



<https://theses.gla.ac.uk/>

Theses Digitisation:

<https://www.gla.ac.uk/myglasgow/research/enlighten/theses/digitisation/>

This is a digitised version of the original print thesis.

Copyright and moral rights for this work are retained by the author

A copy can be downloaded for personal non-commercial research or study,
without prior permission or charge

This work cannot be reproduced or quoted extensively from without first
obtaining permission in writing from the author

The content must not be changed in any way or sold commercially in any
format or medium without the formal permission of the author

When referring to this work, full bibliographic details including the author,
title, awarding institution and date of the thesis must be given

Enlighten: Theses

<https://theses.gla.ac.uk/>
research-enlighten@glasgow.ac.uk

THE ADSORPTION OF SIMPLE MOLECULES
ON SUPPORTED RHODIUM CATALYSTS

by

Karen Green

A thesis submitted for the degree of Doctor
of Philosophy of the University of Glasgow

Department of Chemistry,

November 1988

© Karen Green, 1988

ProQuest Number: 10999379

All rights reserved

INFORMATION TO ALL USERS

The quality of this reproduction is dependent upon the quality of the copy submitted.

In the unlikely event that the author did not send a complete manuscript and there are missing pages, these will be noted. Also, if material had to be removed, a note will indicate the deletion.



ProQuest 10999379

Published by ProQuest LLC (2018). Copyright of the Dissertation is held by the Author.

All rights reserved.

This work is protected against unauthorized copying under Title 17, United States Code
Microform Edition © ProQuest LLC.

ProQuest LLC.
789 East Eisenhower Parkway
P.O. Box 1346
Ann Arbor, MI 48106 – 1346

I know nothing, except the fact of my Ignorance.

Socrates 469-399 BC

Acknowledgements

I would like to express my thanks to my supervisor, Professor Geoff Webb, for his help during the period of this project, and most especially during the writing of this thesis. I am also indebted to both Tommy Boyle and Ken Shepherd, as well as the staff of the various departmental workshops, for their patience and humour in matters technical. Thanks are also due to Dr David Jackson for his help and cooperation with use of equipment.

It would not be fair to mention anyone by name, but the help, encouragement and sympathy I have received during the last three years, from friends and colleagues within the Chemistry Department, will be something I will remember for a very long time. I would also like to take this opportunity to formally thank my parents for the patience and support they have given me during what has been a very difficult period in my life.

My thanks are also extended to the SERC for the maintenance grant I received during the period of this study.

But finally, I would like to dedicate this work to my boyfriend, Stephen, who has probably suffered more than anyone, and without whose help I would never have made it.

TABLE OF CONTENTS

Summary

Chapter 1 Introduction

1.1	Historical Background	1
1.2	The Influence of Experimental Variables on the Reactions of Carbon Monoxide with Hydrogen	3
1.2.1	Catalyst Support Effects	6
1.2.2	Promoter Effects	14
1.2.3	Metal Precursor Effects	16
1.2.4	The Effects of Pre-Treatments and Reduction Procedures	17
1.3	Adsorption Studies	20
1.3.1	The Adsorption of Hydrogen on Rhodium Catalysts	20
1.3.2	The Adsorption of Carbon Monoxide on Rhodium Catalysts	23
1.3.3	The Adsorption of Carbon Dioxide on Rhodium Catalysts	38
1.3.4	The Adsorption of Oxygen on Rhodium Catalysts	40
1.3.5	The Adsorption of Simple Oxygenates on Rhodium Catalysts	43
1.4	Mechanisms	46

Chapter 2 Objectives 57

Chapter 3 Experimental

3.1	Introduction	58
3.2	Materials	60
3.2.1	Catalyst Preparation	60
3.2.2	Gases	62
3.3	Direct Monitoring Techniques	63
3.3.1	The Vacuum System	63
3.3.2	The Reaction Vessel	64
3.3.3	The Counting System	66
3.3.3.1	Plateau Determination	66
3.3.3.2	Background Count Rates	67
3.3.3.3	The Intercalibration Factor	67

3.3.3.4	Dead Time Corrections	68
3.3.4	The Gas Chromatograph and Scintillation Counter	69
3.3.4.1	The Gas Chromatograph	69
3.3.4.2	The Scintillation Counter	72
3.3.5	Preparation of Labelled Gases	72
3.3.5.1	^{14}C -Carbon Dioxide	72
3.3.5.1	^{14}C -Carbon Monoxide	73
3.3.6	Experimental Procedure	74
3.3.6.1	Reduction of Catalysts	74
3.3.6.2	Adsorption Isotherms	74
3.3.6.3	Desorption Measurements	76
3.4	The Pulse-Flow Microreactor (with GC-MS)	77
3.4.1	Introduction	77
3.4.2	The Pulse Flow Vacuum System	77
3.4.3	The Flow System	78
3.4.4	The Sampling System	78
3.4.5	The Reaction Vessel	79
3.4.6	The Gas Chromatograph and Mass Spectrometer	79
3.4.7	Experimental Procedure	80
3.5	Pulse Flow Adsorption System	81
3.5.1	Introduction	81
3.5.2	Apparatus	82
3.5.3	Temperature Programmed Reduction	83
3.5.4	Adsorption Measurements	84
3.5.5	Temperature Programmed Desorptions	84
3.6	Pulse Flow Adsorption System - with Mass Spectrometer	85
3.7	In-situ Fourier-Transformed Infra-Red Measurements	86
3.7.1	Fourier-Transform Infra-Red Spectrometer	86
3.7.2	The Transmission Enviromental Flow Cell	86
3.7.3	Catalyst Preparation	87
3.7.4	Experimental Procedure	88

Chapter 4 Experimental Analysis

4.1	Refinement of Radiochemical Data	90
4.2	Pulse Flow Adsorption Measurements	91

Chapter 5 Adsorption Experiments Using ^{14}C Labels

5.1	Introduction	93
5.2	Carbon Monoxide Adsorption	93
5.2.1	Adsorption Isotherms	93

5.2.2	Molecular Exchange	98
5.2.3	Desorption Measurements	101
5.2.4	Gas-Phase Analysis - Carbon Dioxide Formation	102
5.2.5	The Heat of Adsorption of Carbon Monoxide	103
5.2.6	The Adsorption of Carbon Monoxide on Al_2O_3 , SiO_2 and MoO_3	105
5.3	Carbon Dioxide Adsorption	106
5.3.1	Carbon Dioxide Adsorption Isotherms	106
5.3.2	Molecular Exchange	108
5.3.3	Desorption Measurements	109
5.4	The Influence of Hydrogen on Carbon Monoxide Adsorption	109
5.5	The Influence of Hydrogen on Carbon Dioxide Adsorption	110
5.6	The Influence of Pre-adsorbed Carbon Dioxide on ^{14}C -Carbon Monoxide Adsorption	111
5.7	The Influence of Pre-adsorbed Carbon Monoxide on ^{14}C -Carbon Dioxide Adsorption	112
5.8	The Influence of Oxygen on Carbon Monoxide Adsorption	114
5.9	The Influence of Oxygen on Carbon Dioxide Adsorption	116
5.10	Repeated Reductions	116

Chapter 6 Carbon Monoxide Adsorption Experiments Using Heavy Atom Labels

6.1	Introduction	118
6.2	$^{13}\text{C}^{16}\text{O}$ / $^{12}\text{C}^{18}\text{O}$ Adsorption on 2% Rh/ SiO_2	118
6.2.1	CO Adsorption - Rh/ SiO_2	118
6.2.2	Experiments Using Isotopic Labels - Rh/ SiO_2	121
6.3	$^{13}\text{C}^{16}\text{O}$ / $^{12}\text{C}^{18}\text{O}$ Adsorption on 2% Rh/ MoO_3	123
6.3.1	CO Adsorption - Rh/ MoO_3	123
6.3.2	Experiments Using Isotopic Labels - Rh/ MoO_3	125

Chapter 7 Pulse Flow Experiments

7.1	Introduction	127
7.2	Temperature Programmed Reduction Profiles	127

7.3	Pulse Flow Experiments	129
7.3.1	Introduction	129
7.3.2	Carbon Monoxide Adsorption	130
7.3.3	Carbon Dioxide Adsorption	132
7.3.4	Oxygen Adsorption	133
7.3.5	Carbon Monoxide Adsorption on to a Pre-oxidised Catalyst	134
7.3.6	The Influence of Pre-Adsorbed Carbon Monoxide on Carbon Dioxide Adsorption	135
7.3.7	The Influence of Pre-Adsorbed Carbon Dioxide on Carbon Monoxide Adsorption	135
7.4	Temperature Programmed Desorption Measurements	136
7.4.1	Carbon Monoxide Temperature Programmed Desorption	136
7.4.2	Oxygen Temperature Programmed Desorption	137

Chapter 8 Infra-Red Spectroscopy

8.1	Carbon Monoxide	138
8.1.1	Carbon Monoxide Adsorption on Rh/Al ₂ O ₃	138
8.1.2	Carbon Monoxide Adsorption on Rh/SiO ₂	139
8.1.3	Carbon Monoxide Desorption	140
8.1.4	The Influence of the Reduction Procedure on the Infra-red Spectrum of Adsorbed Carbon Monoxide	141
8.1.5	Carbon Monoxide and Hydrogen Co-Adsorption	142
8.1.5.1	The Co-Adsorption of Carbon Monoxide and Hydrogen on Rh/Al ₂ O ₃	143
8.1.5.2	The Co-Adsorption ² of Carbon Monoxide and Hydrogen on Rh/SiO ₂	144
8.2	Carbon Dioxide	145
8.2.1	Carbon Dioxide Adsorption on Rh/Al ₂ O ₃	147
8.2.2	Carbon Dioxide Adsorption on Rh/SiO ₂	147
8.3	Methanol Adsorption	148
8.3.1	Methanol Adsorption on Rh/Al ₂ O ₃	149
8.3.2	Methanol Adsorption on Rh/SiO ₂	150
8.4	Ethanol Adsorption	151
8.4.1	Ethanol Adsorption on Rh/Al ₂ O ₃	152
8.4.2	Ethanol Adsorption on Rh/SiO ₂	154
8.5	Acetaldehyde Adsorption	155
8.5.1	Acetaldehyde Adsorption on Rh/Al ₂ O ₃	156
8.5.2	Acetaldehyde Adsorption on Rh/SiO ₂	157

Chapter 9 Discussion

9.1	The Catalyst Structure	159
9.2	The Adsorption of Carbon Monoxide	166
9.3	The Adsorption of Carbon Dioxide	187
9.4	The Adsorption of Oxygen	191
9.5	The Competitive Adsorption of Carbon Monoxide Carbon Dioxide, Hydrogen and Oxygen	192
9.5.1	The Competitive Adsorption of Carbon Monoxide and Hydrogen	192
9.5.2	The Competitive Adsorption of Carbon Dioxide and Hydrogen	197
9.5.3	The Competitive Adsorption of Carbon Monoxide and Carbon Dioxide	198
9.5.4	The Competitive Adsorption of Carbon Monoxide and Oxygen	199
9.5.5	The Competitive Adsorption of Carbon Dioxide and Oxygen	202
9.6	The Adsorption of Simple Oxygenates on Rhodium Catalysts	203
9.6.1	Methanol	203
9.6.2	Ethanol	206
9.6.3	Acetaldehyde	209

References

SUMMARY

The adsorption of a number of molecules relevant to the hydrogenation of carbon monoxide to organic oxygenate products over various supported rhodium catalysts has been investigated, under both static and pulsed flow conditions, using radioactive and stable isotope tracer techniques, temperature-programmed desorption and Fourier transform infra red spectroscopy. The catalysts used were 2%(w/w) and 5%(w/w) rhodium on silica, 2%(w/w) rhodium on alumina and 2%(w/w) rhodium on molybdenum trioxide. Temperature-programmed reduction techniques have also been used to characterise the catalysts.

Determination of the [14-C]carbon monoxide and [14-C]carbon dioxide adsorption isotherms, under static conditions, showed that the amounts of each adsorbed were dependent on both the adsorbate and the support. Thus, each catalyst adsorbed considerably more carbon monoxide than carbon dioxide. However, whilst the carbon monoxide would undergo complete exchange at ambient temperature, no such exchange was found with adsorbed carbon dioxide. The average heat of adsorption of carbon monoxide was found to be support independent with a value of -93 ± 6 kJ mol⁻¹. The amounts of carbon monoxide adsorbed by each catalyst decreased in the order alumina > silica > molybdenum oxide.

Exposure of [14-C]carbon monoxide precovered surfaces to either hydrogen or oxygen in the presence of gas phase [14-C]carbon monoxide resulted in an increase in surface

radioactivity. Similar measurements with [14-C]carbon dioxide showed that the presence of hydrogen had little effect, the presence of oxygen dramatically reduced the amount of carbon dioxide adsorbed.

Examination of the effects of preadsorbed carbon monoxide on the adsorption of carbon dioxide, and vice versa, showed that whilst preadsorbed carbon dioxide reduced the adsorption capacity of each catalyst for carbon monoxide, probably through a site-blocking mechanism, preadsorption of carbon monoxide increased the extent of adsorption carbon dioxide on both the silica- and molybdenum trioxide supported catalysts, but decreased the amount of carbon dioxide adsorbed on the alumina-supported catalyst.

Pulsed flow adsorption measurements gave similar results to those obtained under static conditions, except that the amounts adsorbed were less due to the removal of weakly adsorbed species by the flow gas. Determinations of the amounts of carbon monoxide and carbon dioxide adsorbed at a variety of temperatures leads to the conclusion that adsorption of the dioxide is an activated process, whilst that of the monoxide proceeds with minimum activation energy. Adsorption of a 1:1 mixture of $^{13}\text{C}^{16}\text{O}$ and $^{12}\text{C}^{18}\text{O}$ showed that scrambling of the adsorbed species only occurred at elevated temperatures. Evidence is presented to show that this scrambling occurs by a concerted mechanism, rather than via dissociation, whilst the formation of small amounts of carbon dioxide at the elevated temperatures

probably arises from a water gas shift reaction involving water retained by the catalyst following reduction and activation. A surprising feature to emerge from the temperature-programmed desorption studies was that whilst some carbon monoxide is still retained by the catalyst at 593K, this material would readily undergo isotopic exchange with gas phase carbon monoxide.

FTIR studies of the adsorption of carbon monoxide on the rhodium-silica and rhodium-alumina catalysts showed the presence of bands ascribable to linear, bridged and gem adsorbed species on the reduced metal. An additional band ascribed to carbon monoxide adsorbed on a partially reduced rhodium site was also observed. No satisfactory measurements could be made, even in diffuse reflectance, with the rhodium-molybdenum trioxide catalysts, due to the extremely high absorbance of the catalyst samples. The effect of increasing temperature on the spectra of the adsorbed carbon monoxide was to increase the intensity of the bands due to the gem-adsorbed species, whilst the intensity of the linear band simultaneously decreased. This is taken to indicate that the presence of the adsorbed carbon monoxide causes a restructuring of the metal surface, and thereby an increase in the number of isolated rhodium sites on which the gem-dicarbonyl species are adsorbed, as the temperature is increased.

The FTIR spectra of adsorbed carbon dioxide on rhodium-silica and rhodium-alumina revealed bands due to both surface carbonates and adsorbed carbon monoxide, indicating

that at least some of the dioxide is dissociatively adsorbed on the surface.

Investigations of the adsorption of methanol, ethanol and ethanal by infra red spectroscopy showed that, on both rhodium-silica and rhodium-alumina catalysts, decomposition to carbon monoxide occurred at ambient temperature. The extent of this decomposition, which was support dependent, was promoted by increase in temperature and by the presence of hydrogen. Bands due to the presence of surface hydrocarbonaceous species were also observed.

CHAPTER 1
INTRODUCTION

CHAPTER 1 INTRODUCTION

1.1 HISTORICAL BACKGROUND

The hydrogenation of carbon monoxide has been studied with varying amounts of enthusiasm since it was first reported in 1902¹. Much of the early work on this reaction was carried out by Fischer and Tropsch², as they searched for a means to convert Germany's vast coal reserves into more convenient fuels. However, when, after 1945, oil became plentiful and cheap, interest in these reactions quickly waned, so that today it is recognised that the Fischer-Tropsch synthesis of hydrocarbons will only be viable in South Africa, for the foreseeable future. The same, however, may not be true of the oxygen containing compounds which are produced alongside the hydrocarbons. Many of these oxygenates are valuable products in their own right, being produced at present from oil, using complex and therefore expensive processes. The hydrogenation of carbon monoxide could, therefore, prove to be a very attractive route to these products if good commercial catalysts can be developed.

One such process has already been developed by I.C.I. for the low pressure formation of methanol³. Their Cu/ZnO/Al₂O₃ catalysts can now produce methanol with a selectivity of greater than 99%, from a mixture of carbon

monoxide, carbon dioxide and hydrogen.

Many of the recent advances in oxygenate production have been made using homogeneous catalysts⁴, because of the relative ease of studying these systems. Unfortunately, homogeneous catalysts have several severe disadvantages over heterogeneous ones⁵, the first and most obvious problem being that of separating the catalyst from the product mixture. Since the separation procedures which are available usually destroy the catalyst in the process, the catalyst must be cheap and easy to produce, thus adding further constraints to the system. Since the catalyst and products are both in the same phase, the reaction cannot, in most cases, be run as a continuous process, but must be carried out in the batch mode. The stability of many of these homogeneous complexes has also been a problem which has resulted in the use of very high operating pressures. Although many advances have been made in this area, the successful "heterogenation" of these catalysts would probably mean that an even greater improvement in operating conditions would be possible.

Over the years an enormous variety of catalysts have been used for the hydrogenation of carbon monoxide, under a bewildering variety of conditions - see for instance reference 6. This study, however, will concentrate almost exclusively on heterogeneous reactions and, in particular, on those of rhodium catalysts supported on a variety of

inorganic oxide supports.

There has been a great deal of interest lately in the Group VIII metals, because of their ability, depending on the catalyst and the conditions used, to produce both hydrocarbons and oxygenates⁷. Rhodium catalysts have come to prominence because it is known to form the more useful higher molecular weight oxygenates from carbon monoxide and hydrogen. A number of papers have cited rhodium as being active in both homogeneous^{8,9} and heterogeneous catalysts^{10,11}. However, a greater understanding of the catalytic action of rhodium is needed before new and better catalysts can be developed for these processes.

It is also appropriate to mention at this point, that although the reaction mixture, or syngas, for these reaction is produced, at the moment, from natural gas or oil¹², the technology could easily be adapted to run on coal. Thus, when oil becomes scarce or expensive, these reactions could provide a feasible alternative to oil-based chemical feedstocks.

1.2 THE INFLUENCE OF EXPERIMENTAL VARIABLES ON THE REACTIONS OF CARBON MONOXIDE WITH HYDROGEN

A number of factors determine the catalytic behaviour of heterogeneous catalysts, the main ones for rhodium catalysts will be dealt with here, before the adsorption of

the reactants and reaction products is discussed.

The reaction conditions have, not surprisingly, been found to have a considerable effect on the activity of these catalysts and on the products formed. The formation of hydrocarbons is favoured over transition metal catalysts at low pressures, but at higher pressures, especially if the temperature is low, a reasonable yield of oxygenates can be obtained.

Chuang¹³ found that while Rh/TiO₂ produced only a 2% yield of oxygenates at atmospheric pressure, this rose to 17% at ten atmospheres. Similar results have also been reported for palladium and rhodium catalysts supported on SiO₂ and Al₂O₃¹⁴ - at low pressures only hydrocarbons are formed, while at higher pressures large amounts of methanol and ethanol are produced. The overall activity of rhodium catalysts has also been found to be pressure dependent. Thus the Rh (111) face is only active for Fischer-Tropsch synthesis at pressures above one atmosphere¹⁵.

The reaction temperature has a significant effect on the catalyst's selectivity. As the temperature is increased, the yield of hydrocarbons, particularly methane, has been reported to increase¹⁶. Watson¹⁷ found that methanol was the main product below 225°C, while between 225°C and 300°C the yields of acetaldehyde and ethanol were higher. Finally at temperatures greater than 350°C the Rh/Al₂O₃ catalyst was

reported to produce only methane.

The ratio of H_2/CO in the syngas is also very important. A very high ratio promotes the formation of methane, whilst a low ratio increases the production of oxygenates and ethene^{16,18}. Most of the results discussed in this chapter were obtained with a H_2/CO ratio of 2-3, so that the full range of products could be obtained.

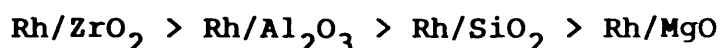
Another experimental factor which can affect the amount and type of products formed is the extent to which secondary reactions are allowed to take place. Kuznetsov¹⁶ found that the higher the space velocity of the system, the better the yield of oxygenates obtained. Bhasin¹⁹ overcame the problem of secondary reactions by looking at the product distribution at very low conversions.

A large number of kinetic studies have been carried out on this system, and although the results obtained vary considerably with experimental conditions, the general consensus appears to be that the reaction is approximately first order in hydrogen and between 0 and -1 order in carbon monoxide²⁰⁻²². The inhibiting effect of a high surface concentration of carbon monoxide has meant that under many reaction conditions it is the surface concentration of hydrogen which is rate limiting.

1.2.1 CATALYST SUPPORT EFFECTS

For many years the oxide supports of transition metal catalysts were simply thought of as inert carriers for the active component, stabilising the formation of very small metal particles. However, a wealth of experimental evidence has now shown that the support can have a much more dramatic and varied role²³. Rhodium foils and single crystals have been found to produce only simple hydrocarbons, such as methane, in the hydrogenation of carbon monoxide¹⁵, yet supported catalysts can form a wide range of both hydrocarbons and oxygenates.

The choice of support can substantially affect both activity and the product distribution of a supported metal catalyst, as many groups have shown. The activity of a series of Ni, Rh, Ru and Pd catalysts were two orders of magnitude higher when the metal was supported on MoO₃ or WO₃, rather than on SiO₂²⁴. While Lizuka²⁵ reported that the activity of rhodium catalysts for the hydrogenation of both carbon monoxide and carbon dioxide decreased in the order:-



Rhodium carbonyl clusters supported on ZnO, MgO, BeO and CaO were found to form mainly methanol⁷, while La₂O₃, ZrO₂, CeO₂, TiO₂ and ThO₂ supported catalysts produced C₂-

oxygenates. Rh/SiO₂ and Rh/Al₂O₃ were found in the same study to form mainly C₁-C₅ hydrocarbons.

Similar effects have also been observed with other Group VIII metals²⁶, even different types of SiO₂ in the support can change a catalyst's behaviour²⁷.

There are several theories to explain these dramatic effects²³, all of which may have some part to play in any particular system. The simplest theory is that the support controls the size and geometry of the metal particles which are formed on reduction. The support thereby controls the number and type of active sites which are formed. When there is a high degree of interaction between the metal particle and the support, the metal will tend to wet the surface of the support, maximising the contact between the two phases and forming large 2-D rafts²⁸. When the interaction energy is low, 3-D crystallites with a totally different set of sites will form. The raft-like particles are easy to both reduce and oxidise, while the 3-D crystallites are more difficult²⁹. A catalyst is likely to have both types of particles on its surface at any one time, but the ratios of the two will be dependent on the specific catalyst and conditions used³⁰.

The activity of the Rh/SiO₂ catalyst was found to increase significantly as the dispersion fell from 0.45 to 0.25³¹. In the same study, methanol was found to be produced selectively at high dispersions, while acetaldehyde

production reached a maximum at 50% dispersion, along with that of ethanol and acetic acid. Methane production increased steadily with increasing particle size.

The support may also determine the crystal habit of the metal particles. Rh/MgO was found to have a lower activity than Rh/Al₂O₃ because, on MgO the metal particles preferentially exposed the less active low index planes³².

It has been suggested that, in some systems, the reported support effects could be due to the bifunctional nature of the catalyst, active sites being present on the support as well as the metal particles. The spillover of atomic hydrogen from the metal on to the support is a well documented process³³⁻³⁶, and it has been suggested that this spillover hydrogen can then react with adsorbed carbon dioxide to form formate species. These species have now been detected on the supports of several catalysts^{37,38}. Since formates decompose on rhodium to form carbon monoxide and water³⁹, the sites for formate production are likely to be situated on the support, rather than the metal particles. Rh/La₂O₃ catalysts have been reported as forming high yields of oxygenates¹⁶, however the same study also found that La₂O₃ was, by itself, a good methanol catalyst.

The support may also act by retaining active species which are formed during the reaction, or the reduction procedure. When RhCl₃ is used as the metal precursor,

traces of chlorine are found to remain on the surface after reduction⁴⁰. This can then be trapped by the support material, dramatically changing the catalyst's characteristics.

There is growing evidence to suggest that certain supports, in particular Al_2O_3 and zeolites, tend to stabilise the lower oxidation states of rhodium⁴¹⁻⁴⁴, through the formation of mixed oxides, which are more resistant to reduction than the original metal precursor. The formation of even a few of these Rh^{n+} sites could then have a significant effect on the catalysts' behaviour.

It has also been reported that clear trends exist between the acidity of the support and the type of products which are formed. Rhodium catalysts with basic supports, such as MgO , form large amounts of methanol, while catalysts with acidic supports form mainly hydrocarbons⁴⁵. Dirske⁴⁶ used Li-naphthalide to remove all acidity from the supports of a Rh/SiO_2 catalyst, and found that the catalyst was almost 100% selective for methanol. A very similar untreated catalyst, with its fairly acidic support, produced only methane.

These support effects have long been associated with some kind of electronic interaction between the support and the metal particles. Since the Fermi levels of a metal are generally higher than those of a semiconductor, Schwab⁴⁷ suggested in 1958 that a flow of electrons would be expected

between the metal and the support. Although this delocalised transfer of charge may be significant after a low temperature reduction (LTR), some groups⁴⁸ believe that a more localised movement of electrons in the opposite direction, that is from the support to the metal, is more important after a higher temperature reduction. This charge transfer may be closely related to the spillover of hydrogen atoms on to the support and the consequential reduction of the support metal³⁵. Evidence for the transfer of electrons from the support to the metal has also been reported from X-ray Photoelectron Spectroscopy (XPS) experiments on Rh/TiO₂⁴⁹.

However, whichever the direction of charge transfer, changing the electron density of the metal particles would be expected to have a dramatic effect on the catalyst's behaviour. Increasing the rhodium's electron density would strengthen the bond between the metal atom and any adsorbed carbon monoxide by increasing the degree of back donation from the metal to the π anti-bonding orbitals of the carbon monoxide. This would promote the dissociation of the carbon monoxide⁵⁰. Whilst decreasing the electron density of the metal would increase the proportion of molecularly adsorbed carbon monoxide, although the overall amount adsorbed may decrease due to less backbonding. The adsorption of carbon monoxide will be discussed in greater detail elsewhere in this chapter.

Solymosi⁵¹ investigated the effects of directly increasing the conductivity of the support, by doping TiO_2 with W^{6+} ions, and found that the amount of surface carbon and the amount of methane produced by the surface increased dramatically when W^{6+} was added. This, he believed, was due to increased electron transfer between the support and the rhodium. However, these effects would tend to be rather short range and would only be significant when a large proportion of the metal atoms were in contact with the support. Chien⁵² found that the degree of interaction between TiO_2 and the rhodium it supported, increased as the particle size decreased.

The reduction procedure has considerable influence in some supported rhodium systems. After a high temperature reduction (HTR), usually above 500°C , these catalysts exhibit the so-called Strong Metal Support Interactions (SMSI). These reactions, which can to a large extent be reversed by exposure to oxygen, result in a decrease in the adsorption capacity of the catalyst for carbon monoxide and hydrogen, as well as changes in the activity and selectivity of certain reactions. The onset of SMSI behaviour is closely connected to the reducibility of the support. Supports such as TiO_2 and MoO_3 which undergo reductions at fairly low temperatures²⁴, tend to show SMSI behaviour. Reduction of the support is often facilitated by hydrogen spillover from the metal particles, but the support must be

able to accommodate the defects caused by this process if it is to show strong metal support interactions⁵.

Currently one of the most widely held theories for SMSI is that the migration of partially reduced support species on to the metal particles strongly modifies their catalytic properties⁴⁸. When reduced samples of Rh/TiO₂ were examined by Auger spectroscopy, the metal particles were found to be covered with a species containing both titanium and oxygen atoms^{49,53}. However, when the surface layers had been removed by ion sputtering, the normal peak due to rhodium metal was obtained. The ratio of the oxygen and the titanium peaks in the initial spectrum was such that it was found to be a suboxide of titanium on the metal particles rather than TiO₂. Extended X-ray Adsorption Fine Structure Analysis (EXAFS)⁴⁹, has shown that there is a higher degree of Rh-O interactions after HTR than LTR, even though the metal particle size, as measured by electron microscopy, appears unchanged. This again appears to be due to the interaction of the metal with support material on its surface.

Somarjai et al⁵⁴ investigated the effects of depositing suboxides of TiO₂ directly on to model rhodium catalysts and found that a 0.15 monolayer of TiO_x produced a threefold increase in methane formation. These results were explained by the formation of special sites at the periphery of the TiO_x islands where the carbon monoxide, interacting perhaps

with Ti^{3+} species, could dissociate more readily. Others found⁵⁵ that when VOCl was deposited on a Rh/SiO_2 catalyst it produced a catalyst which exhibited behaviour which was very similar to that of $\text{Rh}/\text{V}_2\text{O}_3$.

Some suggest^{55,56} that the overlayers are formed when some of the support material dissolves during catalyst preparation, then reprecipitates on reduction. Others believe the driving force for encapsulation to be the formation of bonds between the metal atoms and the partially reduced support⁵⁷. Modification of the rhodium valence levels after HTR suggests that some kind of strong interaction is involved.

The suboxide support decorations, which are formed on the metal particles, appear to reduce hydrogen, carbon monoxide and nitrous oxide adsorption by means of a simple site blocking mechanism⁵⁸. It has been found that those reactions which are most affected by SMSI are those which require a large ensemble of sites⁵⁹. Partial encapsulation, like alloying, breaks up the larger ensembles and so severely hampers these reactions^{49,60}. A new type of site associated with this support material may also be formed⁵⁸ and although the evidence suggests that only a few of these sites are present, their high activity is such that they can significantly affect the overall catalyst behaviour¹⁰.

There are several other theories to explain SMSI behaviour²³, most of which have already been discussed

above. These include the loss of 3D character after HTR, the partial reduction of the support material, the stabilisation of oxidised forms of rhodium, increased spillover / reverse spillover and the formation of new sites due to changes in the particle geometry. However, since support decorations have been reported on rhodium particles after fairly mild reductions⁵⁶, it may be unwise to try and separate SMSI and "normal" support effects.

1.2.2 PROMOTER EFFECTS

Promoters are generally species which are added, in fairly small quantities, to the catalyst during preparation, in order to modify its behaviour. However, the method of preparation appears to be very important⁶¹, as it has been found that with many catalysts the majority of the promoter appears to be situated on the support⁶², where it has little effect. For the promoters to exert their full effects they must be in close proximity to the metal particles.

Ichikawa (fig 3 in ref 5) found that certain transition metal oxides had a significant effect on the activity and selectivity of Rh/SiO₂. V₂O₃ increased the catalyst's production of ethanol dramatically. Alkali metal ions also improve the selectivity of these catalysts for oxygenates, but tend to decrease the overall rate, through decreased

hydrogenation activity^{10,13,14,61-65}. Oxides such as La_2O_3 , CeO_2 , Pr_6O_{11} , Nd_2O_3 , Sm_2O_3 , MnO , MoO_3 and V_2O_3 have all been reported as improving the production of ethanol over Rh/SiO_2 , $\text{Rh}/\text{Al}_2\text{O}_3$ and Rh/TiO_2 , as have Fe and Pt promoters⁶⁶⁻⁷⁶. These oxides appear to produce similar effects whether they are used as promoters or supports. In fact, it has been suggested that the origins of these effects are very similar to those of the support effects discussed in the previous section. The promoters are seen as producing partially reduced species, which then migrate on to the metal particles^{55,73-76}. The overlayers produced, may then simply block certain sites (such as those for carbon monoxide adsorption) or they may form new sites, possibly through the stabilisation of Rh^{n+} species^{69,71}. However, they do not appear to have any effect on the particle size⁷⁵. Naito has reported that Na^+ promoters appear to stabilise oxygen on the surface, perhaps at the promoter associated sites, which may account for the dramatic effect observed in the catalyst behaviour.

Sachtler⁷⁷ suggested that the oxygen end of carbon monoxide is associated with the promoter, in the new sites which are formed. By stabilising both ends of the molecule and reducing its electron density these sites decrease the rate of carbon monoxide dissociation, as is observed with many promoted rhodium catalysts.

1.2.3 METAL PRECURSOR EFFECTS

The choice of metal precursor must also be considered when designing a catalyst to perform a chosen task. Many groups have used metal carbonyl clusters, such as $\text{Rh}_6(\text{CO})_{16}$, to produce well dispersed catalysts with a narrow range of particle sizes⁷⁸⁻⁸¹. These compounds can be reduced under fairly mild conditions to Rh^0 , without losing any of the cluster structure, although there is evidence to suggest that the stability of the cluster depends on the basicity of the support⁷⁸. Catalysts formed from these cluster complexes generally have a very high dispersion and a good selectivity for the oxygenates.

A wide variety of metal salts have also been used as metal precursors. These include $\text{Rh}(\text{NO}_3)_3$, RhCl_3 , Rh_2O_3 , $\text{Rh}_2(\text{SO}_4)_3$ and $[\text{Rh}(\text{OCOCH}_3)_2]_2$ ⁸²⁻⁸⁶. There is evidence to suggest that catalysts produced from these metal precursors still contain a small proportion of Rh^{n+} species after their normal reduction procedures^{41,86}. This incomplete reduction may be related to the retention of anionic species on the surface. Residual chlorine has been detected on several catalysts and has been shown to reduce the selectivity of these catalysts towards oxygenates⁴⁰, although this may depend on the support used⁵⁵. When sulphate or acetate precursors were used the surface was poisoned for carbon monoxide adsorption by respectively, sulphurous and carbonaceous residues⁸⁶.

The type of metal salt may also have an effect. Anhydrous Rh_2O_3 was quickly reduced to the metal under reaction conditions but the hydrated oxide was fairly stable producing large amounts of oxygenates and olefins⁸⁶.

The differences in catalytic behaviour which are observed when different metal precursors are used appear to have similar origins to those of the support and promoter effects. The ease of reduction of the metal precursor may control the size and geometry of the metal particles that are formed, thus affecting the number and type of sites available. Catalysts produced from $\text{Rh}(\text{NO}_3)_3$ appear to show a higher degree of dispersion than those from the more commonly used RhCl_3 . The residue formed by reduction of the precursor may also change the catalyst behaviour, blocking some sites and causing the formation of others. RhCl_3 for instance is thought to be better at stabilising Rh^{n+} than $\text{Rh}(\text{NO}_3)_3$ ⁴³.

1.2.4 THE EFFECTS OF PRETREATMENT AND REDUCTION PROCEDURE

As already noted, certain rhodium catalysts have been observed to show the so called SMSI behaviour when reduced at high temperatures^{20,23}. However, the length of time and temperature of the reduction, as well as the reducing

mixture used, can have more general effects as well.

The average size of the metal particles which are formed on reduction have been found to increase with the reduction temperature and the length of the reduction procedure⁸⁷. These changes in dispersion can affect both the activity and selectivity of the reduced catalyst³¹.

Fully reduced rhodium foils and single crystals have been found to produce only hydrocarbons from carbon monoxide and hydrogen¹⁵. If, however, the catalyst is first oxidised before use the overall activity is much higher and some oxygenates are formed. This transitory effect may be due to a disordering of the rhodium surface which produces new and more active sites⁸⁸, although other theories suggest that oxygen either burns off surface contaminants, such as precursor residues, or that the oxygen atoms themselves have some sort of promotional role to play. After a low temperature reduction, two Rh-O bands were observed by EXAFS measurements⁸⁹, one band due to incomplete reduction of the catalyst was removed by further reduction at 400°C. Duprez et al⁹⁰ found that partially reduced Rh/Al₂O₃ produced high yields of hydrocarbons while preventing the formation of oxygenates - oxygen treatment of rhodium foil increased the production of oxygenates¹⁵.

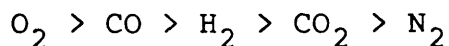
When Rh/SiO₂ was reduced by a 1:1 mixture of carbon monoxide and hydrogen⁹¹, the major products were ethene and propylene, while after hydrogen reduction the corresponding

saturated hydrocarbons were the main products. Reduction under hydrogen and water on the other hand resulted in a high yield of ethanol and acetaldehyde. Similar results have also been observed for other transition metals, such as ruthenium⁹².

In conclusion it can clearly be seen that a number of factors can have a very dramatic effect on the behaviour of supported rhodium catalysts. These include the method of catalyst preparation and reduction which are employed, the metal precursor, support and, if present, the promoter chosen, not to mention the reaction conditions used. However, this list may still be far from complete. In order to understand better the behaviour of these very complex systems, many groups have attempted to simplify the systems as much as possible, investigating the separate interactions of reactants and products with well characterised surfaces under carefully controlled conditions. The next few sections will present some of the information which has been obtained in these experiments. It should, however, be noted that as these experiments were carried out under very different conditions to those at which these reactions would normally be run, caution is needed when extrapolating these results to reaction conditions.

1.3 ADSORPTION STUDIES

The large number of groups which have investigated the adsorption of simple molecules on transition metals, have with few exceptions, found that the strength of adsorption of the various gases decreased in the order:

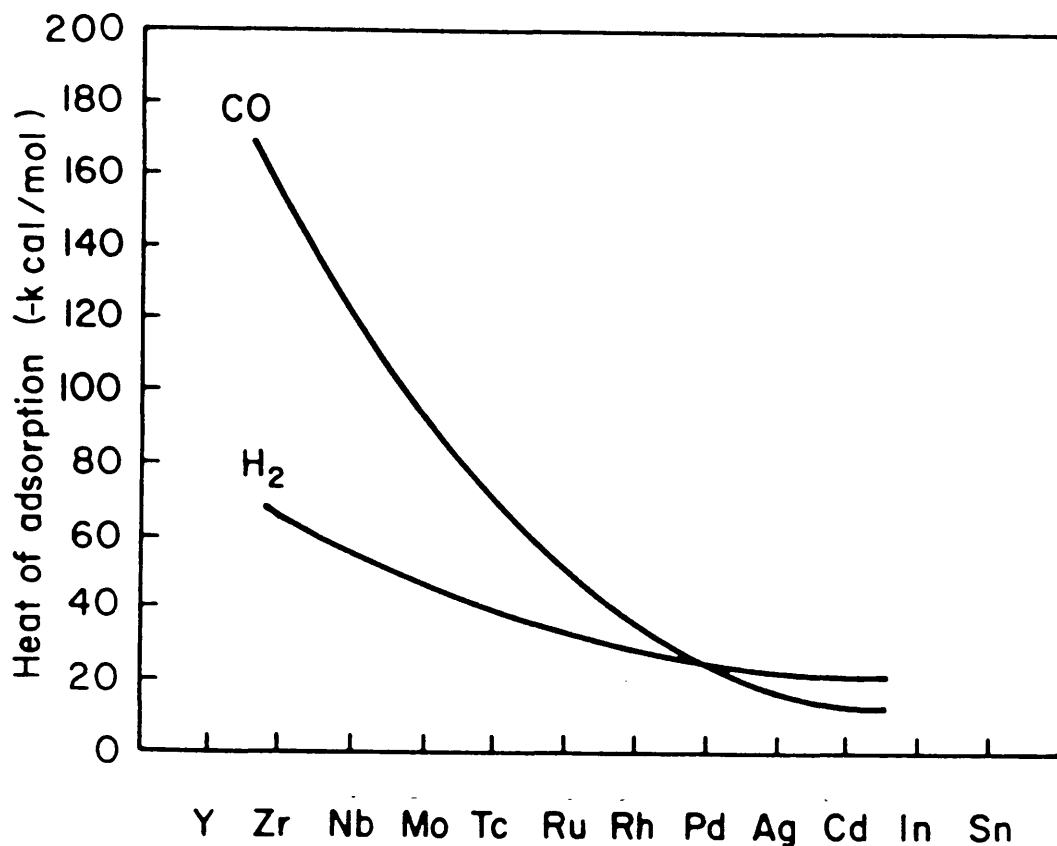


This led to a qualitative classification of the metals, where rhodium, along with platinum and palladium, was thought to be able to adsorb oxygen, carbon monoxide and hydrogen but not carbon dioxide or nitrogen. The ability of the transition metals to adsorb these gases was believed to be related to their ability to stabilise the weakly held precursors of the adsorbed species¹².

1.3.1 THE ADSORPTION OF HYDROGEN

The adsorption of hydrogen on supported metal catalysts appears to be a fairly simple non-activated process³⁶ which varies little as you move across the transition series⁵. The heat of adsorption of hydrogen for instance, varies much less than that of carbon monoxide⁹³ (fig 1.1). The adsorption of hydrogen on rhodium is a dissociative and non-activated process which proceeds via a short-lived mobile precursor above 100K^{5,94}. Hydrogen has a high initial

Fig. 1.1



sticking coefficient⁹⁵ and adsorbs rapidly on all of the rhodium crystal faces, while tungsten, on the other hand, adsorbs hydrogen much faster on its rougher faces than the smooth ones. As hydrogen is adsorbed on rhodium surfaces, the work function of the metal has been reported⁹⁶ to rise, indicating that the adsorbed hydrogen has a partial negative charge. However, there is some evidence to suggest that with platinum at least, the charge on the hydrogen atom is dependent upon the local environment, being negatively charged in the vicinity of steps but carrying a small positive charge when on a flat plane⁹⁷. This may also be true of hydrogen adsorbed on rhodium.

When hydrogen is adsorbed at very low temperatures a small amount of molecular hydrogen has been observed⁹⁶,

which is desorbed from the surface at 110K. This α -hydrogen was found to have a lower heat of adsorption on rhodium than that on platinum or iridium⁹⁵. The same was also true of the dissociated, or β -hydrogen.

The adsorption of simple molecules, such as hydrogen, has been used for many years as a means of measuring the surface metal area of supported catalysts. This method, however, rests on the assumption that one atom of hydrogen will be adsorbed on each metal atom. A growing body of evidence now suggests that this may not be the case^{98,99} as many groups have reported H:Rh ratios of greater than unity. Several theories have been put forward to explain these observations, which include multiple hydrogen adsorption, spillover of hydrogen atoms from the metal to the support and partial reduction of the support material.

Kip et al⁹⁸ have studied the adsorption of hydrogen on several metals supported on SiO₂ and Al₂O₃. They found that the H:M ratio was a linear function of the average coordination number - the H:M ratio fell as the particle size increased. Since the ratio was independent of support but decreased in the order:



they related the high hydrogen adsorption to the formation of polyhydric species on the surface, as the stability of

such complexes would be expected to decrease in the order shown.

Two distinct types of hydrogen adsorption have been reported on Rh/TiO₂¹⁰⁰, the initial fast adsorption is thought to be on to the metal particles themselves, whilst the second type is due to spillover of hydrogen atoms on to the support. Although the careful use of isotopic labels has shown that rapid exchange occurs between the two types of hydrogen¹⁰¹, the hydrogen adsorbed on the metal particles tends to be more strongly held than that on the support³⁵. N.M.R. results suggest that the "metallic" hydrogen is made up of several different species³⁴, with evidence for the formation of a bulk rhodium hydride also being reported⁹⁵. Hydrogen has been observed to be desorbed from rhodium catalysts at several distinct temperatures^{102,36}, with single crystal studies showing that hydrogen is desorbed from the stepped faces before the smooth ones⁹⁵.

Rhodium's ability to dissociate hydrogen molecules has long been recognised¹⁰³ and this, therefore, allows the metal particles to act as "portholes" for the migration of hydrogen atoms on to the support. Although hydrogen spillover is very dependent on the catalyst and conditions used, even supports such as SiO₂ and Al₂O₃, which were previously considered to be unreactive, are now recognised as promoting a limited amount of spillover^{33,36}. With catalyst supported on oxides such as MoO₃, WO₃ and TiO₂,

hydrogen spillover is well known and quite considerable causing a significant reduction of the support²⁴. Paramagnetic Ti^{3+} ions have been detected by e.s.r. on Rh/TiO₂ catalysts as a result of hydrogen spillover^{34,35}. This reduction of the support is thought to take place via the transfer of an electron from the rhodium to the Ti^{4+} ion and the subsequent formation of a Ti^{3+} species, while the proton which is formed reacts with a surface oxygen to form a hydroxyl group. These hydroxyl groups can then combine to form water molecules, which are released from the surface, and a series of support sub-oxides⁵. This process may go quite deep into the crystal lattice of the support, eventually causing its collapse, although the process can be partially reversed by the presence of oxygen.

Hydrogen spillover is promoted, as expected, by high temperatures and a high partial pressure of hydrogen¹⁰¹. A low temperature reduction, with the high dispersion it produces, also increases the amount of hydrogen atoms which are present on the support. This is because the very small particle size means the hydrogen atoms do not have to migrate as far before they reach the support, thus reducing the chances of their recombination and desorption. Thus while more hydrogen is adsorbed by the surface after a low temperature reduction, it is less strongly held than that adsorbed after a high temperature reduction^{35,101}. This is reflected in the shape of the hydrogen isotherms which were obtained for the different samples. The amount of

spillover / reverse spillover which is occurring is believed to have a very significant effect on the catalyst's overall behaviour by increasing the amount of hydrogen which is available on the surface.

Carbon monoxide adsorption has been shown to severely limit the spillover of hydrogen on to the catalyst support³³, by blocking the spillover sites. It has, however, no effect on any hydrogen which is already present on the support.

Hydrogen is believed to be adsorbed very weakly on some of the transition metal ions present⁵ in the supports which have been used. The amounts adsorbed, however, are negligible without the activating presence of the metal particles.

1.3.2 THE ADSORPTION OF CARBON MONOXIDE

Carbon monoxide adsorption on rhodium involves a very similar type of bonding to that occurring in metal carbonyl clusters¹⁰⁴. The bond is formed by a transfer of electrons from the highest filled orbital on the carbon monoxide, which is the 5σ lone pair on the carbon atom, to the unoccupied metal d-orbitals^{50,105,106}. Back-donation then occurs between the filled metal orbitals and the lowest unoccupied orbitals (2π) on the carbon monoxide. Since the

5σ orbitals are essentially non-bonding, loss of electron density from these orbitals has little effect on the C-O bond. The 2π orbitals, however, are anti-bonding, so the back-donation of electrons from the metal results in a weakening, and consequential lengthening, of the C-O bond. These effects can be clearly seen with infra-red spectroscopy. The gas phase stretching frequency of the C-O bond is observed at 2143 cm^{-1} ¹⁰⁷, yet values as low as 1825 cm^{-1} have been reported for carbon monoxide adsorbed on Rh/MgO catalysts³³.

Species which affect the amount of back-donation taking place can dramatically strengthen or weaken the C-O bond. Adsorbed chlorine shifts the C-O stretching frequency to higher wavenumbers as its electron withdrawing ability reduces back-donation⁶⁸.

There has been a great deal of debate in recent years as to whether all of the carbon monoxide is molecularly adsorbed or whether some of it dissociates on the surface into adsorbed carbon and adsorbed oxygen.

Yates et al¹⁰⁸ found that the sticking coefficient of carbon monoxide on the Rh (111) face was very low at less than 10^{-3} per collision. This meant that the maximum possibility of carbon monoxide dissociating on adsorption was less than 10^{-3} per collision with the surface.

Gorodetskii found that no surface carbon could be

detected on surface rhodium after carbon monoxide adsorption and then desorption¹⁰⁹. They were also unable to detect a high temperature desorption peak which had previously been associated with the recombination of dissociated carbon monoxide²³. When carbon monoxide was artificially dissociated in the same system, by electrical discharge, carbon crystals were observed to form on the Rh (111) face, although at 1000K some carbon did diffuse into the bulk. A high temperature carbon monoxide desorption peak as well as some carbon dioxide formation were also observed.

Other workers have quoted the observation of first order desorption kinetics of carbon monoxide^{110,111} as evidence for its molecular adsorption on rhodium. On the other hand, Somorjai et al reported that some carbon monoxide dissociated on both polycrystalline²² and stepped⁴² rhodium surfaces. They believed that although carbon monoxide adsorption was molecular at room temperature, dissociation could occur, especially at elevated temperatures, on the less coordinated sites found at steps and defects.

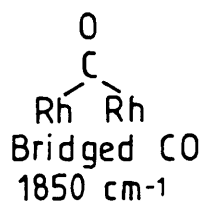
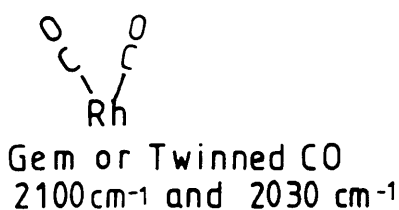
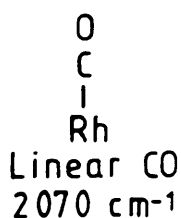
With supported rhodium catalysts the amount and type of surface carbon which is formed from carbon monoxide dissociation appears to be very dependent on the support which is used¹¹³. Rh/TiO₂ has been reported to produce fairly large amounts of carbon, but the carbon produced ages more quickly than that produced on Rh/SiO₂. Under reaction

conditions a variety of rhodium catalysts have been shown to be covered with a layer of carbonaceous material^{23,38,114}, which could only have been formed from carbon monoxide dissociation.

Surface science techniques^{115,116} have shown that carbon monoxide is adsorbed on rhodium surfaces via a mobile precursor state with a very high initial sticking coefficient. Carbon monoxide forms a series of highly regular arrays on the surface which vary as the surface coverage changes.

Molecular carbon monoxide is thought to exist on rhodium catalysts in one of the three major forms shown below:

CO Adsorption Modes on Rh



although other species, such as side-on bonded molecules¹¹⁷ have also been proposed. Most of the evidence for species 1-3 has come from the tremendous amount of infra-red spectroscopy work which has been carried out on this system¹¹⁸⁻¹²⁴. Other techniques, however, such as ¹³C n.m.r. and tunnelling spectroscopy¹²⁵⁻¹²⁸, have also been

useful because of the problems associated with infra-red spectroscopy such as a limited spectral range.

The stretching frequency of the bridged species appears as expected at the lowest frequency ($1800-1900\text{cm}^{-1}$)¹²² due to the high degree of back bonding which is present in this species⁵⁰. On the other hand, the gem species which has the least back bonding, produces a doublet of infra-red (ir) bands at 2100 cm^{-1} and 2031 cm^{-1} ¹²². The structure of the gem species was originally assigned by analogy to the homogeneous $[\text{Rh}(\text{CO})_2\text{Cl}]_2^-$ complexes¹²⁹, where two carbon monoxide molecules are bonded to each rhodium atom. The ir spectra of these complexes consists of a doublet, due to its symmetric and antisymmetric stretching modes, at 2095 cm^{-1} and 2043 cm^{-1} ¹³⁰.

The stretching frequencies of the linear and bridged species are known to shift to higher frequencies as the degree of coverage increases. Rice¹²⁴, for instance, has reported that the peak due to linear carbon monoxide can shift from 2038 cm^{-1} to 2073 cm^{-1} , on $\text{Rh}/\text{Al}_2\text{O}_3$, as the surface concentration of carbon monoxide is increased. This suggests that these species are present on metallic crystallites and it is the degree of interaction between neighbouring molecules which shifts the frequency to higher wave numbers.

The gem peaks do not shift with coverage. It is, therefore, believed that they are present on isolated sites,

where the interaction between neighbouring groups is not important^{120,122}. Very similar conclusions have also been drawn from ¹³C-nmr studies using Rh/Al₂O₃¹²⁸.

As the loading of rhodium increases and the dispersion falls, the intensity of the linear and bridged peaks increases, whilst the gem peaks lose intensity. This phenomenon has been reported by several groups^{42,118,124} and is cited as evidence for the formation of gem carbon monoxide on isolated sites, the concentration of which would tend to decrease as the metal loading is increased.

The angle between the carbonyl groups in the gem species (2a) can be calculated from the relative intensities of the symmetric and antisymmetric ir absorbances using the relation:

$$A_{\text{asym}}/A_{\text{sym}} = \tan^2 \alpha$$

The integrated adsorbance
symmetric stretching mode
of CO = A_{sym}

The integrated adsorbance
antisymmetric stretching mode
of CO = A_{asym}

Since the ratio of A_{asym} / A_{sym} was approximately one, the angle between the two CO moieties was taken to be 90°. This is in very good agreement with the bond angle of 91° calculated for [Rh(CO)₂Cl]₂¹³¹.

A detailed examination of the ir spectrum of carbon monoxide on Rh/Al₂O₃ has led Yao et al¹¹⁹ to report that the

linear species is more "floppy" than the gem, occupying four times the distribution of sites. However ^{13}C -nmr studies suggest¹²⁸ that the gem species is less rigidly held showing a higher degree of motion than the other species.

Several groups have found that the exchange of isotopically labelled molecules occurs much faster with the gem than the linearly adsorbed carbon monoxide^{122,123,132}. In fact, at low temperature, the gem carbon monoxide is the only species which will undergo exchange^{124,127}.

This fast exchange is thought to occur by the coordination of an extra molecule of carbon monoxide to form a very transient $\text{Rh}(\text{CO})_3$ species¹²². Evidence for this tricarbonyl species comes from homogeneous inorganic chemistry. When a solution of $[\text{Rh}(\text{CO})_2\text{Cl}]_2$ is subjected to a high pressure of carbon monoxide, $\text{Rh}(\text{CO})_3\text{Cl}$ is formed^{133,134}. The ir spectrum of this species has bands at 2107, 2072 and 2030 cm^{-1} . Very similar bands were detected when carbon monoxide was adsorbed on $\text{Rh}/\text{Al}_2\text{O}_3$ ¹³² or Rh/SiO_2 ¹³³, suggesting a small amount of $\text{Rh}(\text{CO})_3$ was present. When $[\text{Rh}(\text{CO})_2\text{Cl}]_2$ was deposited on SiO_2 and then exposed to carbon monoxide the tricarbonyl was again reported to form. Similar species, with their three ir active carbonyl bands, have also been reported in molybdenum¹³⁵ and manganese¹³⁶ complexes.

Each of the three types of carbon monoxide present on rhodium appear to have different reactivity, as would be

expected from their differences in bonding, however there seems to be some dispute as to which is the most reactive.

Tanaka³² and Fujimoto²¹ both report that the bridged carbon monoxide reacts with hydrogen before the linear does, and that the gem carbon monoxide desorbs from the surface without reacting. Zhang¹²⁰, on the other hand, states that the activity with respect to both hydrogen and oxygen decreases in the order:

gem > linear > bridged

When hydrogen is present, under reaction conditions, only linear carbon monoxide can be detected on the surface, and this appears at a lower frequency than before^{32,137-139}. This shift to lower frequency may be due to the formation of a carbonyl-hydride species^{138,139}, or may simply be a consequence of the low concentration of carbon monoxide on the surface³².

The presence of hydrogen appears to have little effect on the adsorption of carbon monoxide at room temperature¹⁰⁶, although a low temperature repulsion between coadsorbed carbon monoxide and hydrogen results in their segregation on Rh (111) faces¹¹⁶. This is in contrast to the enhanced adsorption which has been observed on various other metals¹⁴⁰. Carbon and oxygen, on the other hand, have a rather profound inhibitory effect on the adsorption of

carbon monoxide¹⁰⁶. Due to carbon laydown during the initial period of the reaction, as little as 29% of the amount of carbon monoxide initially adsorbed, can be adsorbed on the rhodium catalysts in the steady state¹⁴¹.

The effect of oxygen is more complex, being different for the different carbon monoxide species. Both the presence of oxygen and pre-oxidation of the catalyst surface reduce the amount of linear and bridged carbon monoxide on the surface, but appear to have little effect on the gem carbon dioxide present^{83, 118, 132, 142}. Only the bridged and linear forms of carbon monoxide have been reported to react with oxygen to form carbon dioxide¹²⁴. This may be due to the inability of the gem sites to coordinate two carbonyl groups and an oxygen atom. The linear and bridged sites have been reported to adsorb oxygen whilst the gem sites did not⁸³ but this effect appears to be dependent on the metal precursor used⁸².

Many factors appear to affect the amounts of the various forms of carbon monoxide present on the surface. The dispersion of the catalyst is perhaps the most important factor, but the reduction temperature can also have a substantial effect. As the temperature of reduction is increased, the amount of gem carbon monoxide which is observed decreases with respect to the other species^{124, 143, 144}. However, when the length of reduction is increased the gem peak is unaffected, whilst the linear

peak increases and the bridged falls⁴⁹. An increase in the adsorption temperature also promotes the formation of gem carbon monoxide³². This appears to be an activated process which will only occur above 170K¹²³. There has been a great deal of debate in the recent literature as to whether gem carbon monoxide is adsorbed on a metallic Rh⁰ or a Rh⁺ site.

As discussed earlier, the presence of oxygen^{116,132} or water^{69,85} appears to stabilise the gem carbon monoxide and promote its formation, whilst hydrogen¹⁴² has the opposite effect. This suggests that a partially oxidised surface⁸⁹, as would be found after a low temperature reduction, increases the concentration of the gem species on the surface^{49,88,143,144}. Even after a fairly rigorous reduction, some rhodium is found to be in a higher oxidation state¹⁴⁵, and it is at these sites that the twinned carbonyl is thought to be formed. The ratio of gem to linear carbon monoxide increased in the presence of an unreduced rhodium phase.

The structure of the gem species was first proposed because of the similarity of its ir spectrum to that produced by [Rh(CO)₂Cl]₂, yet in this complex rhodium is in the 1+ oxidation state.

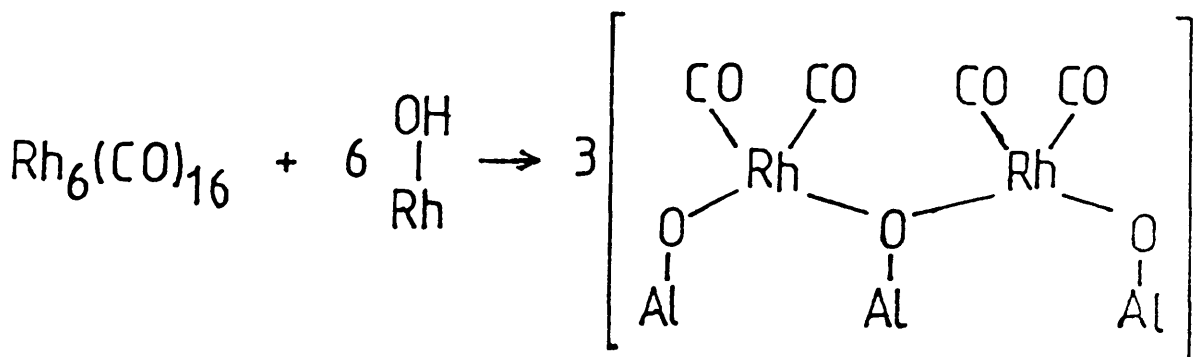
When Rh³⁺ ions were deposited on either Al₂O₃¹²² or zeolites¹⁴⁶, the rhodium was reduced by carbon monoxide to

form $[\text{Rh}^{\text{I}}(\text{CO})_2]^-$ species, which had an identical ir spectrum to that of the gem species on $\text{Rh}/\text{Al}_2\text{O}_3$. $\text{Rh}^{\text{I}}(\text{CO})_2$ has also been formed by the decarboxylation of $\text{Rh}_6(\text{CO})_{16}$ clusters¹⁴⁷.

XPS studies¹⁴⁸ have provided more evidence for the existence of $\text{Rh}^{\text{I}}(\text{CO})_2$ on $\text{Rh}/\text{Al}_2\text{O}_3$ catalysts, these species are thought to form at the edges of 2-dimensional rhodium rafts.

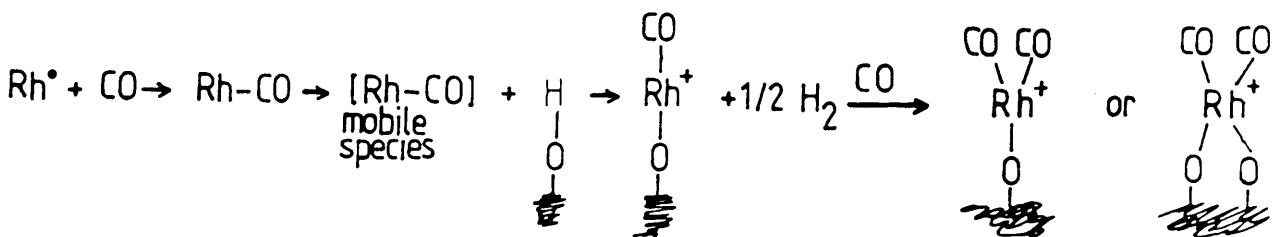
Prinet⁴⁸ and several other groups¹²¹ have suggested that these positively charged sites are produced by the oxidative dissociation of carbon monoxide. Others disagree, and report the importance of hydroxyl groups in the formation of gem carbon monoxide¹⁴⁸.

Smith et al¹⁴⁷ have investigated the behaviour of $\text{Rh}_6(\text{CO})_{16}$ clusters supported on Al_2O_3 , SiO_2 and MgO . They have found that when the support is impregnated in air the doublet due to gem carbon monoxide appears immediately following the adsorption of carbon monoxide. However, when the impregnation takes place in vacuo, both bands due to carbon monoxide adsorbed on metallic sites at 2065 cm^{-1} and 1800 cm^{-1} , and the gem doublet appeared. Dehydration of the support prior to impregnation or reduction of the catalyst in hydrogen, produced a spectrum which contained only the "metallic" bands, although the gem bands reappeared after treatment with water or oxygen. These results, the authors suggest, are due to the formation of $\text{Rh}^{\text{I}}(\text{CO})_2$ species on the surface by the route shown below:



Hydrogen was found to desorb at high temperatures. Other groups¹⁴⁴ examining more conventional Rh/SiO₂ and Rh/Al₂O₃ catalysts came to very similar conclusions. They found that as the concentration of gem carbon monoxide (as measured by ir spectroscopy) increased, that of the non-hydrogen bound hydroxyl groups on the surface fell. This process was faster on the Al₂O₃ support, which contained more hydroxyl groups, than on the SiO₂¹⁴⁷. The presence of hydrogen appeared to reverse this process, increasing the concentration of the hydroxyl groups and the linear carbon monoxide, whilst simultaneously reducing that of the gem species, although the effect of hydrogen appeared to be dependent on the dispersion of the catalyst, being greatest when the dispersion was low. This, the authors believe, suggests the need for metallic spillover sites, if the hydrogen is to reduce and aggregate the Rh^I species which were formed by interaction with the hydroxyl group.

The process, which is strongly activated, is thought to go via the route shown overleaf.



However alternative views on the centres for twinned carbon monoxide also exist. Yates et al^{28,121,122}, for instance, believe that the gem carbon monoxide is formed on isolated Rh⁰ atoms or Rh⁰ atoms with a very low coordination number, such as those on the edge of metallic rafts. Although it has been suggested that, because of their very low coordination numbers, these sites possess a slight positive charge⁵.

A number of groups have reported that the adsorption of carbon monoxide on to supported rhodium catalysts, results in the disruption of the small rhodium particles, and the formation of isolated Rh^I(CO)₂ species^{143,149-151}.

Of all the techniques available to the catalytic chemist EXAFS (Extended X-ray Adsorbance Fine Structure) spectroscopy has proved the most useful in this area. This technique measures the interaction between neighbouring surface species and especially those of neighbouring rhodium atoms, providing information on the short range ordering of the surface as well as the average Rh-Rh bond length and coordination number¹⁴⁹. Carbon monoxide may disrupt the Rh-Rh bonds of metal particles because of the relatively high energy of the Rh-CO bond (185 kJmol⁻¹) compared to that of

the Rh-Rh bond (44.5 kJmol^{-1}). The extent of disruption depends on the size of the metal particles¹⁵¹. Small particles of less than 1 nm can be broken up completely by the action of carbon monoxide. However, larger particles are disrupted less because the above mechanism releases insufficient energy to break all of the Rh-Rh bonds which are present in the crystallite. This disruption can also occur when no gas phase, only adsorbed, carbon monoxide is present, although, under these conditions the process will only occur rather slowly¹⁴³.

Similar phenomena have been reported for platinum and palladium catalysts where the dissociative adsorption of hydrocarbons has also been reported to disrupt the metal particles¹⁵⁰.

While even very small amounts of NO have been found to greatly accelerate the disruptive process which carbon monoxide produces¹⁵², temperatures above 175°C , particularly in the presence of hydrogen¹⁵³, have been found to result in the re-agglomeration of the monomeric $\text{Rh}^{\text{I}}(\text{CO})_2$ species. This aggregation to form large metallic clusters is probably concentrated at faults and defects in the support.

1.3.3 THE ADSORPTION OF CARBON DIOXIDE ON RHODIUM CATALYSTS

The very slight extent to which carbon dioxide can be adsorbed on rhodium catalysts has led some groups to report

that it is not adsorbed at all^{12,111}. Yet carbon dioxide can be hydrogenated at a much faster rate³² and with a much lower activation energy than carbon monoxide. This is a direct consequence of its weak adsorption. Since carbon dioxide is much less strongly held by the catalyst than carbon monoxide, a higher concentration of hydrogen can develop on the surface as carbon dioxide cannot block adsorption sites to the same extent as carbon monoxide. This, therefore increases the rate of the reaction compared to that of carbon monoxide hydrogenation where the concentration of hydrogen limits the rate.

Carbon dioxide has been reported to dissociate to a slight extent on rhodium, but only at elevated temperatures or pressures^{138,154}, giving rise to an ir spectrum which consists of bands due to carbonate species and linear carbon monoxide.

No gem carbon monoxide has been detected from carbon dioxide dissociation and the linear band appears at lower wavenumbers (2020 cm^{-1}) than is observed with carbon monoxide adsorption¹⁵⁵. These observations have been explained by the formation of a $\text{Rh}(\text{CO})(\text{H})$ species on the surface¹³⁸. Although others have suggested that the shift in the linear peak is simply due to the very low concentration of carbon monoxide which is present¹⁵⁵.

Both the presence of hydrogen and of boron impurities

in the rhodium promote the dissociation of carbon dioxide on rhodium catalysts¹³⁸, as does elevated temperatures¹⁵⁵.

Hydrogen enhances the amount of carbon dioxide which is adsorbed by the catalysts, mainly due to the formation of formate ions on the support³⁷. This is an activated process, and very dependent on the catalyst support. The formates are either formed by the spillover and reaction of activated hydrogen with carbon dioxide adsorbed on the support, or by the reaction of hydrogen and carbon dioxide on the rhodium itself. Since formates are known to decompose on rhodium¹³⁸, the former process appears to be more likely.

1.3.4 THE ADSORPTION OF OXYGEN ON RHODIUM CATALYSTS

Oxygen has a number of important effects on the behaviour of supported rhodium catalysts. It can affect both the dispersion¹¹⁹ and the oxidation state⁹⁰ of the metal particles which are formed. It can also control the way in which carbon monoxide bonds to the catalyst surface and appears to bring about a partial reversal of the so called SMSI behaviour.

As H:Rh and CO:Rh ratios of greater than unity have been obtained from the adsorption of these molecules on to rhodium catalysts⁹⁹, it is now widely agreed that these experiments do not provide an accurate method of determining

the dispersion of a supported catalyst. Some, however, have suggested that hydrogen-oxygen titrations may provide more useful results¹⁵⁶.

On reduction, rhodium catalysts consist of two distinct types of metal particles³⁰, the relative proportions of which change with the catalyst and the conditions. The first type of particle is very small and easily oxidised / reduced, whilst the second is larger and more difficult to oxidise / reduce. Conesa et al³⁵ have shown that after a low temperature reduction 65% of the rhodium can be oxidised whilst, after a higher temperature reduction, only 15% will oxidise. This suggests that hydrogen / oxygen titrations must be carried out very carefully to avoid a more than superficial oxidation of the smaller particles.

Oxygen adsorption proceeds by a very fast adsorption on to both the metal and its support¹⁰⁰, followed, especially at high temperature, by a slower bulk oxidation of the metal particles. Rh_2O_3 formation can occur with as little as 10^{-2} torr of oxygen present¹⁵⁷. It has been reported to form preferentially on the high index planes of rhodium catalysts.

Gorodetskii⁹⁶ has observed both molecular and dissociated oxygen molecules on rhodium catalysts, but only the dissociated oxygen reacts with hydrogen atoms to form water. In the presence of hydrogen, the adsorbed oxygen

tends to form into isolated islands and it is at the edge of these islands, or on stepped surfaces, that the water formation reaction is most active. Reaction of the bulk rhodium oxide with hydrogen has also been reported at high temperatures.

The strength of oxygen adsorption appears to be a function of the acidity of the catalyst support⁸¹. Acidic supports such as Al_2O_3 adsorb oxygen very strongly, while more basic supports such as ZrO_2 do not. The amount of oxygen adsorbed by some catalysts has been reported to decrease as the adsorption temperature is increased.

Although pre-adsorbed oxygen reacts very quickly with carbon monoxide to form carbon dioxide⁸², the effect of pre-adsorbed carbon monoxide on oxygen adsorption appears to be dependent on the metal precursor used. When $\text{Rh}(\text{NO}_3)_3$ is used as the precursor, oxygen is adsorbed and carbon monoxide simultaneously displaced. Rh_2O_3 , however, again adsorbs oxygen but then desorbs carbon dioxide. Catalysts formed from RhCl_3 do not adsorb any oxygen at all. These effects were reported as being due to differing metal particle geometries and/or precursor residues on the surface. $\text{Rh}_6(\text{CO})_{16}$ clusters supported on zeolites have been shown to decarboxylate under the influence of oxygen without any loss of the cluster structure¹⁴⁵.

Under reaction conditions, there should be very little oxygen in contact with the catalyst surface, yet Na^+ ion

promoters appear to increase the catalytic yield of oxygenates through the stabilisation of oxygen atoms on the surface¹⁴. These oxygen atoms are probably formed through the dissociative adsorption of carbon monoxide as adsorbed carbon and oxygen atoms. This oxygen is usually removed from the surface by reaction with hydrogen or carbon monoxide to form water or carbon dioxide. However, when its concentration builds up on the surface, it can deactivate reactions such as carbon monoxide oxidation^{158,159}, this is especially important at high temperatures when the concentration of carbon monoxide is low.

Water too has a role to play in both the reversal of the SMSI state⁴⁹ and in the formation of gem carbon monoxide¹⁴⁷. It is adsorbed on a rhodium surface via a weakly held precursor state¹⁶⁰, which increases in concentration until a complete monolayer is formed. As the concentration is further increased multilayer adsorption is observed but unlike on other metals such as iron, water does not dissociate on rhodium unless boron impurities are present.

1.3.5 THE ADSORPTION OF SIMPLE OXYGENATES ON RHODIUM CATALYSTS

While a great deal of work has been reported concerning the adsorption of carbon monoxide on rhodium catalysts, relatively little is known about the adsorption of the

oxygenates and hydrocarbons which are formed during carbon monoxide hydrogenation over these catalysts. Yet it is of interest to investigate the adsorption of these molecules because, if the principle of microscopic reversibility is to hold true, it should be possible to produce the same intermediates whether we adsorb the reactants or the products.

Methanol is adsorbed on the Rh (111) face at 100K¹⁶¹ with an initially high sticking coefficient which decreases slightly as monolayer coverage is approached. The adsorbed species appear to consist of a condensed layer of molecules which are only very weakly held, a physically adsorbed layer and two different chemisorbed states. The chemisorbed states are those of the initial dissociative adsorption to form methoxy groups on the surface and the more weakly held associatively adsorbed molecules. The methoxy groups which are formed were not found to be stable, either being hydrogenated to methanol or decomposed to adsorbed carbon monoxide and hydrogen. The molecules appeared to be randomly adsorbed, showing no long range ordering on the surface.

The adsorption of methanol and ethanol on nickel¹⁶², palladium¹⁶³, aluminium¹⁶⁴ and iron¹⁶⁵ catalysts all produced unstable alkoxy groups which decomposed near room temperature.

Methanol and ethanol have also been reported to form alkoxy groups on Al_2O_3 ^{166,167} and SiO_2 ¹⁶⁸. These species appear to be more stable than those formed on the metal particles although at high temperature some decomposition was evident as well as the formation of formate or acetate species. On Al_2O_3 ¹⁶⁹ adsorption of these alcohols is thought to occur via the elimination of a molecule of water between the alcohol and a surface hydroxyl group. Iso-propanol, however, does not appear to form stable alkoxy groups owing to unfavourable interactions between the methyl groups and the surface.

Both formic acid¹⁷⁰ and formaldehyde^{39,171} have been found to decompose on supported rhodium catalysts to form carbon monoxide, carbon dioxide and hydrogen, although no "HCO" species have yet been identified¹⁷². The decomposition was found to be first order¹⁷⁰ but its extent was very dependent on the catalyst support. The Rh/TiO₂ catalyst was found to be two orders of magnitude more active than the Rh/MgO sample. Although the aldehydes and carboxylic acids are only very minor products, large amounts of formate species have been detected on many catalysts under reaction conditions¹³⁷. The ir spectra of formic acid on the various supports alone have been found to be identical to that on the supported catalysts¹⁷⁰ and indeed, formates have often been reported when no metal particles were present³⁸. This very strongly suggests that while formates are stable on the supports at low temperatures, at higher

temperatures, or when formed on the rhodium particles, they quickly decompose.

It should be stressed that because a species is detected on the catalyst surface it does not necessarily mean that it plays a major role in the reaction, the formate species being a case in point. These species are present in large amounts on the support but appear to have little effect on the catalytic activity. In fact, some workers have expressed the view⁵ that if an intermediate is stable enough to be detected in large amounts on the surface, then it is too stable to be an important intermediate in the catalytic reaction.

1.4 MECHANISMS

But why should rhodium prove to be a fairly active catalyst for carbon monoxide hydrogenation, forming a wide range of products, when similar elements are much less active and / or form only one major product ?

Vannice¹⁷³, whilst studying the formation of hydrocarbons over a variety of SiO_2 supported metals, found that a graph of the rate of methane formation as a function of the heat of adsorption of carbon monoxide (fig 1.2) produced a volcano shaped plot with cobalt at the top and rhodium half-way up the downward side.

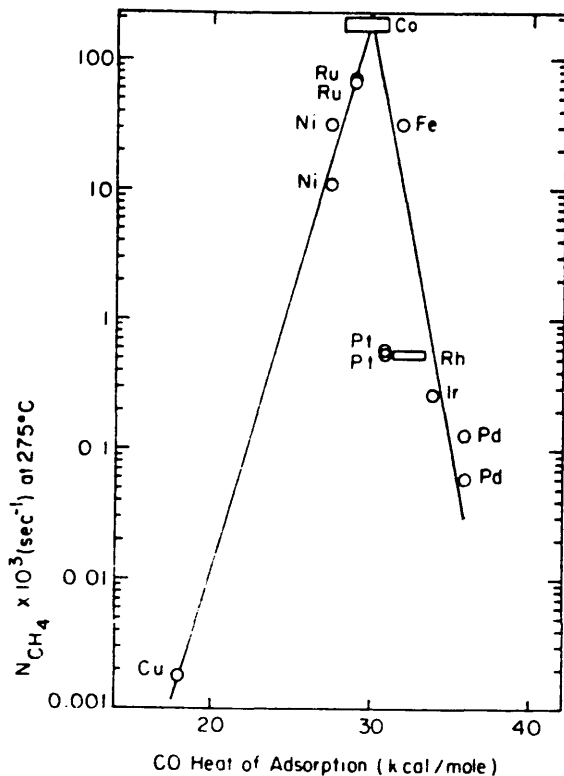


Fig. 1.2

In order to react, the carbon monoxide must interact fairly strongly with the metal, however, if it is held too tightly then reaction is impossible. Copper is a less active methanation catalyst than rhodium because its low heat of adsorption suggests that the carbon monoxide does not interact very strongly with its surface. Palladium, on the other hand, has a higher heat of adsorption than rhodium, and tends to hinder the reaction by interacting too strongly with the carbon monoxide. Rhodium, with a heat of adsorption of 132 kJmol^{-1} ¹⁹⁶ would, therefore be expected to show a reasonable activity.

The way in which carbon monoxide is adsorbed is also important. Metals such as cobalt, nickel and ruthenium

which are known to dissociate carbon monoxide very easily, form only hydrocarbons from syngas. Others, such as platinum, copper and palladium, which adsorb carbon monoxide associatively form only methanol.

This, and other evidence, strongly suggests that the hydrocarbon products of carbon monoxide hydrogenation are formed by the hydrogenation of some kind of surface carbonaceous species formed, in turn, from the dissociation of carbon monoxide⁶. Whilst methanol formation involves the hydrogenation of associatively adsorbed carbon monoxide molecules⁵.

The situation is more complex on metals such as rhodium or iron which adsorb carbon monoxide in both forms⁵. These catalysts have been shown to produce the widest range of products involving hydrocarbons and methanol as well as the higher oxygenates such as ethanol. If the first two mechanisms are correct then it is conceivable that the higher oxygenates are formed by the interaction of hydrocarbon producing sites, which dissociate carbon monoxide, and those which produce methanol; one site producing the hydrocarbon moiety of the molecule and the other the oxygen containing part.

Evidence for these mechanisms comes from a wide variety of sources, many involving the use of isotopic labels. When a 1:1 mixture of $^{13}\text{C}^{16}\text{O}$ and $^{12}\text{C}^{18}\text{O}$ was allowed to react over

Rh/TiO₂¹⁷⁴, very little scrambling of the labels was observed in the methanol formed. However, when the isotopic composition of the ethanol produced was examined¹⁷⁵, it was comparable with a completely dissociative mechanism.

During the initial non-steady state of these reactions there is a laydown of hydrocarbonaceous material on the surface¹¹⁴; this blocks many of the adsorption sites and results in a decrease in the overall catalytic activity and the production of hydrocarbons. If, however, the reaction mixture is then switched to a flow of pure hydrogen, vast amounts of methane can be produced, as well as a little ethane¹⁷⁶. The large amounts of methane formed, corresponding to sixty monolayers¹⁷⁷ or more, suggests that the carbonaceous residue is a polymeric material, which may be partially situated on the support. Methane can also be produced by the hydrogenation of surface carbon formed by the dissociation of carbon monoxide¹⁷⁸. In some cases the surface carbon has been shown to be preferentially hydrogenated even in the presence of gas phase carbon monoxide, but the reactivity of the carbon formed is very dependent on the conditions and the supports used^{114,184}.

The hydrogenation of surface carbon proceeds much faster than the steady state formation of methane from carbon monoxide and hydrogen^{86,179}, which implies that a high surface concentration of carbon monoxide has an inhibitory effect on the reaction rate.

Many workers have observed a large isotopic effect when deuterium is used instead of hydrogen^{22,25}. This strongly suggests that, under reaction conditions, the rate determining step involves the hydrogenation of a surface carbon containing species and that the surface concentration of hydrogen is rate limiting⁷¹. This conclusion is supported by the rate law of the reaction which is usually found to be first order in hydrogen and slightly negative in carbon monoxide²⁰. Supports which increase the amount of hydrogen at the surface, by increased spillover / reverse spillover, do tend to show a high activity²⁴. Vannice¹⁸ recognised a distinct compensation effect in the behaviour of a variety of catalysts where the activity was determined by a delicate balance between the surface concentrations of carbon monoxide and hydrogen.

Several groups have reported an initial induction period for the formation of higher oxygenates^{10,40,114}. This may be due to the formation with time of special sites for oxygenate formation or may be a consequence of the need to have the correct balance of carbon monoxide, hydrogen and CH_x species on the surface before these reactions can take place to any appreciable extent.

Methanol formation has been shown to be linearly correlated to the amount of extractable Rh^+ on the catalyst and some feel⁵ that the higher oxygenates may also be formed on the same charged sites, where carbon monoxide is

associatively adsorbed. Under most reaction conditions some $\text{Rh}^{\alpha+}$ is likely to be present on the surface. Supports and promoters which would be expected to stabilise these sites, have proved to produce catalysts with a high selectivity for oxygenates. Partial oxidation of the surface can increase this yield still further¹⁵. However, other groups have found no correlation between the oxidation state of the rhodium and the catalyst activity for higher oxygenates¹¹³. Some have even found that the amount of C_2 -oxygenates formed was inversely proportional to the amount of Rh^+ in the catalyst⁴⁴. Duprez et al⁹⁰, in fact, found that a partially reduced sample of $\text{Rh}/\text{Al}_2\text{O}_3$ produced no oxygenates at all, whereas a more thorough reduction procedure resulted in a significant yield of ethanol.

A large number of reaction schemes have been proposed to account for the experimental evidence which is available, some of which are listed below.

1. Dissociative adsorption of carbon monoxide and the hydrogenation of the carbon formed into various CH_x species.
2. The further hydrogenation and / or polymerisation of these CH_x species and their desorption as hydrocarbons.
3. The stepwise hydrogenation of molecular carbon monoxide and its desorption as methanol. However, this mechanism must take into account the fact that carbon monoxide is

adsorbed "carbon-down", yet methanol is desorbed from an "oxygen-down" state.

4. Carbon monoxide insertion into a CH_x species, possibly to form an alkyl intermediate which may then undergo a rearrangement to an alkoxide:-

- a) hydrogenation and desorption of the resulting species as a higher oxygenate.
- b) the dehydration and hydrogenation of the resulting species to form a hydrocarbon.

5. Addition of water into a surface carbene (ketene or oxinene) and then its further hydrogenation to form a oxygenate.

6. Addition of carbon monoxide into a surface carbene and its hydrogenation to form an oxygenate.

7. Polymerisation of methanol-like intermediates to form higher oxygenates.

8. Carbon monoxide insertion into methanol-like intermediates to form higher oxygenates.

9. Polymerisation of two molecules of carbon monoxide to form a C_2 -species, which can then be hydrogenated.

The mechanism which has perhaps attracted most attention is that of carbon monoxide insertion into a CH_x species^{60,180}. When ^{13}CO was added to the feed gas of some

steady state catalysts, the label appeared almost immediately in the aldehyde part of acetaldehyde¹⁸¹ but only appeared very slowly in the methane, methanol and ethanol which were also formed. Although this lends evidence to the carbon monoxide insertion theory, it also suggests that ethanol and acetaldehyde are formed by different routes¹⁰. Addition of acetaldehyde to the reaction mixture did not increase the production of ethanol. When ¹³C is deposited on the catalyst surface and then the reaction mixture changed to ¹²CO/H₂, the label quickly appears in the methyl group of both ethanol¹⁴ and acetaldehyde^{182,183}.

If the C_x hydrocarbons and the C_{x+1} oxygenates are considered as being formed from a common intermediate, then the distribution of products formed, is found to be very close to that predicted by the Schulz-Flory Distribution function¹⁷⁵. This equation assumes the one-by-one addition of monomer units onto a growing polymer chain and a constant probability of chain growth. Agreement is less exact when the distribution of carbon atoms in the products is simply used directly.

When palladium catalysts, which normally produce only methanol, were supplied with CH₂ units from CH₂Cl₂, fairly substantial amounts of ethanol were formed¹⁸⁴. This implies that it is the shortage of CH_x units on the surface of palladium catalysts which do not dissociate carbon monoxide readily, that accounts for their very limited production of

higher oxygenates. Rhodium can dissociate carbon monoxide and, under normal conditions, has little shortage of CH_x units. However, if labelled CH_2 units are supplied¹⁸⁵ (from CH_2Cl_2 but not from CH_3Cl) the label appears in the methyl group of ethanol.

If the insertion of a molecule of carbon monoxide into a CH_x species is the correct mechanism, what are the reaction sites and the surface intermediates for higher oxygenate formation ?

Several groups believe^{44,71} that rhodium catalysts are bifunctional in nature, in that hydrocarbons are formed from carbon monoxide dissociation on metallic sites, while methanol is produced on rhodium ions. The higher oxygenates are then thought to form from the insertion of carbon monoxide, at a Rh^+ site, into a CH_x species formed on a metallic site.

Evidence exists for an acetate-like intermediate in the formation of higher oxygenates¹⁸⁵. Most of the evidence for this species comes from the use of ^{18}O labelled carbon monoxide¹⁸³ - approximately 50% of the label was found to have exchanged in the higher oxygenates. This suggests an acetate type species where one of the oxygens comes from the support^{183,185} and the other from the carbon monoxide. Both acetate and acetyl species have been reported on the surface of rhodium catalysts¹⁸⁶. Other workers, however, suggest that the observed scrambling need not come from an acetate

intermediate¹⁷⁷, but may be due to exchange with the surface hydroxyl groups¹⁸⁷, or through the occurrence of several reversible steps.

Formate species have also been detected on some catalysts during the reaction of carbon dioxide¹³⁷ and hydrogen, and on Al_2O_3 ¹⁸⁸ during the hydrogenation of carbon monoxide. However since this species is only formed on some supports and quickly reaches a high but constant concentration, it is assumed to be present on the support and to play little part in the reaction. Formates³⁹ are known to dissociate very easily on rhodium catalysts. The formation of oxygenates by the addition of carbon monoxide into a surface carbene can be neglected as it would imply a common intermediate for both the C_x hydrocarbons and oxygenates and this is not found to be the case¹⁷⁵. The addition of labelled methanol to a Rh/TiO_2 catalyst did result in the formation of a small amount of ethanol from methanol homologation¹⁸⁹. However, since 90% of the ethanol was formed from carbon monoxide hydrogenation, methanol is unlikely to be an important intermediate in these reactions (mechanisms 7 & 8).

Although many groups have tried to identify reaction intermediates on the surface¹⁷², this work has proved very difficult. Lin et al¹⁹⁰, however, using the rather novel technique of pulsed laser atomic probe imaging, claim to have direct evidence of surface carbon, CH , CH_2 and CH_3

species on the surface of a rhodium crystal. This technique uses a laser to heat up a very small area of the crystal face causing any surface species to be desorbed; they are then analysed by a time of flight mass spectrometer.

As discussed earlier, both the support and any promoter present can have a marked effect on the catalyst behaviour. How they exert these effects is also an area of considerable discussion. Some suggest that the promoter and / or the support simply block certain sites and change the amounts and ratios of the surface species present^{60,63,71}. Others believe they interact with the adsorbed carbon monoxide, so as to promote dissociation⁷⁵, or interact with the reaction intermediates in such a way that their stability is altered¹⁴. A third group suggest that some supports and promoters interact with the rhodium crystals to produce new or more active sites^{73,187}. Rh^+ sites could, for instance, be formed from a metal oxide which was only partially reduced.

Although a great deal of effort has been directed towards the understanding of this system, many questions still remain to be answered before active rhodium catalysts can be produced for specific reactions.

CHAPTER 2

OBJECTIVES

The object of this study was to further the understanding of the catalytic action of supported rhodium in the hydrogenation of carbon monoxide, through a detailed examination of the adsorption characteristics of the reactants, and oxygenate products from, this reaction. Four different catalysts were used, 2% Rh/SiO₂, 2% Rh/Al₂O₃, 2% Rh/MoO₃ and 5% Rh/SiO₂ in these experiments to investigate the influence of both the oxide support and the metal loading on the catalysts characteristics.

To this end, both the separate and the competitive adsorption of carbon monoxide and carbon dioxide were investigated using FTIR spectroscopy, ¹⁴C-tracer experiments and pulse-flow adsorption, the influence of hydrogen and oxygen on the adsorption of these molecules was also examined. FTIR was used to study the adsorption of methanol, ethanol and acetaldehyde.

Where possible, as well as carrying out each of the above experiments at ambient temperature, each of the experiments was also repeated at elevated temperatures and under flow conditions, in order to mimic reaction conditions.

CHAPTER 3

EXPERIMENTAL

CHAPTER 3. EXPERIMENTAL

3.1 INTRODUCTION

Although modern science has developed a wide array of techniques to investigate the interaction of molecules at or with a surface, none is yet powerful enough to produce a complete picture of any particular system. In any catalytic study it has therefore proved necessary to use several complementary techniques, and so it is important at this point to consider why the various approaches used in the present work were chosen.

A direct monitoring technique which could be used to measure the adsorption of radiolabelled molecules was developed at Glasgow¹⁹¹ several years ago. While this approach produced a great deal of information regarding the adsorption processes occurring at the catalyst surface, it could provide no information on the chemical form of the surface species. The use of Geiger-Muller tubes in the system also meant that experiments could not be run above room temperature due to their temperature sensitivity. Some other means had, therefore, to be found to identify the adsorbed species.

Various groups have used temperature programmed desorption together with mass spectrometry to overcome this problem, attempting to analyse the various species which

desorb from the catalyst surface as the temperature is increased. This technique has produced some very interesting results, but has the inherent disadvantage, by its very nature, of disrupting the catalytic system.

In situ infra-red spectroscopy on the other hand allows the surface to be investigated in the steady state and under a fairly wide variety of conditions. Infra-red adsorption experiments can provide a wealth of information, not only regarding the surface species which are present, but also on how these species change with time and experimental conditions. In some cases information concerning the nature of the surface itself can also be inferred from infra-red data. However, unless very elaborate calibration measurements are made, infra-red data cannot be used to determine the absolute, or even the relative, amounts of the various species present on the surface.

Pulse-flow chemisorption techniques, especially those employing a mass spectrometer detection system, can provide a measure of the amount of material held on the surface under appropriate conditions. Since most of these systems are designed to work at atmospheric or higher pressures, under flow conditions, they provide a more realistic model of the adsorption processes taking place than direct monitoring techniques. They also have the advantages of being operational under a wide range of temperature and not being restricted to the adsorption of gases which can be

labelled with suitable radio-isotopes.

Temperature programmed reduction and desorption studies provide information on the number, chemical form and reactivity of surface species, although no detailed information on the form of the surface material without the use of a mass spectrometer, useful "fingerprint" data can easily be obtained.

3.2 MATERIALS

3.2.1 CATALYST PREPARATION

4.35g of $\text{RhCl}_3 \cdot 3\text{H}_2\text{O}$ (Johnson, Matthey and Co. Ltd.) were dissolved in distilled water and made up to 500ml. This solution was then used to prepare the catalysts employed in this study by the incipient wetness technique.

Enough RhCl_3 solution was added to an appropriate amount of the support material to produce a catalyst which nominally contained 2% w/w Rhodium. The slurry produced was then evaporated, with constant stirring to ensure an even distribution of the Rhodium salt. When almost dry, the catalyst was placed in a vacuum dessiccator for 24 hours, before being ground into a fine powder for use. As most of the supports used had a very large surface area and tended to adsorb atmospheric water, the catalysts were stored in an

oven at about 70°C when not in use.

The supports used in these studies were SiO₂ (Aerosil), Al₂O₃ (Degussa c), and MoO₃ (Koch-Light). Details of the catalysts and supports used are shown in Table 3.1. Each of the catalysts was prepared to be 2% w/w Rhodium, except for one 5% w/w Rh/SiO₂ sample which was used to investigate the effects of metal loading. The actual Rhodium content, listed in Table 3.1, was determined by atomic adsorption measurements. The total surface areas of the catalysts were calculated using the B.E.T. method of nitrogen adsorption at -196°C.

Table 3.1 Catalyst Composition

<u>Catalyst</u>	<u>%Rh w/w</u>	<u>Total Surface Area</u> (m ² /g)	<u>Average Particle Diameter From TEM</u>
Rh/SiO ₂	1.9	173.5	2.73 nm
Rh/Al ₂ O ₃	1.9	79.8	3.01 nm
Rh/MoO ₃	1.6	11.1	4.29 nm
Rh/SiO ₂	4.1	161.1	-
SiO ₂	-	210.4	-
Al ₂ O ₃	-	89.66	-
MoO ₃	-	6.66	-

3.2.2 GASES

Below is a list of all the gases used in this study together with their stated purities. All were supplied by B.O.C. Ltd. and were used without any further purification unless otherwise stated.

Table 3.2

He - 99.9%	pure	6% H ₂ in N ₂ - 99.9%	pure
CO - 99.5%	pure	6% H ₂ in Ar - 99.9%	pure
CO ₂ - 99.995%	pure	10% CO in He - 99.9%	pure
O ₂ - 99.5%	pure	33.4% CO in H ₂ - 99.9%	pure

The carrier gas was passed through a 5A molecular sieve trap and then through an acetone / dry ice bath to remove any moisture before entering the Fourier Transformed infra-red cell. All other gases entered the cell via the acetone / dry ice bath.

Carbon dioxide was added directly to the vacuum system described in section 3.3.1, but was further purified before use by a series of freezing - thawing cycles to remove any non-condensable impurities; two such cycles were usually sufficient.

3.3 DIRECT MONITORING TECHNIQUES

3.3.1 THE VACUUM SYSTEM

The apparatus consisted of the conventional glass vacuum system depicted in fig 3.1. The system was maintained at pressures of less than 10^{-4} torr by a mercury diffusion pump, backed up by a rotary oil pump. Each of the pumps was fitted with a liquid nitrogen cold trap, to protect against contamination.

Non-radioactive gases were added directly into the secondary manifold via tap F and were then stored in the 2 litre storage bulbs attached to the secondary manifold by means of 4mm taps. Radio-labelled gases were stored in the two adjacent 1 litre storage bulbs, both of which were fitted with side arms for the attachment of ampoules of ^{14}C labelled material. Small, controlled amounts of the various gases could be expanded, via tap T, into the reaction vessel (volume 352cm^3).

Small pressure changes within the reaction vessel were measured by a differential pressure transducer (SE Labs (EMI) Ltd. SE21/V) to within ± 0.0025 torr. The output from the pressure transducer was displayed graphically by a potentiometric chart recorder (Servogar 420). The pressure transducer was calibrated against the mercury manometer to allow absolute pressure changes to be measured.

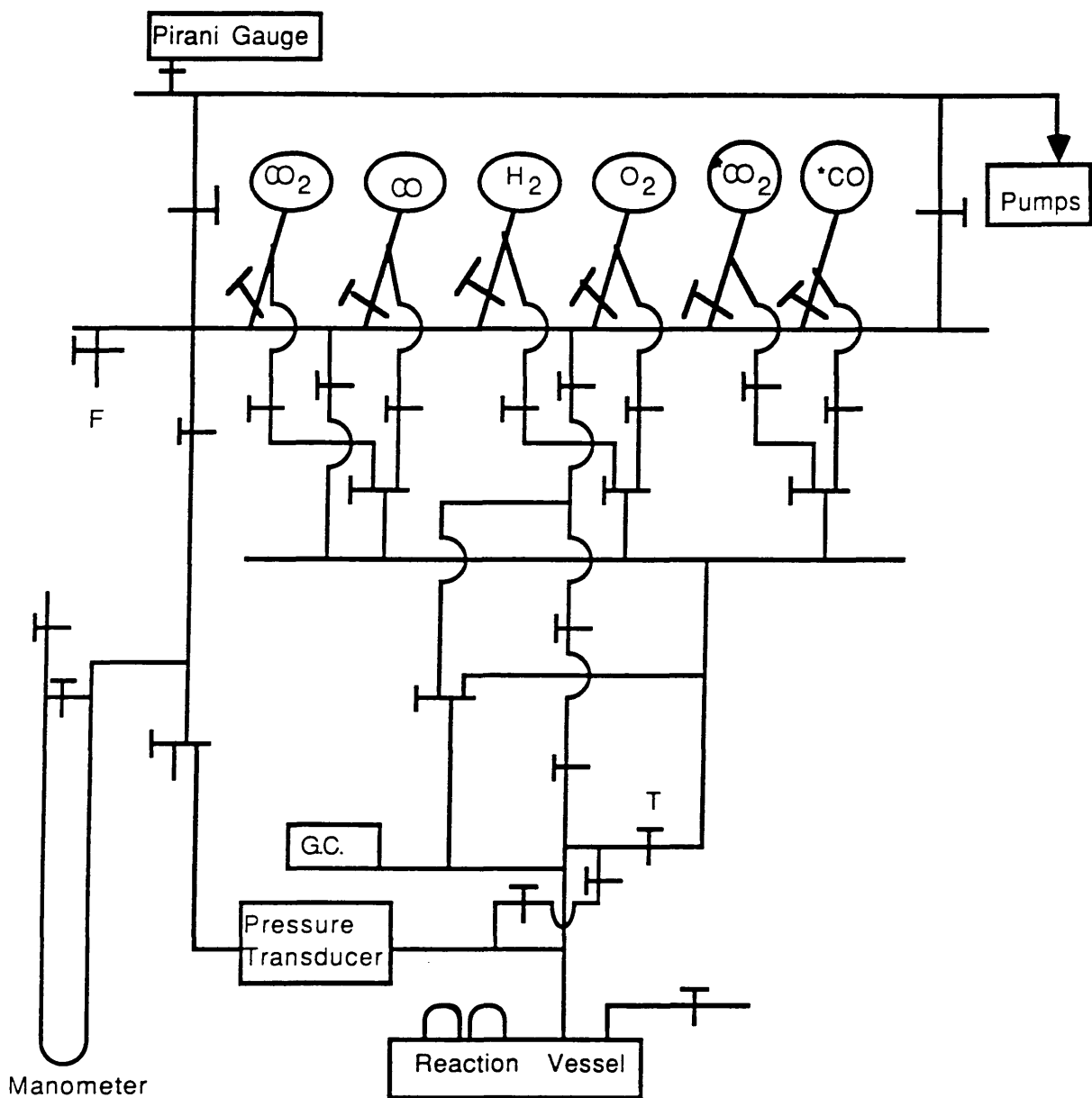


Fig 3.1 The Vacuum System

The reaction vessel was connected to the gas chromatograph - scintillation counter to allow analysis of the gas phase above the catalyst. It was also connected to the secondary manifold, via 4mm taps, to allow rapid and effective evacuation of the reaction vessel.

3.3.2 THE REACTION VESSEL

A diagram of the reaction vessel is shown in fig 3.2. It consisted of a glass vessel containing three B34 sockets together with a furnace region where the catalyst samples could be reduced "in-situ".

A B34 stopper was fitted into one of the sockets, this could then be removed for easy access into the reaction vessel. Two Geiger-Muller tubes, sealed by "Araldite" into B34 cones, were placed in the other sockets. Once in place the Geiger-Muller (GM) tubes were therefore positioned directly above the two equal sections of the catalyst boat.

The samples of catalyst were deposited in section 2 of the boat by slurring the sample with distilled water and then evaporating this slurry on to the walls of the boat. The catalyst was then moved into the furnace region of the vessel by means of an external magnet and the enclosed metal bar which was attached to the catalyst boat. The catalyst was reduced by a flow of 6% H₂ in N₂ and was maintained in this flow at 320°C overnight. The catalyst temperature was

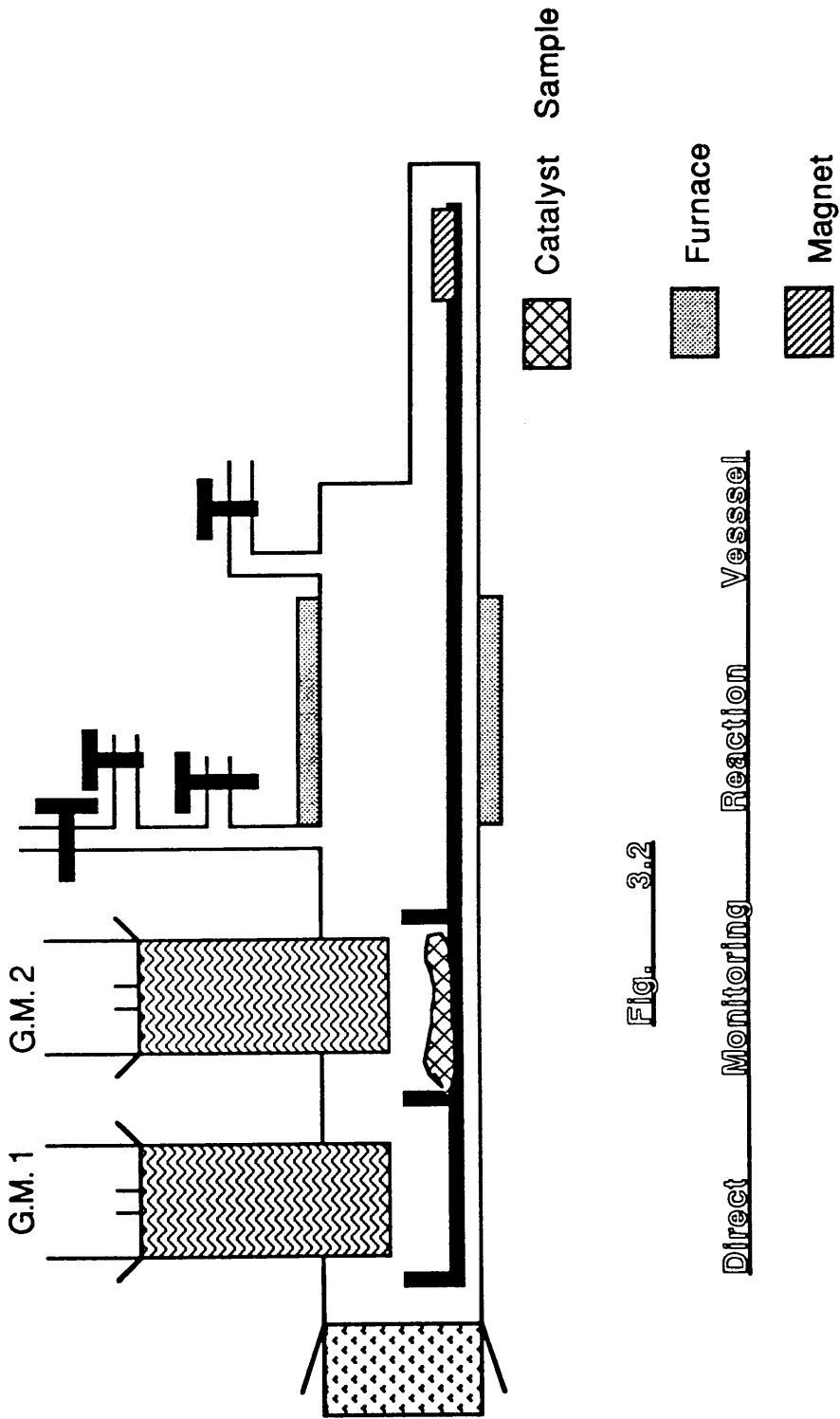


Fig. 3.2

Direct Monitoring Reaction Vessel

measured by a thermocouple embedded in the wall of the furnace region, very close to where the catalyst would be during the reaction procedure. The temperature of the furnace being controlled by a "Regulac" variable transformer.

After reduction, the boat was returned to its original position and the catalyst cooled under vacuum to ambient temperature. When small aliquots of ^{14}C -labelled gases were then admitted into the reaction vessel, GM2 measured any activity on the surface of the catalyst, together with that in the gas phase above, whilst GM1 measured only gas phase activity.

When a ^{14}C -polymethylmethacrylate source was placed in section 2 of the catalyst boat, no activity was detected by GM1 and vice versa, because of the glass dividing wall between the two sections.

If it is assumed that both GM tubes give identical count rates, the count rate of GM2 minus that of GM1 would be a direct measure of the amount of ^{14}C on the catalyst surface and so a measure of the amount of adsorption which has taken place. However, since the two GM tubes did not give identical count rates, several correction factors, detailed in the section below, had to be applied before any useful data could be obtained.

3.3.3 THE COUNTING SYSTEM

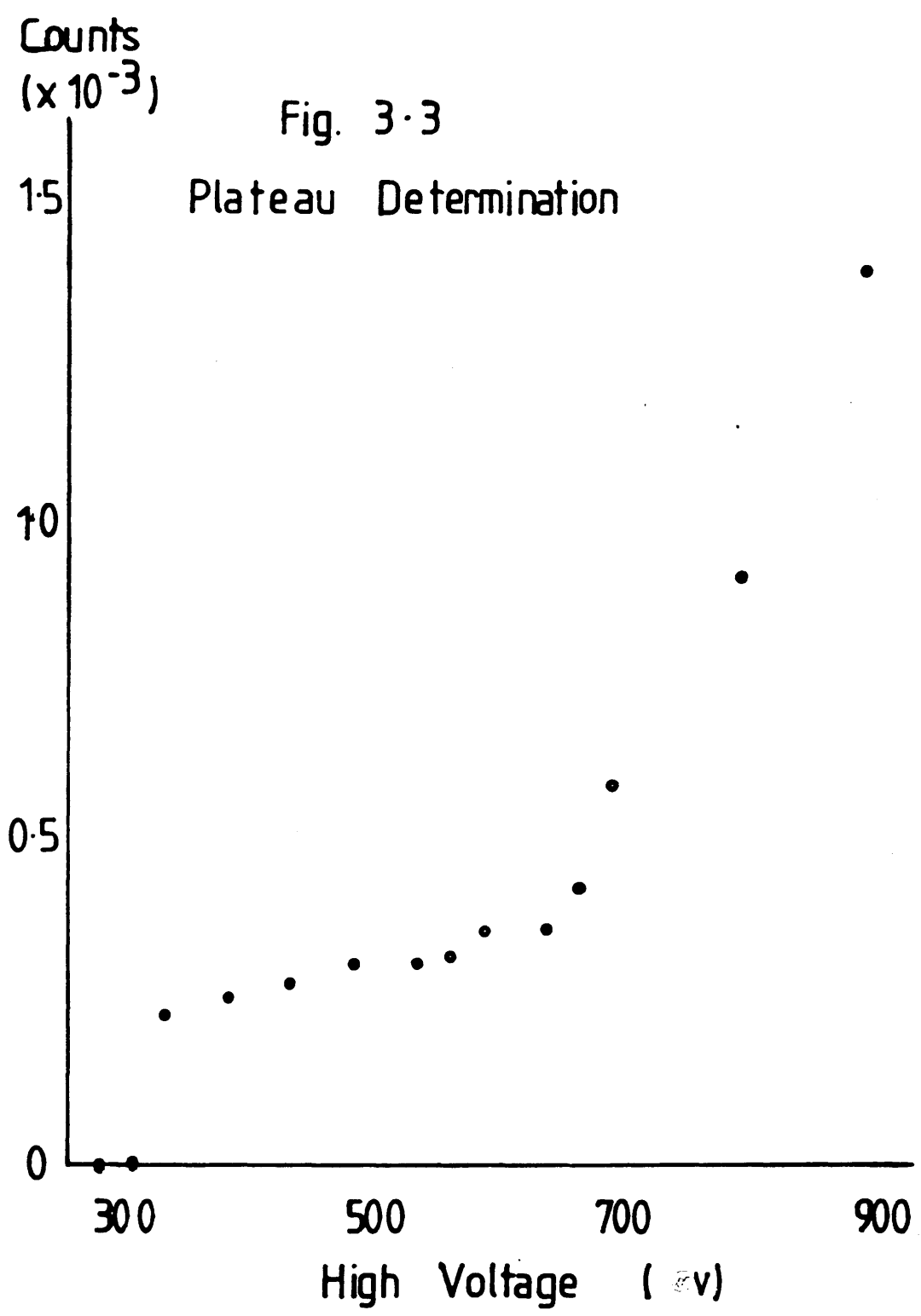
The GM tubes used in this study were the Mullard ZP1481 end window type, filled with a mixture of neon, argon and halogen. Each tube was connected to a Nuclear Enterprises Ltd. SR5 scaler rate meter.

3.3.3.1 PLATEAU DETERMINATION

The plateau region of the GM tubes is the region where the count rate is independent of any small variations (± 20 V) in the applied voltage.

This was determined by admitting a small amount of ^{14}C -carbon dioxide into the reaction vessel and then measuring the count rate as a function of the applied voltage, without any catalyst present. A typical result is shown in fig 3.3. The working voltage was then taken as being in the middle of this plateau region. It was found to be between 500 and 550 V depending on the particular tube used.

At the working voltage, any variations in count rate were found to be within those predicted by statistical error. Since nuclear disintegration is a completely random process, the standard deviation of the count rate is equal to the square root total counts. This means, of course, that the higher the count the lower the error on that



reading will be. In practice, since the radiolabelled gases used had fairly high activities, a counting time of only 300 seconds was sufficient to produce counts with individual errors of less than 3%.

3.3.3.2 BACKGROUND COUNT RATES

Background count rates were determined before each experiment and were subtracted from each reading. Background count rates were never more than 40 counts per minute (cpm) whilst experimental count rates were never less than 150cpm.

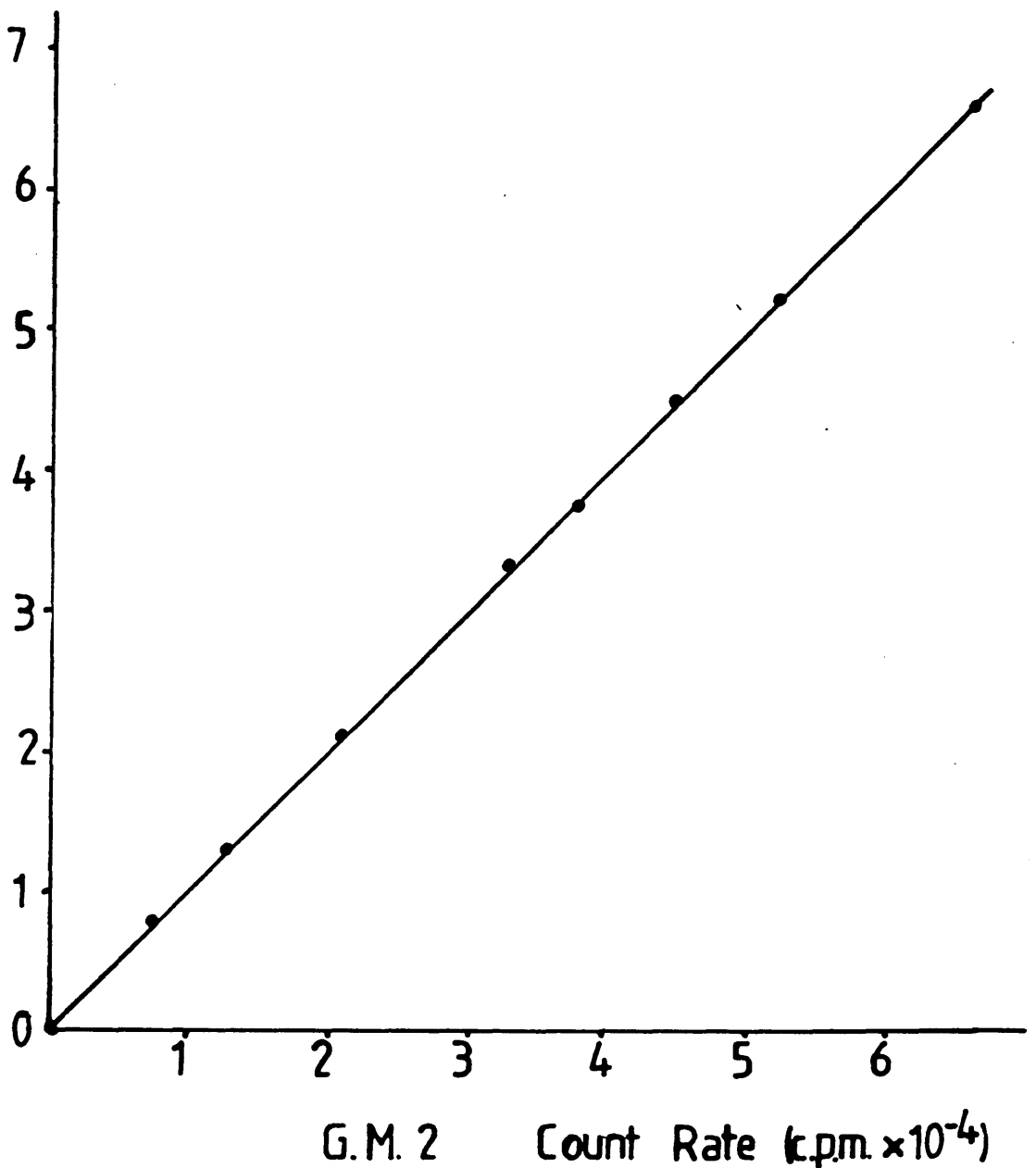
3.3.3.3 THE INTERCALIBRATION FACTOR

The direct monitoring technique outlined above is only valid when both GM tubes measure the same amount of radioactivity. Since the tubes were at slightly different heights above the catalyst and had different counting efficiencies, this was not the case. It was, however, a simple matter to determine an intercalibration factor which overcame these difficulties. This was done by admitting various amounts of radio-labelled gas into the reaction vessel with the boat, but no catalyst, in place and then analysing the count rates from both GM tubes. If the count rate of GM1 is plotted against that of GM2 (fig 3.4), the

The Intercalibration Factor Fig. 3.4

G.M. 1 Count Rate
(c.p.m. $\times 10^{-4}$)

Gradient = 0.971



gradient of the straight line which results is the intercalibration factor.

3.3.3.4 DEAD TIME CORRECTIONS

When radiation passes through a gas, some of its energy is absorbed by the molecules of that gas, causing them to ionise into positive ions and electrons. When an electric field is applied across the gas, these ions and electrons can be detected. The magnitude of the resulting current being proportional to the amount of radiation responsible for the initial ionisation.

This is the principle upon which GM tubes work. However, in commercial GM tubes, the applied field is so high that the resulting acceleration of the original ions and electrons, causes almost complete ionisation of all the gas in the vicinity of the anode. This means that the detector is incapable of measuring another event, until the anode potential has been generated again by migration of the cations to the cathode. This recovery, known as Dead Time, becomes increasingly important at higher count rates.

If N_t (sec^{-1}) is the true count rate, then it is related to the observed count rate (N_o) by equation 3.1.

Equation 3.1

$$N_t = \frac{N_o}{(t - N_o D)} \quad \text{where } D = \text{Dead Time} \quad (\text{sec}^{-1})$$

This can then be rearranged to give:

Equation 3.2

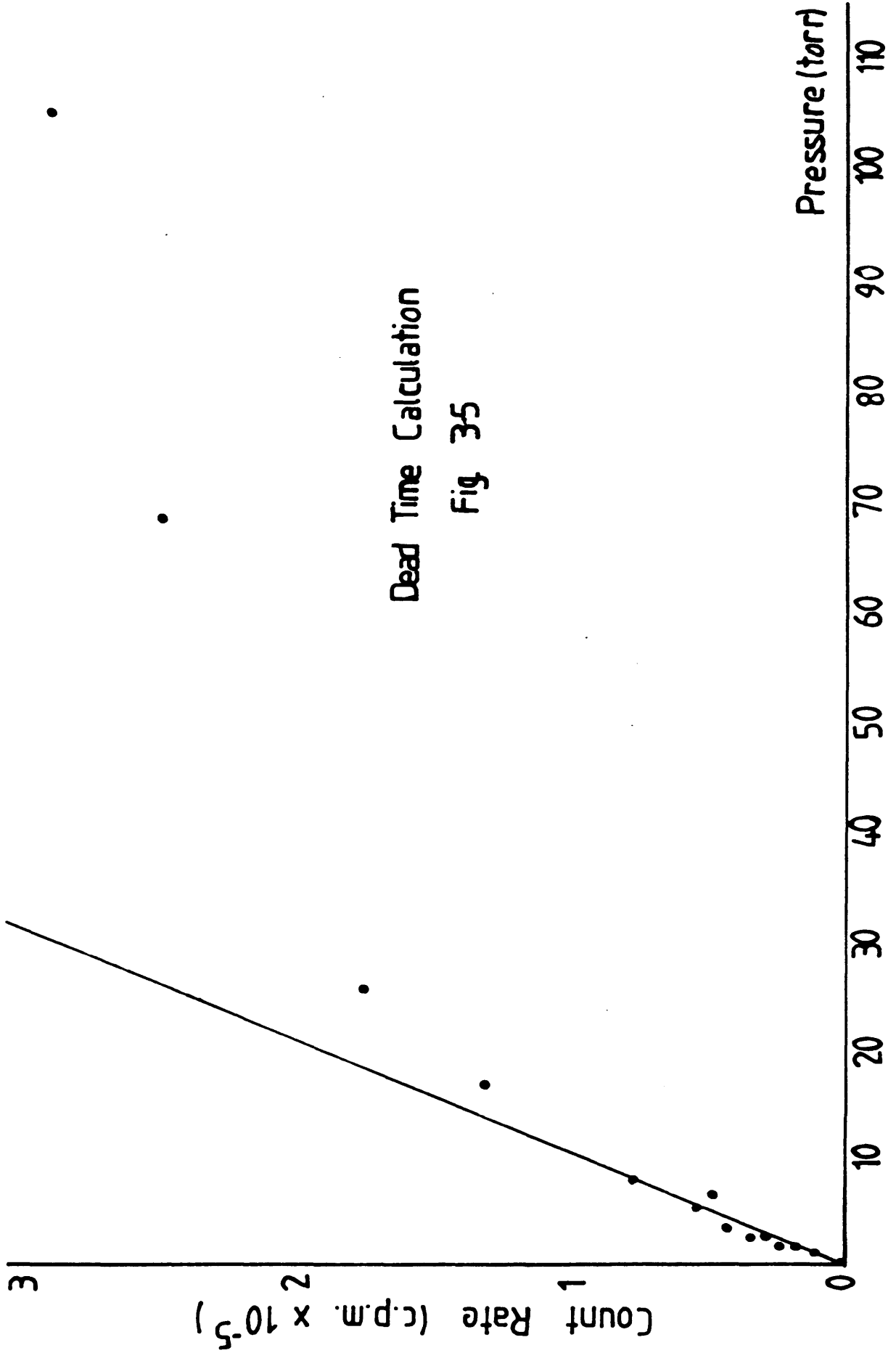
$$D = \frac{N_t - N_o}{N_t N_o}$$

To calculate D, the count rates measured for various amounts of ^{14}C - carbon dioxide, in the reaction vessel when no catalyst was present, were plotted against the amount of ^{14}C -carbon dioxide present. From fig 3.5 it can be seen that a linear relationship exists initially between the measured count rate and the amount of radioactive material in the system. But, as the count rate increases, the dead time starts to take effect and the curve deviates from the straight line relationship. This deviation, or $N_t - N_o$, can then be used to calculate the dead time of the counter. This was calculated to be approximately 5.137×10^{-4} sec, which compares very favourably with the manufacturers value of 5×10^{-4} sec. All count rates were therefore corrected according to equation 3.1.

3.3.4 THE GAS CHROMATOGRAPH AND SCINTILLATION COUNTER

3.3.4.1 THE GAS CHROMATOGRAPH

Analysis of the gas phase during adsorption experiments was carried out by a gas chromatograph (GC) connected to the reaction vessel by the gas sampling system shown in fig 3.6.



Dead Time Calculation
Fig 35

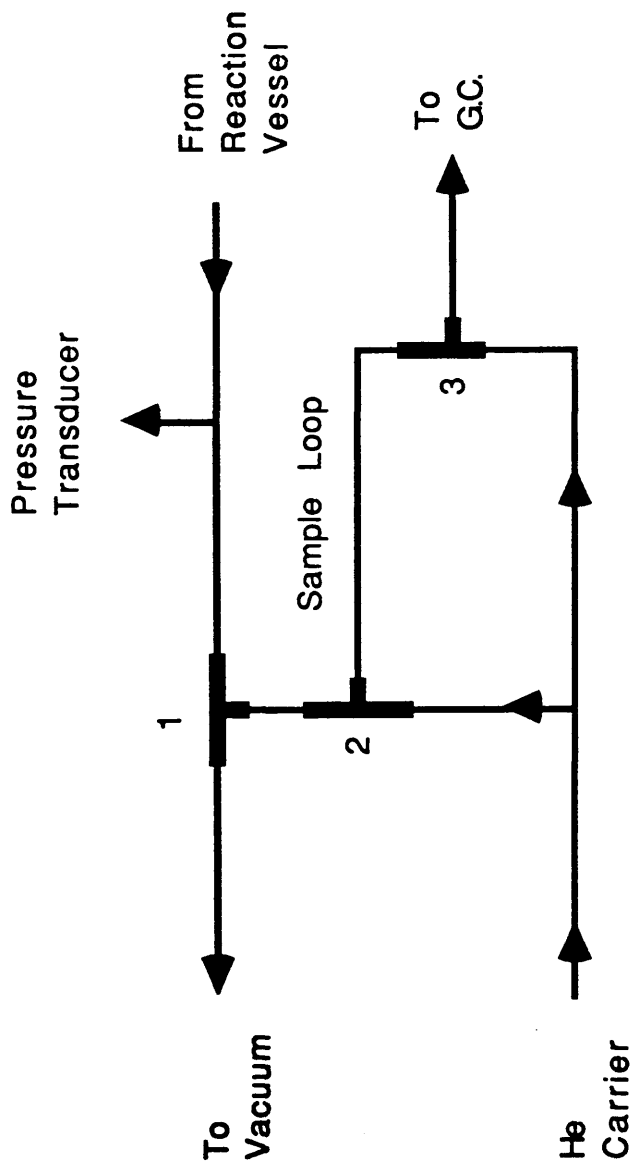


Fig. 3.6 Gas Chromatograph Sampling System

This was constructed from 1/8 inch stainless steel tubing and Whitey 3 way valves. It was connected to the secondary manifold and the reaction vessel by glass to metal seals.

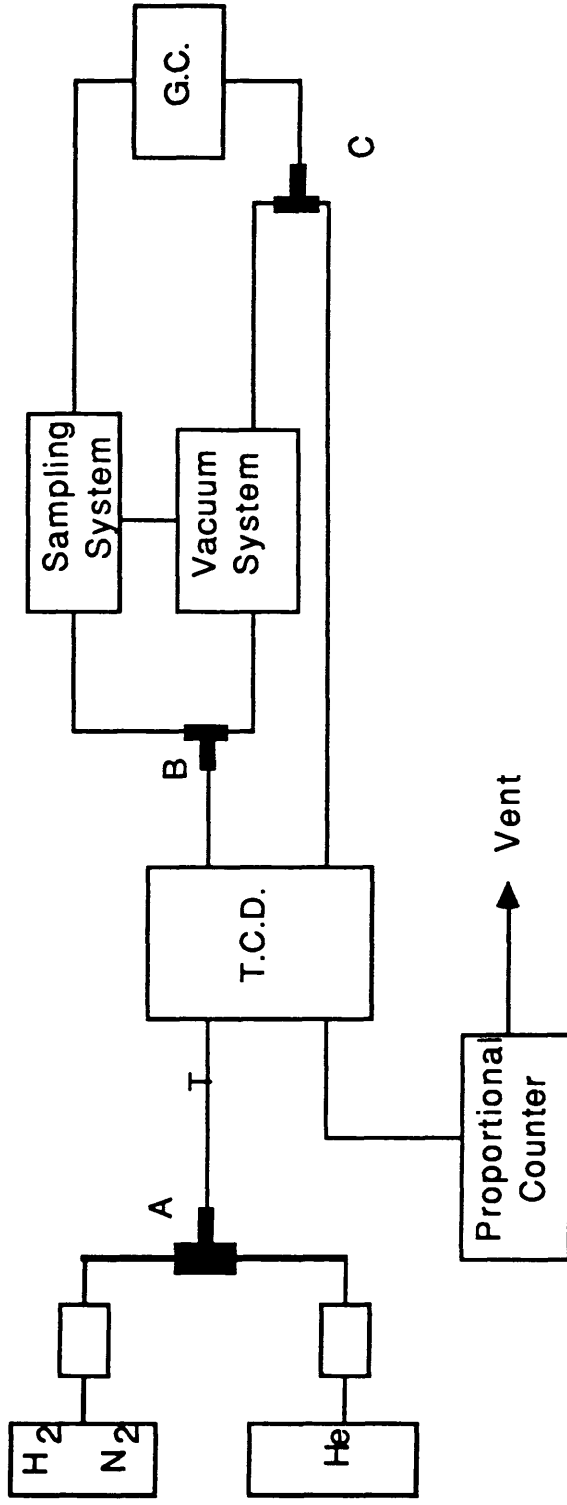
The 0.4ml sample loop was evacuated by manipulating taps 1 and 2. Further manipulation allowed the expansion of gas samples from the reaction vessel into the evacuated sample loop. The pressure of gas in the sample loop could then be measured by isolating the pressure transducer from the reaction vessel and connecting it to the sampling system.

Helium entered the system (fig 3.7) through Whitey Valve A, and then passed through a Negretti - Zambra flow control and needle valve which controlled the flow rate through the entire system. It then flowed through the reference arm of the thermal conductivity detector (TCD) and, if valve C was in its initial position, entered the GC column without passing through the sample loop. However, by simultaneously switching valves B and C, the helium flow could be diverted so that it flushed any gas in the sample loop onto the column. After leaving the GC column, the gases passed through the other arm of the TCD before flowing into the scintillation counter.

The reaction gas mixture was separated using a 6ft long, 1/8 inch o.d. stainless steel column containing 1.9065g of Carbosieve B (mesh 80/100). The gases were

Fig. 3.7

Schematic Diagram of Gas Flow System



3.3.4.2 THE SCINTILLATION COUNTER

The GC system was usually used in conjunction with a spiral cell gas flow scintillation counter (Isoflo - Nuclear Enterprises) which was operated at a voltage of 1088V. The cell (Type IIA - internal volume 200ul) consisted of a long coil of scintillating plastic tubing. The Isoflo was connected to an Apple IIc personal computer equipped with a dual disc drive, Apple monitor and Epson RX-80 printer. Nuclear Interfaces' Isomess 1m 2000 Single Trace Radio - Chromato - Graphic programme system was used to process and integrate the data produced by the scintillation counter.

3.3.5 PREPARATION OF LABELLED GASES

3.3.5.1 ^{14}C - CARBON DIOXIDE

Labelled carbon dioxide was produced by the action of dilute hydrochloric acid on a sample of Barium(^{14}C) Carbonate (Radiochemical Centre, Amersham), the specific activity of which was specified as being 5mCi. The carbon dioxide produced was dried over silica gel and magnesium perchlorate before being frozen at -196°C and pumped to remove any non-condensable impurities.

It was then divided into five equal portions, each with an activity of approximately 1mCi, by expansion into

evacuated glass ampoules. These provided a way of transferring the labelled gas into the evacuated storage bulb, via a break seal in the ampoule. The labelled carbon dioxide was diluted with ^{12}C - carbon dioxide to produce a more convenient pressure and specific activity.

3.3.5.2 ^{14}C - CARBON MONOXIDE

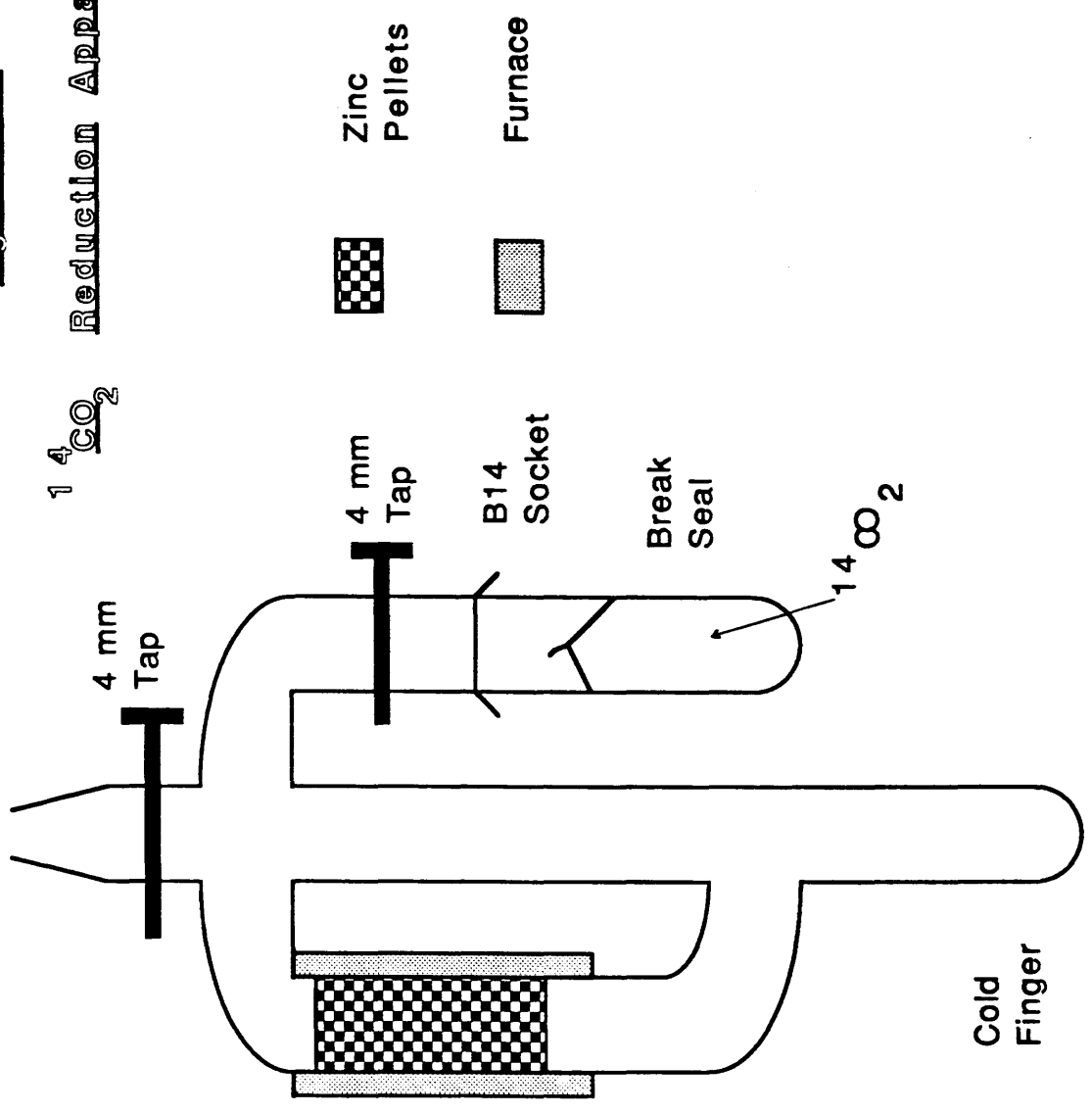
^{14}C - carbon monoxide was prepared by reducing the labelled carbon dioxide, obtained as described above, with metallic zinc. This was carried out in the apparatus shown in fig 3.8.

Zinc pellets, prepared from a moistened mixture of 95% Analar zinc dust and 5% Aerosil Silica, were loaded into one arm of the Pyrex reaction vessel and the whole system evacuated. The zinc pellets were then kept at 320°C for 24 hours, by the external furnace which surrounded them, while the system was pumped to remove any moisture present. After this period, the reaction vessel was isolated from the vacuum system and the ^{14}C - carbon dioxide contained in the ampoule expanded into the reaction vessel. Natural convection currents in the vessel then allowed the ^{14}C - carbon dioxide to circulate over the hot zinc pellets for 72 hours. Any unconverted carbon dioxide remaining after this period was frozen out before the ^{14}C - carbon monoxide produced was expanded into the storage bulb and was diluted before use.

To Storage Vessel

Fig. 3.8

Reduction Apparatus



3.3.6 EXPERIMENTAL PROCEDURE

3.3.6.1 REDUCTION OF CATALYSTS

Between 0.1 and 1g of the catalyst powder was loaded into the catalyst boat and carefully evacuated. Since all of the catalysts were in the form of very fine powders, rapid evacuation tended to blow the catalyst through the entire system and had to be avoided.

A cylinder of 6% H₂ in N₂ was connected to Tap F (fig 3.1) and the system arranged so that gas flowed through the secondary manifold, down into the reaction vessel and out via the vent. A simplified gas flow diagram is shown in fig 3.7.

The catalyst was placed in the furnace region and the temperature increased to 320°C. The catalyst was reduced overnight at this temperature under a 10mlmin⁻¹ flow of 6% H₂ in N₂. When the reduction was complete the H₂/N₂ flow was switched off, the catalyst evacuated and then cooled in vacuum to ambient temperature over a period of thirty minutes.

3.3.6.2 ADSORPTION ISOTHERMS

With the catalyst positioned under GM2, small aliquots of the adsorbate gas were admitted into the reaction vessel via a series of pressure reducing volumes, so that the

amount which entered the reaction vessel could be carefully controlled.

When adsorption was rapid, as when carbon monoxide adsorbed on Rh/Al₂O₃, the gas and surface count rates could be determined almost immediately. However, when adsorption was slower, an equilibrium period of at least 5 minutes was needed before any measurements were made. The count rate was determined over a period of 5 minutes. This counting time was not normally repeated unless the catalyst had not reached pseudo-equilibrium in this period.

This technique could also be used when the surface was already covered with another non-labelled species.

If, after building up a radio-labelled isotherm, a known amount of an unlabelled gas was admitted into the reaction vessel, the extent and rate of exchange could be measured by taking counts at regular intervals. When the surface count rate fell significantly, whilst that of the gas phase rose, exchange had taken place between labelled surface and unlabelled gas phase species.

At any time during an adsorption experiment, but usually at the end, a sample of the gas above the catalyst could be analysed by passing it through the GC and scintillation counter - the GC separated the various gases and determined how much of each was present, whilst the scintillation detected any ¹⁴C which was present.

3.3.6.3 DESORPTION MEASUREMENTS

After building up an adsorption isotherm the reaction vessel was opened to the vacuum, so that any gas phase or weakly held material was removed. After 30 minutes evacuation the surface count rate was again determined.

The catalyst boat could then be moved into the furnace region and, by manipulating Whitey valves A, B and C, a 20 mlmin⁻¹ flow of helium directed through the secondary manifold, over the catalyst surface and thence to the scintillation counter. Any radio-labelled material, which was removed from the surface over a 30 minute period, was therefore measured by the scintillation counter. If required, the catalyst sample could be returned to its original position and the surface count rate determined by the GM tubes.

With the catalyst in the furnace region the temperature was increased to 320°C, the reduction temperature, while the helium stream carried any desorbing species into the scintillation counter for counting. This technique, however, did not permit the identification of any of the desorbing species and the temperature programme was not sufficiently refined to give a detailed picture of the desorption process.

3.4 THE PULSE-FLOW MICROREACTOR (WITH GC-MS)

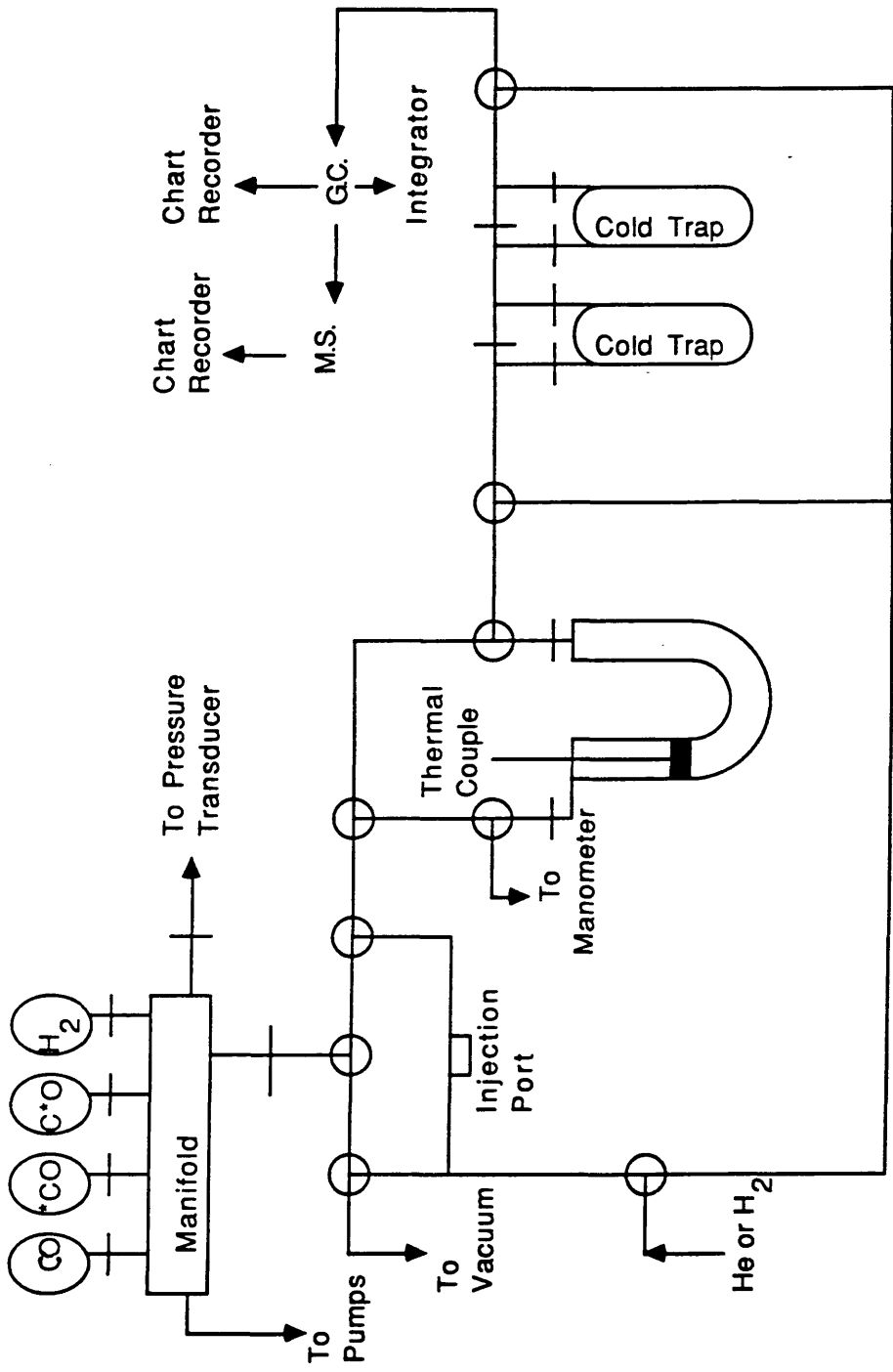
3.4.1 INTRODUCTION

The apparatus used in these experiments consisted of a conventional glass pulse-flow microreactor equipped with a GC and mass spectrometer (MS). The catalyst was reduced in situ before being saturated with pulses of carbon monoxide injected into the helium carrier gas. Analysis of the exit gases during the adsorption and thermal desorption of carbon monoxide was carried out by GC-MS.

3.4.2 THE PULSE-FLOW VACUUM SYSTEM

The vacuum system depicted in fig 3.9, consisted of a glass manifold, which could be maintained at less than 10^{-4} torr by a mercury diffusion pump, backed up by a rotary oil pump, both of which were equipped with liquid nitrogen traps. Four 2 litre storage bulbs were connected to the manifold via 4mm taps and contained heavy atom labelled and unlabelled carbon monoxide.

The manifold was also attached to a pressure transducer (Transamerican Instruments) and a mercury manometer, for the accurate measurement of the pressure within the system. This allowed gas mixtures of known pressure and composition to be made up in the manifold, samples of which could be expanded into the attached sample loop (fig 3.10).

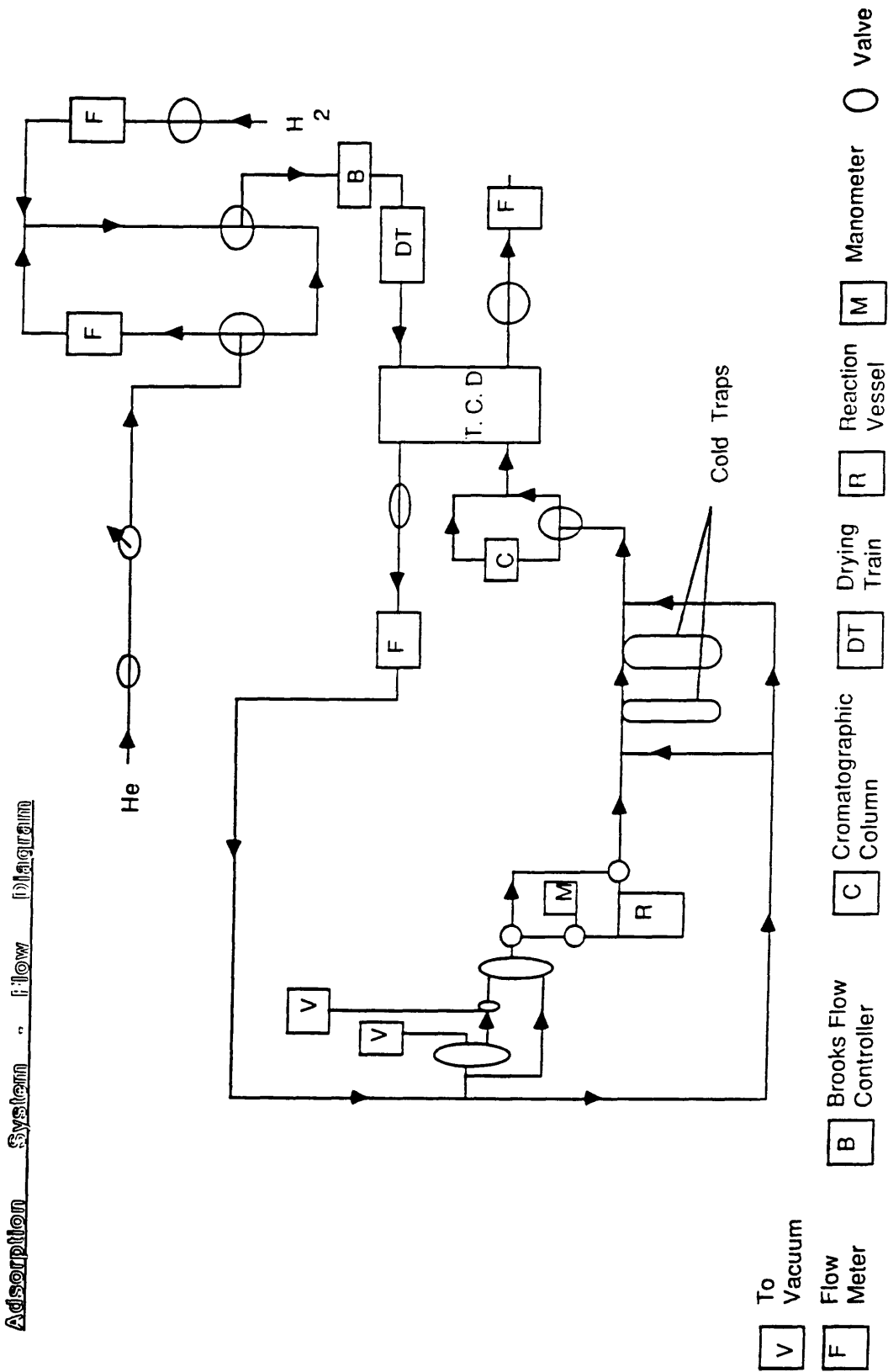


+ 2-Way Tap
 ⊕ 3-Way Tap

Fig. 3.9

Pulse Flow Adsorption System

Fig. 3.10
Adsorption System Flow Diagram



V To Vacuum

F Flow Meter

B Brooks Flow Controller

C Chromatographic Column

DT Drying Train

R Reaction Vessel

M Manometer

O Valve

A 1:1 mixture of 25.3 torr $^{13}\text{C}^{16}\text{O}$ (Amersham) and 23.2 torr $^{12}\text{C}^{18}\text{O}$ (Amersham) was made up and stored in the manifold, for use in these experiments.

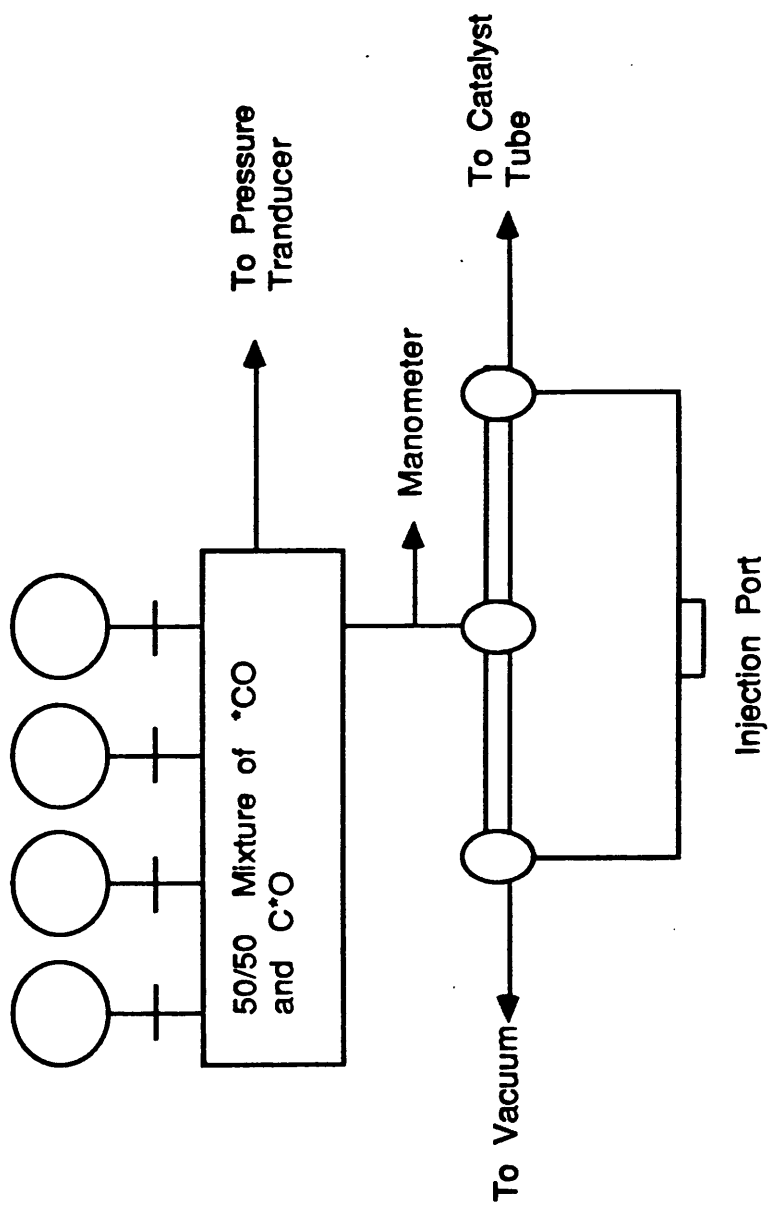
3.4.3 THE FLOW SYSTEM

Helium, hydrogen or a mixture of the two gases could be introduced into the system through a series of Whitey valves, needle valves and flow meters (fig 3.11). The gases then flowed through the reference arm of the TCD before passing through either the sample loop and reaction tube, or the by pass. The gas then passed through two cold traps and the other arm of the TCD, before venting to the atmosphere or entering the MS.

3.4.4 THE SAMPLING SYSTEM

The sampling system shown in some detail in fig 3.10 consisted of a glass sample loop (volume = 2.05 ml) which could be evacuated by manipulating taps 1 and 2. It was filled, from the manifold, by turning tap 2, the pressure of gas in the sample loop being read directly from the manometer. By manipulating taps 1, 2 and 3 the helium carrier gas then flushed the gas sample into the rest of the system, where it could either flow over the catalyst sample or into the bypass. An injection port fitted into the

Fig. 3.11 Adsorption System - Sampling Loop



sampling system meant that a measured amount of gas could also be injected directly into the carrier gas by syringe.

3.4.5 THE REACTION VESSEL

The catalyst sample, about 1cm^3 , was held above a glass sinter in the U-shaped Pyrex reaction vessel. A Digitron 275-K thermocouple was held in a small well near the centre of the catalyst bed. To reduce the catalyst and to carry out desorption measurements a furnace, controlled by a Neutronic Temperature Controller, could be positioned around the reaction vessel.

3.4.6 THE GAS CHROMATOGRAPH AND MASS SPECTROMETER

The GC consisted of a Pye 104 chromatographic oven which maintained a 2m Poropax Q column at 30°C and a TCD which used a bridge current of 240 mA. The flow rate through the system was 50 mlmin^{-1} .

The outputs from both the detector and the catalyst thermocouple were fed to a Servoscribe chart recorder. The TCD was also connected to a LDC 308 computing integrator which measured the retention time and area of each of the peaks produced.

The mass spectrometer was a Spectromass 1000 Quadropole

Mass Spectrometer, set for a 10 second scan time and having a typical internal pressure of 10^{-7} torr. The output from the mass spectrometer was fed to another Servoscribe chart recorder.

3.4.7 EXPERIMENTAL PROCEDURE

The catalyst sample (0.3 - 1.0g) was loaded into the reaction vessel and reduced by rapidly heating the catalyst to 320°C in a 50 mlmin^{-1} flow of pure hydrogen. After 5 minutes at 320°C the catalyst was cooled in hydrogen to ambient temperature, before the carrier gas was switched to helium.

During the reduction procedure, especially with the Rh/MoO₃ catalyst, a great deal of water was produced. This had to be flushed from the system, before any experimental work could be done.

Pulses of carbon monoxide (3.17×10^{18} - 1×10^{19} molecules) were passed over the catalyst surface at ambient temperature, until adsorption, as measured by an analysis of the eluant gases, was complete.

The catalyst was then heated very rapidly to 320°C and any desorbing species were identified and measured by GC-MS. Any carbon dioxide which desorbed as the temperature was increased, was trapped out in the liquid nitrogen cooled

traps and analysed separately after the desorption was complete.

On cooling to ambient temperature, another adsorption / desorption cycle could be carried out. Alternatively the catalyst could be maintained at 250°C and a high temperature carbon monoxide adsorption carried out.

3.5 PULSE-FLOW ADSORPTION SYSTEM

3.5.1 INTRODUCTION

The experiments carried out in this and the next section are very similar to those described in section 3.4, but with two important differences in the experimental procedure used. The catalyst oven used in this system could be accurately temperature programmed. Thus temperature programmed reduction (TPR) and desorption (TPD) profiles could be obtained in much greater detail. The second point, however, was that as the system was not equipped with either an MS or GC column, no detail could be determined regarding the chemical identity of the desorbing species.

A liquid nitrogen trap was incorporated into the system to condense out any carbon dioxide that was present in the effluent gases. However, because the large amount of water produced during the reduction procedure tended to block this trap, cutting off the gas flow to the TCD, its use had to be discontinued.

3.5.2 APPARATUS

The pulse-flow adsorption system used in these experiments is depicted in fig 3.12. The entire system was made of stainless steel tubing connected using Crawford Swagelock couplings. All of the experiments carried out in this section were performed at atmospheric pressure although the system was capable of operating at higher pressures.

Helium, or the reducing mixture of 6% H_2 in N_2 , was split into two streams as it entered the system. One stream acted as reference gas, passing over the reference arm of the TCD (Gowmac 1097) before going to vent. The other stream passed through a 'GO' valve and a Unit Instruments (URS 100.5) mass flow controller - these controlled the pressure and flow rate of gas going through the system. After passing through a 'Valco' ten port sampling valve the gas flowed through the catalyst tube or bypass section before passing over the other arm of the TCD. The output from the TCD was fed to a Servoscribe 2 chart recorder.

The adsorbing gas (carbon monoxide, carbon dioxide or oxygen) entered the system by a different route. After passing through a 'GO' valve and mass flow controller, this gas stream could either be added to the carrier gas to form a mixture, the composition of which was controlled by the mass flow controller, Or alternatively, it could flow into the gas sampling valve. This allowed pulses of the

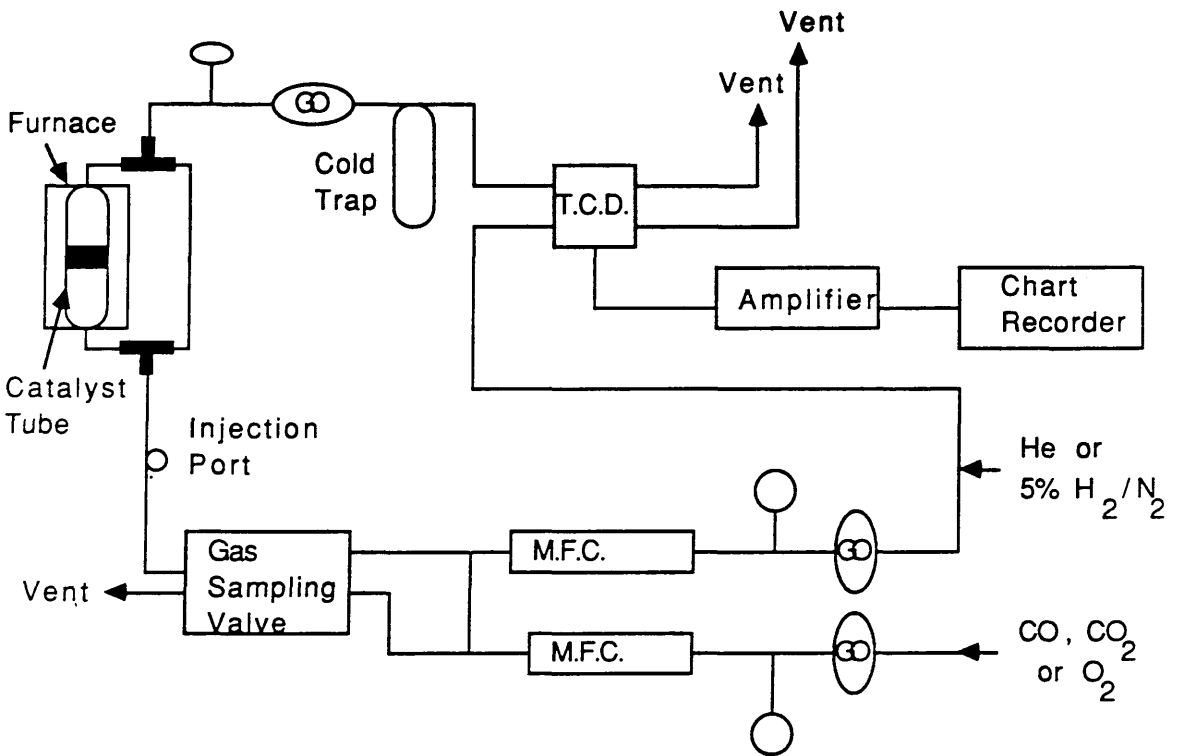
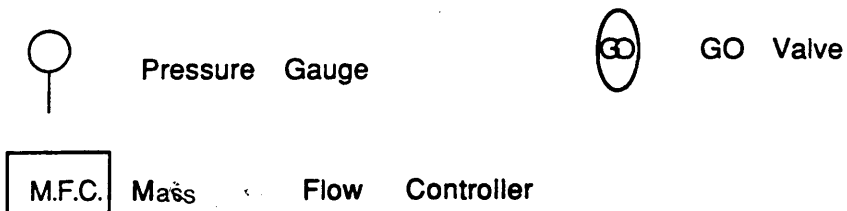


Fig. 3.12 Pulse Flow Adsorption Apparatus



adsorbing gas to be admitted into the carrier stream and so to pass over the catalyst sample.

The sample of catalyst (typically 0.1 - 0.5g) was loaded into a glass lined 1/4 inch stainless steel tube then placed in a Pye oven which could be temperature programmed. The catalyst in the form of a fine powder was held in place by small plugs of silica glass wool.

All of the gauges shown in fig 3.12 (Budenberg) were capable of measuring pressures of up to 100 psi. Gases entered the system at approximately 40 psi and the flow rate, as measured by the flowmeters on the major vents, was approximately 40 mlmin^{-1} .

The ten port sampling valve was pneumatically switched by a Valco Helical Drive Air Actuator, and allowed 500ul samples of gas to be pulsed into the main carrier stream.

3.5.3 TEMPERATURE PROGRAMMED REDUCTIONS

A 40 mlmin^{-1} flow of 6% H_2 in N_2 was passed over the catalyst surface as the temperature was increased at the steady rate of 5°Cmin^{-1} to 300 or 500°C . The catalyst was then held at this temperature for one hour before being cooled to ambient temperature in the 6% H_2 stream. During this time the output from the TCD was fed to a Servoscribe chart recorder which produced an accurate record of the amount of hydrogen taken up with time or temperature.

3.5.4 ADSORPTION MEASUREMENTS

Pulses of the adsorbing gas were passed, in a stream of helium, through the bypass and into the TCD. This produced a series of reference peaks on the chart recorder. When the area of these peaks was stable, the helium carrier was redirected, by taps 1 and 2 to the catalyst sample. A large initial deflection was usually observed due to H_2/N_2 remaining from the reduction in the catalyst tube. Once the base line had settled down, pulses of gas could be admitted to the catalyst and the extent of adsorption measured.

It was possible using this system to carry out adsorption experiments at a variety of temperatures, from $-196^{\circ}C$ to $500^{\circ}C$ if necessary.

3.5.5 TEMPERATURE PROGRAMMED DESORPTIONS

When, following the adsorption procedure described above, the catalyst had reached apparent saturation, the temperature of the oven was increased at the rate of $10^{\circ}Cmin^{-1}$ to $500^{\circ}C$. The TCD profile of the desorbing species was then recorded as a series of peaks on the chart recorder.

3.6 THE PULSE-FLOW ADSORBANCE SYSTEM - WITH MASS SPECTROMETER

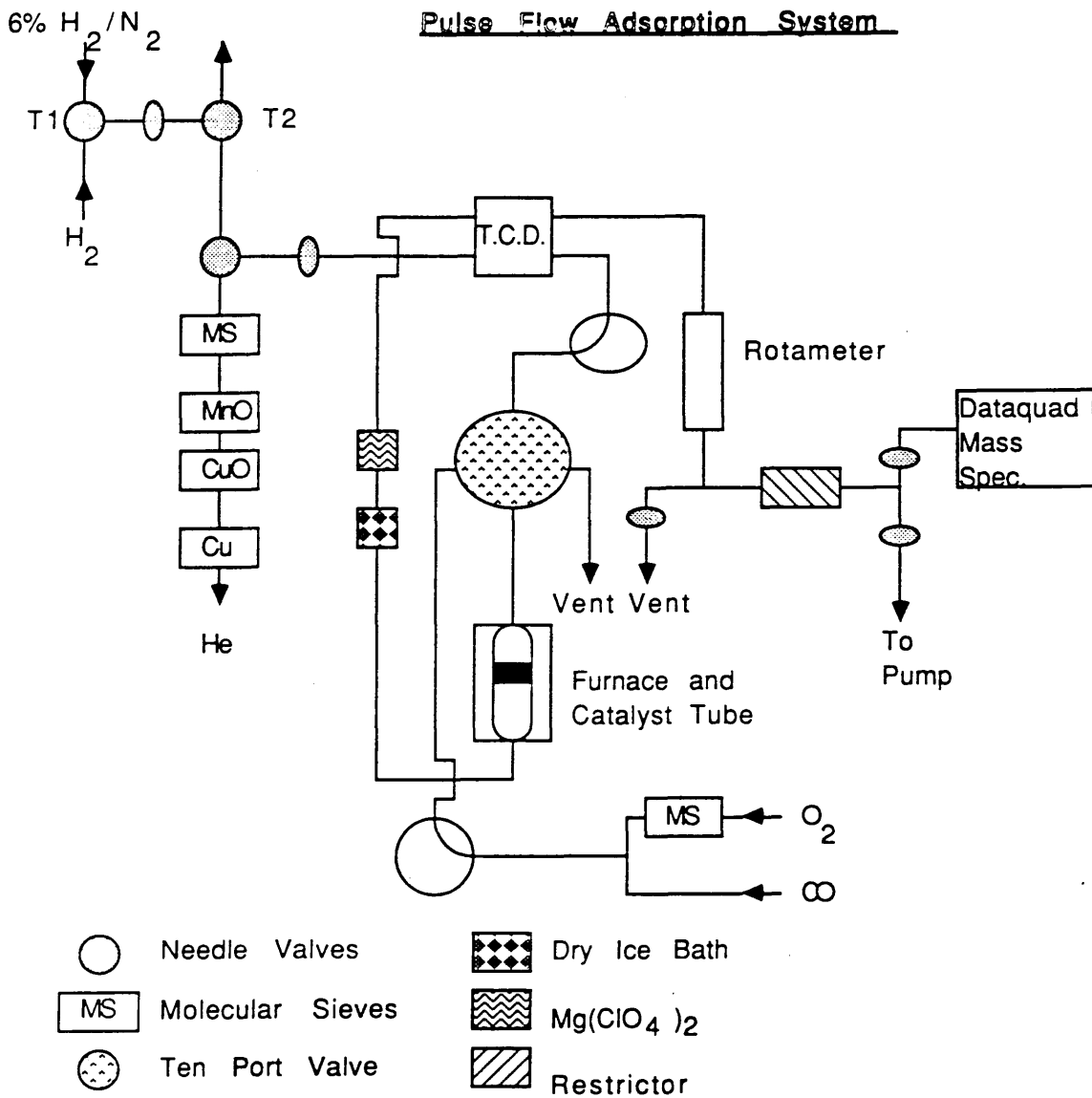
Carbon monoxide, carbon dioxide and oxygen adsorption experiments were also carried out using the apparatus illustrated in fig 3.13. This system was very similar to that described in the previous section, both in its construction and its operation, the only difference being the quadrupole mass spectrometer (Dataquad), situated on the main vent, which allowed the identification of the gas phase species.

To reduce the catalyst sample, 6% H₂ in N₂ was passed through three Whitey valves, two needle valves, the reference arm of the TCD and a ten port sample valve (Valco), before flowing over the catalyst and out through the other arm of the TCD. The flow rate was approximately 50mlmin⁻¹ and the temperature of the catalyst was increased at 5°Cmin⁻¹ to 300°C. The furnace temperature was controlled by a Cambridge Process Controller (702) which used a thermocouple close to the catalyst bed to monitor the catalyst temperature. The catalyst was then maintained at 300°C for one hour before being cooled in the 6% H₂ mixture to ambient temperature.

After changing the gas flow to helium, 50ul pulses of gas could be passed over the catalyst surface by means of the ten port sampling valve. The amount of gas not adsorbed was then detected by the TCD (Gowmac 1097), the output from which was displayed on a potentiometric chart recorder.

Fig. 3.13

Pulse Flow Adsorption System



3.7 IN-SITU FOURIER-TRANSFORMED INFRA-RED MEASUREMENTS

3.7.1 FOURIER TRANSFORMED INFRA-RED SPECTROMETER

The infra-red spectrometer used in this section of the project was a single beam Nicolet 5.Dxc interferometer system, which could be used in either the transmission or diffuse reflectance mode.

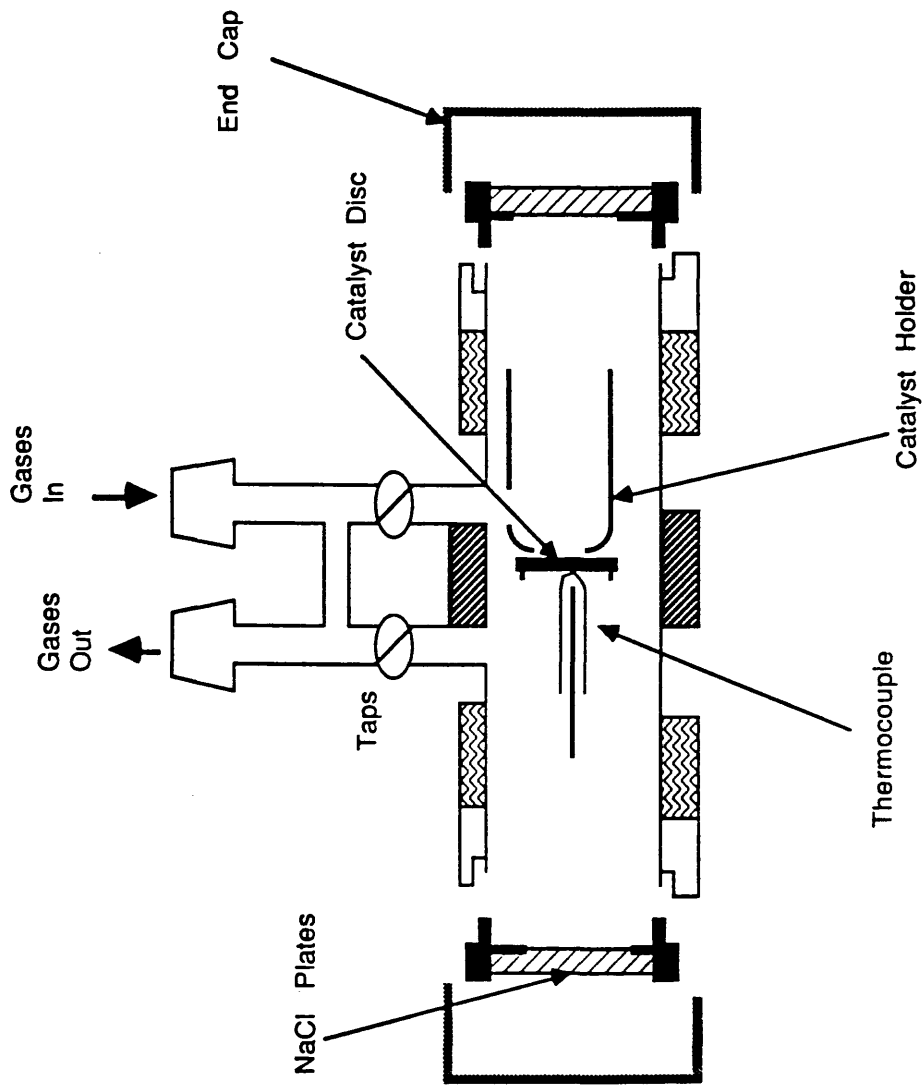
Fourier transformed infra-red (FTIR) spectroscopy was chosen rather than conventional infra-red, because of its far greater speed and better signal to noise ratio when small quantities of species which are difficult to detect are present.

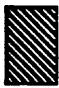
A Nicolet 1280 micro computer, equipped with a double disc drive, was used to transform and process the spectra obtained, allowing greater manipulation of the spectra, background subtraction etc.

A Hewlett-Packard 4770A digital plotter was used to produce a permanent record of the spectra.

3.7.2 TRANSMISSION ENVIRONMENTAL FLOW CELL

The layout of the cell used to obtain in-situ spectra of the catalysts¹⁹² is shown in detail in fig 3.14. It consisted of a Pyrex tube through which various gases were



 Furnace

 Cooling Water

Fig. 3.14 The Infra - Red Cell

flowed at approximately 50 mlmin^{-1} . These gases passed over the surface of a self-supporting catalyst wafer, situated in its holder in the central region of the cell. A furnace, controlled by a Variac variable transformer, surrounded the catalyst sample. A thermocouple situated in a well close to the wafer measured the catalyst temperature. The cell was supported on a cradle within the sample compartment of the spectrometer.

The infra-red beam entered and left the cell through a pair of highly polished NaCl windows, which were mounted by Araldite in two stainless steel rings. These in turn were held in place by two Cajon "Ultra-Torr" threaded jackets. The whole cell was made gas-tight by two compressed Viton O-rings. The window fittings were water cooled to prevent any damage by thermal shock.

The helium carrier gas used in most of these experiments passed through a trap fitted with 5A molecular sieves to remove any water present. All non-condensable gases entered the cell via an acetone-dry ice cold trap which removed any water that was left. The flow rate into the cell was controlled by a needle valve and the flow rate out of the cell was measured by a bubble flow meter.

3.7.3 CATALYST PREPARATION

To prevent excess scattering from the very small catalyst particles which were present, the catalyst samples

were compressed into thin, self-supporting discs. A pressure of 1.5 tonnes was sufficient to form the Rh/Al₂O₃ discs, but a pressure of 4 to 5 tonnes was needed to form Rh/SiO₂ discs.

These discs were then cut to fit into the wafer holder of the flow cell. The wafers used for infra-red measurements were approximately 15mm long by 10mm wide and with a density of between 18 and 30 mgcm⁻¹. Since MoO₃ absorbs infra-red radiation very strongly, no transmission spectra of the Rh/MoO₃ catalyst could be obtained.

3.7.4 EXPERIMENTAL PROCEDURE

The infra-red cell was kept at 320°C for at least 15 minutes, to remove water which had condensed in the cell, before any spectra were taken. Background spectra were taken, without any catalyst present, at both 320°C and at ambient temperature and these were then automatically subtracted from any subsequent spectra.

The catalyst wafers were reduced at 320°C for 30 minutes in a 50 mlmin⁻¹ flow of 6% H₂ in argon. The catalyst was then cooled in the same gas to room temperature. Reference spectra were taken at 320°C and ambient temperature - these could be subtracted from adsorption spectra if desired.

50mlmin⁻¹ of the adsorbing gas was passed over the catalyst surface for approximately 5 minutes. The gas flow was then changed to helium and the cell flushed to remove any gas phase or loosely held material. The surface spectra was then taken.

It was also possible to either study the adsorption of a particular molecule at elevated temperature or to slowly increase the temperature of the catalyst and investigate the desorption of surface species. If the adsorbing material was a volatile liquid it could be injected directly into the carrier stream by syringe, through the injection port at the top of the cell.

CHAPTER 4

EXPERIMENTAL ANALYSIS

CHAPTER 4. EXPERIMENTAL ANALYSIS

4.1 REFINEMENT OF RADIOCHEMICAL DATA

As was previously mentioned in section 3.3.3, the count rate during an adsorption experiment could not be used to calculate the adsorption isotherm before a number of correction factors had been applied. This procedure is described in this section. If:

$$A(I) = \text{count rate GM1}$$

$$B(I) = \text{count rate GM2}$$

$$D = \text{dead time (secs)}$$

$$T = \text{counting time (secs)}$$

then the dead time corrected count rates are given by:

$$\text{GM1(cps)} = C(I) = \frac{A(I)}{T - A(I)D}$$

$$\text{GM2(cps)} = D(I) = \frac{B(I)}{T - B(I)D}$$

$$\text{True count rate GM1(cpm)} = E(I) = (C(I) - A)60$$

$$\text{True count rate GM2(cpm)} = F(I) = (D(I)*Z - B)60$$

where:

$$A = \text{background count rate GM1(cps)}$$

$$B = \text{background count rate GM2(cps)}$$

$$Z = \text{intercalibration factor}$$

If the surface count rates ($S(I) = F(I) - E(I)$) are then plotted against the gas phase counts ($E(I)$), the adsorption isotherms discussed in chapter 5 are obtained.

4.2 PULSE-FLOW ADSORPTION MEASUREMENTS

Although three slightly different sets of apparatus (sections 3.4, 3.5 and 3.6) were used to obtain these results, the method by which the amount of gas adsorbed by the catalyst sample could be calculated from the type of trace shown in fig 4.1 was the same in each case.

The number of molecules of gas present in a reference pulse (N) was easily calculated from the volume and pressure of gas injected.

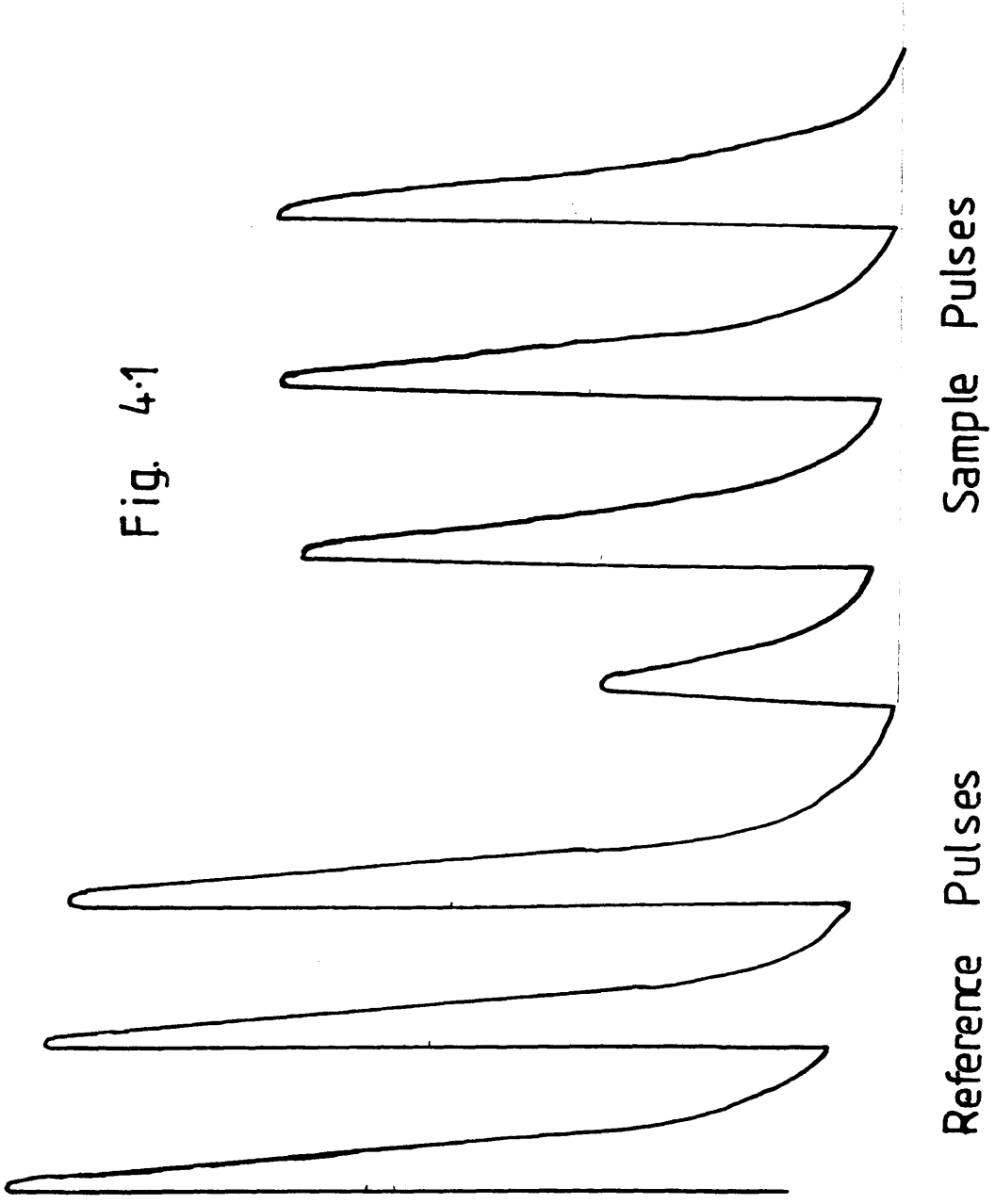
$$N = \frac{PV}{RT} \cdot N_A$$

A conversion factor, F can then be calculated:

$$F = \frac{N}{\text{Area of peak produced}}$$

The number of molecules in a pulse which went over the catalyst should be approximately the same as that in a reference pulse produced under identical conditions.

Fig. 4.1



Therefore, at catalyst saturation the sample peak should be of a very similar area to the reference one. However, this is not the case; the sample peaks were always smaller than the reference ones. This is because the carrier gas is continually stripping adsorbed molecules from the catalyst surface which are then replenished from the next pulse of adsorbing gas. As complete saturation never appears to be reached, it was necessary for calculation purposes to use the area of the largest peak produced at saturation, rather than the reference peak, as the standard from which the amount of gas adsorbed was calculated.

$A(\text{sat})$ = area of peak at saturation

$A(I)$ = area of peak I

$(A(\text{sat}) - A(I)) \times F$ = no of molecules of gas
adsorbed from pulse I

If the pulses are put in at regular intervals, a plot of $\sum(A(\text{sat}) - A(I)) \times F$ against pulse number will be a measure of the amount of material on the surface with time.

Desorption results can be treated in a similar way, where:.

Amount of material on the Surface	-	Amount desorbed	=	Amount Still on the Surface
(Estimated from adsorption Expts)		(Peak area x F)		

CHAPTER 5

ADSORPTION EXPERIMENTS USING ^{14}C LABELS

CHAPTER 5. ADSORPTION EXPERIMENTS USING ^{14}C LABELS

5.1 INTRODUCTION

This chapter describes a series of comparative adsorption studies, carried out using the apparatus described in section 3.3.

Since, due to changes in counting geometry and sample size, it was not possible to quantitatively compare results from one experiment to the next, this study will concentrate on the more general trends observed in such things as the amount of material adsorbed by the surface.

Where percentage changes are quoted, these were calculated as a percentage of the final count rate, of the initial reference isotherm, for each sample.

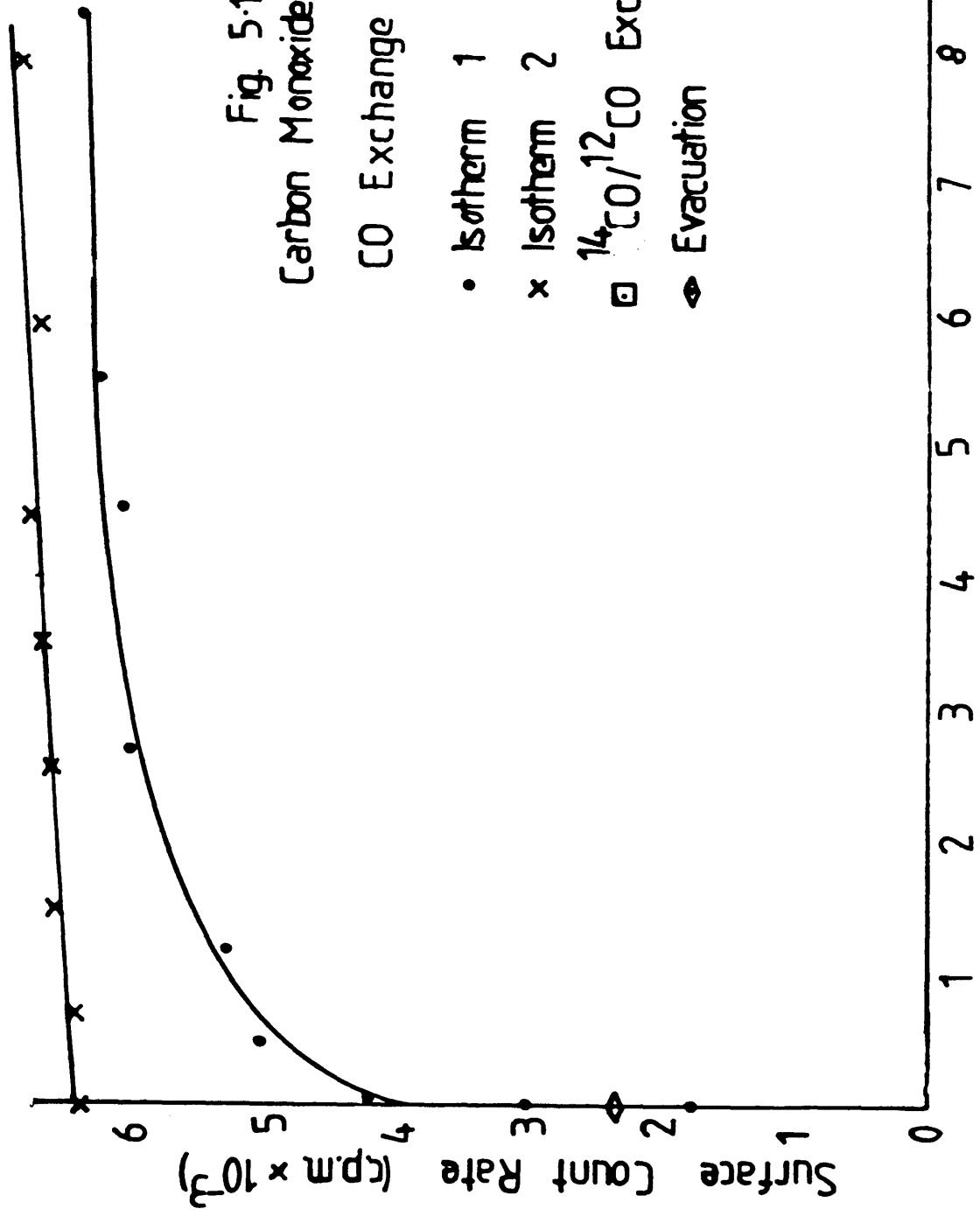
5.2 CARBON MONOXIDE ADSORPTION

5.2.1 ADSORPTION ISOTHERMS

Prerduced samples of catalyst were exposed to a series of small aliquots of ^{14}C - carbon monoxide and the count rates measured at each stage to obtain the type of isotherms illustrated in fig 5.1, 5.2 and 5.3. The samples were then evacuated for thirty minutes, before a second isotherm was

Fig. 5.1
Carbon Monoxide on Rh/Al₂O₃
CO Exchange Without Evacuation

- Isotherm 1
- × Isotherm 2
- ◻ ¹⁴C/¹²C Exchange
- ◊ Evacuation



Gas Phase
Count Rate
(c.p.m. × 10⁻³)

Surface Count Rate (c.p.m. × 10⁻³)

Fig 5.2 Carbon Monoxide on 5% Rh/SiO₂
CO Exchange Without Evacuation

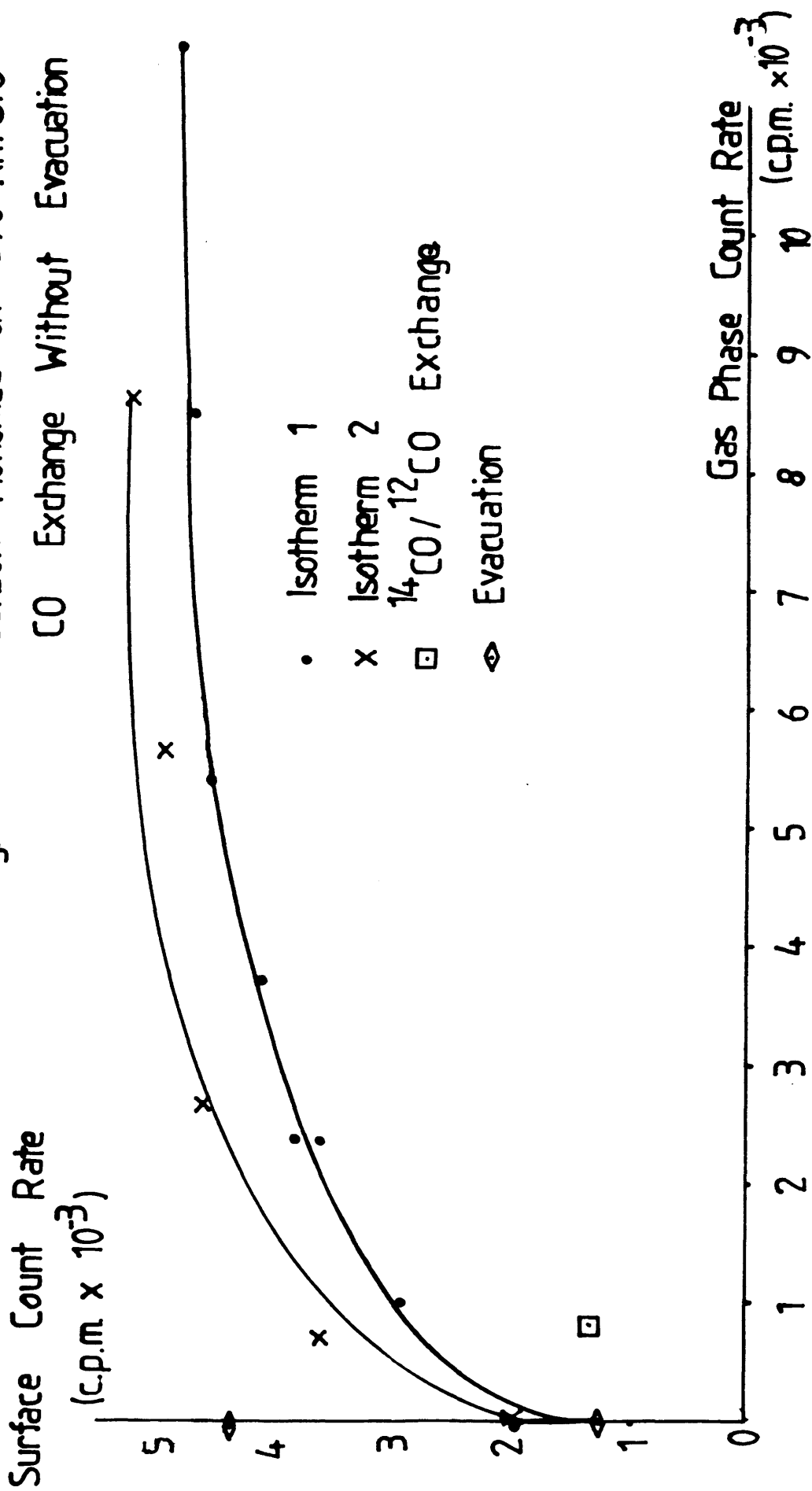
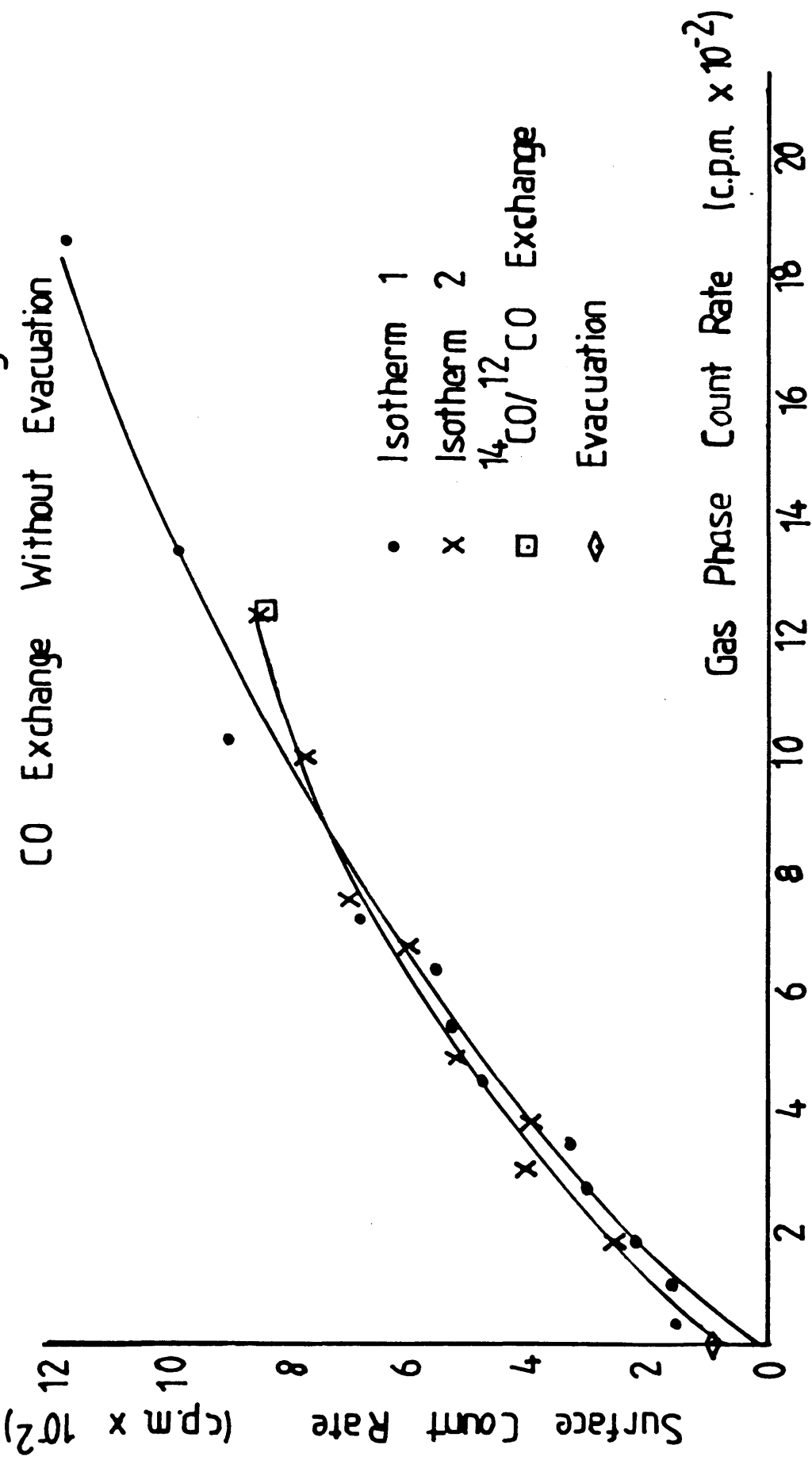


Fig. 5.3 Carbon Monoxide on Rh/MoO₃



determined.

As fig 5.1 shows, the 2% Rh/Al₂O₃ sample initially adsorbed all of the carbon monoxide which was admitted into the reaction vessel and hence the surface count rate increased very rapidly. However, as more carbon monoxide was added, and saturation approached the increase gradually slowed, until in the second portion of the graph the isotherm was almost horizontal, corresponding to complete saturation of the surface. A subsequent period of evacuation only removed 2% of the surface carbon monoxide, suggesting a very strong bond between it and the catalyst. Very little carbon monoxide was then taken up in the second isotherm as the catalyst was already covered with a layer of very strongly held carbon monoxide. The shape of the second isotherm was identical to that of the second portion of Isotherm 1.

The 2% Rh/SiO₂ catalyst was such a fine powder that it tended to be sucked through the apparatus when it was placed under vacuum. This meant it could not be used in these experiments. The more dense 5% Rh/SiO₂ catalyst was, therefore, used in its place.

The behaviour of the 5% Rh/SiO₂ catalyst (fig 5.2) was very similar to that of the 2% Rh/Al₂O₃ one, although a higher pressure of carbon monoxide was needed before saturation was reached. 6% of the adsorbed carbon monoxide was removed by 30 minutes evacuation. The second isotherm

had a similar shape to that of the first, although the saturation surface count rate was somewhat higher.

The 2% Rh/MoO₃ catalyst, on the other hand, behaved rather differently (fig 5.3). Much less carbon monoxide was adsorbed on the Rh/MoO₃ catalyst than on the other two catalysts, indicating a much lower dispersion of metal particles on the Rh/MoO₃ sample. However, the most striking difference between the Rh/MoO₃ and the other catalysts was in the shape of the isotherm. The initial large adsorption of carbon monoxide was completely absent, and although there was a slight change of gradient, the Rh/MoO₃ sample never appeared to reach saturation, even at relatively high concentrations of carbon monoxide. Upon evacuation, up to 93% of the surface carbon monoxide could be removed at ambient temperature. The shape of the second isotherm was very similar to that of the first and again surface saturation was not reached within the limits of adsorbate pressure used in these experiments. These results are summarised in table 5.1, overleaf.

If it is assumed that carbon monoxide only interacts with the rhodium particles and that one molecule of carbon monoxide adsorbs on each rhodium atom, then the amount of carbon monoxide adsorbed by each of these catalysts can be used to calculate the proportion of the rhodium atoms present, which are on the catalyst's surface. These results, quoted as the percentage dispersion are listed

below in table 5.2

Table 5.1 Carbon Monoxide Adsorption (20°C)

<u>Procedure</u>	<u>Surface Count Rate</u> (cpm)	<u>Relative Total Change</u> (%)
<u>2% Rh/Al₂O₃</u>		
(sample size = 0.0945g)		
a) ¹⁴ C ¹⁴ O adsorption to surface saturation (4.80 torr)	6454	100
b) Evacuation for 30 minutes	6326	98
c) ¹⁴ C ¹⁴ O adsorption to surface saturation (4.59 torr)	6908	107
<u>5% Rh/SiO₂</u>		
(sample size = 0.1154g)		
a) ¹⁴ C ¹⁴ O adsorption to surface saturation (6.75 torr)	4713	100
b) Evacuation for 30 minutes	4399	93
c) ¹⁴ C ¹⁴ O adsorption to surface saturation (5.03 torr)	5179	110
<u>2% Rh/MoO₃</u>		
(sample size = 0.3502g)		
a) ¹⁴ C ¹⁴ O adsorption to surface saturation (10.75 torr)	1175	100
b) Evacuation for 30 minutes	82	8
c) ¹⁴ C ¹⁴ O adsorption to surface saturation (7.12 torr)	853	73

The amount of carbon monoxide adsorbed by the catalyst samples can also be used to calculate the average metal particle size on the surface. These calculations again assume that one molecule of carbon monoxide is adsorbed on each metal atom, but, also that each molecule of carbon monoxide takes up a surface area of 16.8×10^{-20} m, a figure which is supported by experimental evidence. The following expression can then be used to estimate "r", the average metal particle radius.

$$SA = \frac{4\pi r^2}{\frac{4}{3}\pi r^3 \rho} = \frac{3}{\rho r}$$

where:

SA = Surface Area of rhodium per gram of Rh present

r = average metal particle radius (m)

ρ = density of the metal (gm^{-3})

Table 5.2 Dispersions and Metal Particle Size

Catalyst	Rh/Al ₂ O ₃	Rh/SiO ₂	Rh/MoO ₃
Dispersion (%)	18.3	10.9	0.89
Metal Surface Area (m ² /g of Rh)	179	107.5	8.77
Average Particle Radius (nm)	1.35	2.25	27.6

5.2.2 MOLECULAR EXCHANGE

After building up a ^{14}C - carbon monoxide isotherm, a measured amount of unlabelled carbon monoxide was admitted into the reaction vessel, to measure any molecular exchange between labelled surface molecules and unlabelled gas phase carbon monoxide, which might occur. If after a period of time the surface count rate had decreased, while that of the gas phase had increased significantly, then exchange had occurred. However, it should be noted that the change in surface count rate observed would be dependent on the ratio of labelled and unlabelled molecules of carbon monoxide present in the system.

If the gas phase was evacuated off before any unlabelled material was admitted, the amount of irreversibly held carbon monoxide which exchanged with that in the gas phase, could be determined.

The results of both these experiments are shown in table 5.3.

Approximately 50% of both the reversibly and irreversibly held carbon monoxide on the $\text{Rh}/\text{Al}_2\text{O}_3$ and Rh/SiO_2 catalysts exchanged with that in the gas phase. The results for the Rh/MoO_3 catalyst are somewhat more difficult to explain. No exchange was observed when the gas phase was still present, yet 81% of the irreversibly held carbon monoxide exchanged with that in the gas phase.

Table 5.3 Molecular Carbon Monoxide Exchange Experiments

(i) Molecular Exchange without Evacuation (20°C)

<u>Procedure</u>	<u>Surface Count Rate</u> (cpm)	<u>Relative Total Change</u> (%)
<u>2% Rh/Al₂O₃</u>		
(sample size = 0.0945g)		
a) ¹⁴ CO adsorption to surface saturation (4.59 torr)	6908	100
b) Admission of 4.31 torr of ¹² CO		
- initial	2936	42.5
- overnight	2825	40.9
<u>5% Rh/SiO₂</u>		
(sample size = 0.1478g)		
a) ¹⁴ CO adsorption to surface saturation (4.27 torr)	10067	100
b) Admission of 5.42 torr of ¹² CO		
- initial	5503	54.7
<u>2% Rh/MoO₃</u>		
(sample size = 0.3502g)		
a) ¹⁴ CO adsorption to surface saturation (7.12 torr)	853	100
b) Admission of 2.63 torr of ¹² CO		
- initial	862	101

Table 5.3 cont.

(ii) Evacuation followed by Molecular Exchange 20°C

<u>Procedure</u>	<u>Surface Count Rate</u>	<u>Relative Total Change</u>
2%Rh/Al₂O₃		
(sample size = 0.1934g)		
a) ¹⁴ CO adsorption to surface saturation (3.66 torr)	13158	100
b) 30 minutes evacuation	12953	98
c) Admission of 2.58torr of ¹² CO		
- initial	7347	56
- overnight	7184	55
5% Rh/SiO₂		
(sample size = 0.1154g)		
a) ¹⁴ CO adsorption to surface saturation (2.54 torr)	4713	100
b) 30 minutes evacuation	4399	93.3
c) Admission of 6.74 torr of ¹² CO		
- initial	1834	38.9
- overnight	1317	27.9
2%Rh/MoO₃		
(sample size = 0.4848g)		
a) ¹⁴ CO adsorption to surface saturation (3.08 torr)	1437	100
b) 30 minutes evacuation	651	45.3
c) Admission of 5.03 torr of ¹² CO		
- initial	345	21.9
- overnight	123	8.4

5.2.3 DESORPTION MEASUREMENTS

After saturating a catalyst with ^{14}C - carbon monoxide and evacuating it for 30 minutes, it was possible in the system used to pass a stream of helium over the catalyst and to measure the amount of carbon monoxide which desorbed from the surface. Helium was flowed over the surface for 30 minutes before the surface and gas phase count rates were again determined. Any material removed from the catalyst then passed through the scintillation counter where its activity was measured.

The sample was then placed in the catalyst oven and the amount of ^{14}C labelled material which desorbed from the surface as the temperature was increased to 320°C was measured using the scintillation counter. After the catalyst had been held at 320°C for 10 minutes it was moved back into the counting region of the reaction vessel and the count rates measured. It was not possible with the apparatus used to identify the chemical form of the desorbing species.

The results from these experiments are shown in table 5.4. A summary of the results discussed in section 5.2 is shown in figures 5.4 - 5.6.

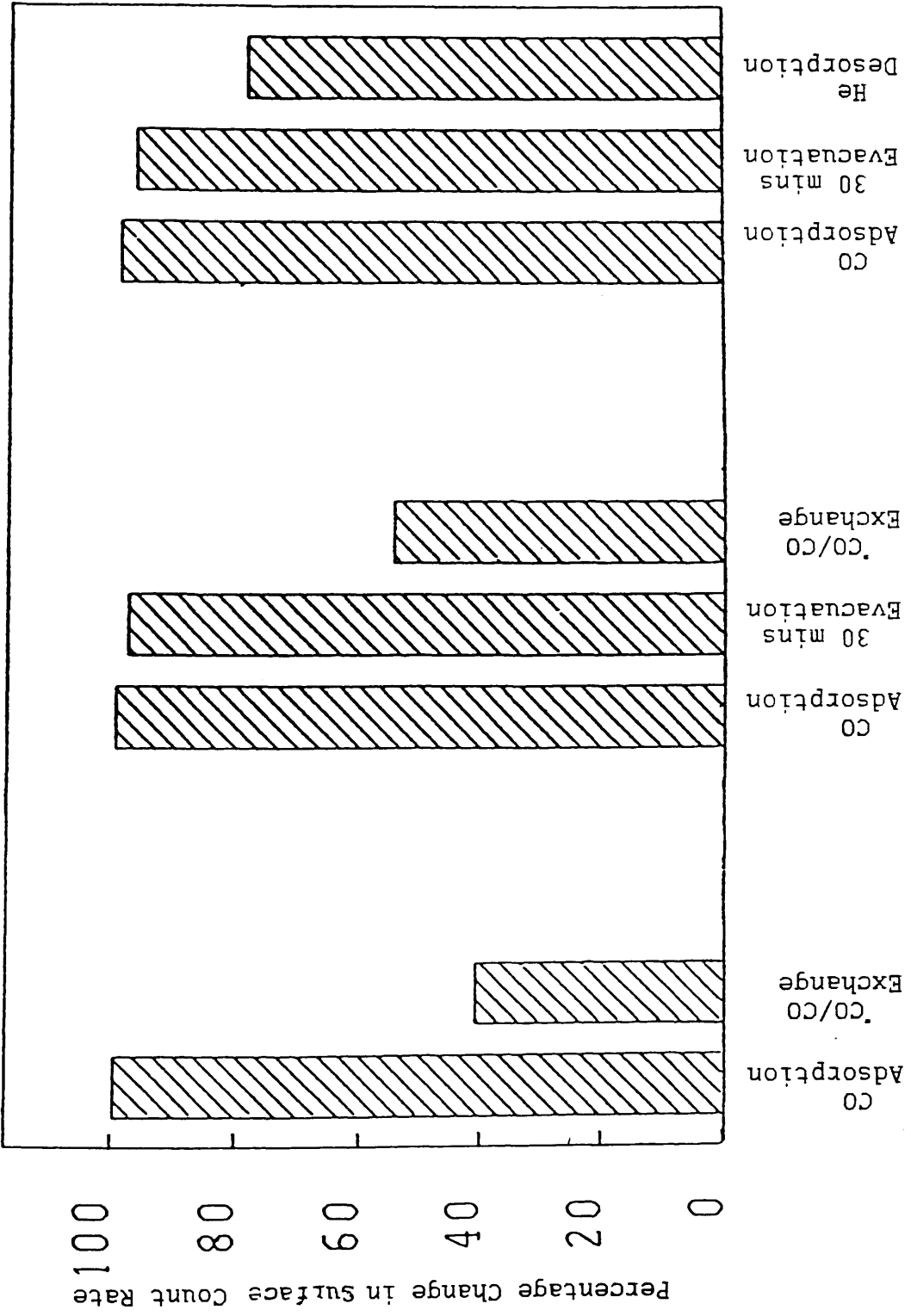


Fig. 5.4

Carbon Monoxide
on Rh/Al₂O₃

Fig. 5.5

Carbon Monoxide Adsorption
on Rh/SiO₂

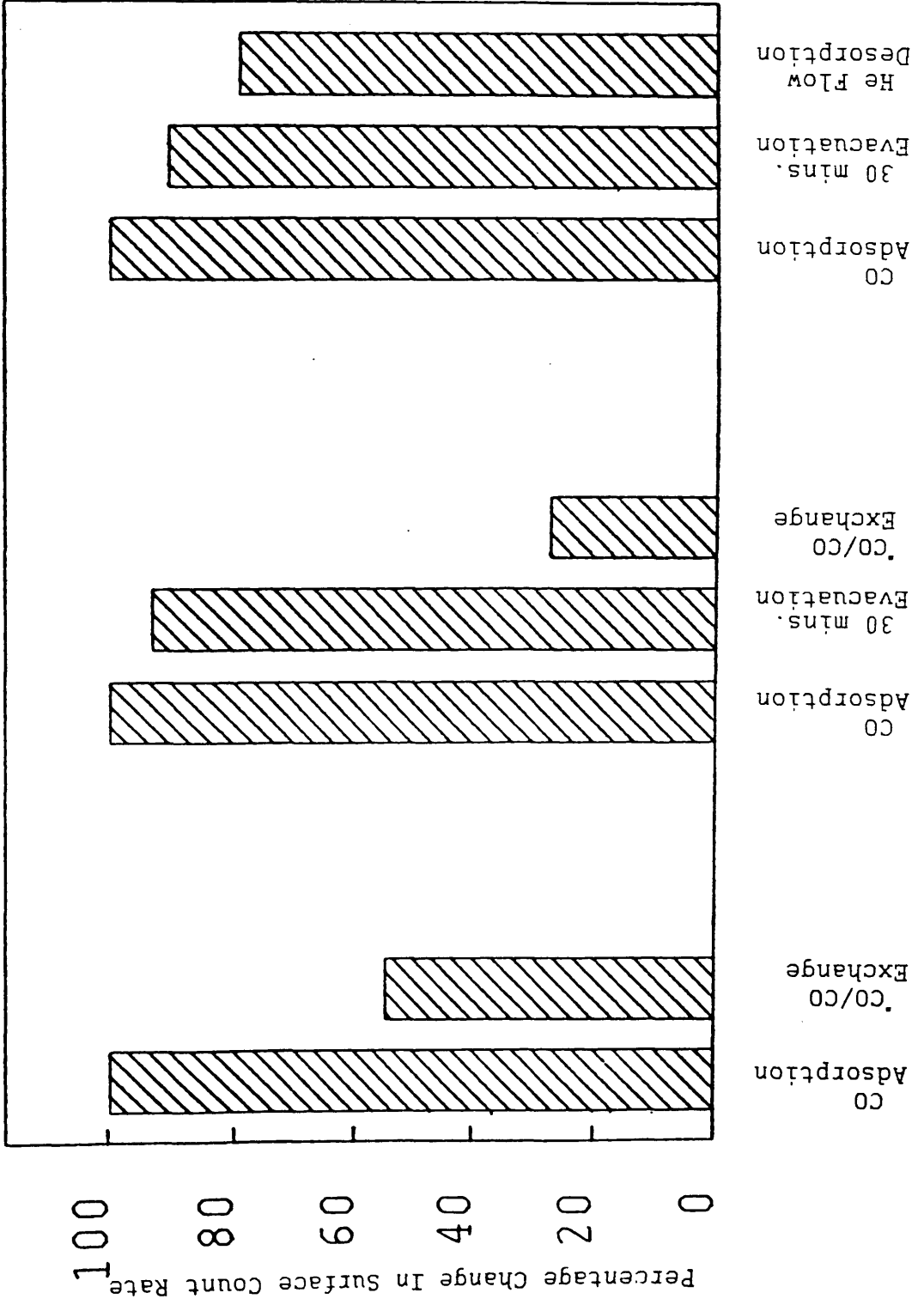


Fig. 5.6

Carbon Monoxide
on Rh/MoO₃

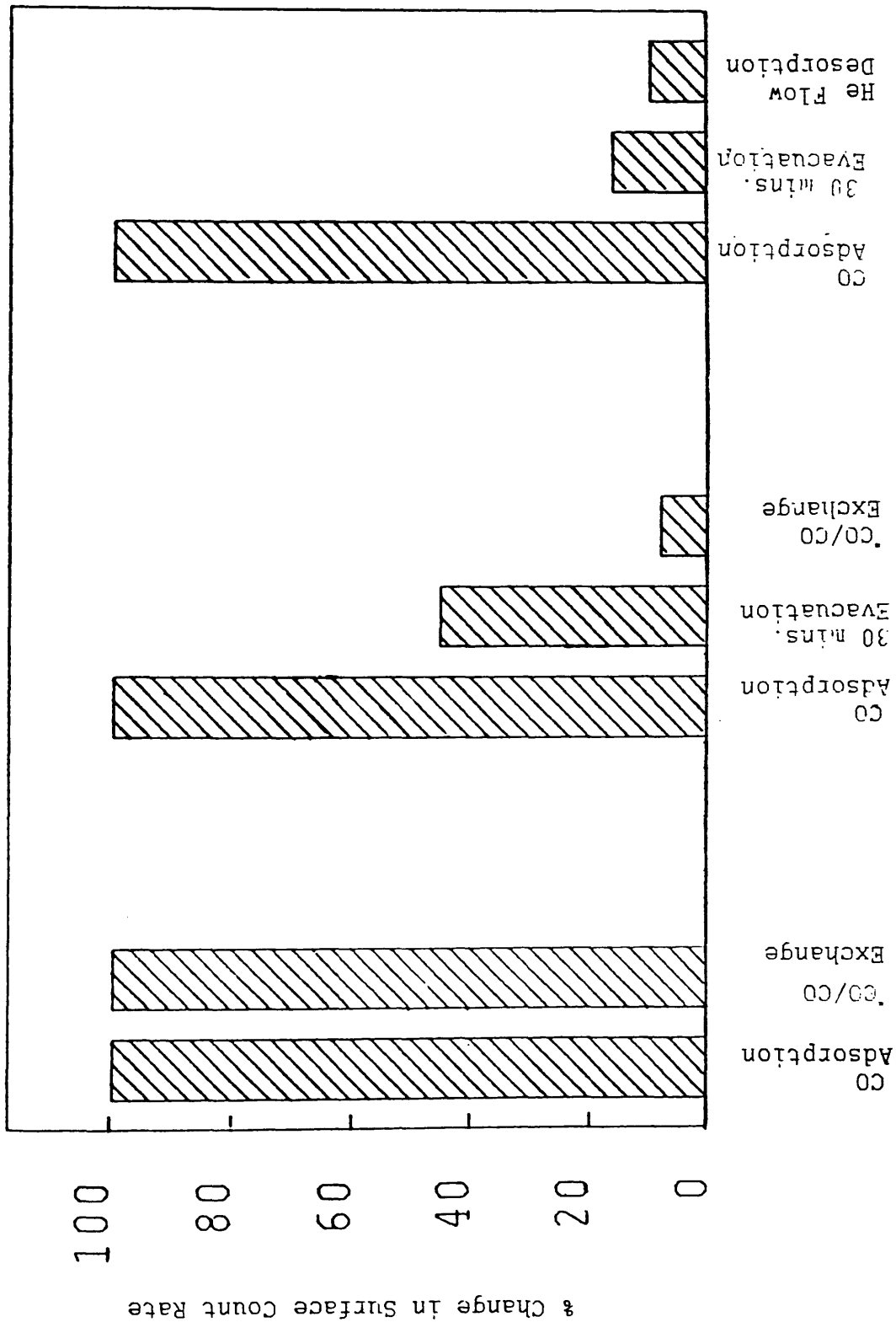


Table 5.4 Carbon Monoxide Desorption

Rh/Al₂O₃ (0.1934g)	Surface Count Rate (cpm)	Relative Total Change (%)
a) Surface Saturation with ¹⁴ C ¹⁸ O (3.67 torr)	7185	100
b) 30 minutes evacuation	6990	97.3
c) 30 minutes helium flow	5669	78.9
d) Thermal desorption at 320°C in flowing helium	13	0.2

5% Rh/SiO₂ (0.2267g)

a) Surface saturation with ¹⁴ C ¹⁸ O (2.74 torr)	6955	100
b) 30 minutes evacuation	6305	90.7
c) 30 minutes helium flow	5508	79.2
d) Thermal desorption at 320°C in flowing helium	19	0.3

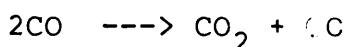
Rh/MoO₃ (0.5773g)

a) Surface saturation with ¹⁴ C ¹⁸ O (3.01 torr)	4445	100
b) 30 minutes evacuation	736	16.6
c) 30 minutes helium flow	458	10.3
d) Thermal desorption at 320°C in flowing helium	9	0.2

5.2.4 GAS PHASE ANALYSIS - CARBON DIOXIDE FORMATION

The gas phase above the catalyst was analysed by GC-scintillation counter at the end of each of these experiments - no carbon dioxide was detected in the gas

phase. This does not eliminate the possibility of some carbon dioxide formation by one of the routes outlined below, but the concentration of carbon dioxide, present in the gas phase, was too low to detect.



5.2.5 THE HEAT OF ADSORPTION OF CARBON MONOXIDE

Langmuir's theories of adsorption may be tested using the carbon monoxide isotherms described in section 5.2.1, if the surface count rate is taken as being equivalent to the volume of gas adsorbed by the catalyst sample, V , and the gas phase count rate as equal to the residual pressure within the reaction vessel.

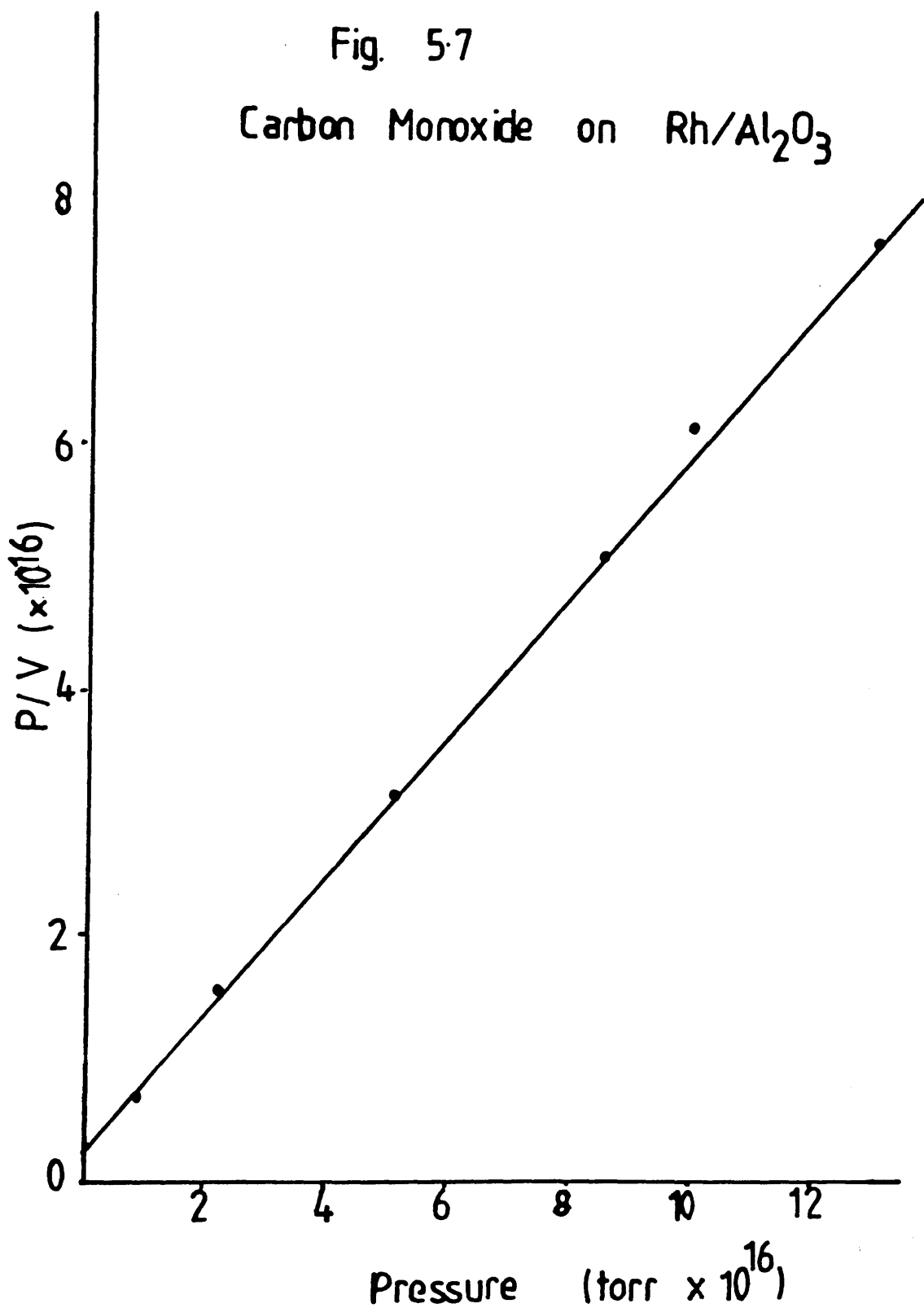
$$\text{Since } \frac{P}{V} = \frac{1}{V_m} P + \frac{1}{bV_m} \quad \text{where: } b = \frac{\text{rate of adsorption}}{\text{rate of desorption}}$$

$$V_m = \text{volume adsorbed at monolayer coverage}$$

a plot of P/V against P should be a straight line of gradient $1/V_m$ (fig 5.7-5.9). This was found to be the case for all three catalysts, when the best fit lines of P/V against P were plotted for values of P which were greater than 500 cpm.

Fig. 5.7

Carbon Monoxide on Rh/Al₂O₃



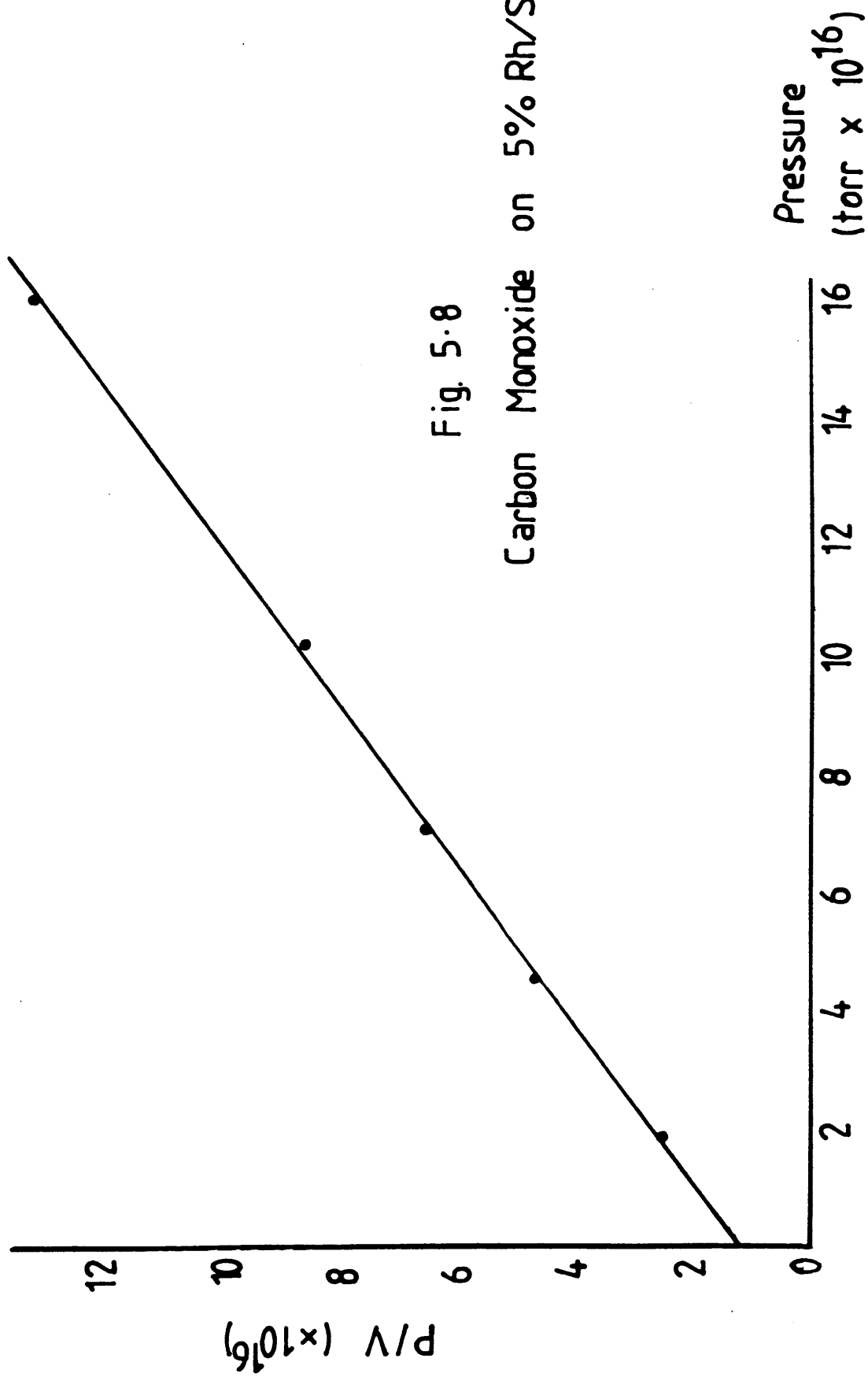


Fig. 5.8

Carbon Monoxide on 5% Rh/SiO₂

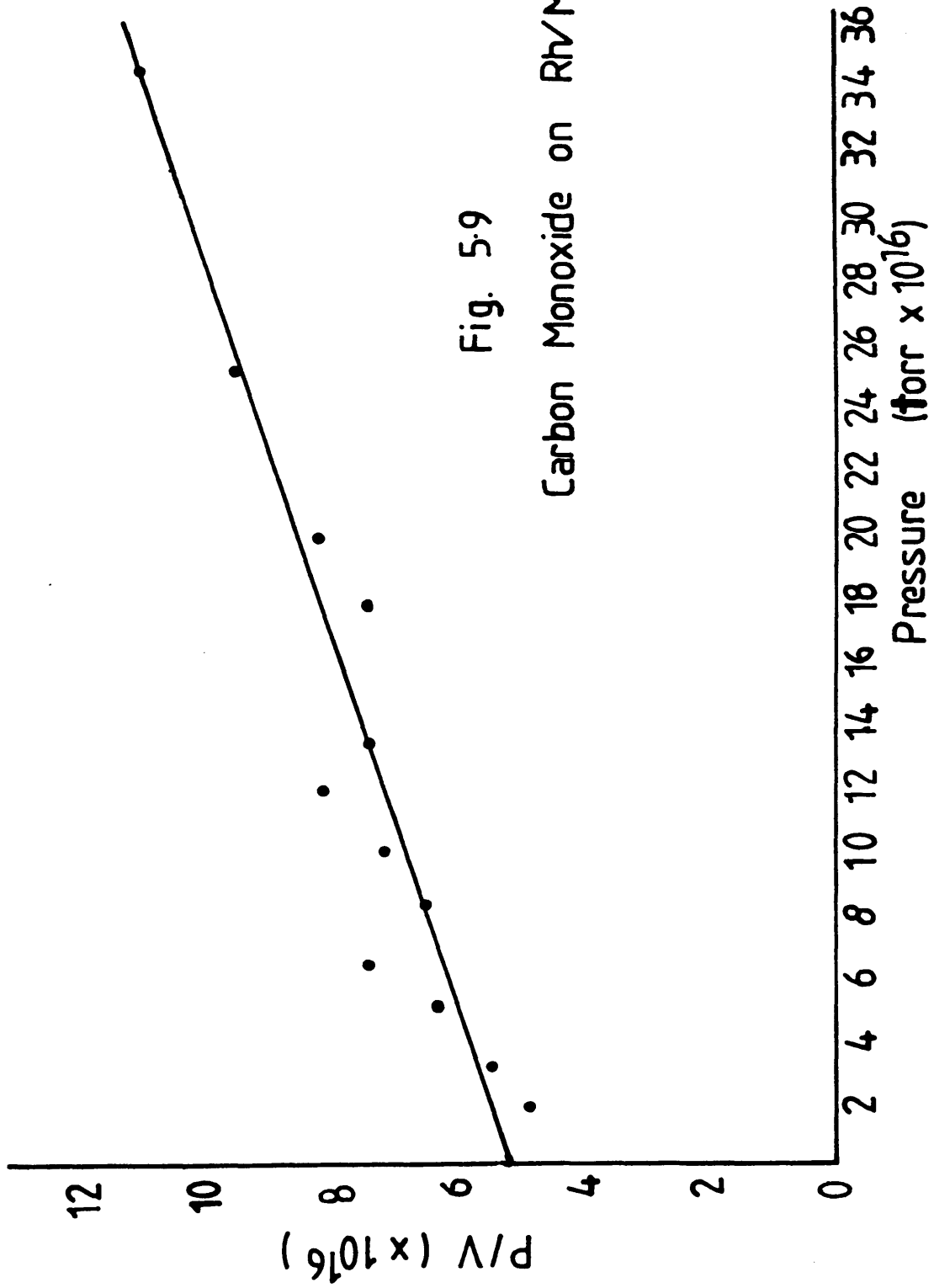


Fig. 5-9

Carbon Monoxide on Rh/MoO₃

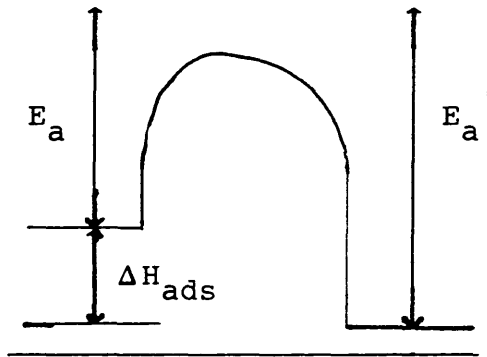
Once values for V_m have been obtained these may be used to calculate θ , the fraction of the surface covered as:

$$\theta = V/V_m$$

The equilibrium constant, b , can also be evaluated since:

$$b = \frac{\theta}{P(1 - \theta)}$$

If we consider the reaction profile of carbon monoxide adsorption, it is clear that $E_a' = E_a + \Delta H_{ads}$



- E_a' = Activation energy of desorption
- E_a = Activation energy of adsorption
- H_{ads} = Average heat of adsorption

Therefore:-

$$\text{rate of adsorption} = A_a \exp(-E_a/RT)$$

$$\text{rate of desorption} = A_d \exp(-E_a'/RT)$$

$$= A_d \exp(-E_a/RT) \exp(-\Delta H_{ads}/RT)$$

A_d = Pre-exponential factor for desorption

A_a = Pre-exponential factor for adsorption

$$b = \frac{A_a \exp(-E_a/RT)}{A_d \exp(-E_a/RT) \exp(-\Delta H_{ads}/RT)}$$

If we assume that A_a/A_d is approximately one this expression simplifies to:

$$b = 1/\exp(-\Delta H_{ads}/RT)$$

$$\ln b = \Delta H_{ads}/RT$$

from which ΔH_{ads} can be calculated. The values of V_m , b and ΔH_{ads} which were obtained are shown in Table 5.5.

Table 5.5 Average Heats of Adsorption of Carbon Monoxide

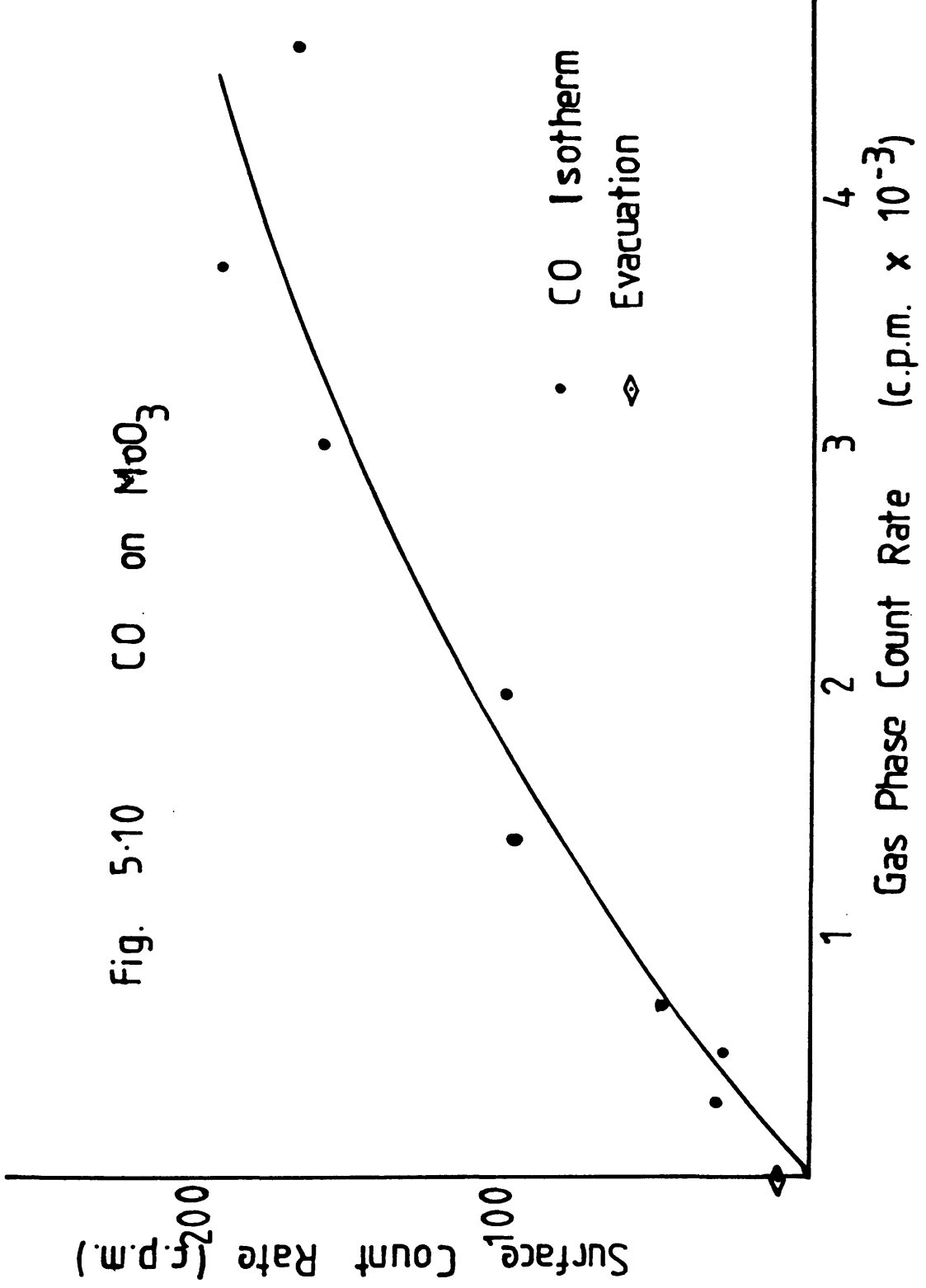
	V_m (cm ³)	b	ΔH (kJmol ⁻¹)
Rh/Al ₂ O ₃	1.767	2.27×10^{-16}	-86.80
Rh/SiO ₂	1.36	6.14×10^{-17}	-92.49
Rh/MoO ₃	0.587	3.25×10^{-18}	-99.77

5.2.6 THE ADSORPTION OF CARBON MONOXIDE ON Al₂O₃,

SiO₂ and MoO₃

The adsorption of carbon monoxide on the Al₂O₃, SiO₂ and MoO₃ supports themselves (without any rhodium present) was also investigated. Only on MoO₃ was any adsorption detected (fig 5.10) and this was fairly limited in the absence of any rhodium particles.

Fig. 5.10 CO on MoO_3



5.3 CARBON DIOXIDE ADSORPTION

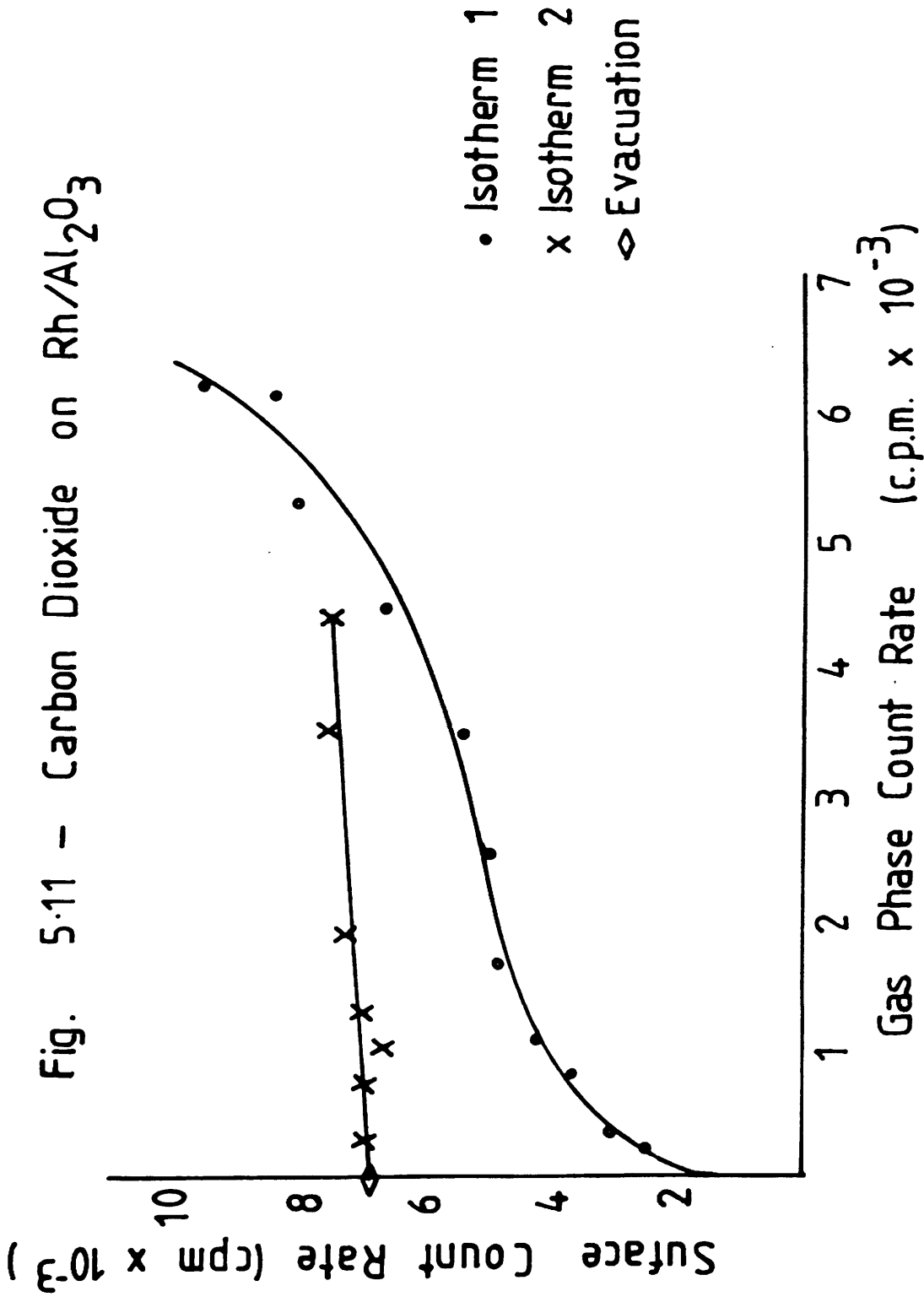
Carbon dioxide was found in this work to adsorb rather slowly on rhodium catalysts. This has meant that the measurements made in these experiments were not carried out under strictly equilibrium conditions. However where comparable results rather than absolute values are of interest this approximation was found to be satisfactory.

5.3.1 CARBON DIOXIDE ADSORPTION ISOTHERMS

^{14}C - carbon dioxide isotherms were determined in an identical manner to that described in the previous section. Rhodium was found to adsorb carbon dioxide much more weakly and to a lesser extent than it can carbon monoxide. The individual points on the carbon dioxide isotherms detailed here have therefore got a large inherent error in them, due to the lower number of counts being measured. This has led to a greater spread of points in these isotherms, making their shapes less distinct.

When carbon dioxide was adsorbed on to a freshly reduced sample of $\text{Rh}/\text{Al}_2\text{O}_3$ the isotherm obtained was sigmoidal in shape (fig 5.11). After an initial period when the surface counts increase rapidly as the pressure is increased, the curve flattens out at approximately 500 cpm. before showing a second sharp increase. Under the

Fig. 5.11 - Carbon Dioxide on Rh/Al₂O₃



conditions used in this experiment the catalyst did not reach saturation.

In contrast the isotherms of Rh/SiO₂ (fig 5.12) and Rh/MoO₃ (fig 5.13), show a linear increase in the surface concentration of carbon dioxide. Rh/SiO₂ adsorbs very little carbon dioxide as expected but adsorption by Rh/MoO₃ is quite considerable.

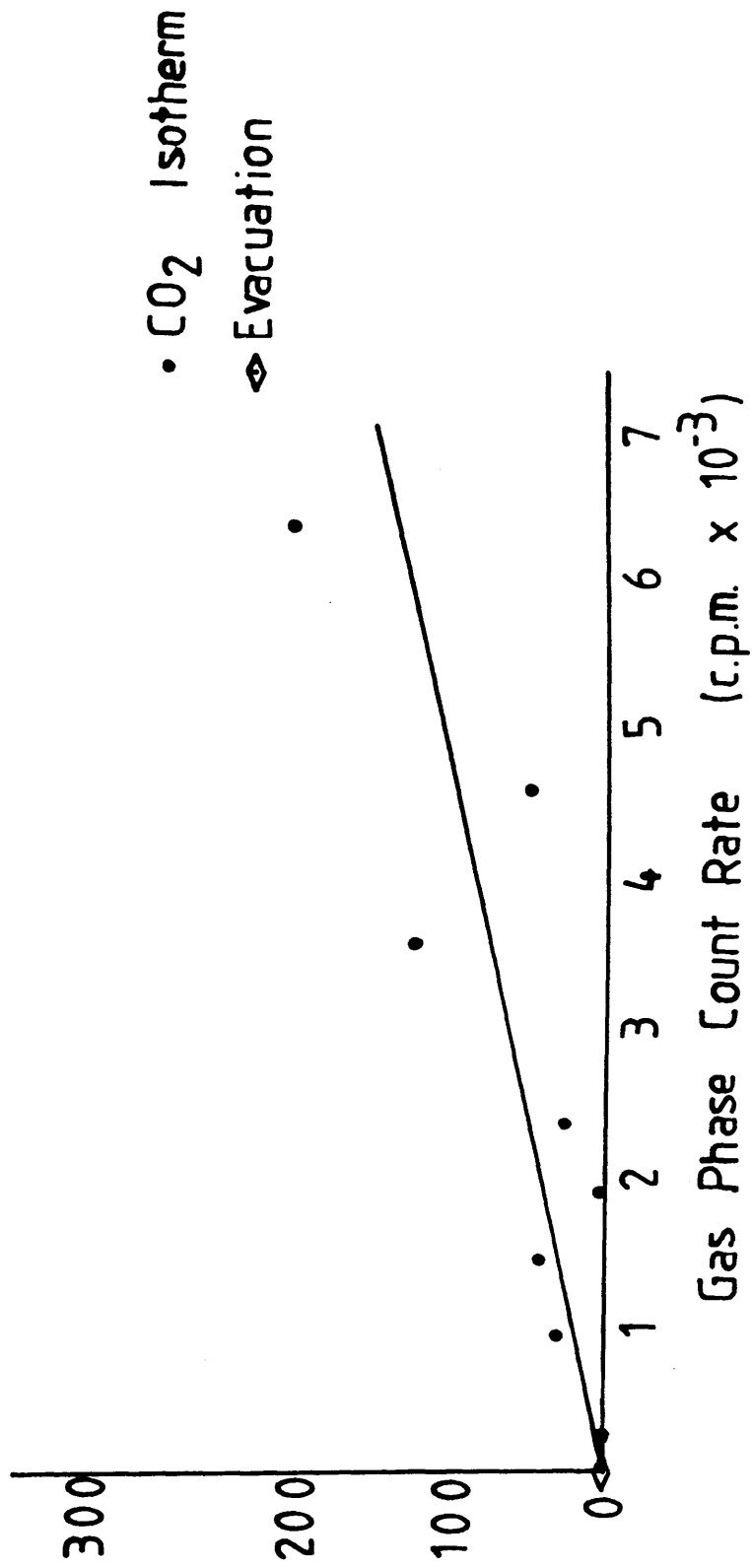
Upon evacuation, almost all of the adsorbed carbon dioxide was removed from the Rh/MoO₃ and Rh/SiO₂ catalysts, yet only 40% of that adsorbed on the Rh/Al₂O₃ catalyst was removed.

Table 5.6 Carbon Dioxide Adsorption 20°C

<u>Rh/Al₂O₃ (0.1934g)</u>	<u>Surface Count Rate</u>	
	cpm	Initial Count Rate
a) ¹⁴ CO ₂ adsorption (4.30 torr)	960	100
b) 30 mins evacuation	596	62.1
<u>5% Rh/SiO₂ (0.1749g)</u>		
a) ¹⁴ CO ₂ adsorption	222	100
b) 30 mins evacuation	0	0
<u>Rh/MoO₃ (0.4299g)</u>		
a) ¹⁴ CO ₂ adsorption	2135	100
b) 30 mins evacuation	31	1.5

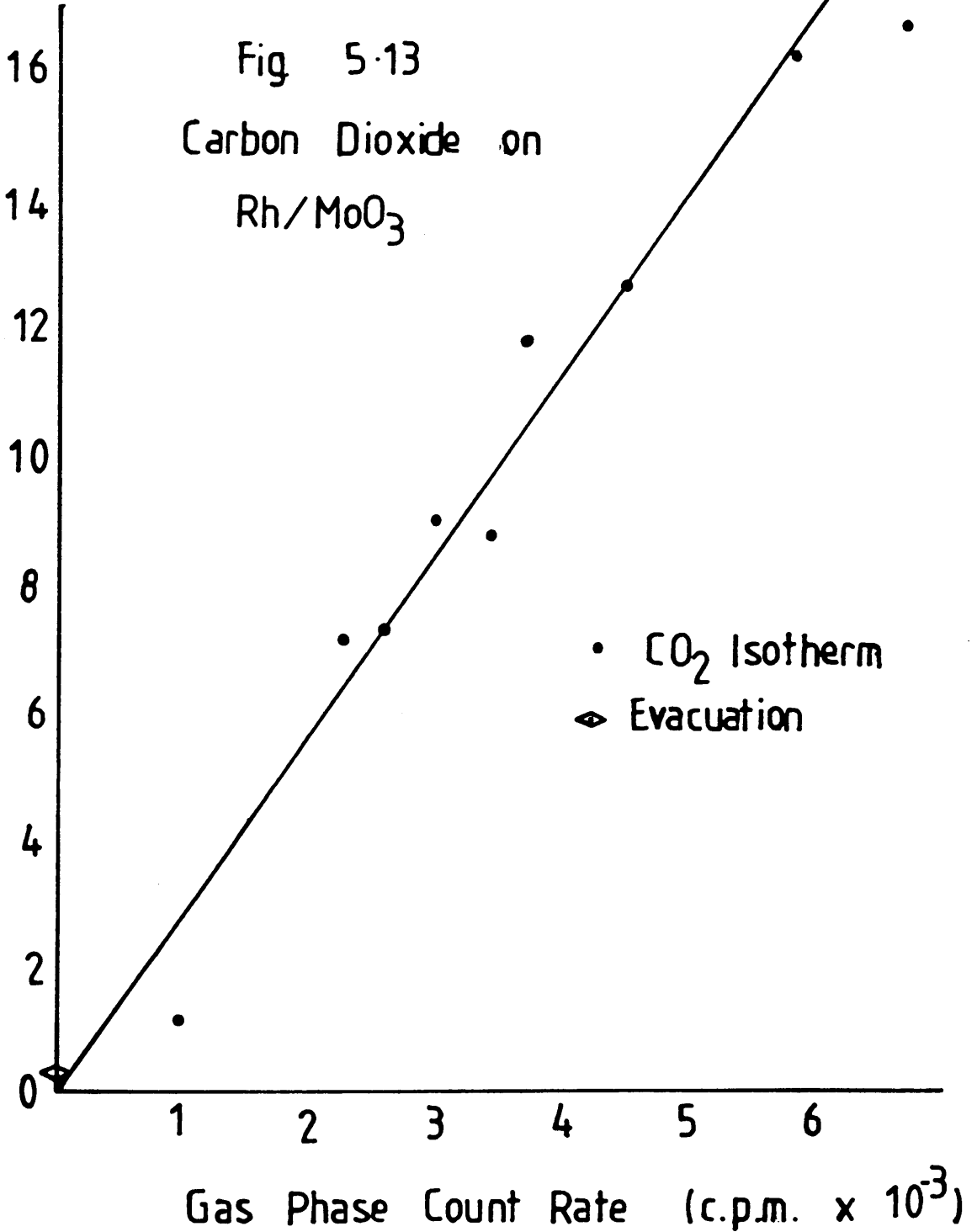
Fig. 5.12

Carbon Dioxide on 5% Rh/SiO₂



Surface Count
Rate
(c.p.m. $\times 10^{-2}$)

Fig 5.13
Carbon Dioxide on
Rh/MoO₃



5.3.2 MOLECULAR EXCHANGE

In these experiments, the catalyst surface was exposed to a measured amount of ^{14}C - carbon dioxide for a period of 2-3 hours. Unlabelled carbon dioxide was then admitted to the reaction vessel and the count rates determined, immediately, and after 3 hours, to determine if any exchange had taken place between labelled surface molecules and unlabelled gas phase ones.

Table 5.7 Molecular Carbon Dioxide Exchange
without Evacuation

Rh/ Al_2O_3 (0.4492g)	Surface Count Rate	Initial Count Rate
a) $^{14}\text{CO}_2$ adsorption(4.61 torr)	472.4	100
b) Admission of 3.92 torr of $^{12}\text{CO}_2$ - 3 hours	471.0	99.7
5% Rh/SiO₂ (0.2937g)		
a) $^{14}\text{CO}_2$ adsorption(4.39 torr)	214.9	100
b) Admission of 5.13 torr of $^{12}\text{CO}_2$ - 3 hours	215.8	100.4
Rh/MoO₃ (0.5377g)		
a) $^{14}\text{CO}_2$ adsorption(4.98 torr)	504.9	100
b) Admission of 4.44 torr of $^{12}\text{CO}_2$ - 3 hours	487.3	96.5

5.3.3 DESORPTION MEASUREMENTS

The same desorption experiments that were carried out for carbon monoxide desorption (section 5.2.3) were also attempted with carbon dioxide. However, carbon dioxide was so weakly bound to the surface that simple evacuation was sufficient to remove most of the surface material.

No ^{14}C -carbon monoxide was detected in the gas phase after any of the ^{14}C -carbon dioxide adsorption experiments. None of the supports adsorbed carbon dioxide,

The results of all the experiments detailed in this section are summarised in figs 5.14-5.16.

5.4 THE INFLUENCE OF HYDROGEN ON CARBON MONOXIDE ADSORPTION

When a catalyst saturated with ^{14}C -carbon monoxide was exposed to a known amount of hydrogen, the amount of carbon monoxide taken up by the surface immediately increased. After 1 hour the surface count rate for each of the catalysts had increased between 19 and 35% (Table 5.8).

Fig. 5.14

Carbon Dioxide Adsorption on Rh/Al₂O₃

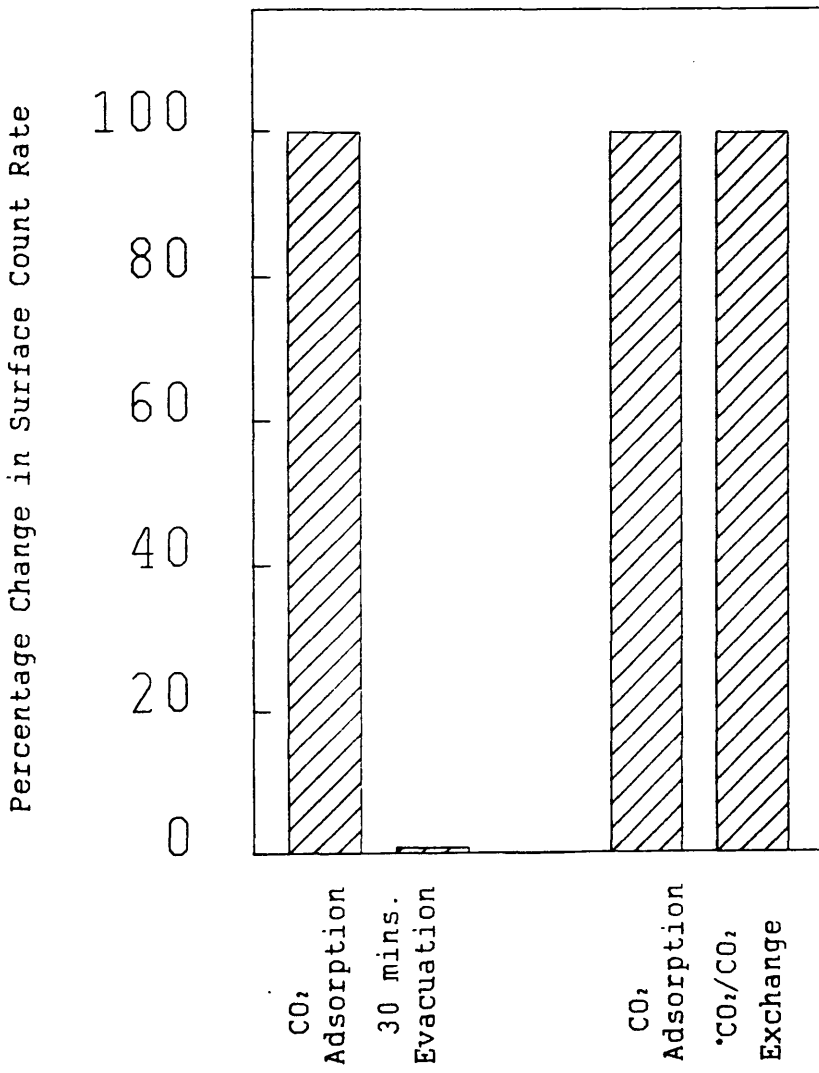


Fig. 5.15

Carbon Dioxide Adsorption on Rh/Al₂O₃

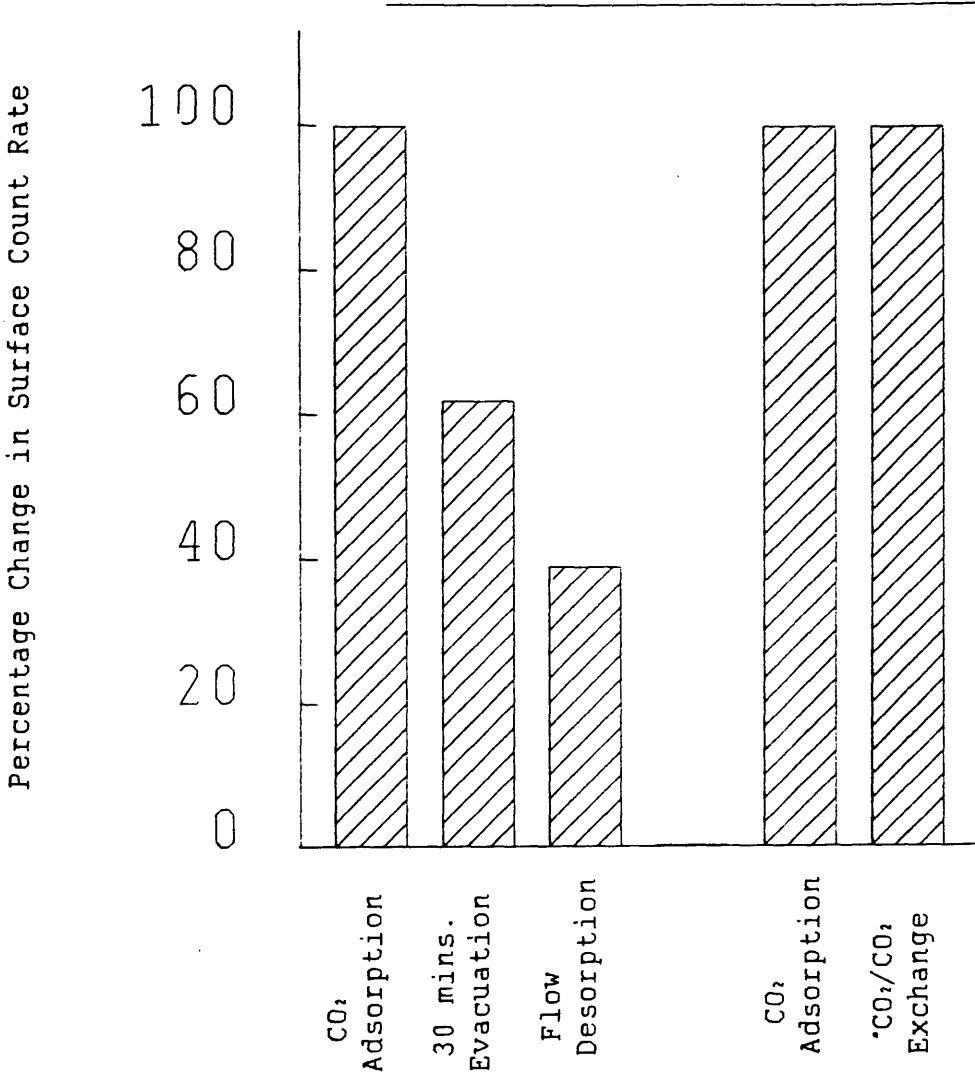


Fig. 5.16

Carbon Dioxide Adsorption on Rh/Al₂O₃

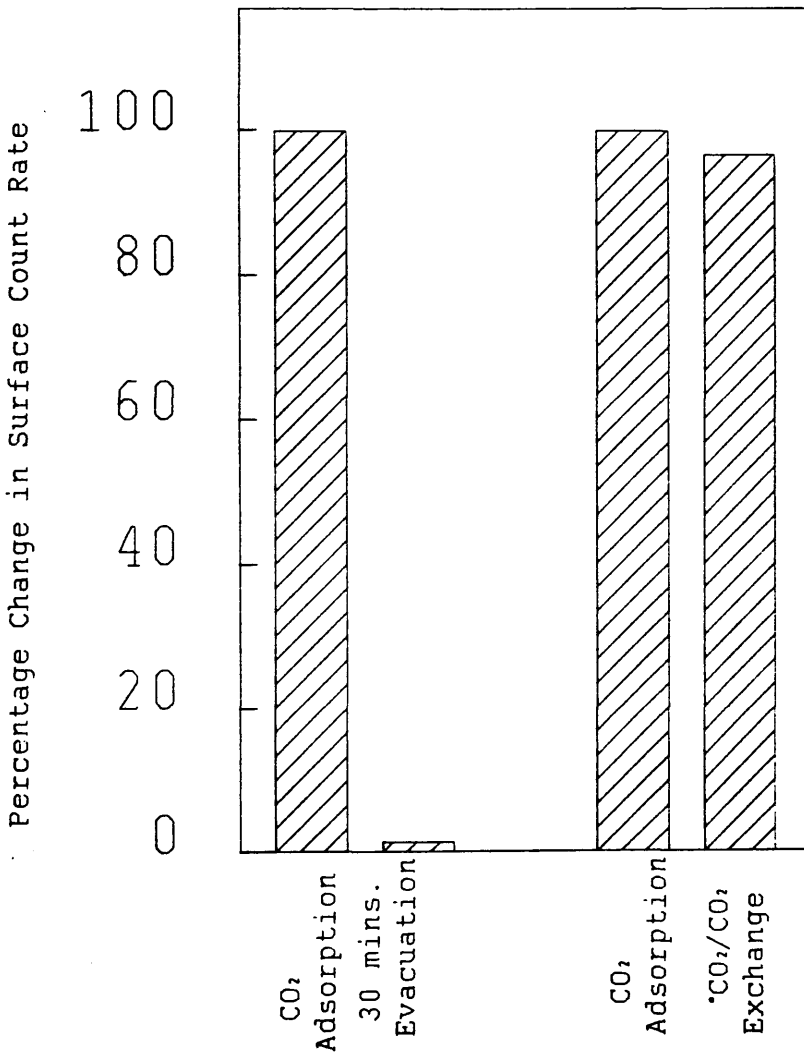


Table 5.8 The Influence of Hydrogen on Carbon Monoxide
Adsorption 20°C

Rh/Al ₂ O ₃ (0.2313g)	Surface Count Rate	Ratio of Initial Count Rate
a) Surface saturation with ¹⁴ C- ¹⁴ CO (4.47 torr)	13062	100
b) Admission of 3.75 torr of H ₂	15581	119
5% Rh/SiO₂ (0.2164g)		
a) Surface saturation with ¹⁴ C- ¹⁴ CO (11.4 torr)	11660	100
b) Admission of 4.29 torr of H ₂	15686	135
Rh/MoO₃ (0.5088g)		
a) Surface saturation with ¹⁴ C- ¹⁴ CO (3.83 torr)	831	100
b) Admission of 2.95 torr of H ₂	1066	128

5.5 THE INFLUENCE OF HYDROGEN ON CARBON DIOXIDE ADSORPTION

In these experiments a catalyst sample covered with ¹⁴C-carbon dioxide was exposed to a measured amount of pure hydrogen. The results are shown in table 5.9.

**Table 5.9 The Influence of Hydrogen on Carbon Dioxide
Adsorption 20°C**

Rh/ Al_2O_3 (0.1934g)	Surface Count Rate	%age of Initial Count Rate
a) $^{14}\text{CO}_2$ Adsorption (3.57 torr)	89.9	100
b) Admission of 2.04 torr of H_2 - overnight	99.3	111
5% Rh/SiO_2 (0.1749g)		
a) $^{14}\text{CO}_2$ Adsorption (4.42 torr)	52.3	100
b) Admission of 3.62 torr of H_2 - 3 hours	71.8	137
Rh/MoO_3 (0.4299g)		
a) $^{14}\text{CO}_2$ Adsorption (4.22 torr)	766	100
b) Admission of 6.93 torr of H_2 - 2 hours	734	95.8

An increase in the surface count rates of both the Rh/ SiO_2 and Rh/ Al_2O_3 catalysts was detected, whilst that of the Rh/ MoO_3 sample decreased slightly. It should, however, be noted that the error on the Rh/ SiO_2 count rate was fairly large ($\pm 14\%$), due to the low number of counts detected.

5.6 THE INFLUENCE OF PRE-ADSORBED CARBON DIOXIDE ON ^{14}C -CARBON MONOXIDE ADSORPTION

After equilibrating a catalyst sample with unlabelled carbon dioxide, a ^{14}C -carbon monoxide isotherm was determined to investigate the effect of pre-adsorbed carbon dioxide on carbon monoxide adsorption. Since the gas phase carbon dioxide was not evacuated before ^{14}C carbon monoxide

was admitted, the carbon monoxide was adsorbing competitively on to a fully saturated surface. The isotherms obtained are shown in figs 5.17-5.19.

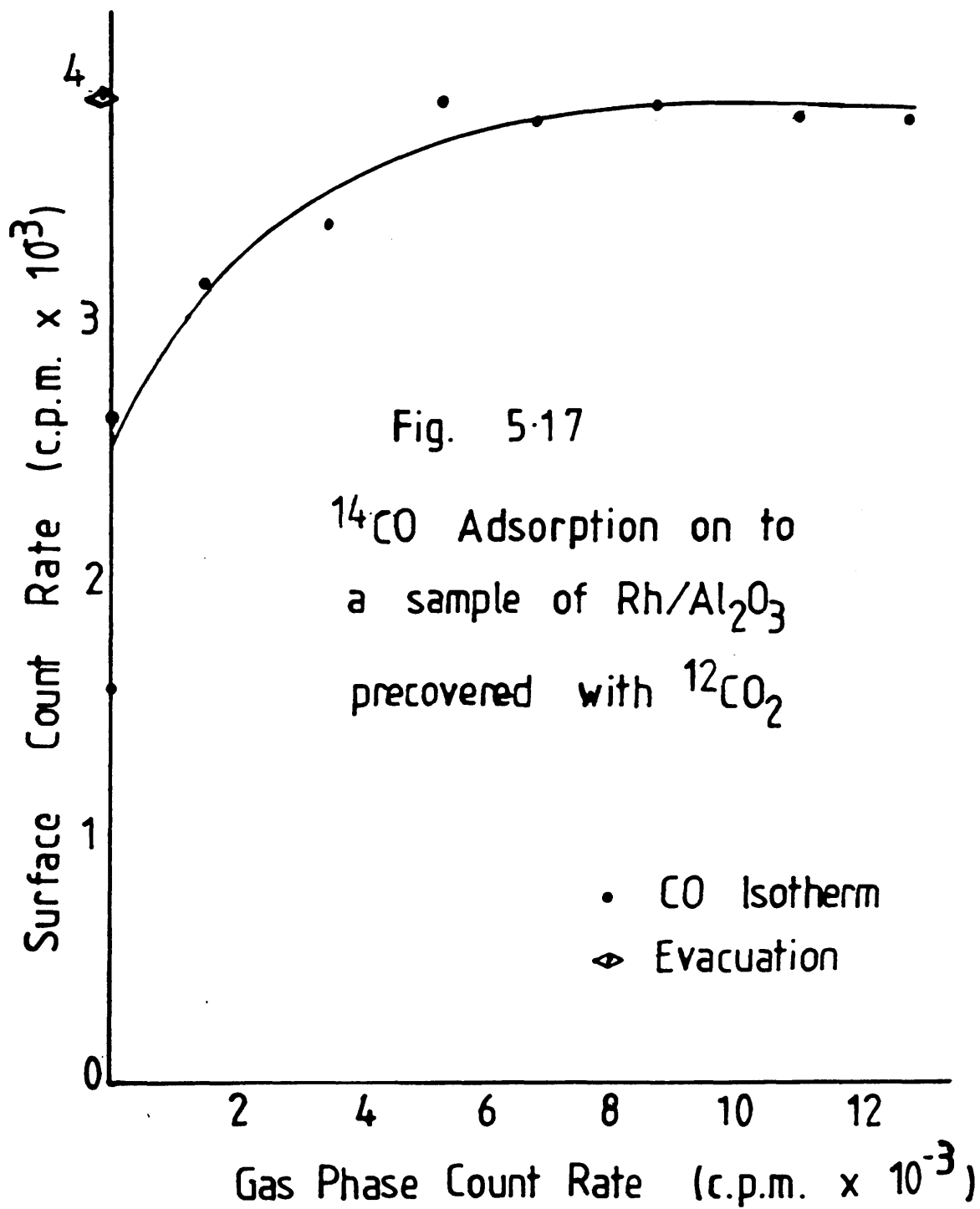
In each case, the shape of the isotherm was very similar to that obtained when no carbon dioxide was present. However, the amount of carbon monoxide adsorbed (maximum count rate) was somewhat less than that adsorbed during a typical carbon monoxide isotherm, such as those shown in fig 5.1-5.3.

It would be unwise to quantitatively compare the results of experiments carried out with this apparatus on two different catalyst samples. However, the figures quoted in table 5.10 strongly suggest that, at least for the Rh/Al₂O₃ and Rh/SiO₂ catalysts, pre-adsorbed carbon dioxide has blocked some carbon monoxide adsorption. To aid the comparison between catalysts the maximum count rates quoted in table 5.10 have been quoted as counts per minute per gram of rhodium present.

Table 5.10 The Influence of Preadsorbed Carbon Dioxide

	<u>on ¹⁴C - Carbon Monoxide Adsorption</u>					
	Rh/SiO ₂ MCR	%	Rh/Al ₂ O ₃ MCR	%	Rh/MoO ₃ MCR	%
¹⁴ CO Adsorption	712126	100	262838	100	41964	100
¹⁴ CO Adsorption in the presence of Preadsorbed CO ₂	149059	21	149655	57	44112	105

(MCR = Maximum Count Rate)



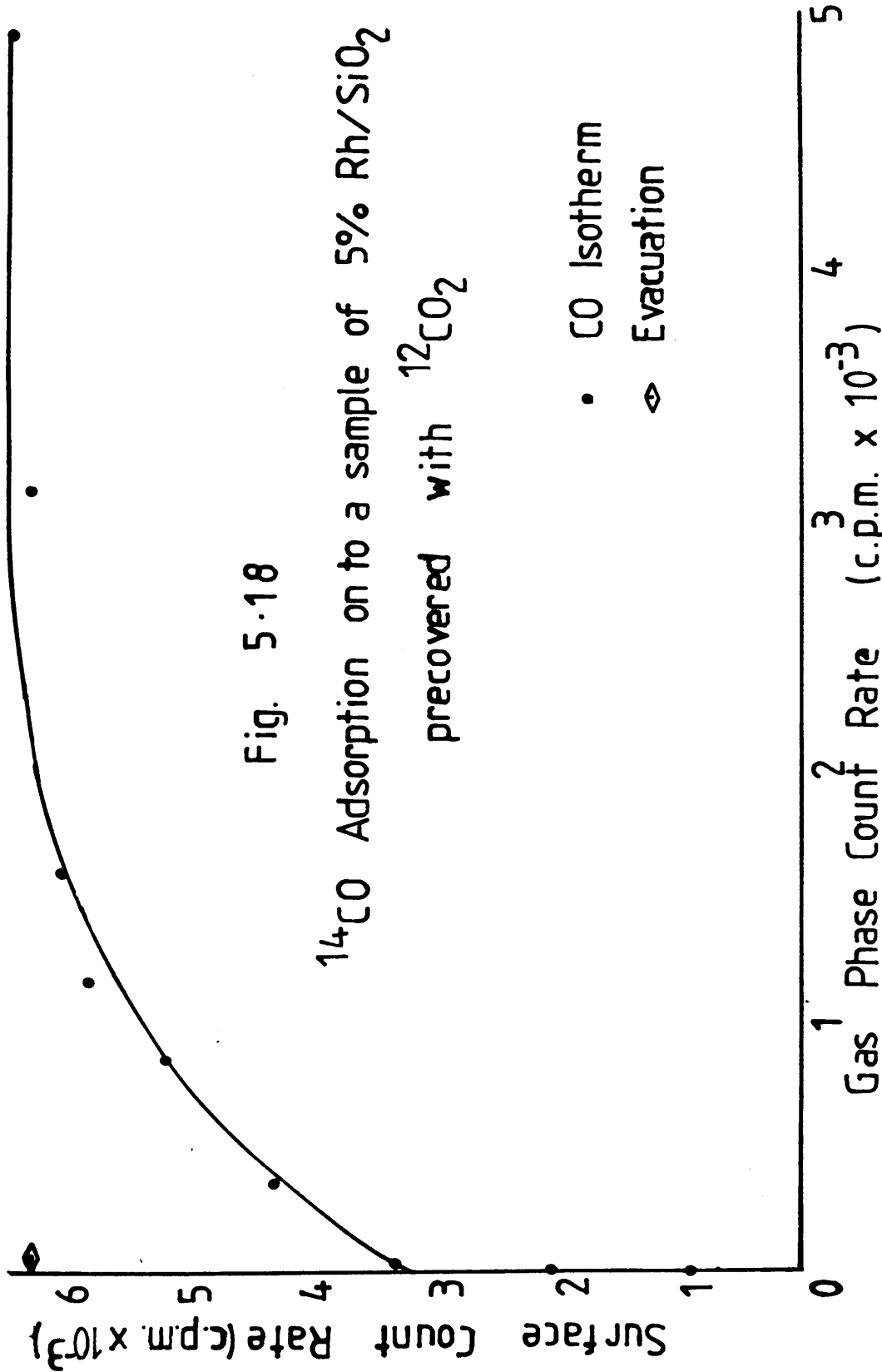
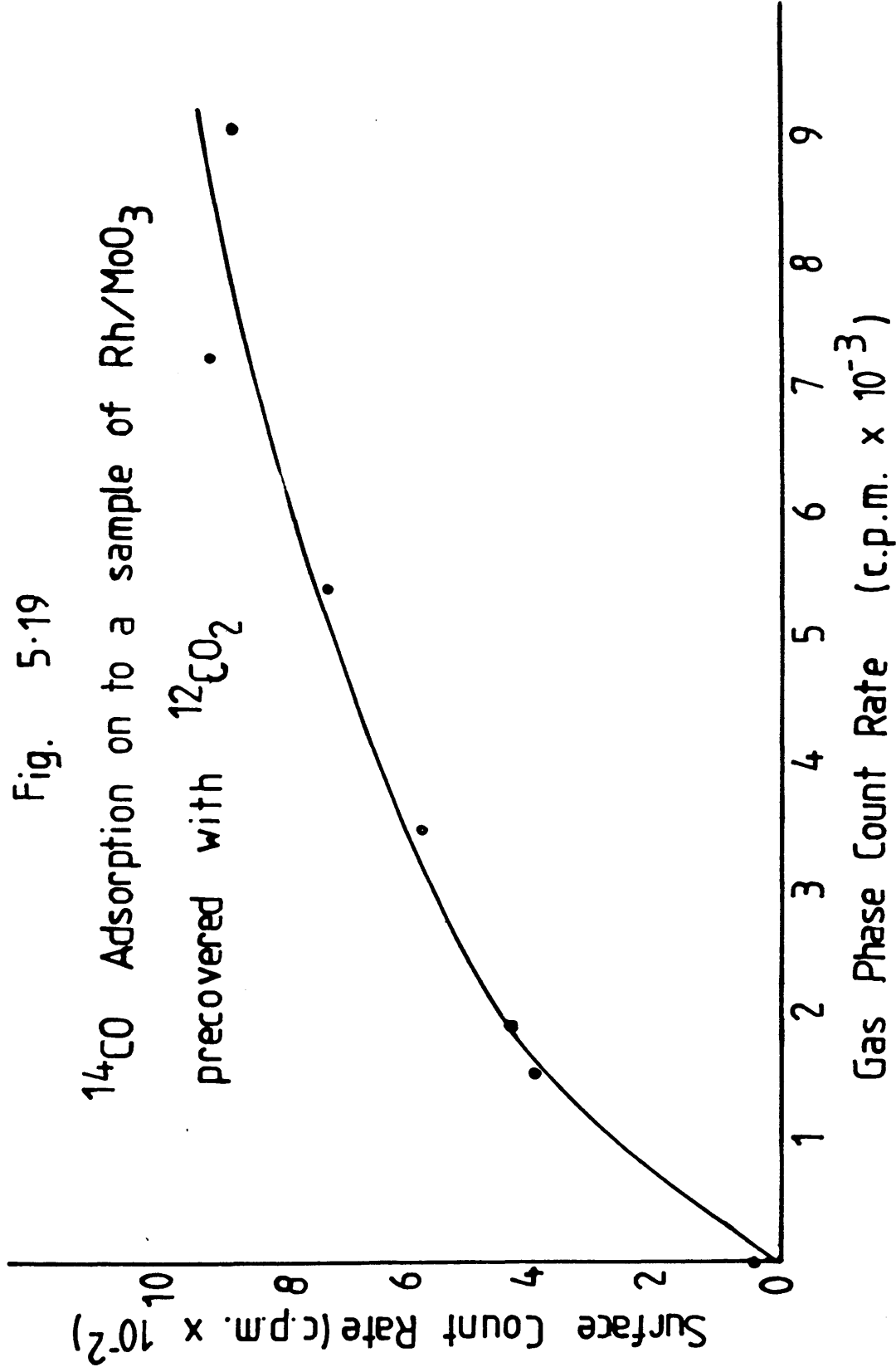


Fig. 5-19

^{14}CO Adsorption on to a sample of Rh/MoO_3

precovered with $^{12}\text{CO}_2$



The small increase in the amount of carbon monoxide adsorbed by the Rh/MoO₃ catalyst is within the experimental error of the experiment.

5.7 THE INFLUENCE OF PRE-ADSORBED CARBON MONOXIDE ON ¹⁴C-CARBON DIOXIDE ADSORPTION

The effect of preadsorbed carbon monoxide on carbon dioxide adsorption was investigated in exactly the same way as that of preadsorbed carbon dioxide on carbon monoxide adsorption. A freshly reduced sample of catalyst was exposed to unlabelled carbon monoxide, before a ¹⁴C - carbon dioxide isotherm was determined (fig 5.20 - 5.22). The shape of the isotherms were again similar to those obtained in the absence of carbon monoxide, although the Rh/MoO₃ isotherm is rather more curved than before. When these results are compared with those of isotherms determined in the absence of carbon monoxide the results are rather interesting (Table 5.11)

Table 5.11 The Influence of Preadsorbed Carbon Monoxide
on ¹⁴C - Carbon Dioxide Adsorption

	Rh/SiO ₂		Rh/Al ₂ O ₃		Rh/MoO ₃	
	MCR	%	MCR	%	MCR	%
¹⁴ CO ₂ Adsorption	52251	100	6206	100	62078	100
¹⁴ CO ₂ Adsorption in the presence of Preadsorbed CO	3391	6.5	11740	189	96145	155

(MCR = Maximum Count Rate)

Fig. 5.20

$^{14}\text{CO}_2$ Adsorption on a sample of $\text{Rh}/\text{Al}_2\text{O}_3$
precovered with ^{12}CO

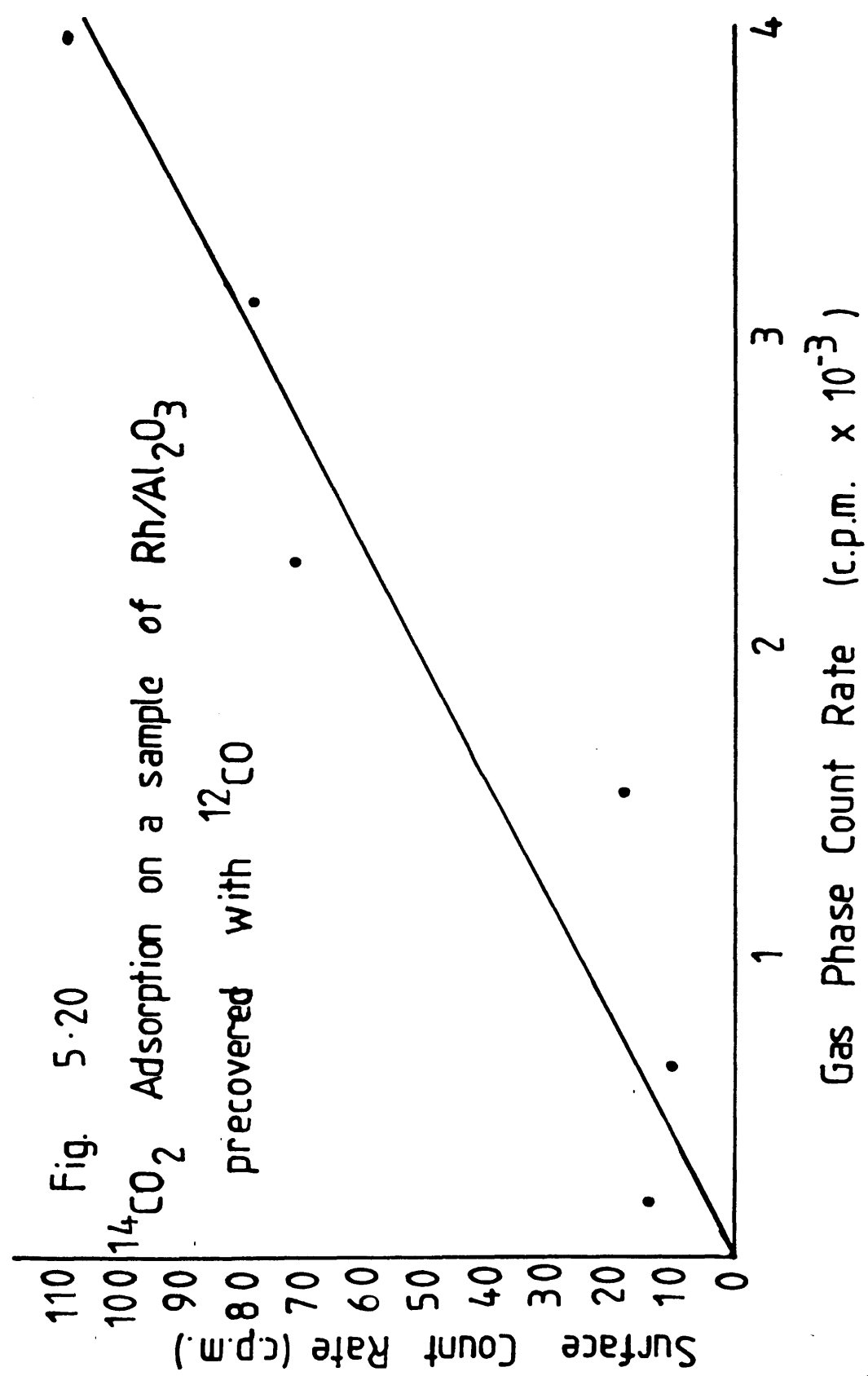
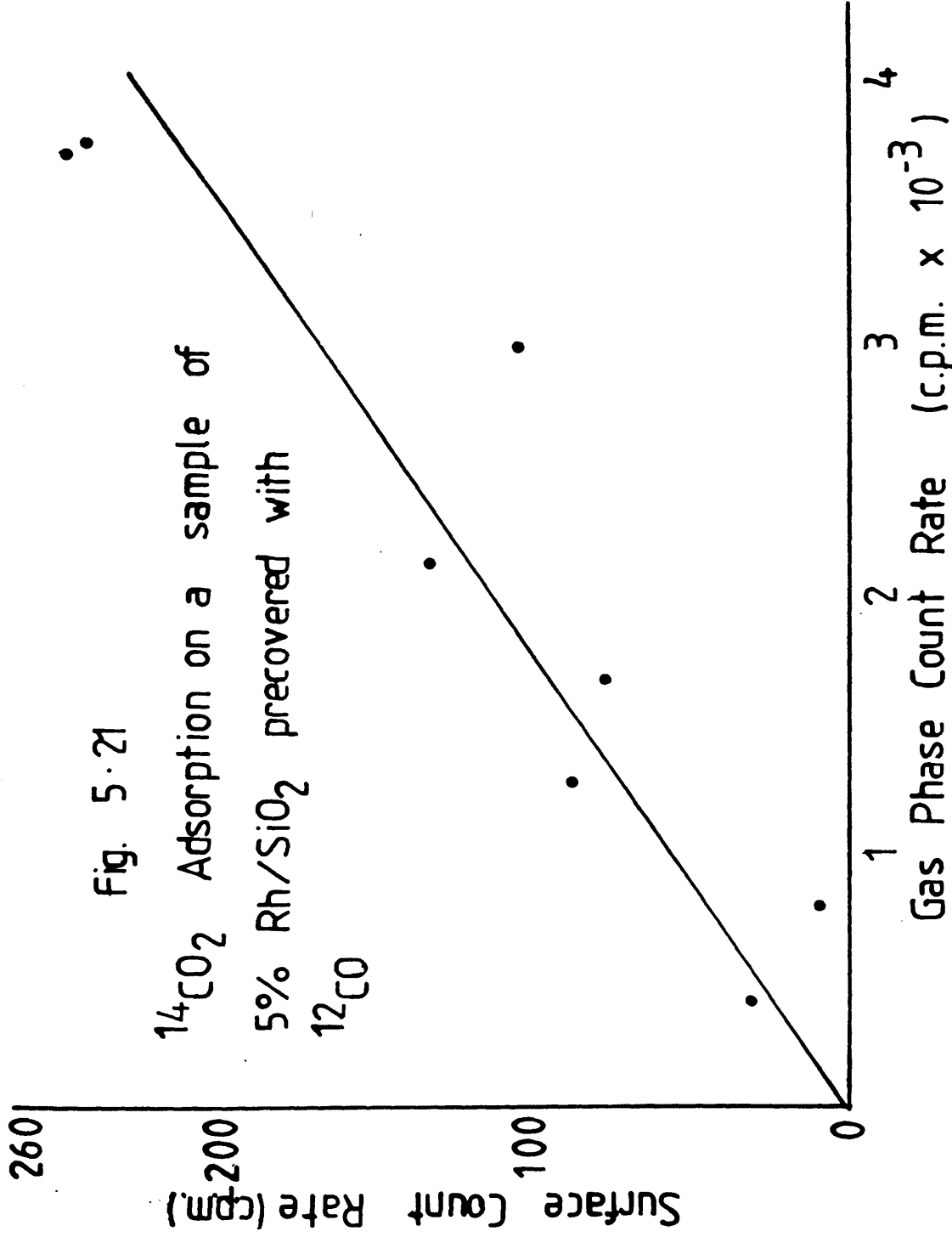


Fig. 5.21

$^{14}\text{CO}_2$ Adsorption on a sample of
5% Rh/SiO₂ precovered with
 ^{12}CO



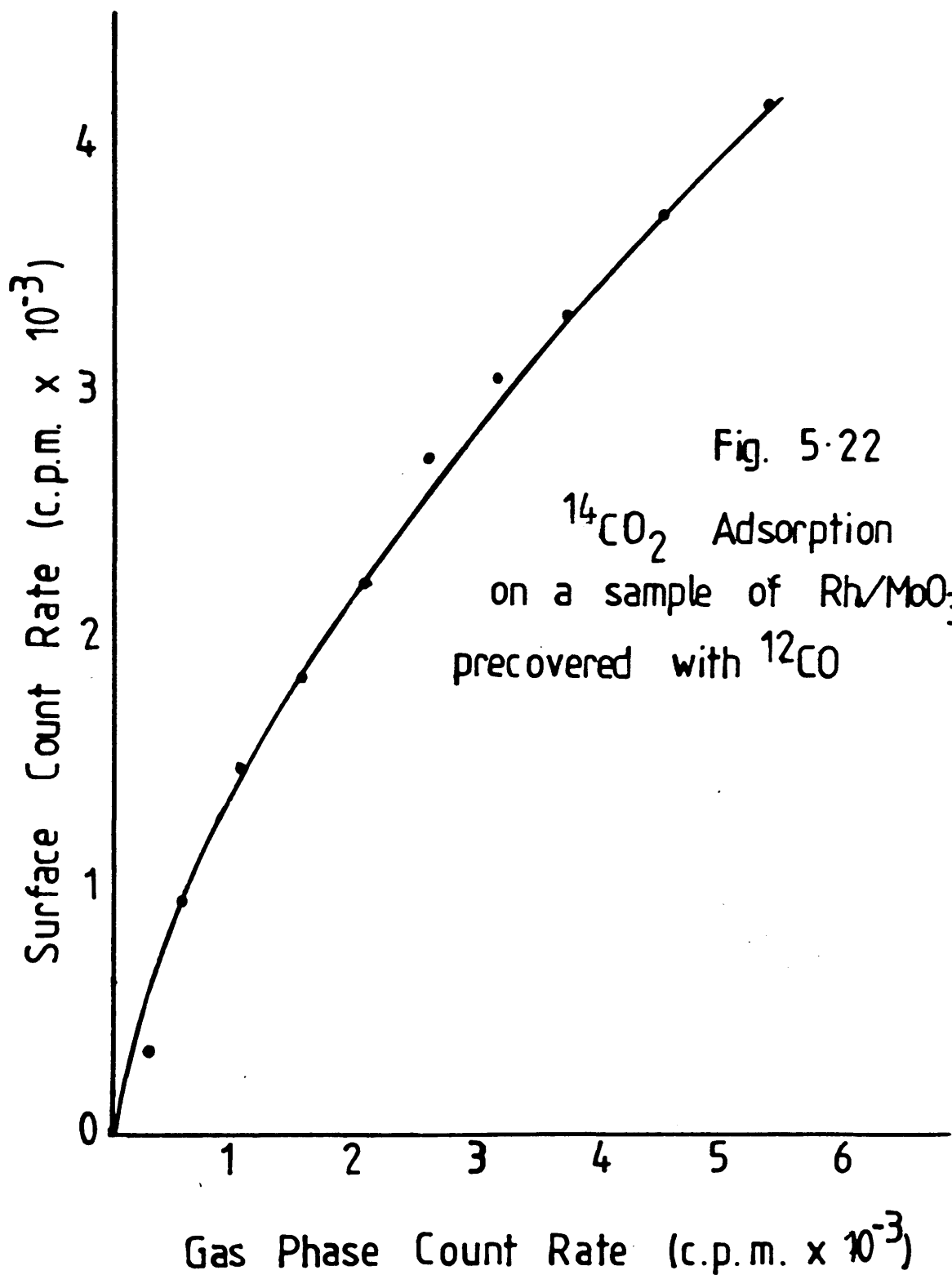


Fig. 5-22
 $^{14}\text{CO}_2$ Adsorption
on a sample of Rh/MoO_3
precovered with ^{12}CO

The maximum count rates are again quoted in counts per minute (cpm) per gram of rhodium. The amount of carbon dioxide adsorbed on a precovered sample of Rh/Al₂O₃ was dramatically reduced compared to that adsorbed on to a freshly reduced sample. On the other hand the amount of carbon dioxide adsorbed by the other two catalysts increased in the presence of carbon monoxide.

The results described in sections 5.4 - 5.7 are summarised in figures 5.23 - 5.25.

5.8 THE INFLUENCE OF OXYGEN ON CARBON MONOXIDE ADSORPTION

The effects of oxygen on carbon monoxide adsorption were investigated in three different ways. Freshly reduced samples of catalyst were exposed to a measured amount of oxygen for 30 minutes, to form a preoxidised surface, before being evacuated for 30 minutes. A ¹⁴C - carbon monoxide isotherm was then determined, this was then followed by a second period of evacuation and a second isotherm. When saturation had been reached a known amount of oxygen was admitted in to the reaction vessel to measure any exchange or displacement of surface carbon monoxide caused by the gas phase oxygen. After 60 minutes the gas phase was evacuated and a second charge of oxygen added to the reaction vessel. The adsorption of carbon monoxide was then investigated by building up a third isotherm, in the presence of this gas phase oxygen.

Fig. 5.23

Hydrogen, Carbon Monoxide
and Carbon Dioxide Adsorption

on Rh/Al₂O₃

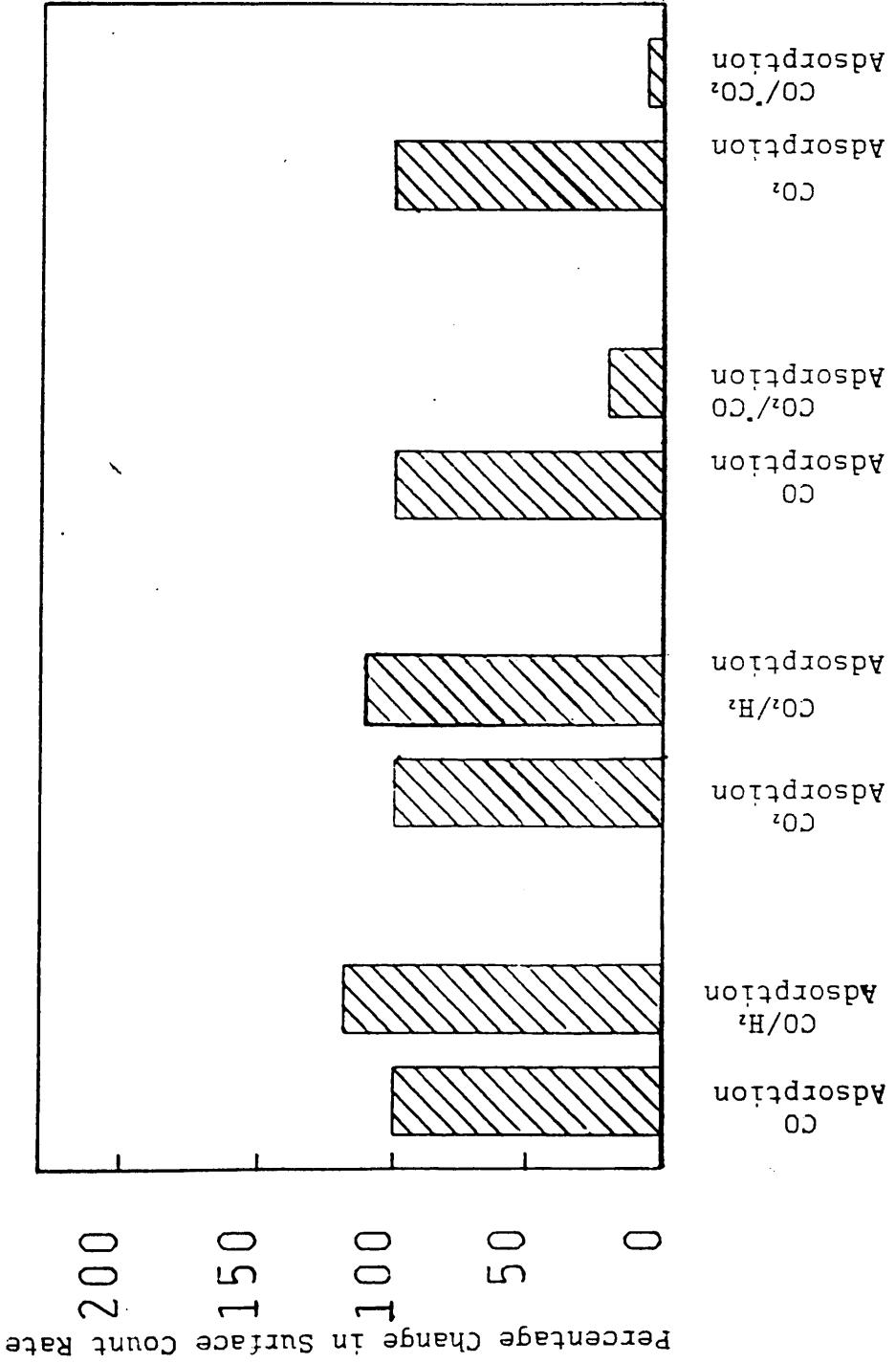
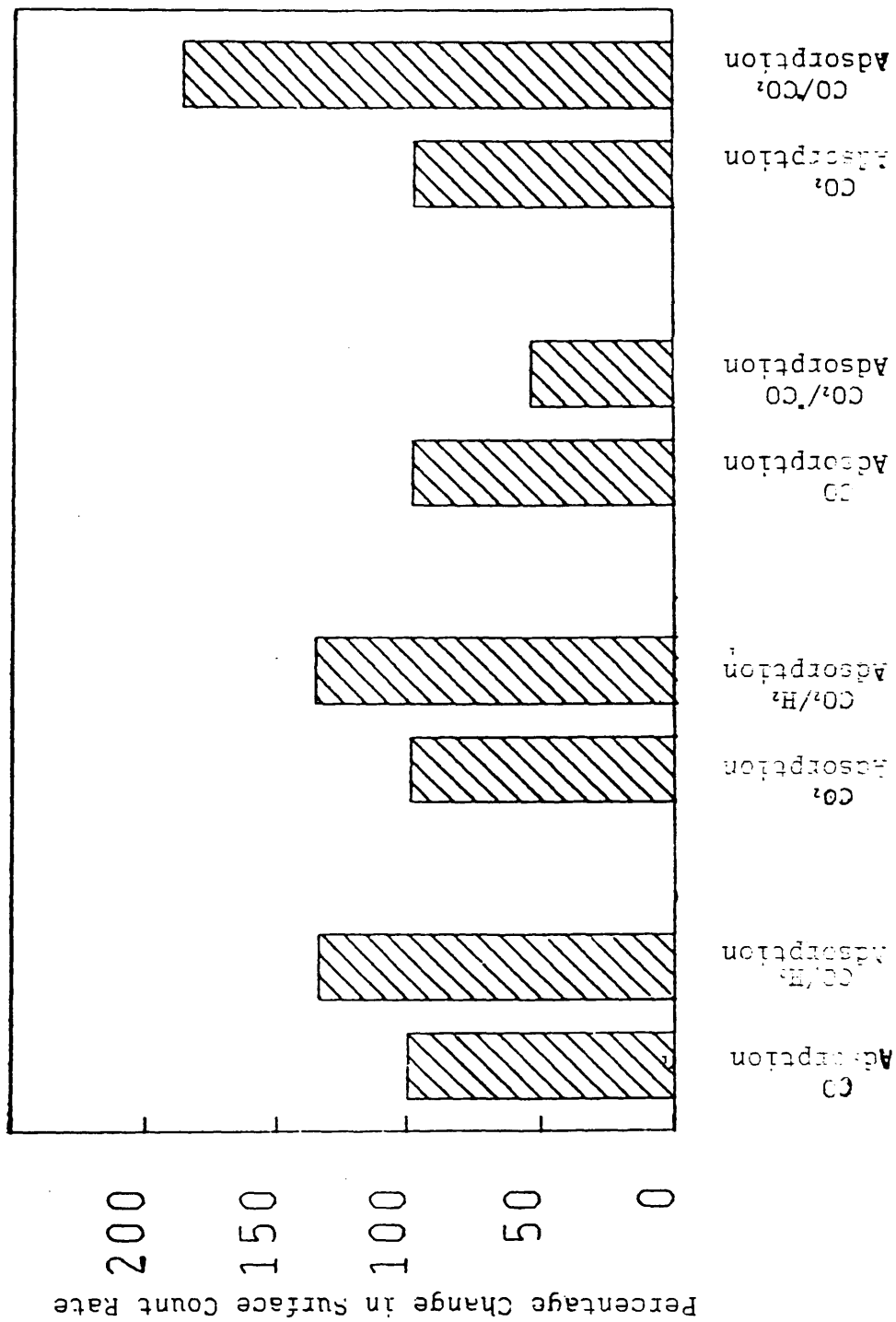


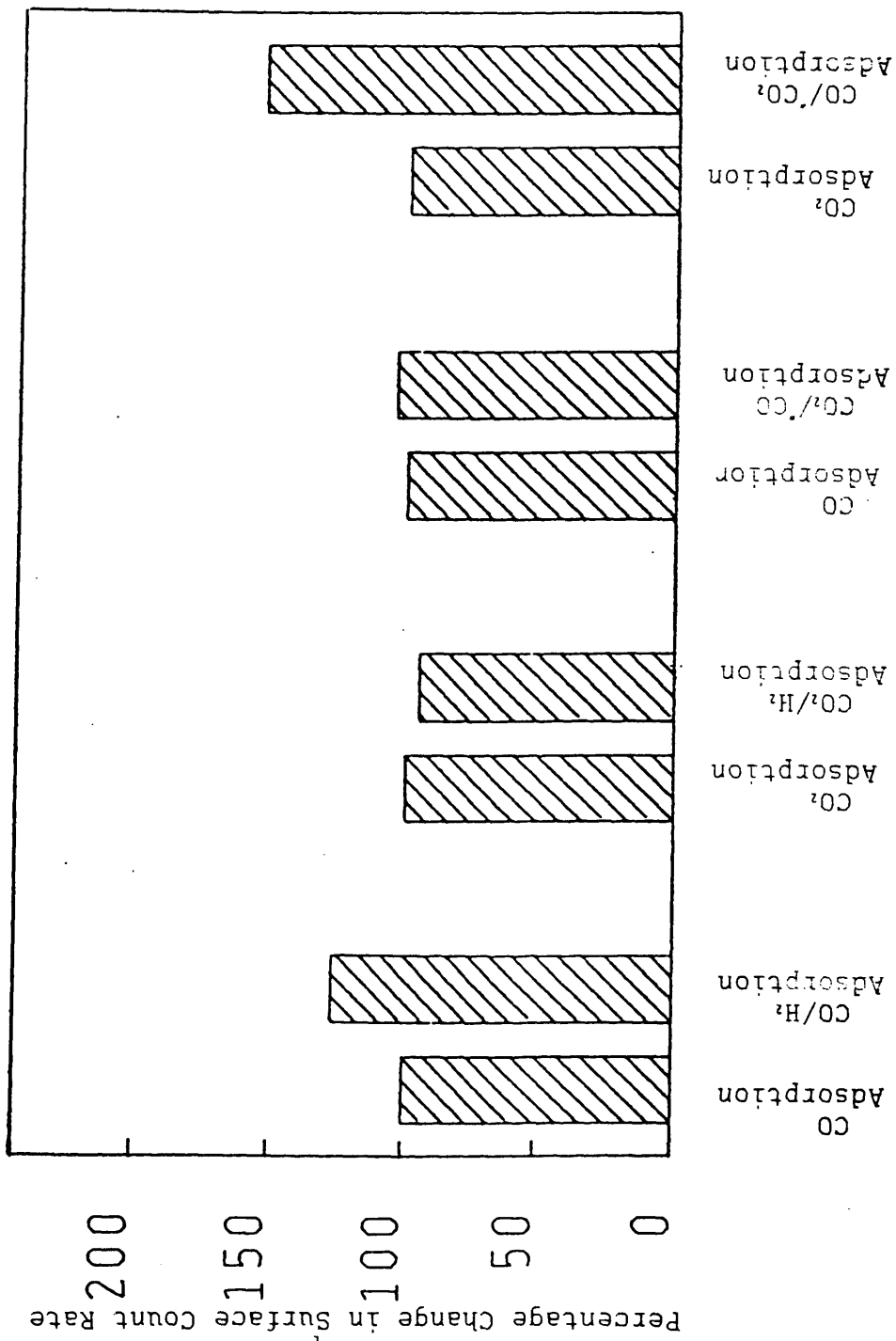
Fig. 5.24

Hydrogen, Carbon Monoxide
and carbon Dioxide
Adsorption on Rh/SiO₂



Fig, 5.25

Hydrogen, Carbon Monoxide
and Carbon Dioxide
Adsorption on Rh/MoO₃



All three catalysts adsorbed significant quantities of carbon monoxide even when the surface had been oxidised (fig 5.26-5.28). However, less carbon monoxide was adsorbed than on the freshly reduced sample and higher pressures of carbon monoxide were necessary to reach saturation with the Rh/SiO₂ and Rh/Al₂O₃ catalysts. The Rh/MoO₃ catalyst adsorbed much more carbon monoxide after oxidation, with a higher proportion of the adsorbed material being stable to evacuation on the preoxidised samples of Rh/MoO₃ than on the fully reduced ones. Only 13% of the surface ¹⁴C could be removed by evacuation from the oxidised catalyst, compared to 93% of that adsorbed on to the reduced samples. A comparison between the behavior of the oxidised and reduced catalysts is shown in figure 5.29.

No exchange was observed between surface carbon monoxide and gas phase oxygen, but after 60 minutes in the presence of oxygen the surface count rate had increased significantly.

Carbon monoxide isotherms determined in the presence of gas phase oxygen, showed a linear increase in the surface count rate with the pressure of carbon monoxide in the reaction vessel. Significantly more carbon monoxide was adsorbed under these conditions, than on the preoxidised surfaces, by each of the three catalysts.

The Key to Figs. 5.26 - 28

- CO Adsorption on a Pre-oxidised Surface
- x CO Adsorption after Evacuation
- ⊙ Co-Adsorption of CO and O₂

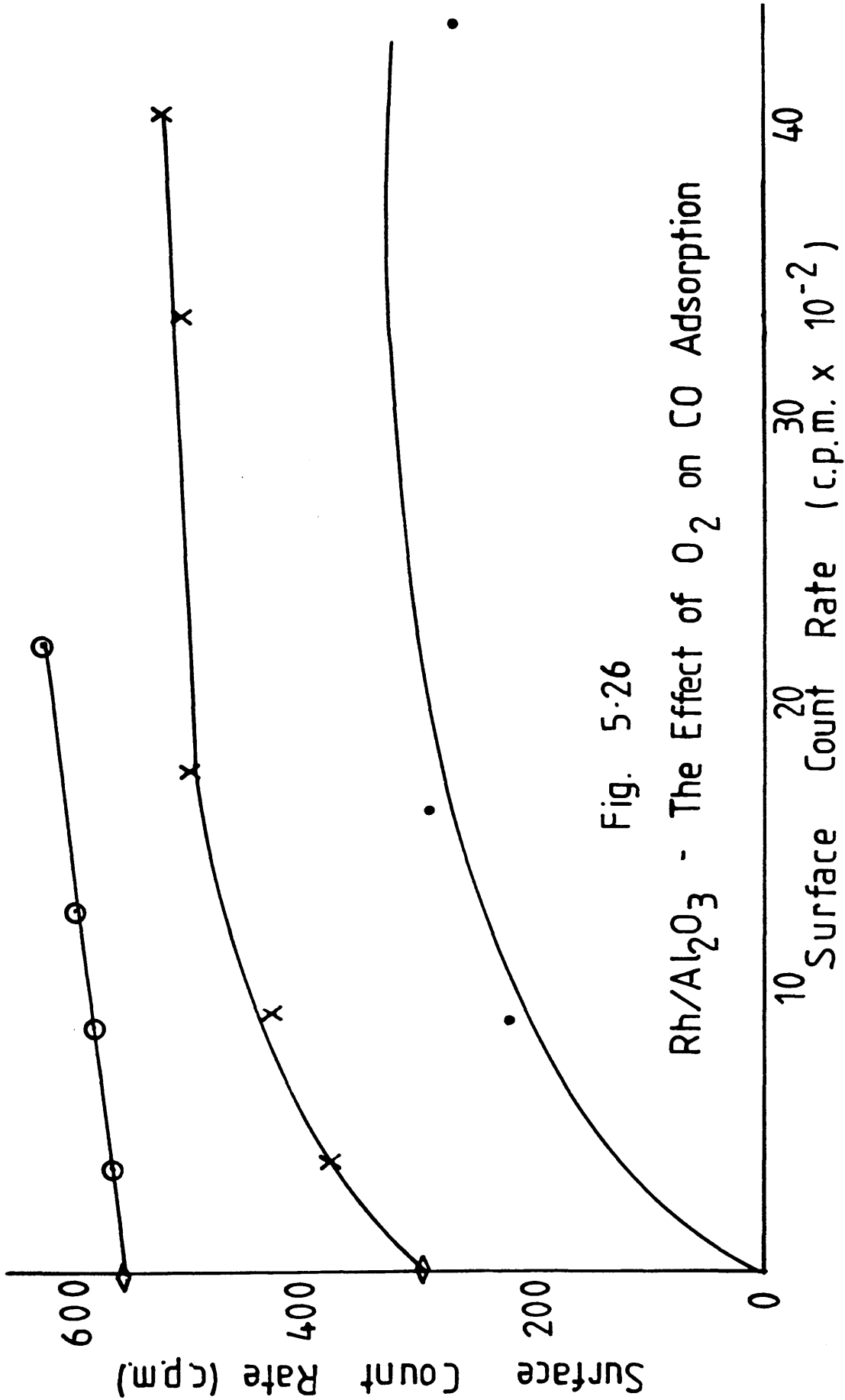
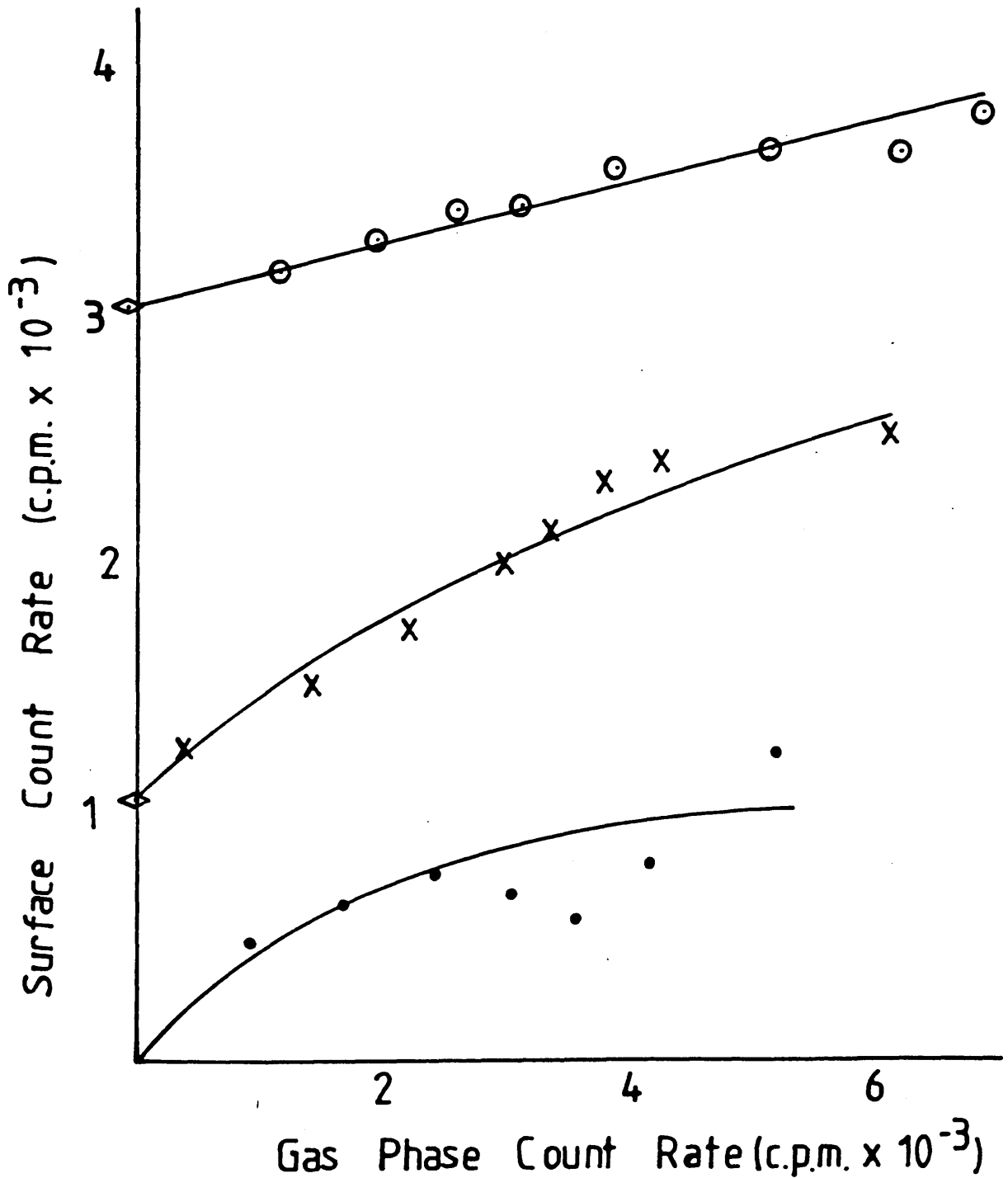


Fig. 5-26

Rh/Al₂O₃ - The Effect of O₂ on CO Adsorption

Fig. 5.27

The Effect of O_2 on the Adsorption of
CO on to 2% Rh/SiO₂



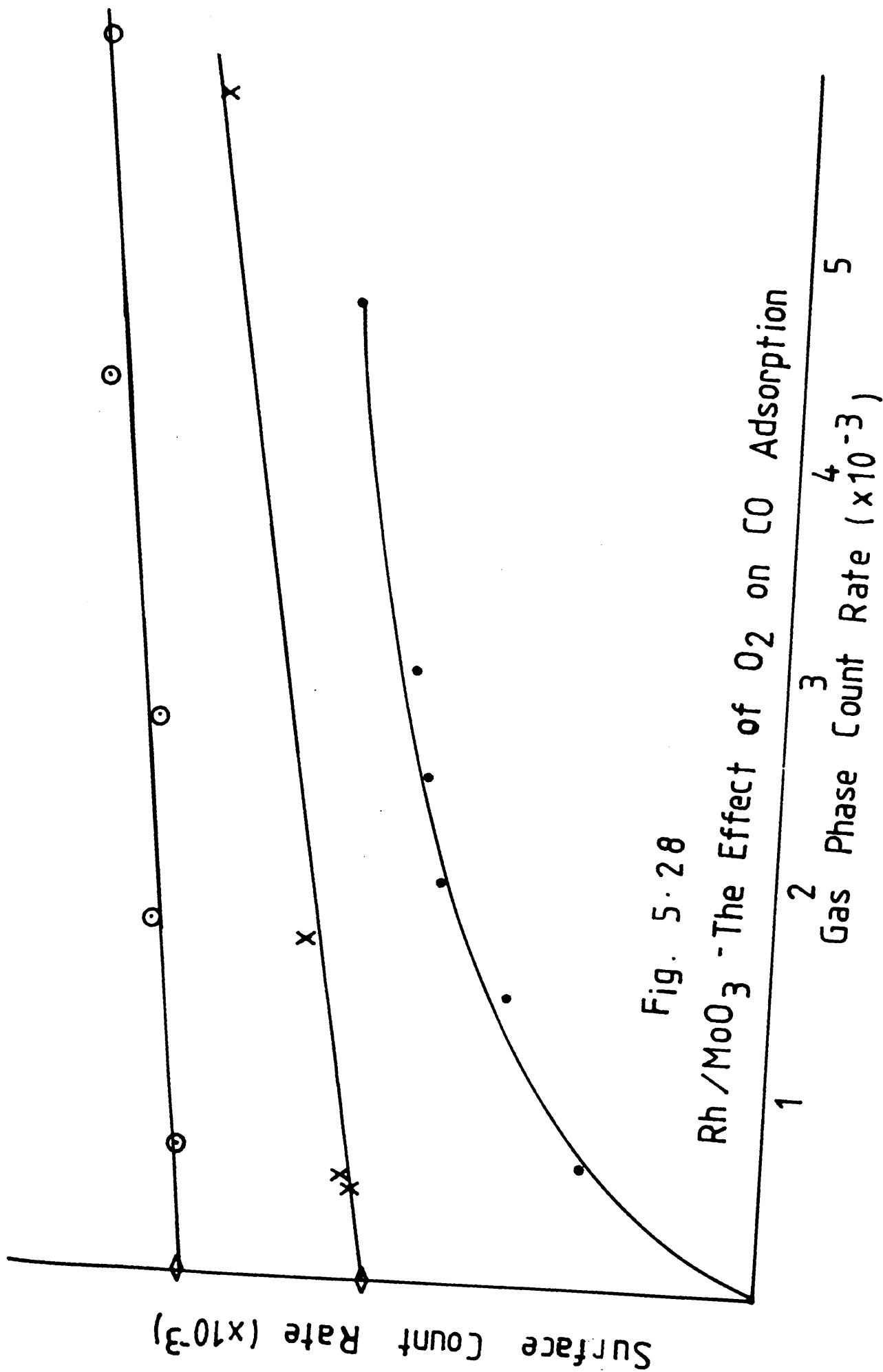


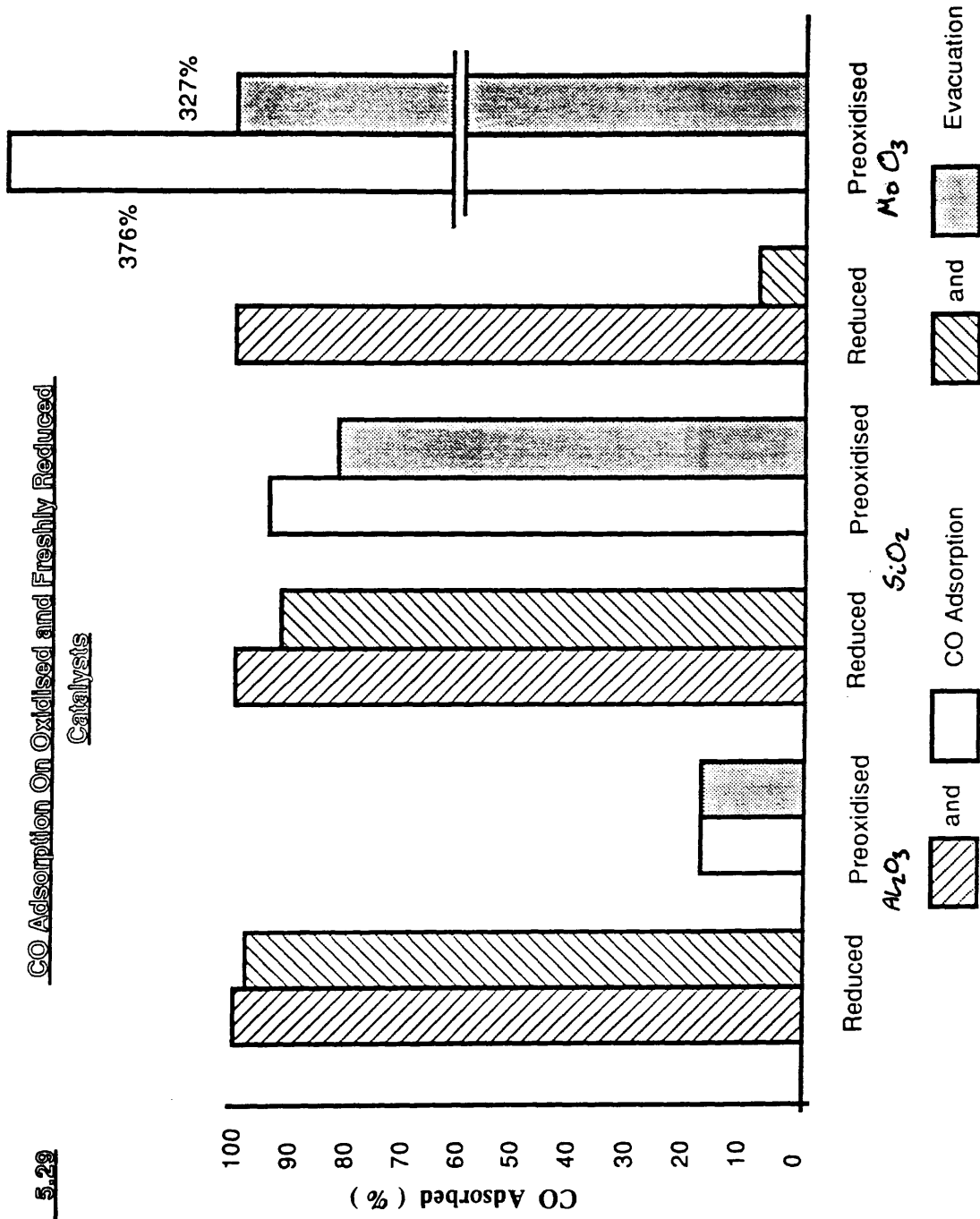
Fig. 5.28

Rh / MoO₃ - The Effect of O₂ on CO Adsorption

Gas Phase Count Rate ($\times 10^{-3}$)

Fig. 5.29

CO Adsorption On Oxidised and Freshly Reduced Catalysts



5.9 THE INFLUENCE OF OXYGEN ON CARBON DIOXIDE ADSORPTION

The procedure used in these experiments was identical to that described in section 5.8. Carbon dioxide adsorption was measured on a preoxidised surface and in the presence of oxygen. Carbon dioxide - oxygen exchange was also investigated (fig 5.30-5.32).

The adsorption of carbon dioxide by all three catalysts was severely limited by the oxidation procedure. The isotherms show a rather wide scatter of point because the low count rates being measured meant that each measurement has a fairly large error. This makes it difficult to obtain a clear picture of what is happening at the catalyst surface. Surface oxidation appears to have a more profound and longer lived effect on carbon dioxide adsorption than it does on carbon monoxide. Co-adsorption of carbon dioxide and oxygen, decreased the amount of carbon dioxide adsorbed on the surface from that which would adsorb on the preoxidised catalyst.

5.10 REPEATED REDUCTIONS

In these experiments the effects of repeated reduction cycles on carbon monoxide adsorption were investigated to determine whether a catalyst sample could be re-used. This was desirable as it would eliminate some of the variables, such as sample size, between experiments.

The Key to Figs. 5.30-32

- CO Adsorption on a Pre-oxidised Surface
- x CO Adsorption after Evacuation
- ⊙ Co-Adsorption of CO and O₂

Fig. 5.30

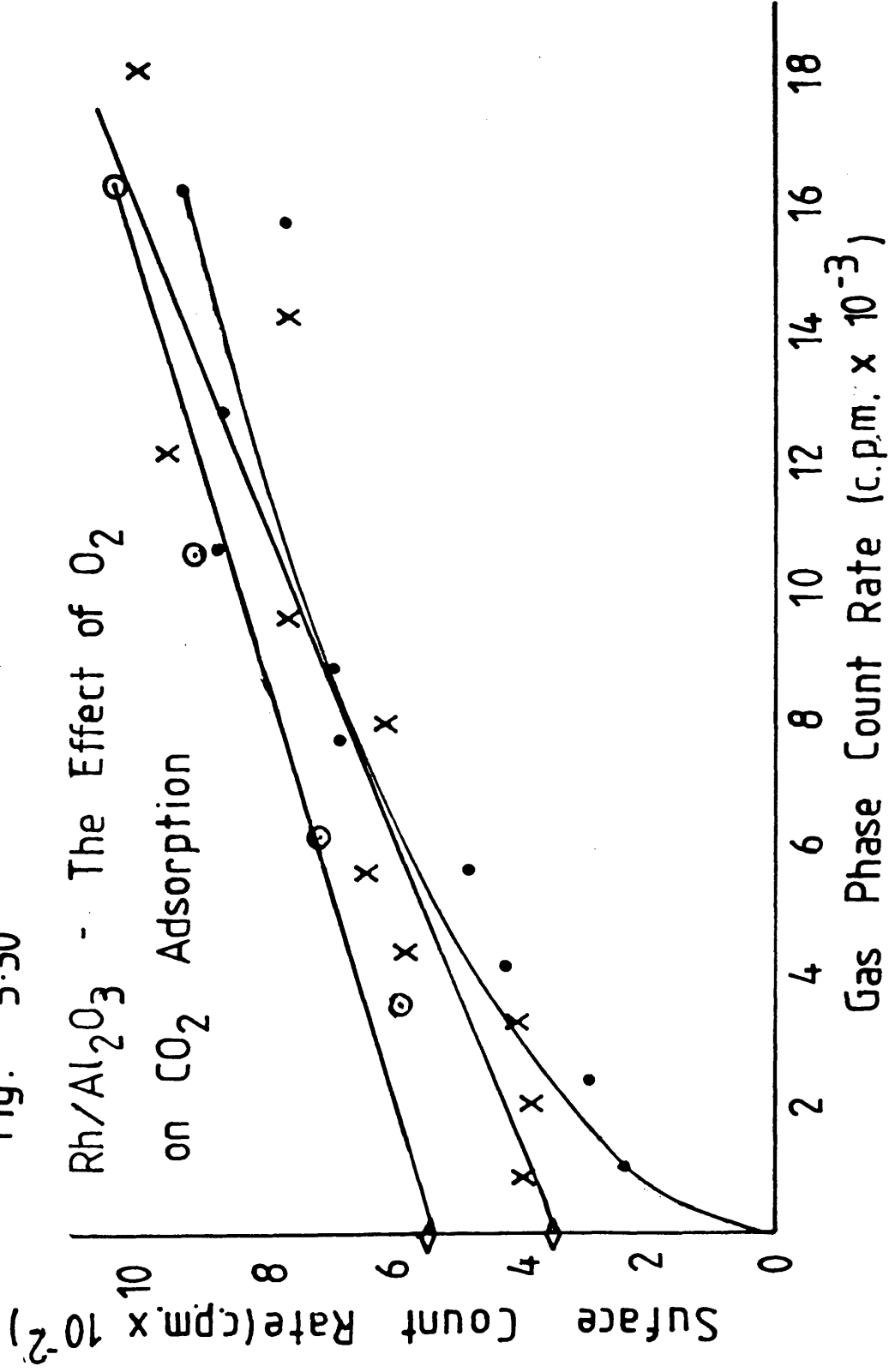


Fig. 5-31
 2% Rh/SiO₂ - The Effect
 of O₂ on CO₂ Adsorption

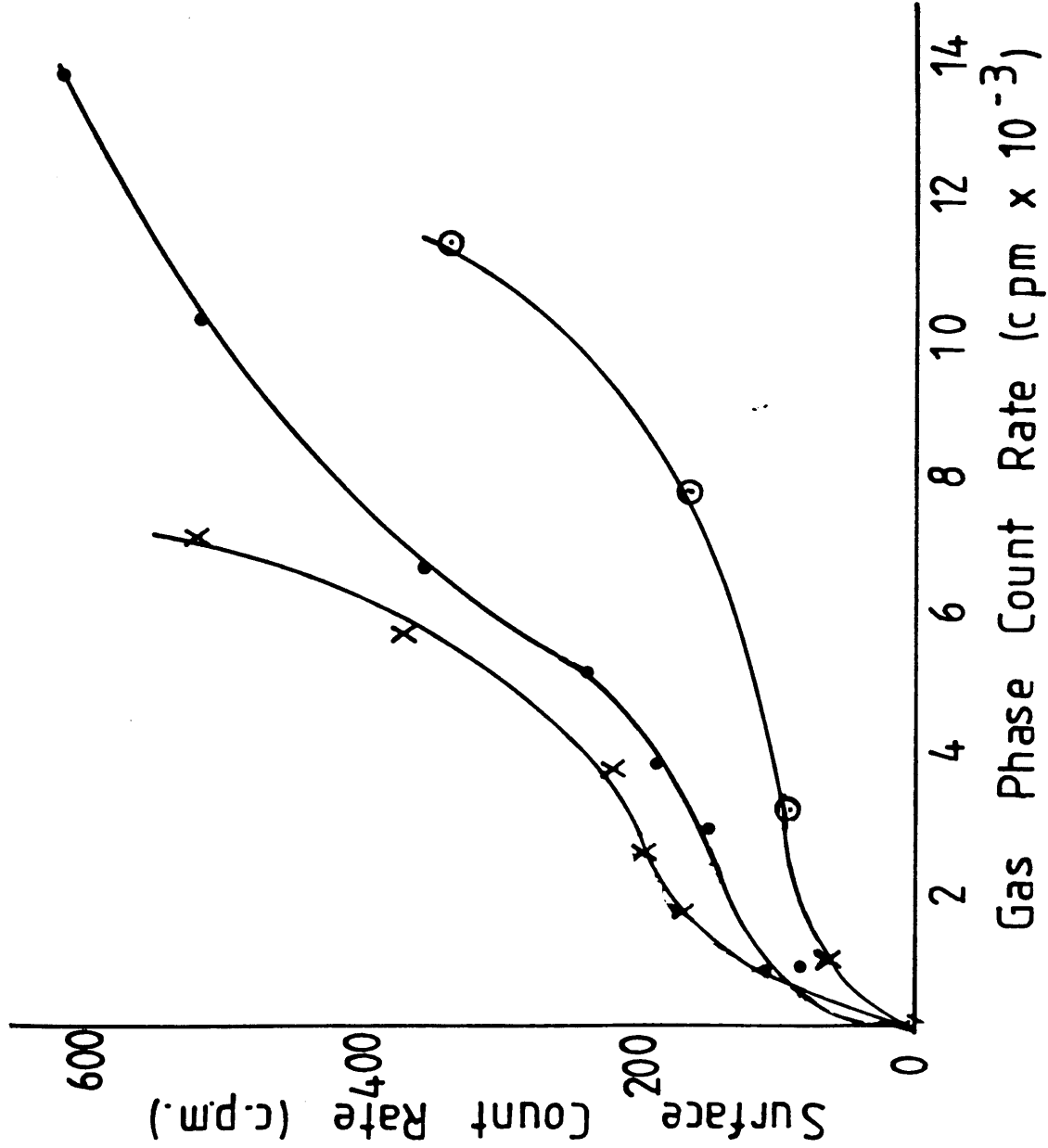
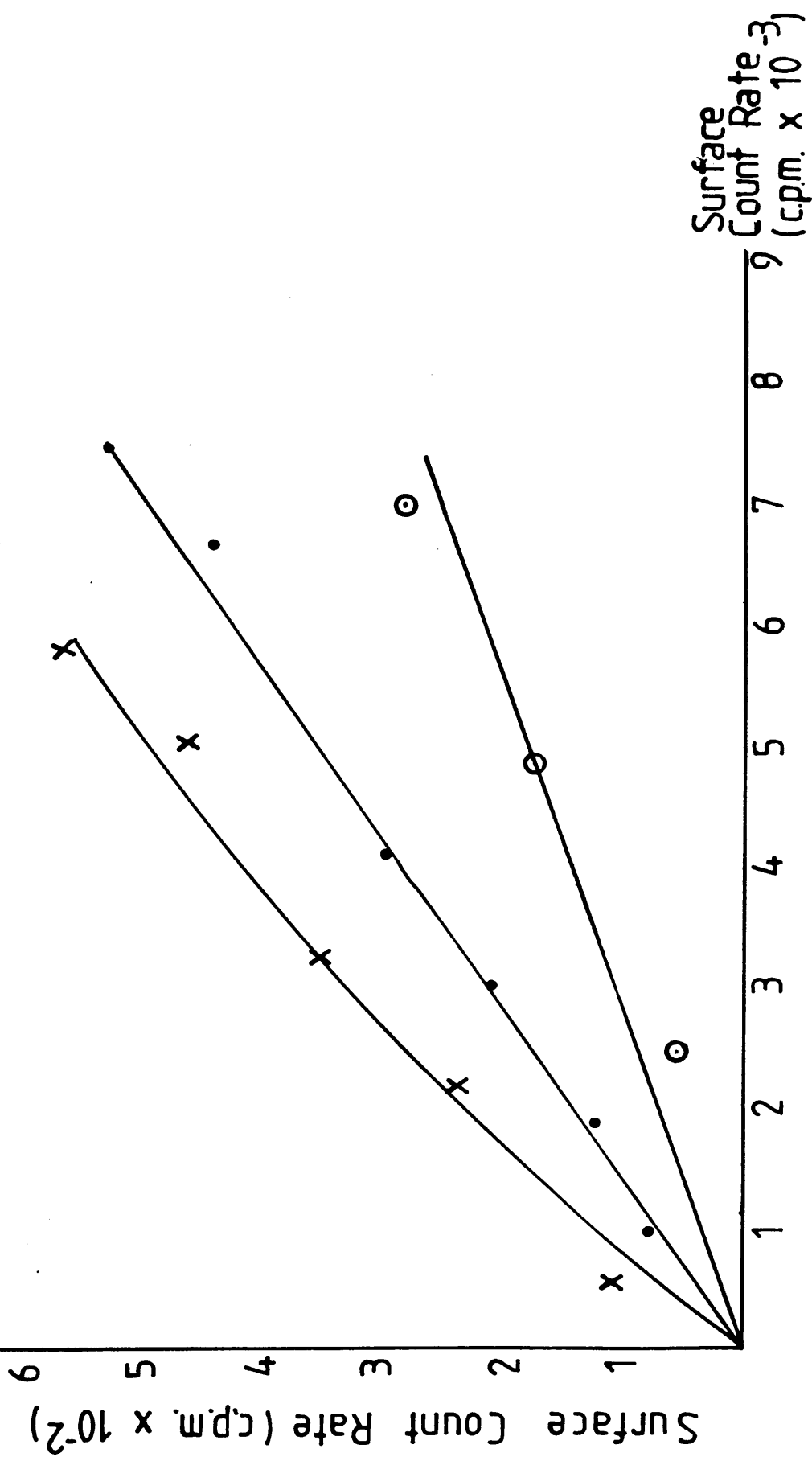


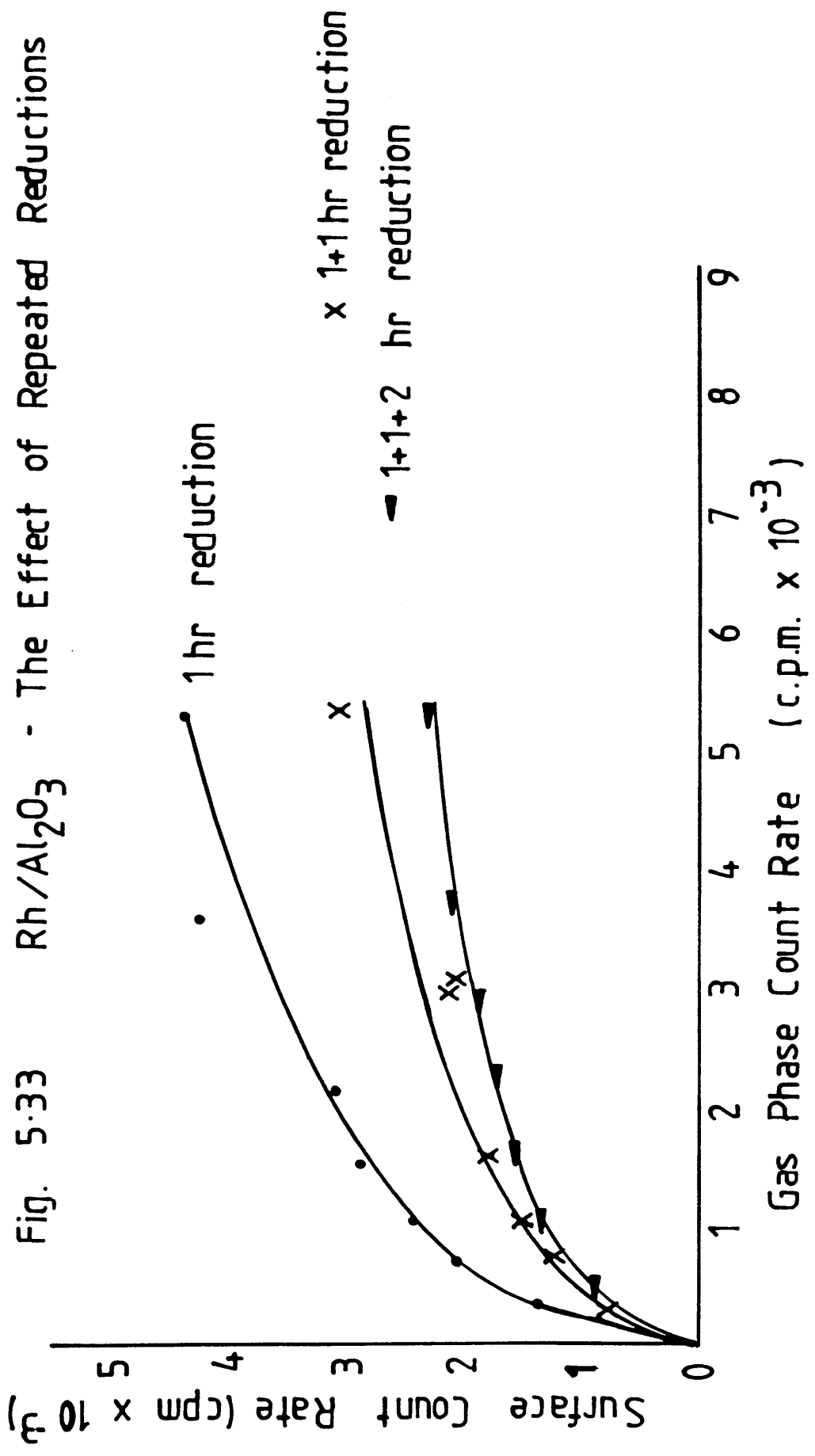
Fig. 5.32: Rh/MoO₃ - The Effect of O₂ on CO₂ Adsorption



The catalyst samples were reduced overnight at 320°C before being cooled under vacuum for 30 minutes in the normal way. After determining a ^{14}C - carbon monoxide isotherm, the catalyst was reduced, under the same conditions, for a further hour and again cooled under vacuum, before a second isotherm was determined. This procedure was then repeated once more.

Figures 5.33 - 5.35 clearly show that the amount of carbon monoxide adsorbed by each of the catalysts is very dependent on the reduction procedure. Since even after three reduction periods the catalysts had not reached a steady state, it was decided that catalyst samples should not be re-used.

Fig. 5.33 Rh/Al₂O₃ - The Effect of Repeated Reductions



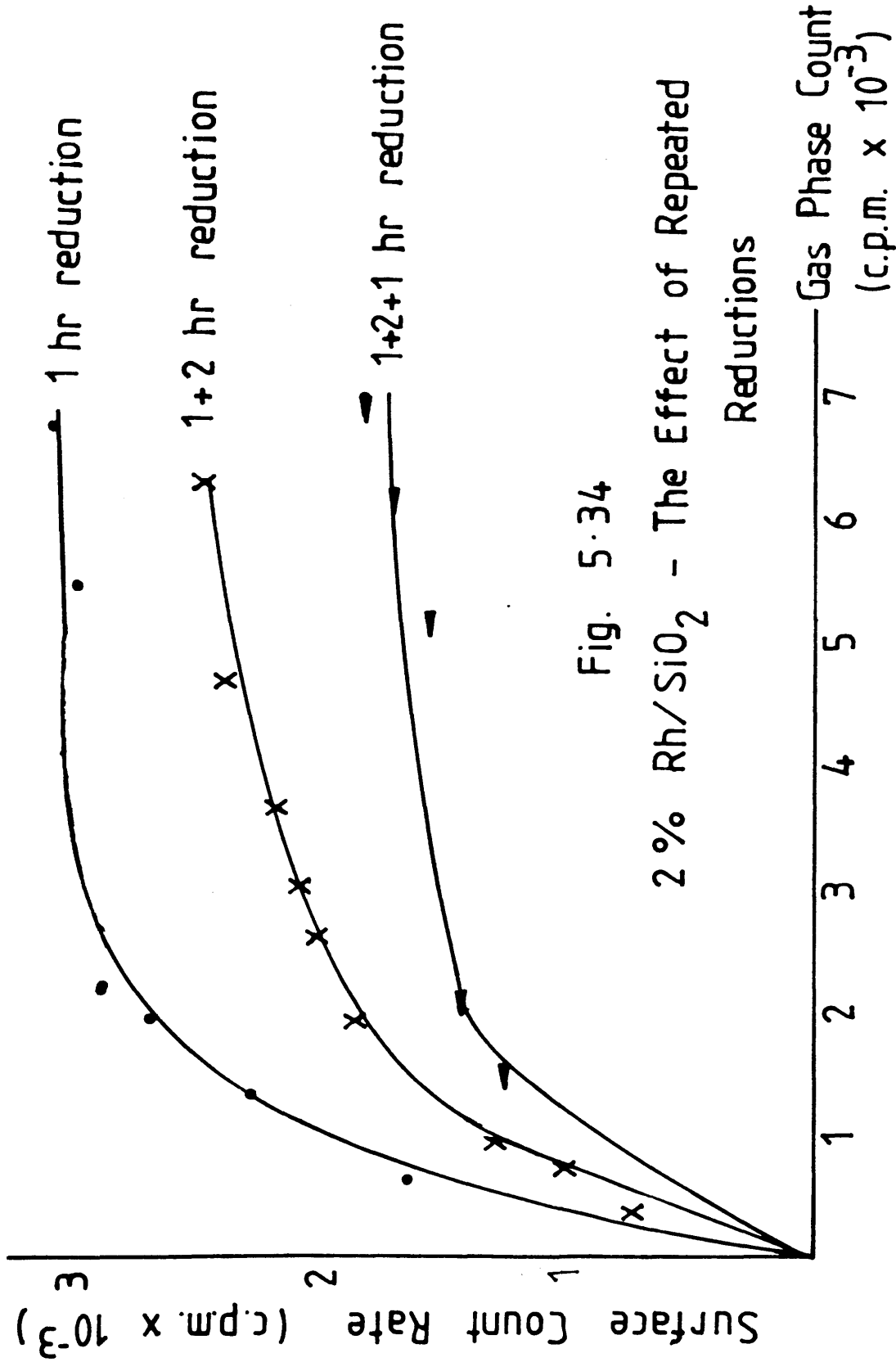


Fig. 5.34

2% Rh/SiO₂ - The Effect of Repeated

Reductions

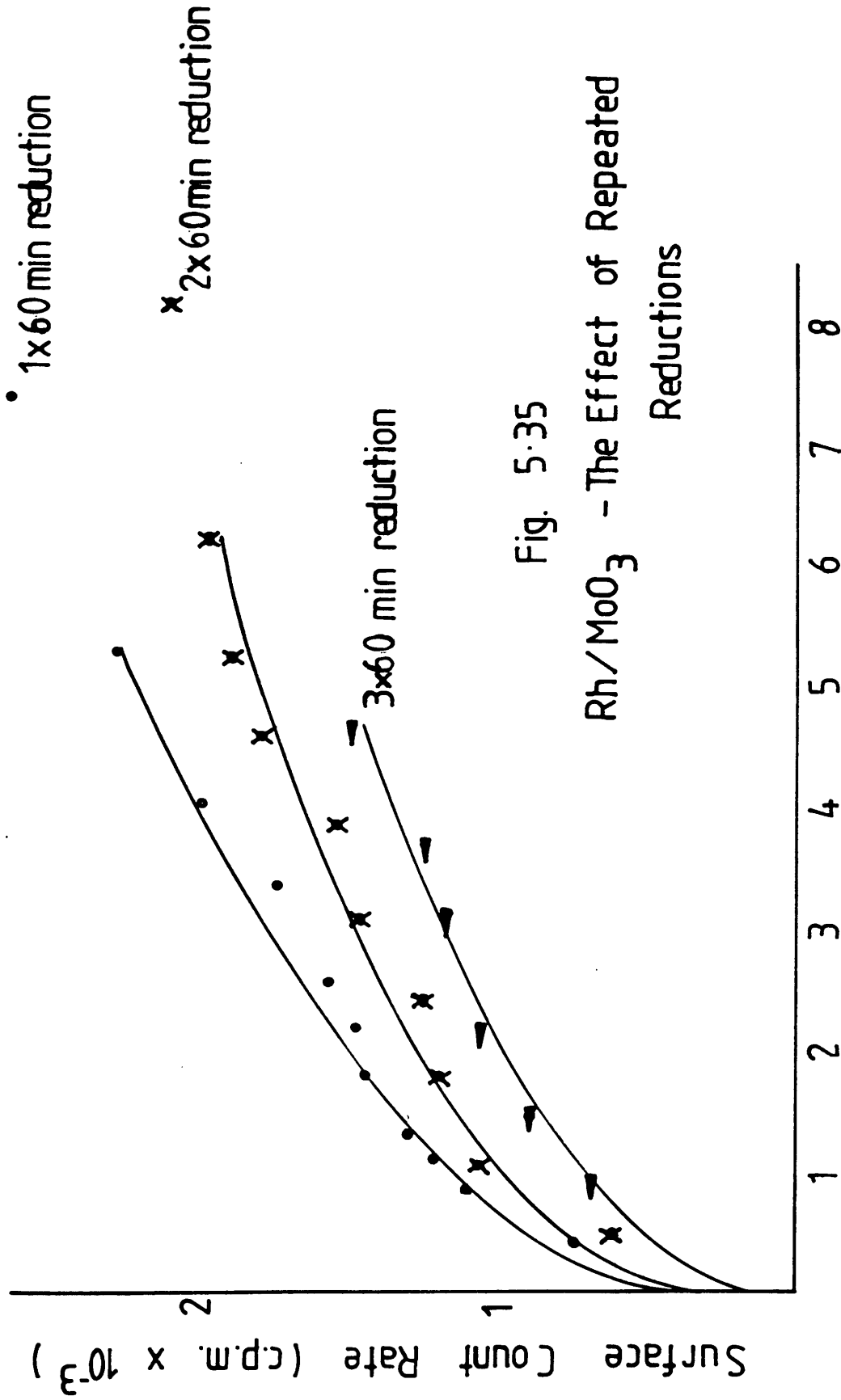


Fig. 5.35

Rh/MoO₃ - The Effect of Repeated Reductions

Gas Phase Count Rate (c.p.m. $\times 10^{-3}$)

CHAPTER 6

CARBON MONOXIDE ADSORPTION EXPERIMENTS

USING HEAVY ATOM LABELS

CHAPTER 6. CARBON MONOXIDE ADSORPTION EXPERIMENTS
USING HEAVY ATOM LABELS

6.1 INTRODUCTION

The experiments described in this chapter used two heavy atom labels - ^{13}C and ^{18}O - to investigate the adsorption of carbon monoxide on Rh/SiO_2 and Rh/MoO_3 catalysts. Of particular interest in these experiments was the scrambling of carbon monoxide at the catalyst surface and the labelling of any surface carbon formed. Details of the apparatus and procedure used are given in section 3.4.

6.2 $^{13}\text{C}^{16}\text{O}/^{12}\text{C}^{18}\text{O}$ ADSORPTION ON 2% Rh/SiO_2

6.2.1 CO ADSORPTION - Rh/SiO_2

Pulses of either labelled or unlabelled carbon monoxide were passed over a pre-saturated sample of catalyst at room temperature. When "saturation" had been reached the catalyst temperature was quickly raised to 320°C and the desorption products analysed.

As the reference peaks were always larger than those of pulses which had passed over the catalyst, "true" saturation was never reached. A portion of the adsorbed carbon monoxide was continually being stripped from the surface by the helium carrier stream. These experiments, therefore,

only refer to that carbon monoxide which was stable on the surface at ambient temperature over the period of the experiment, this is usually referred to as irreversibly held carbon monoxide.

This adsorption / desorption cycle was then repeated. After three or four cycles the catalyst was assumed to be in its steady state. The catalyst was then heated to 250°C, where another high temperature adsorption / desorption cycle was carried out. The results of these experiments are summarised in table 6.1.

Table 6.1 Summary of Results - Rh/SiO₂

	Initial State	Steady State	250°C
Total adsorption of CO	1.49×10^{19}	6.9×10^{18}	1.17×10^{19}
CO ₂ Produced	Nil	Nil	1.34×10^{17}
Thermal Desorption (320°C)			
- CO	4.91×10^{18}	3.41×10^{18}	Nil
- CO ₂	1.02×10^{18}	8.02×10^{17}	3.33×10^{17}
Amount of Material left on Surface	8.97×10^{18}	2.68×10^{18}	1.14×10^{19}

(Units = molecules of CO or CO₂)
per gram of Rh

Initially 1.49×10^{19} molecules of carbon monoxide were adsorbed on the 0.30g sample of Rh/SiO₂ used. However, this fell to only 6.9×10^{18} molecules when the catalyst was in its steady state. The initial dispersion of the sample was calculated at 42.73% but, due to the reaction conditions, this is only a measure of the number of sites adsorbing carbon monoxide irreversibly.

During carbon monoxide adsorption the eluting gas was analysed for carbon dioxide. At room temperature very little carbon dioxide was formed and this amount decreased with the number of pulses of carbon monoxide which had passed over the catalyst surface. The amount of both carbon monoxide and carbon dioxide which desorbed from the surface also decreased by a small amount in going from the initial to the steady state.

The amount of material left on the surface after each adsorption / desorption cycle - that is the difference between the amount of material which adsorbed on to the surface and that which desorbed - decreased in the steady state to about 30% of its initial value. However, when the catalyst was heated to 250°C even apparent saturation did not appear to be reached within the limits of these experiments and 1.17×10^{19} molecules of carbon monoxide adsorbed on to the surface. The amount of carbon monoxide adsorbed by the catalyst increased dramatically and

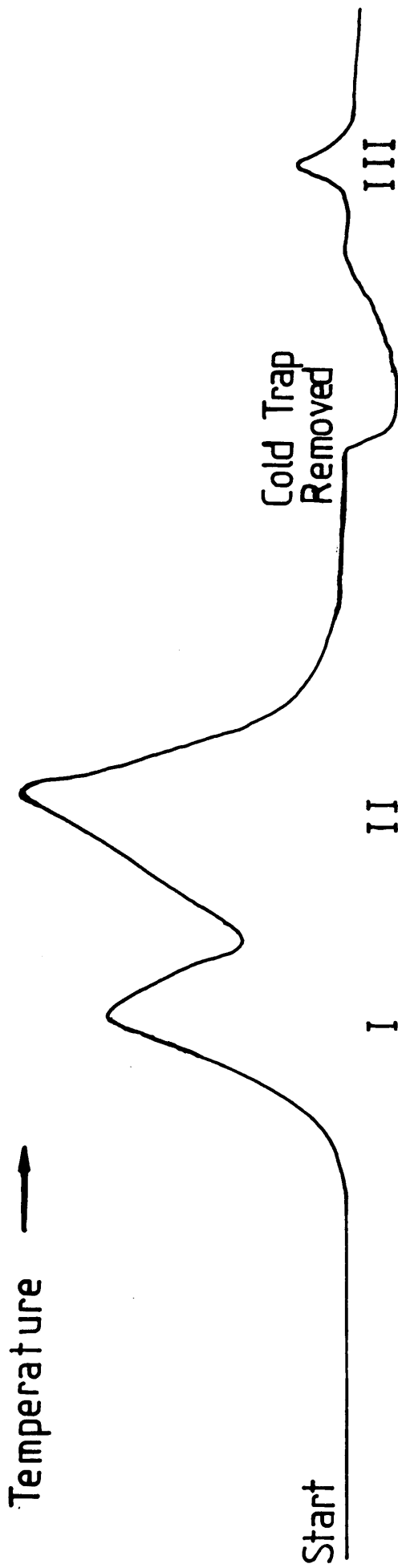
substantial amounts of carbon dioxide were formed during these higher temperature adsorptions.

During the desorption process no carbon monoxide and less carbon dioxide than expected came off the surface after high temperature adsorption. This left rather a large amount of material on the surface. Most of this material was stable to H_2 at $320^\circ C$.

6.2.2 EXPERIMENTS INVOLVING ISOTOPIC LABELS - Rh/SiO₂

When pulses of a 1:1 mixture of ^{13}CO and $C^{18}O$ were passed over a sample of freshly reduced catalyst at room temperature, no scrambling of the labels was detected in the effluent gas. Analysis of the desorption products of the sample indicate that at least three different species were present on the surface (fig 6.1).

Two peaks due to carbon monoxide were produced. In the first, smaller, peak, the carbon monoxide was not scrambled. However, in the second peak, not only was there complete scrambling, but the gas was greatly enriched with ^{16}O . When the cold trap was warmed up and the carbon dioxide produced was analysed, it was also found to be scrambled and ^{16}O enriched. A little water was also produced during thermal desorption, but this did not contain detectable levels of $H_2^{18}O$.



- Peak I Non-Scrambled CO
- Peak II Scrambled and O^{16} Enriched CO
- Peak III Scrambled and O^{16} Enriched CO₂

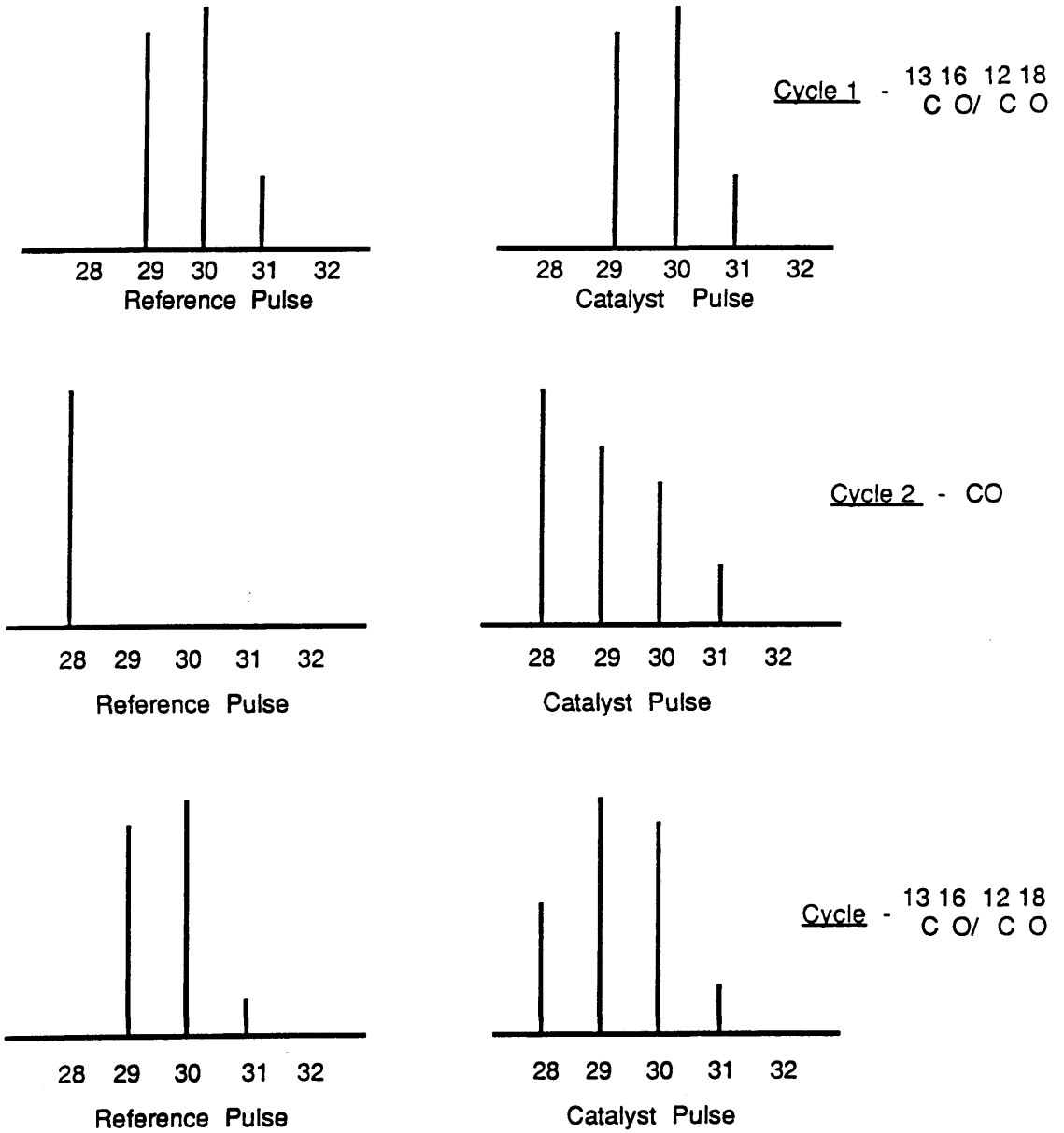
Fig. 6.1 CO Desorption from Rh/SiO₂

The catalyst was cooled to room temperature before it was exposed to pulses of unlabelled carbon monoxide. Comparison of the mass spectrum of a reference pulse with that of the effluent gas (fig 6.2) shows quite clearly that after an initial period when only unlabelled carbon monoxide comes through, unlabelled gas phase carbon monoxide has displaced labelled material from the surface. In fact, 70% of labelled material left on the surface from the previous adsorption / desorption cycle was displaced by unlabelled gas phase molecules. The labelled carbon monoxide which is displaced is both scrambled and ^{16}O enriched.

After carrying out a thermal desorption, pulses of labelled carbon monoxide were again passed over the catalyst surface. This time unlabelled carbon monoxide was displaced by the gas phase molecules. This was followed by a second labelled cycle. The carbon monoxide which desorbed during the chemisorption of $^{13}\text{CO}/\text{C}^{18}\text{O}$ was scrambled and slightly enriched with ^{16}O , probably due to displacement of scrambled material from previous cycles.

When labelled carbon monoxide was adsorbed at 250°C , both the carbon monoxide which was not retained on the surface and the carbon dioxide which was formed were completely scrambled and enriched with ^{16}O . The carbon dioxide which was subsequently thermally desorbed was also scrambled.

Fig. 6.2 The Displacement of Surface Material
by Gas Phase Molecules of CO



6.3 $^{13}\text{C}^{16}\text{O}/^{12}\text{C}^{18}\text{O}$ ADSORPTION ON 2% Rh/MoO₃

6.3.1 CARBON MONOXIDE ADSORPTION - Rh/MoO₃

Exactly the same procedure as that detailed above was carried out using a 1g sample of Rh/MoO₃. A larger sample of the Rh/MoO₃ catalyst had to be used because of its far greater density; the catalyst volume was approximately the same as that of Rh/SiO₂ in the experiments above. The results are shown in Table 6.2.

Table 6.2 SUMMARY OF RESULTS - Rh/MoO₃

	Initial State	Steady State	250°C
Total Adsorption of CO	4.11 x 10 ¹⁸	1.37 x 10 ¹⁸	1.60 x 10 ¹⁸
CO ₂ Produced	Nil	Nil	6.93 x 10 ¹⁸
Thermal Desorption (320°C)			
- CO	3.48 x 10 ¹⁸	9.13 x 10 ¹⁷	4.08 x 10 ¹⁷
- CO ₂	3.44 x 10 ¹⁷	3.30 x 10 ¹⁷	9.71 x 10 ¹⁷
Amount of Material left on Surface	3.20 x 10 ¹⁷	1.30 x 10 ¹⁷	2.20 x 10 ¹⁷

(Units = molecules of CO or CO₂)
per gram of catalyst

Only 4.11×10^{18} molecules of carbon monoxide adsorbed initially on the catalyst sample; much less than that which adsorbed on the smaller sample of Rh/SiO₂. From this an initial dispersion of only 3.33% was calculated.

The amount of carbon monoxide adsorbed in the steady state was again considerably lower than that of the original adsorption. Both carbon monoxide and carbon dioxide were evolved from the catalyst surface during thermal desorption. The amount of material desorbed from the surface and that left on the surface by each adsorption / desorption cycle also decreased slightly in going from the initial to the steady state.

At 250°C the amount of carbon monoxide adsorbed by the catalyst was only slightly higher than that adsorbed at room temperature on to the steady state surface. During carbon monoxide desorption a large amount (6.93×10^{18} molecules) of carbon dioxide was produced. On raising the temperature to 320°C both carbon monoxide and carbon dioxide desorbed from the surface, leaving only a very small amount of material on the surface.

When the catalyst sample was originally reduced, large amounts of water were produced: subsequent desorption sequences produced even more.

6.3.2 EXPERIMENTS USING ISOTOPIC LABELS - Rh/MoO₃

No scrambling of the labels was observed in the carbon monoxide which was not retained on the Rh/MoO₃ catalyst during the initial adsorption cycle. Two desorption peaks, due to carbon monoxide, were again detected when the temperature was raised to 320°C. The second of these peaks being completely scrambled. The carbon dioxide which was produced was also scrambled and enriched with ¹⁶O.

When unlabelled carbon monoxide was pulsed over the catalyst surface, labelled carbon monoxide, left on the surface by the previous cycle, was displaced. This carbon monoxide was scrambled and ¹⁶O enriched.

Only one carbon monoxide desorption peak was detected but it appears to be composed of two overlapping peaks. Only unlabelled carbon monoxide and carbon dioxide were produced during the desorption.

When labelled carbon monoxide was exposed to a catalyst surface which had previously been saturated with unlabelled carbon monoxide, no unlabelled carbon monoxide was detected in the gas stream leaving the reaction vessel. This was probably due to the very small amount of ¹²C¹⁶O which had been left on the surface by the previous cycle.

During the fourth adsorption / desorption cycle a very small amount of air was detected in the carrier stream.

However, this appears to have had little effect on the catalyst's behaviour; the only difference being that the first carbon monoxide desorption peak was scrambled and enriched with ^{16}O .

During the high temperature adsorption of carbon monoxide, carbon dioxide was formed which was both scrambled and ^{16}O enriched. Both carbon monoxide and carbon dioxide were produced during the thermal desorption, but only one peak of scrambled carbon monoxide was detected.

CHAPTER 7

PULSE FLOW EXPERIMENTS

CHAPTER 7 PULSE-FLOW EXPERIMENTS

7.1 INTRODUCTION

This chapter will discuss a series of experiments which were carried out on the "Pulse-flow" systems described in sections 3.5 and 3.6.

7.2 TEMPERATURE PROGRAMMED REDUCTION PROFILES

Temperature programmed reduction (TPR) studies were carried out on all four catalysts, typical results are shown in figs 7.1-7.3. The TPR of 2% Rh/SiO₂ was found to be identical to that of the 5% catalyst.

The exact position and height of the various peaks produced often varied from one experiment to another, but the overall shape of the curves proved to be a constant and unique "fingerprint" for each particular catalyst.

The TPR of Rh/Al₂O₃ consisted of two well separated peaks at about 120°C and 240°C (fig 7.1), whilst with Rh/SiO₂, hydrogen consumption was observed at 105°C and 138°C. The TPR of Rh/MoO₃ was more complex, consisting of a very large peak at 190°C with a second, smaller peak at 290°C. A shoulder often appeared on the initial peak at about 150°C, together with a very broad peak whose maxima

Fig. 7.1
TPR of Rh/Al₂O₃
β = 5°/min → 500°C
0.547g.Rh/Al₂O₃

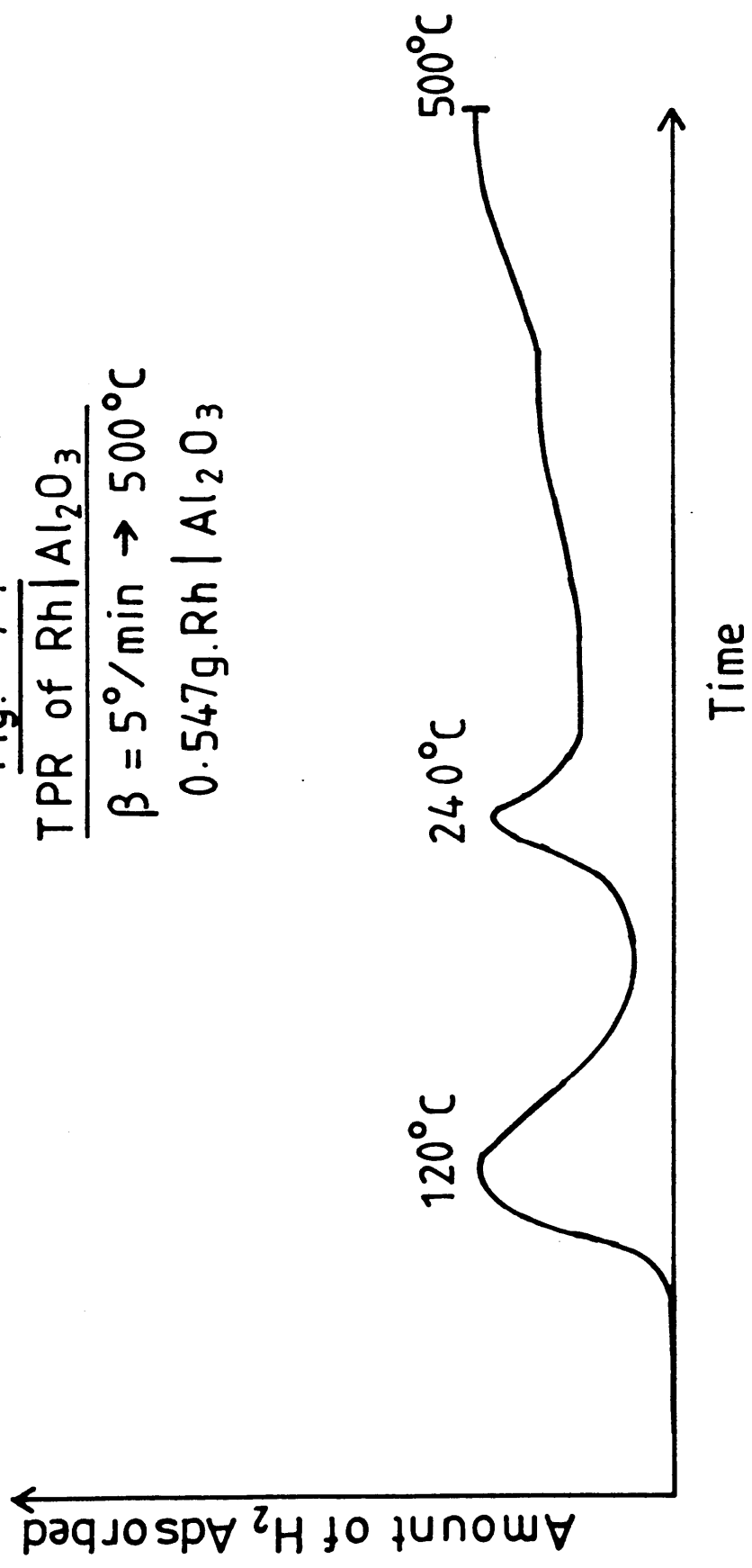


Fig. 7.2

TPR of RhI SiO₂

$\beta = 5^\circ/\text{min} \rightarrow 500^\circ\text{C}$

0.162 g. RhI SiO₂

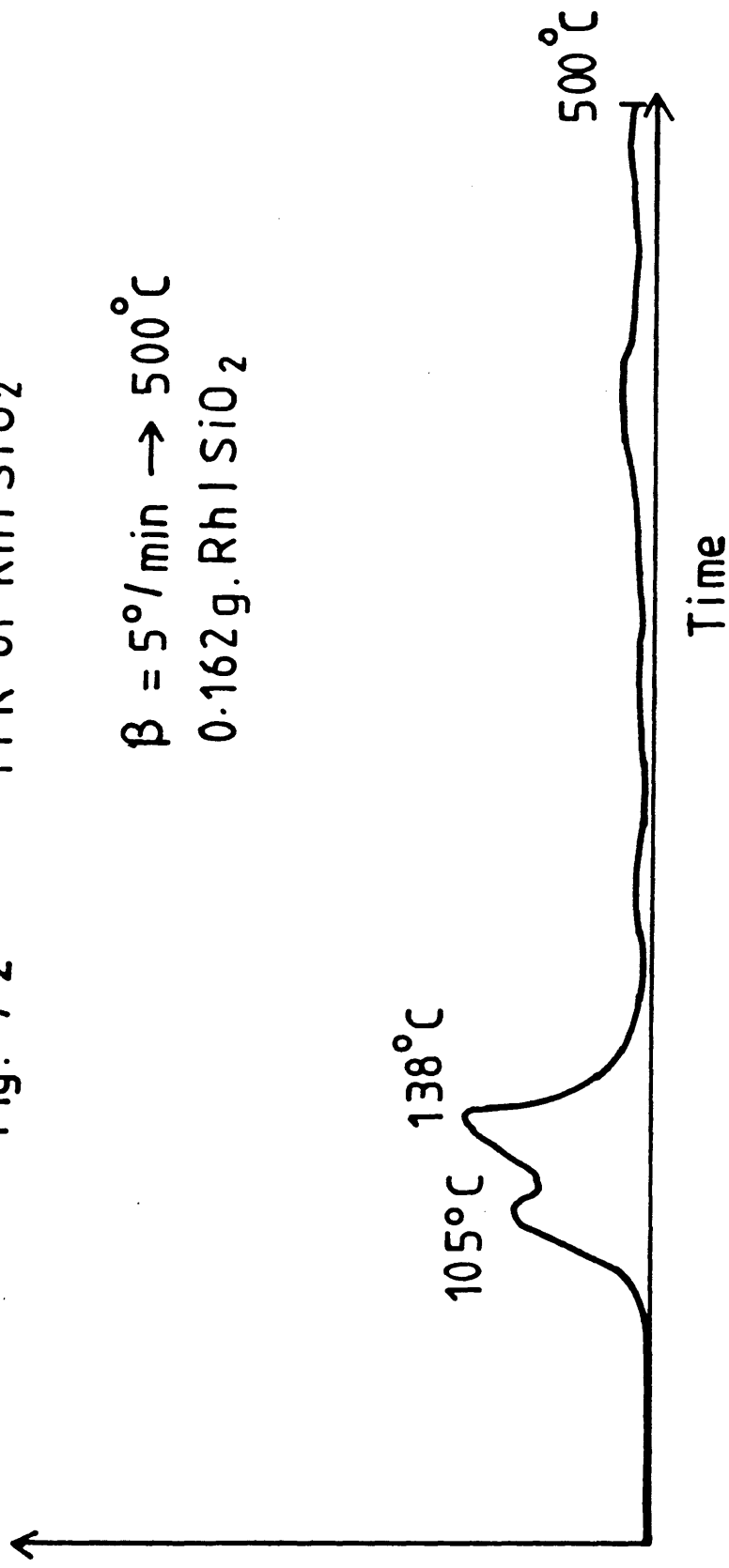
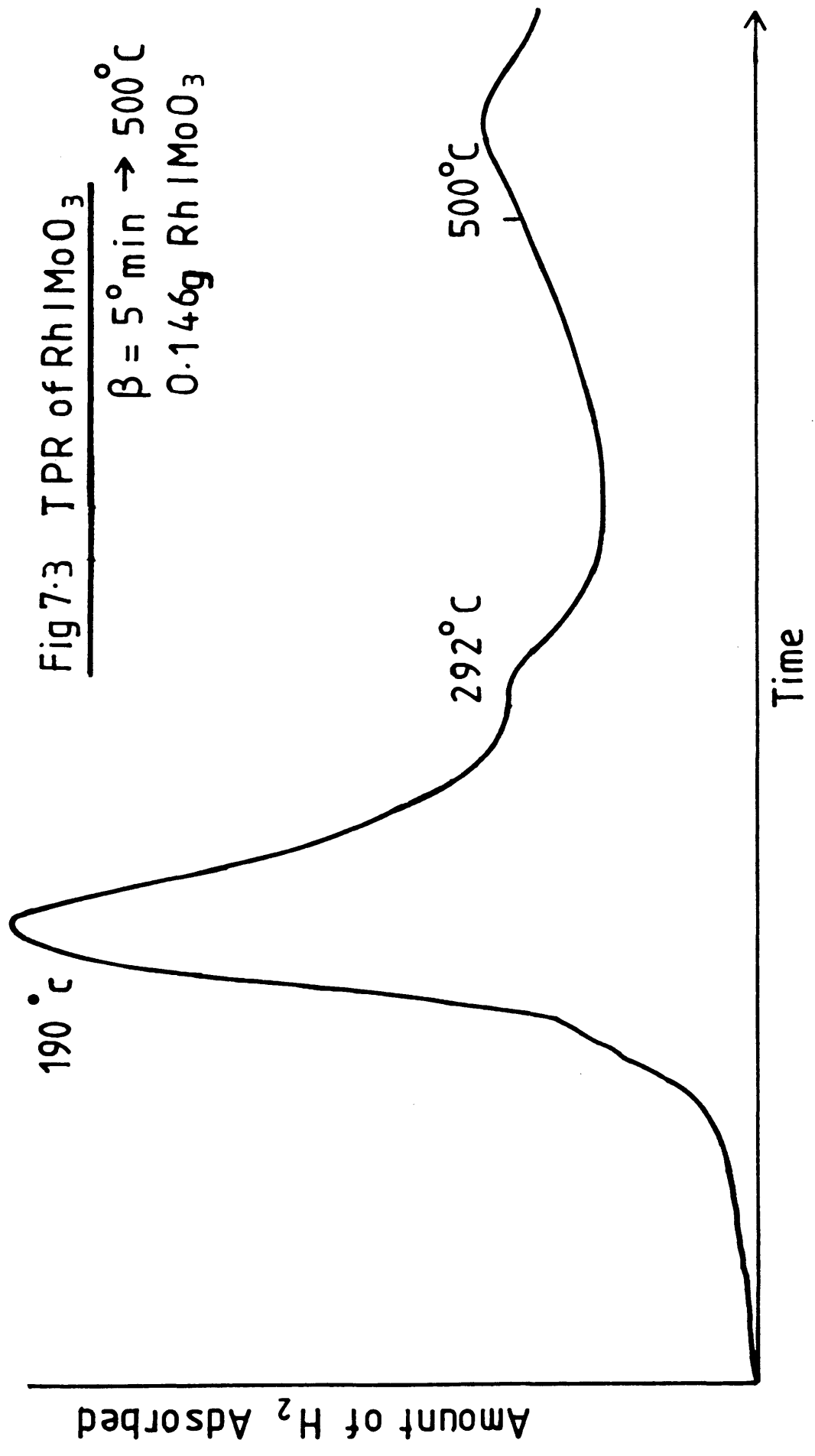


Fig 7.3 TPR of Rh1MoO₃

$\beta = 5^\circ \text{min} \rightarrow 500^\circ \text{C}$
0.146g Rh1MoO₃



was at 500°C, the highest temperature used in these experiments.

TPR profiles were also obtained for the three supports. While alumina and silica adsorbed very little hydrogen, MoO₃ (fig 7.4) showed two distinct reduction peaks at 410°C and ca. 500°C.

Table 7.1 summarises the results obtained. In the second and third columns adsorption is expressed in units of molecules/g of catalyst.

Table 7.1 TPR data

	Peak Positions (°C)	H ₂ Adsorbed	Theoretical Adsorption
2%Rh/SiO ₂	124,147	1.83 x 10 ¹⁹	1.67 x 10 ²⁰
5%Rh/SiO ₂	119,144	3.42 x 10 ¹⁹	3.60 x 10 ²⁰
2%Rh/Al ₂ O ₃	115,246	1.29 x 10 ¹⁹	1.67 x 10 ²⁰
2%Rh/MoO ₃	140,202,305,500	3.71 x 10 ²⁰	1.41 x 10 ²⁰

The peak positions shown are the average maxima positions taken over a series of experiments. The amount of hydrogen adsorbed is also an average value and is quoted in molecules per gram of catalyst to allow comparisons between catalysts to be drawn. If we assume that during the reduction procedure all the Rh³⁺ ions present are reduced to rhodium metal according to the reaction shown below

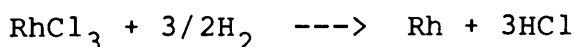
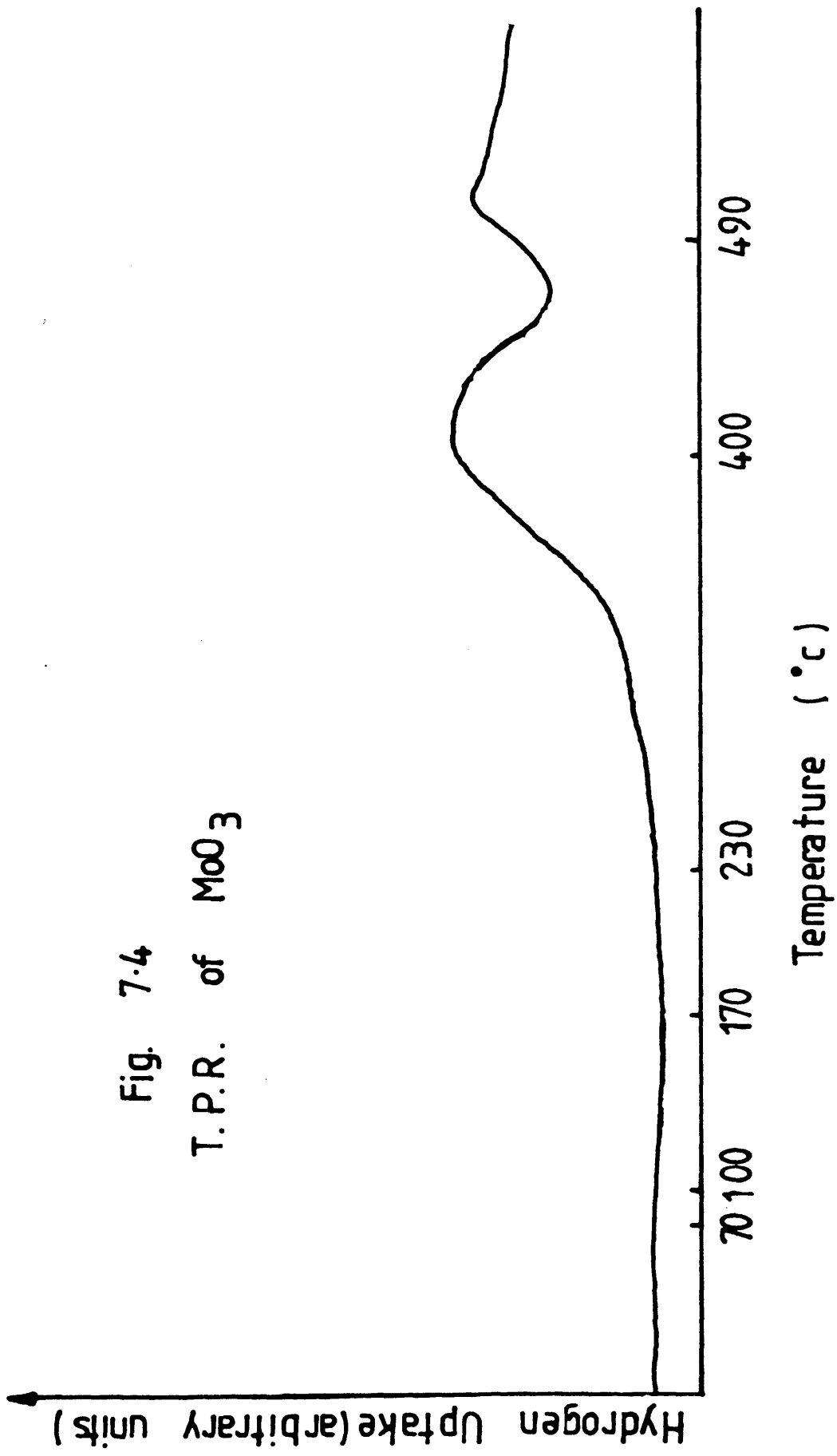


Fig. 7.4
T.P.R. of MoO_3



then the amount of hydrogen the catalyst would, theoretically, be expected to adsorb, can be calculated and is quoted in table 7.1.

It can clearly be seen from table 7.1 that only the Rh/MoO₃ catalyst was reduced completely during the reduction procedure. The Rh/Al₂O₃ catalyst appeared to be the most difficult one to reduce as it took up least hydrogen per gram of catalyst. The Rh/MoO₃ sample on the other hand adsorbed more than twenty times the amount of hydrogen per gram of catalyst than any of the other three. While the 5% Rh/SiO₂ catalyst was found to adsorb less hydrogen per gram of rhodium than the 2% catalyst.

7.3 PULSE-FLOW EXPERIMENTS

7.3.1 INTRODUCTION

When pulses of carbon monoxide were passed over a freshly reduced sample of catalyst, some carbon monoxide was adsorbed by the surface and some was not. The amount of carbon monoxide retained by the catalyst was taken as the difference in area of a peak due to carbon monoxide which had passed over the sample, and that of an identical reference pulse which had not passed over the catalyst.

It was found, however, that the extent of adsorption was very dependent on the time interval between pulses,

everything else being constant. This is illustrated in fig. 7.5 for the 2% Rh/SiO₂ catalyst.

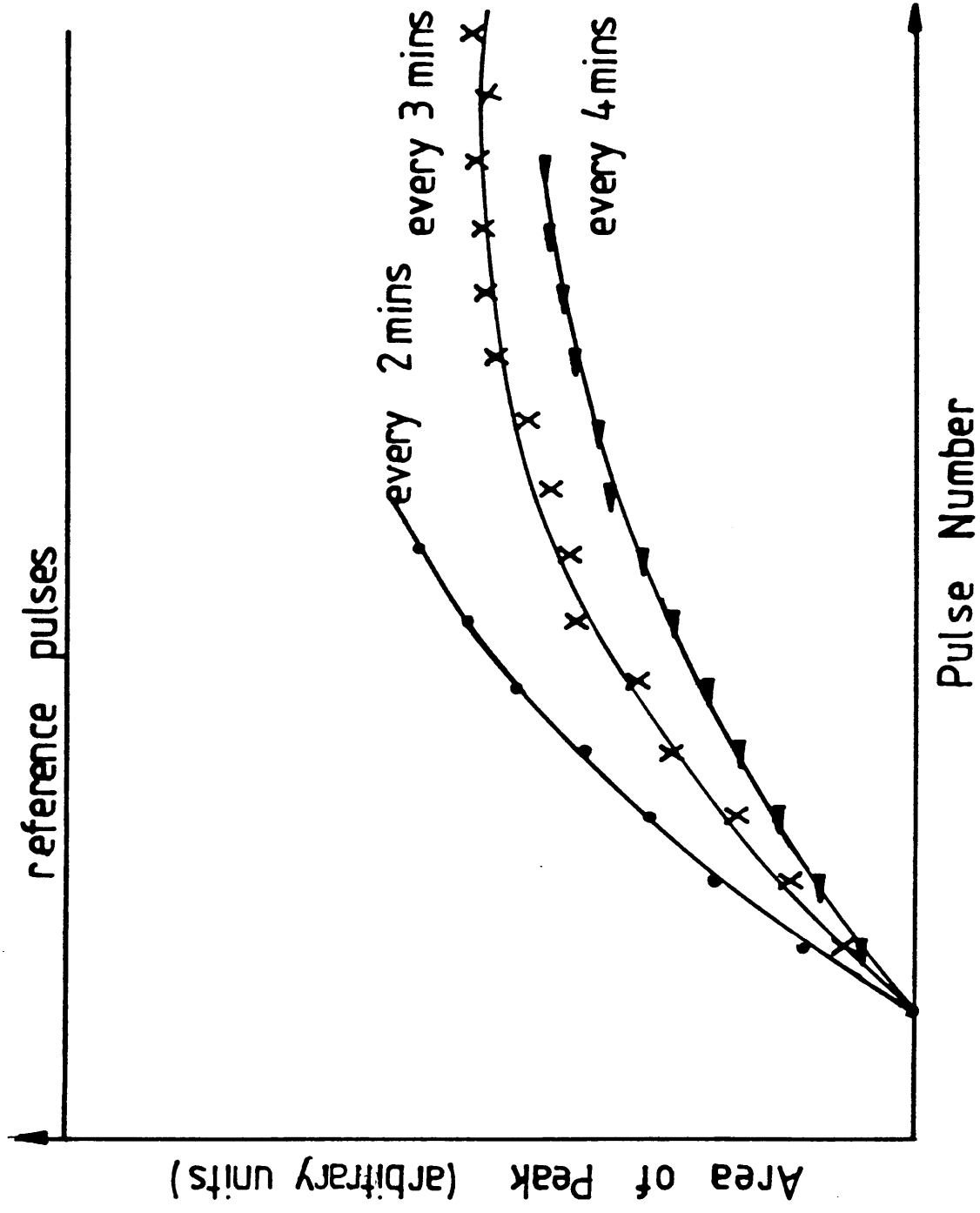
Moreover, even at "saturation", the area of a pulse which had passed over the catalyst surface was always considerably less than those of the reference pulses. Together, these facts strongly suggest that full saturation is never reached in this system, and that the helium carrier stream is continually removing some form of weakly adsorbed carbon monoxide from the catalyst surface.

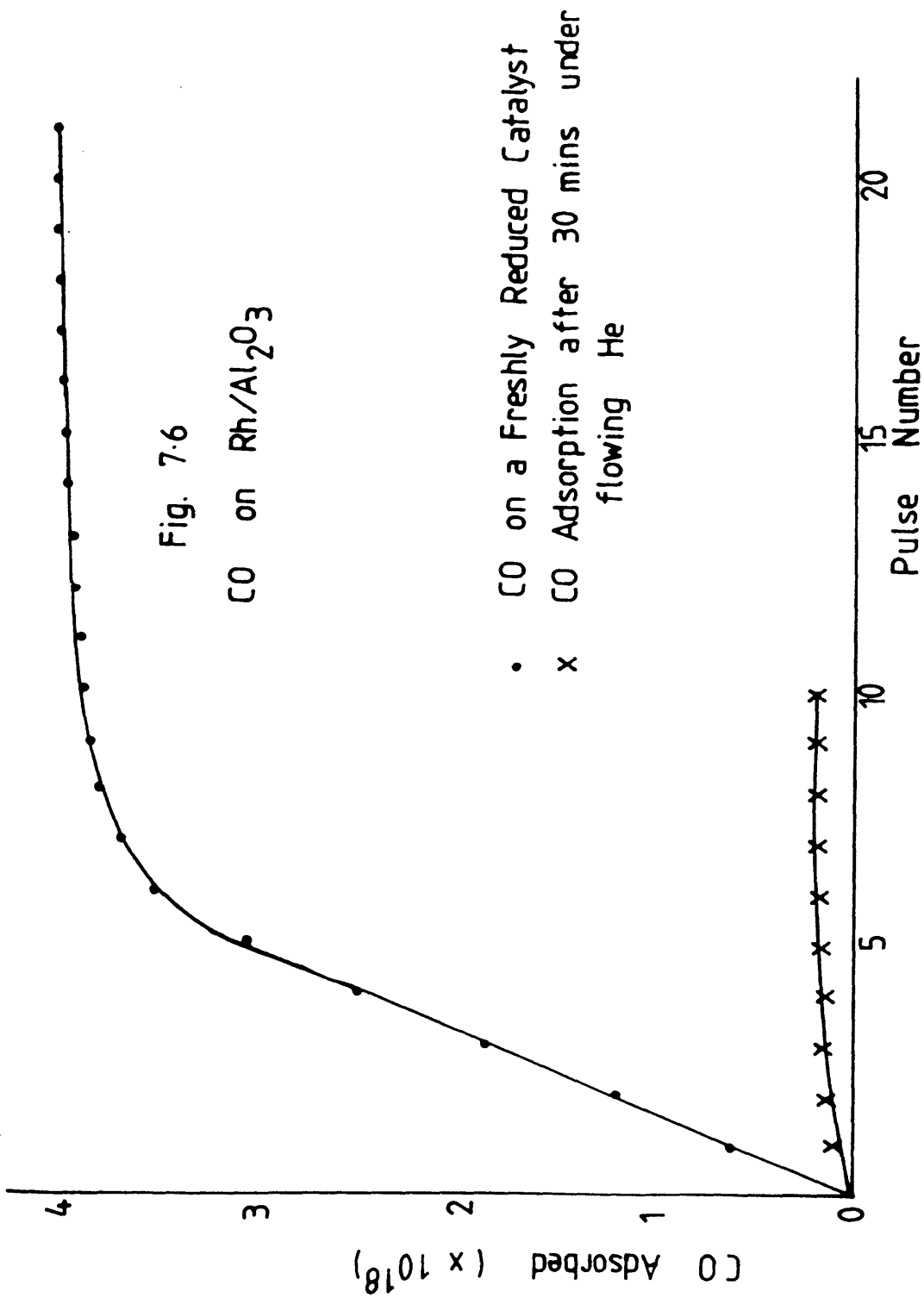
Since this effect was quite substantial, even at the relatively low flow rates used in these experiments, the pulses of the adsorbing gas had to be injected into the carrier stream at carefully regulated intervals, usually every minute, in order to obtain reproducible results.

7.3.2 CARBON MONOXIDE ADSORPTION

If the amount of carbon monoxide on the catalyst surface is plotted against the pulse number, the type of curves shown in fig 7.6-7.9 are obtained. These curves have a similar shape to those of the adsorption isotherms discussed in section 5.2, but should not be compared with them as the amount of carbon monoxide on the surface is plotted here against a time base (pulse number) rather than pressure.

Fig. 7.5
CO Adsorption on
Rh/SiO₂ as a
function of the
Interval Between
Pulses





CO Adsorbed
($\times 10^6$ moles)

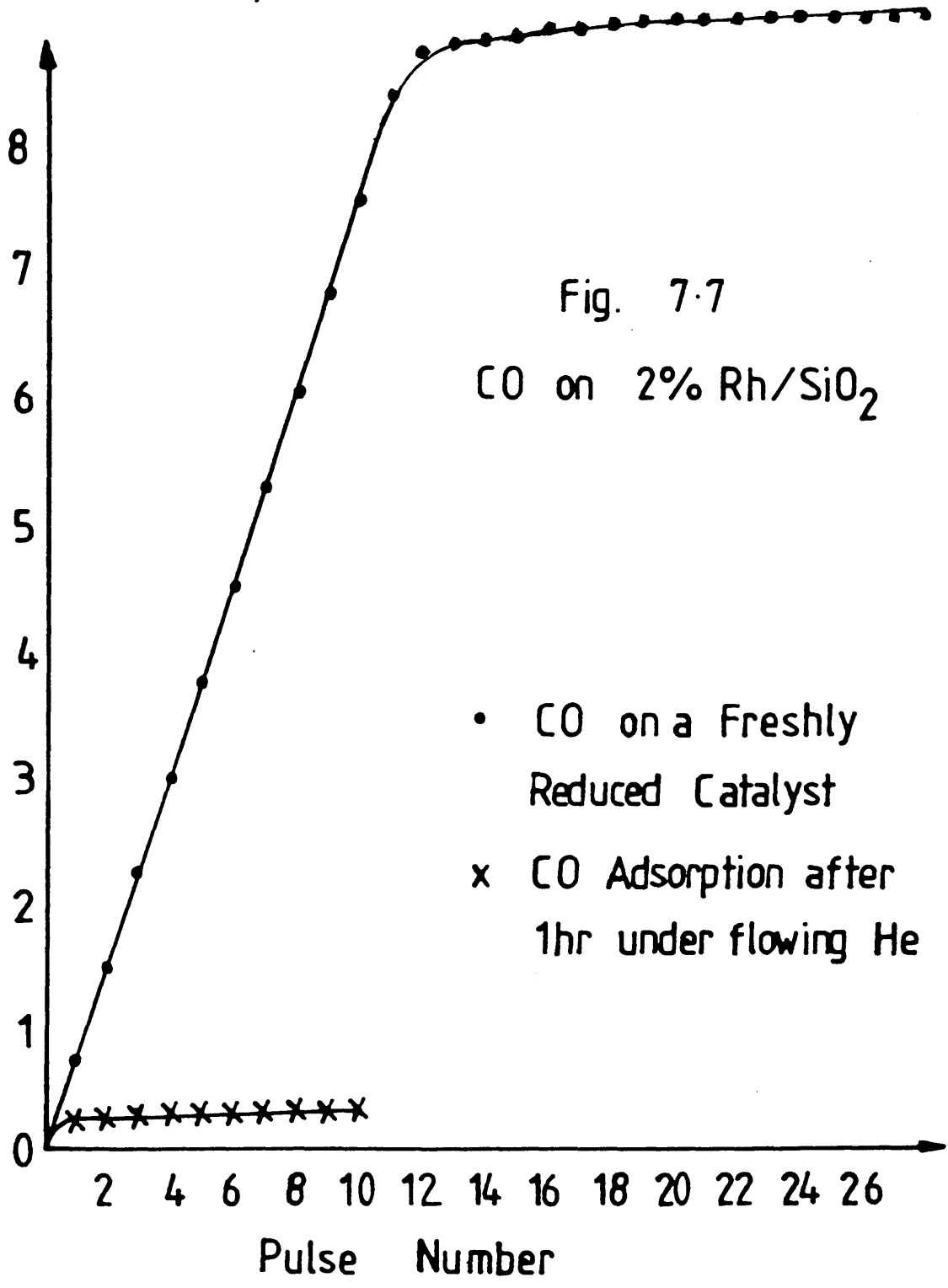


Fig. 7.7

CO on 2% Rh/SiO₂

- CO on a Freshly Reduced Catalyst
- x CO Adsorption after 1hr under flowing He

Fig. 7.8

CO on 5% Rh/SiO₂

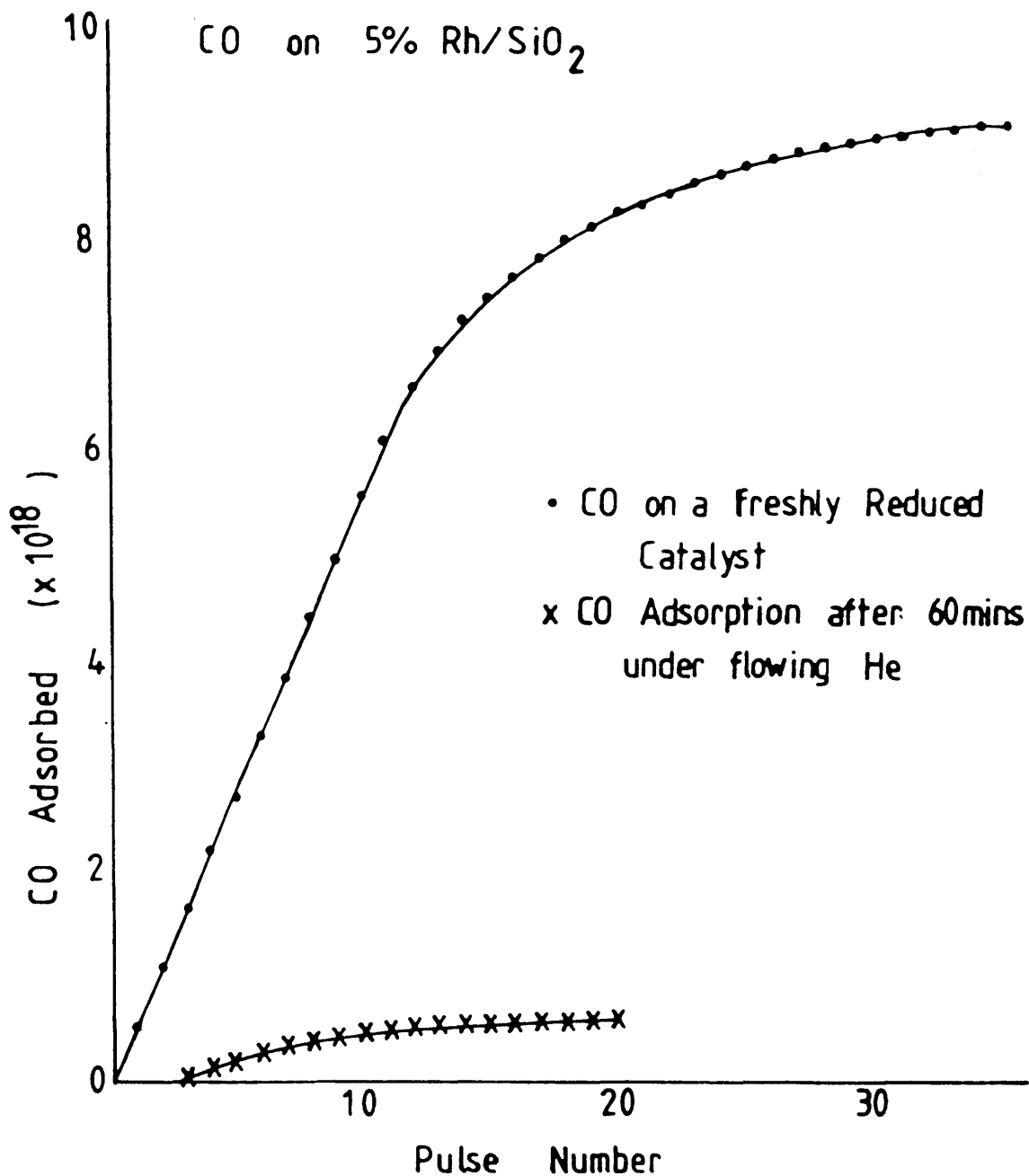
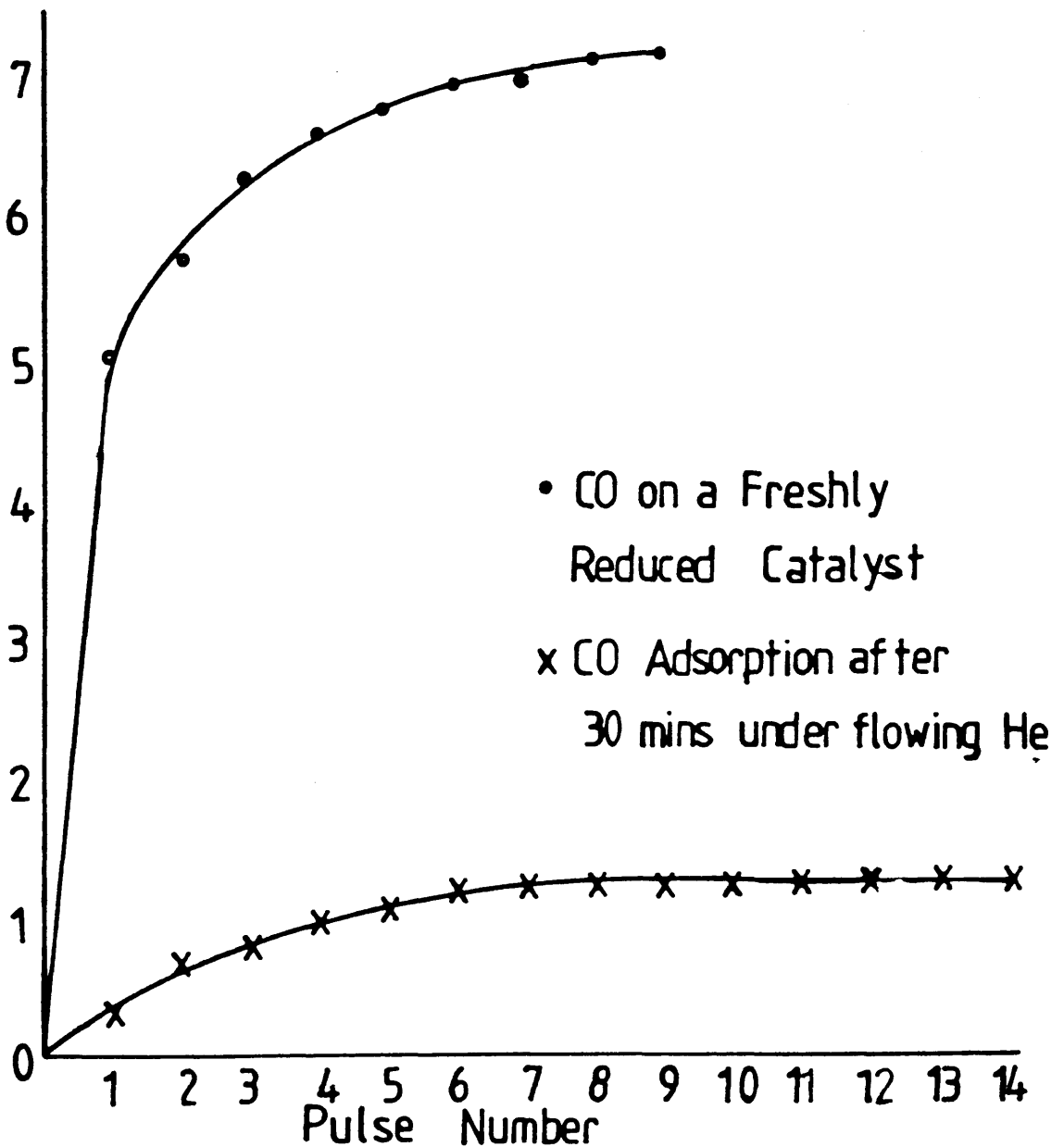


Fig. 7.9

CO on Rh/MoO₃

Amount of CO
Adsorbed
($\times 10^7$ moles)



After reduction, pulses of carbon monoxide were passed over the catalyst surface until a steady-state had been obtained. The catalyst was then left in a flow of helium for a period of 10-60 minutes, before again being exposed to carbon monoxide. Any carbon monoxide taken up in this second phase of adsorption, was due to molecules replacing those removed by the helium carrier stream.

The amount of carbon monoxide taken up by each of the catalysts is detailed below, together with the percentage dispersion of the catalyst calculated from that figure. In calculating the percentage dispersions it was assumed that one molecule of carbon monoxide would adsorb on each rhodium atom. As is discussed elsewhere this may not be a valid assumption, but for simple comparative purposes is perfectly acceptable. Since the amount of carbon monoxide adsorbed varied considerably between experiments an average value is quoted in Table 7.2. The adsorption figures are quoted in units of molecules of carbon monoxide per gram of rhodium.

Table 7.2 Carbon Monoxide Adsorption

	1 st CO Ads ⁿ	%Dispersion	2 nd CO Ads ⁿ	Average Ads ⁿ
2%Rh/SiO ₂	6.40 x 10 ²⁰	10.98	2.62 x 10 ¹⁹	1.10 x 10 ²¹
5%Rh/SiO ₂	5.58 x 10 ²⁰	9.54	3.63 x 10 ¹⁹	1.34 x 10 ²¹
Rh/Al ₂ O ₃	1.07 x 10 ²¹	18.30	5.26 x 10 ¹⁹	8.7 x 10 ²⁰
Rh/MoO ₃	5.22 x 10 ¹⁹	0.89	9.02 x 10 ¹⁸	2.53 x 10 ²⁰

The Rh/SiO₂ and Rh/Al₂O₃ catalysts adsorbed comparable amounts of carbon monoxide whilst the Rh/MoO₃ catalyst adsorbed less than a tenth of this amount.

Only 5% of the carbon monoxide adsorbed initially by the Rh/SiO₂ and Rh/Al₂O₃ was adsorbed during the second period of adsorption. This compares with a value of 17% for the MoO₃ supported catalyst.

All of the above experiments were carried out at ambient temperature. A limited number of adsorption experiments were also carried out at 0°C to try and eliminate, or reduce, the effect of the carrier stream. However, the lower temperature had little effect on the amount of carbon monoxide adsorbed by each of the catalysts.

7.3.3 CARBON DIOXIDE ADSORPTION

The adsorption of carbon dioxide on each of the catalysts was also investigated at a variety of temperatures. After reduction, the catalyst was heated to 100°C and exposed to pulses of carbon dioxide. The temperature was then increased to 150°C and then 250°C where the adsorption of carbon dioxide was again measured. The amount of carbon dioxide adsorbed by each of the catalysts at 100°C is shown in table 7.3. Less carbon dioxide was adsorbed at ambient temperature than at 100°C, suggesting

that the adsorption of carbon dioxide is an activated process.

Table 7.3 Carbon Dioxide Adsorption

Amount of CO ₂ Adsorbed (Molecules of CO ₂ per gram of Rh)		
2% Rh/SiO ₂	6.23 x 10 ¹⁸	Temp. = 100°C
Rh/Al ₂ O ₃	2.47 x 10 ¹⁹	
Rh/MoO ₃	1.09 x 10 ¹⁸	

7.3.4 OXYGEN ADSORPTION

The amount of oxygen adsorbed on to Rh/SiO₂, Rh/Al₂O₃ and Rh/MoO₃ was determined, the results of these measurements being shown in table 7.4.

The Rh/SiO₂ and Rh/Al₂O₃ catalysts reached saturation very quickly, however, even after forty one pulses of oxygen, the Rh/MoO₃ sample had still not reached equilibrium.

Table 7.4 Oxygen Adsorption

	Amount of O ₂ Adsorbed (Molecules of O ₂ per g Rh)	% Dispersion
2% Rh/SiO ₂	5.02 x 10 ²⁰	17%
Rh/Al ₂ O ₃	2.11 x 10 ²¹	72%
Rh/MoO ₃	1.66 x 10 ²¹	57%

Fig. 7.10

Rh/Al₂O₃ - The Effect of
Oxidation on CO Adsorption

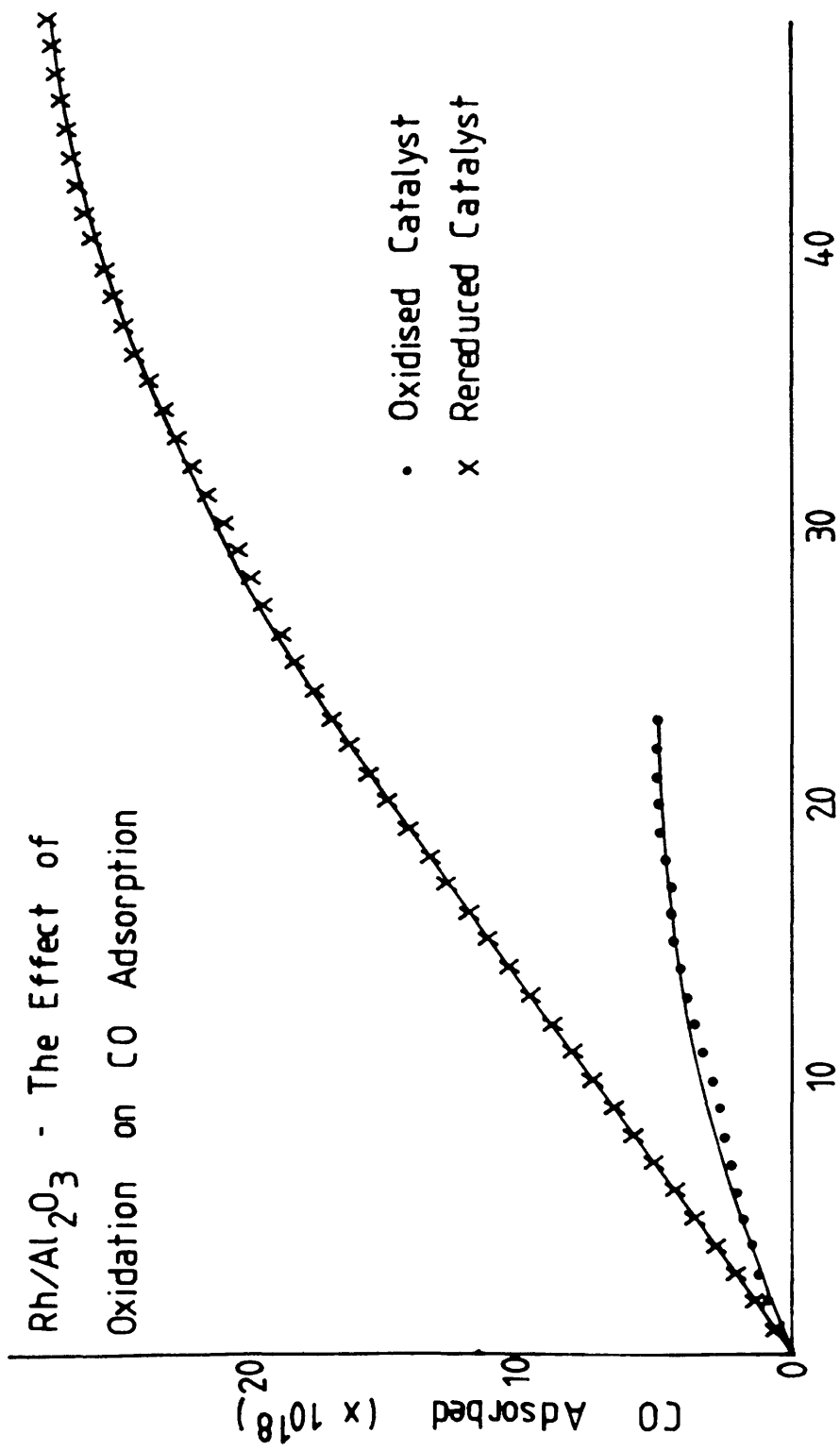
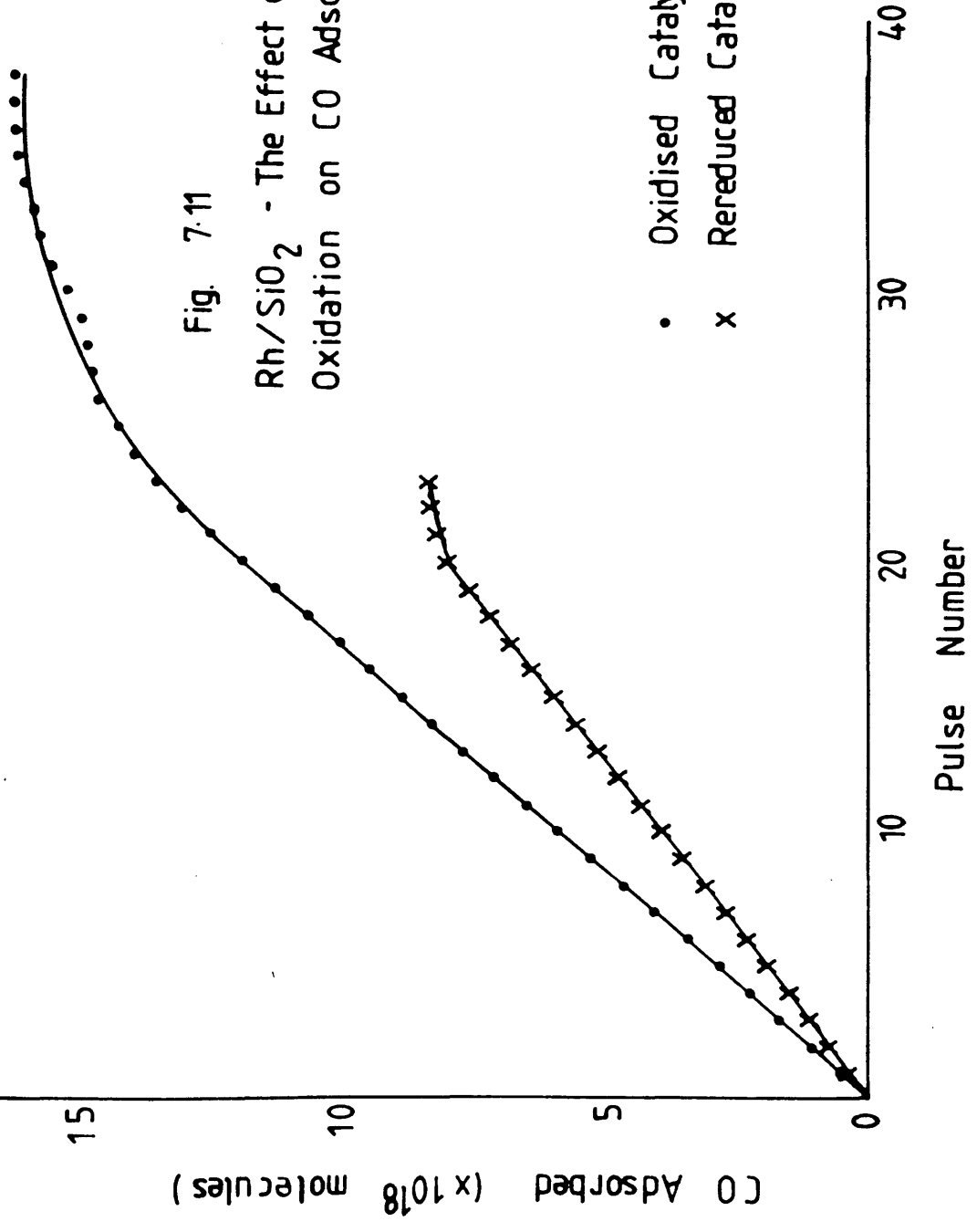


Fig. 7.11
Rh/SiO₂ - The Effect of
Oxidation on CO Adsorption

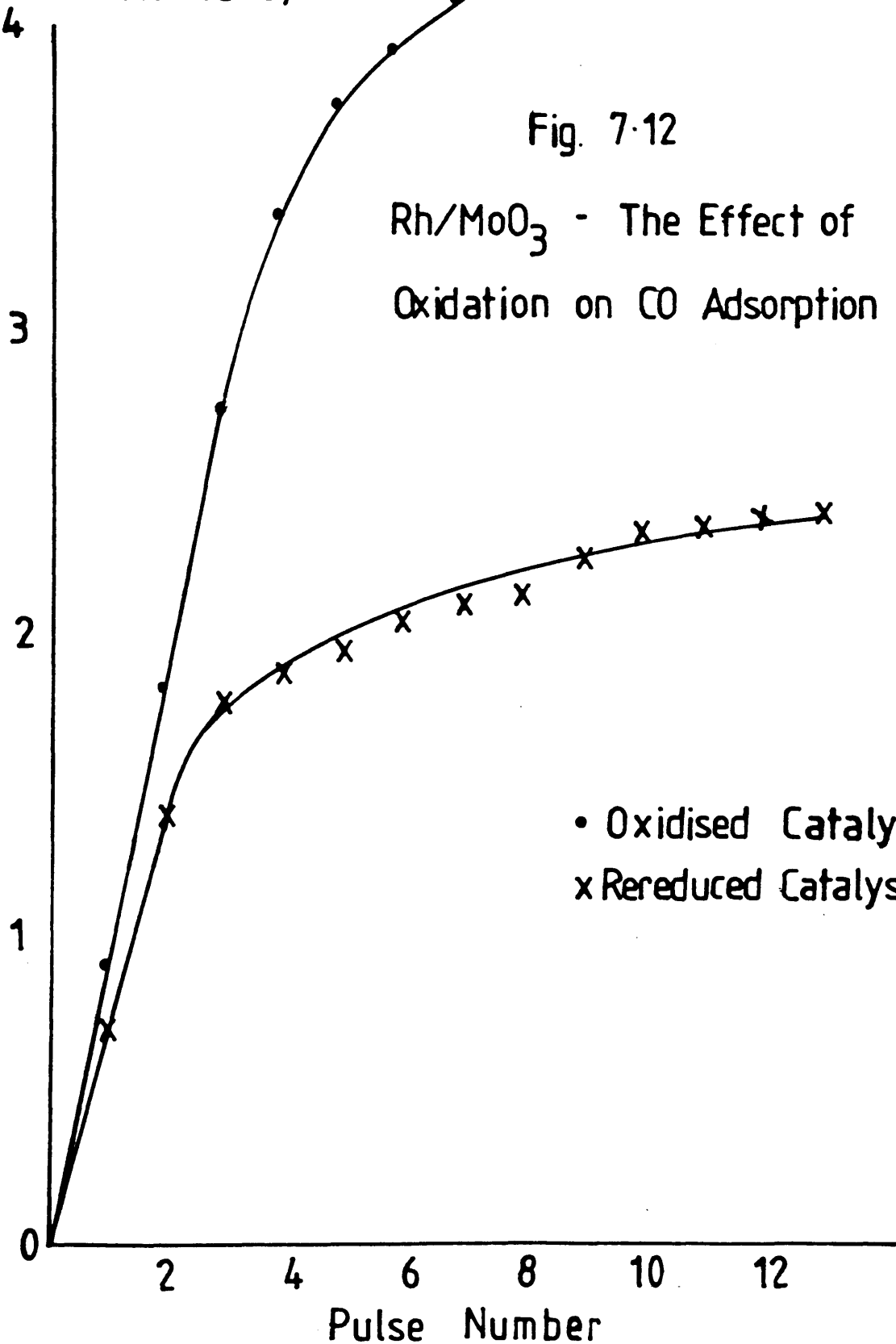


CO Adsorbed
($\times 10^{-18}$ molecules)

Fig. 7-12

Rh/MoO₃ - The Effect of
Oxidation on CO Adsorption

• Oxidised Catalyst
x Rereduced Catalyst



**7.3.5 CARBON MONOXIDE ADSORPTION ON TO A
PREOXIDISED CATALYST**

Freshly reduced catalyst samples were saturated with oxygen before being exposed to pulses of carbon monoxide. When the catalyst had reached "saturation" it was re-reduced in 6% hydrogen in nitrogen at 300°C for one hour. The amount of carbon monoxide taken up by the oxidised and re-reduced surfaces is shown in table 7.5 and in figs 7.10-7.12.

**Table 7.5 Carbon Monoxide Adsorption
on Preoxidised Catalyst Samples**

	CO Adsorption (Molecules of CO per g Rh)		
	Oxidised Surface	Rereduced Surface	Typical Result
2%Rh/SiO ₂	1.57 x 10 ²¹	8.14 x 10 ²⁰	1.1 x 10 ²¹
Rh/Al ₂ O ₃	7.21 x 10 ²⁰	4.02 x 10 ²¹	8.7 x 10 ²⁰
Rh/MoO ₃	5.61 x 10 ²⁰	2.91 x 10 ²⁰	2.53 x 10 ²⁰

Pre-adsorbed oxygen decreases the amount of carbon monoxide which will adsorb on the Rh/Al₂O₃ catalyst. After re-reduction of the oxidised surface, the other two catalysts adsorbed slightly less carbon monoxide, suggesting a loss of surface area during the oxidation-reduction cycle.

7.3.6 THE INFLUENCE OF PREADSORBED CARBON MONOXIDE ON CARBON DIOXIDE ADSORPTION

Each of the catalyst samples were exposed to carbon monoxide before the amount of carbon dioxide adsorbed by the catalyst was determined (Table 7.6). The catalysts were then re-reduced and the amount of carbon dioxide taken up by the re-reduced surface measured.

In each case more carbon monoxide was adsorbed on the pretreated surface than on the re-reduced one, although in each case a loss of surface area during the reduction cycle was also indicated.

Table 7.6 The Influence of Preadsorbed Carbon Monoxide on Carbon Dioxide Adsorption

	CO ₂ Adsorption (Molecules of CO ₂ per g Rh)		
	CO Treated Surface	Re-reduced Surface	Typical Value
2%Rh/SiO ₂	1.08 x 10 ¹⁹	2.32 x 10 ¹⁸	6.93 x 10 ¹⁸
Rh/Al ₂ O ₃	4.87 x 10 ¹⁹	1.49 x 10 ¹⁹	2.47 x 10 ¹⁹
Rh/MoO ₃	3.82 x 10 ¹⁹	6.74 x 10 ¹⁸	1.03 x 10 ¹⁸

7.3.7 THE INFLUENCE OF PREADSORBED CARBON DIOXIDE ON CARBON MONOXIDE ADSORPTION

Using a similar procedure to that described above, the influence of pretreating the catalysts with carbon dioxide before adsorbing carbon monoxide was investigated. Less

carbon monoxide was adsorbed on to the catalyst after the adsorption of carbon dioxide.

Table 7.7 **The Influence of Preadsorbed Carbon Dioxide**
on Carbon Monoxide Adsorption

	CO Adsorption (Molecules of CO per g Rh)		
	CO ₂ Treated Surface	Re-reduced Surface	Typical Values
2%Rh/SiO ₂	3.69 x 10 ²⁰	8.14 x 10 ²⁰	1.1 x 10 ²¹
Rh/Al ₂ O ₃	6.62 x 10 ²⁰	4.02 x 10 ²¹	8.7 x 10 ²⁰
Rh/MoO ₃	1.90 x 10 ²⁰	2.91 x 10 ²⁰	2.53 x 10 ²⁰

7.4 TEMPERATURE PROGRAMMED DESORPTION MEASUREMENTS

7.4.1 CARBON MONOXIDE TEMPERATURE PROGRAMMED DESORPTION

Pure carbon monoxide was passed over a freshly reduced sample of catalyst, at room temperature for ten minutes prior to the desorption measurements. The surface was then flushed with helium for a further ten minutes, before the temperature of the catalyst was increased at a steady 10°/min to 500°C.

Desorption peaks from the Rh/Al₂O₃ catalyst were detected at approximately 200°C and 330°C, but no identification of the desorbing species was made. Rh/SiO₂

produced a low temperature peak at 110°C which appeared to be a combination of two separate peaks which were very close together, and a high temperature peak at 375°C. The Rh/MoO₃ catalyst produced two small and ill-defined peaks at about 125°C and 165°C.

7.4.2 OXYGEN TEMPERATURE PROGRAMMED DESORPTION

Using exactly the same procedure as detailed above the Temperature Programmed Desorption (TPD) profile of oxygen adsorbed on these supported rhodium catalysts was determined. The Rh/Al₂O₃ catalyst produced a small but broad peak at about 480°C, while the silica supported catalyst had a profile which consisted of two small peaks at 225°C and 435°C. Rh/MoO₃ did not appear to desorb oxygen below 500°C, the highest temperature used in these experiments.

CHAPTER 8

INFRA - RED SPECTROSCOPY

All of the spectra described in this section were recorded in the environmental transmission cell discussed in section 3.7.4.1, using the experimental procedure described.

8.1 Carbon Monoxide

Figure 8.1 shows the infra-red spectrum of gas phase carbon monoxide at atmospheric pressure and ambient temperature. It consists of two peaks centred at 2174 cm^{-1} and 2115 cm^{-1} , with the second peak showing some evidence for infra-structure.

8.1.1 Carbon Monoxide on Rh/Al₂O₃

When carbon monoxide was adsorbed on to a freshly reduced sample of Rh/Al₂O₃, the spectrum shown in fig. 8.2 was obtained. This consisted of two very sharp bands at 2098 cm^{-1} and 2025 cm^{-1} , with a third, much broader peak at about 1845 cm^{-1} .

After saturating a sample of Rh/Al₂O₃ with carbon monoxide, the temperature of the catalyst was slowly increased, using the external furnace, and the infra-red spectrum of the surface was recorded (fig. 8.3).

Fig. 8.1

Gas Phase Carbon Monoxide

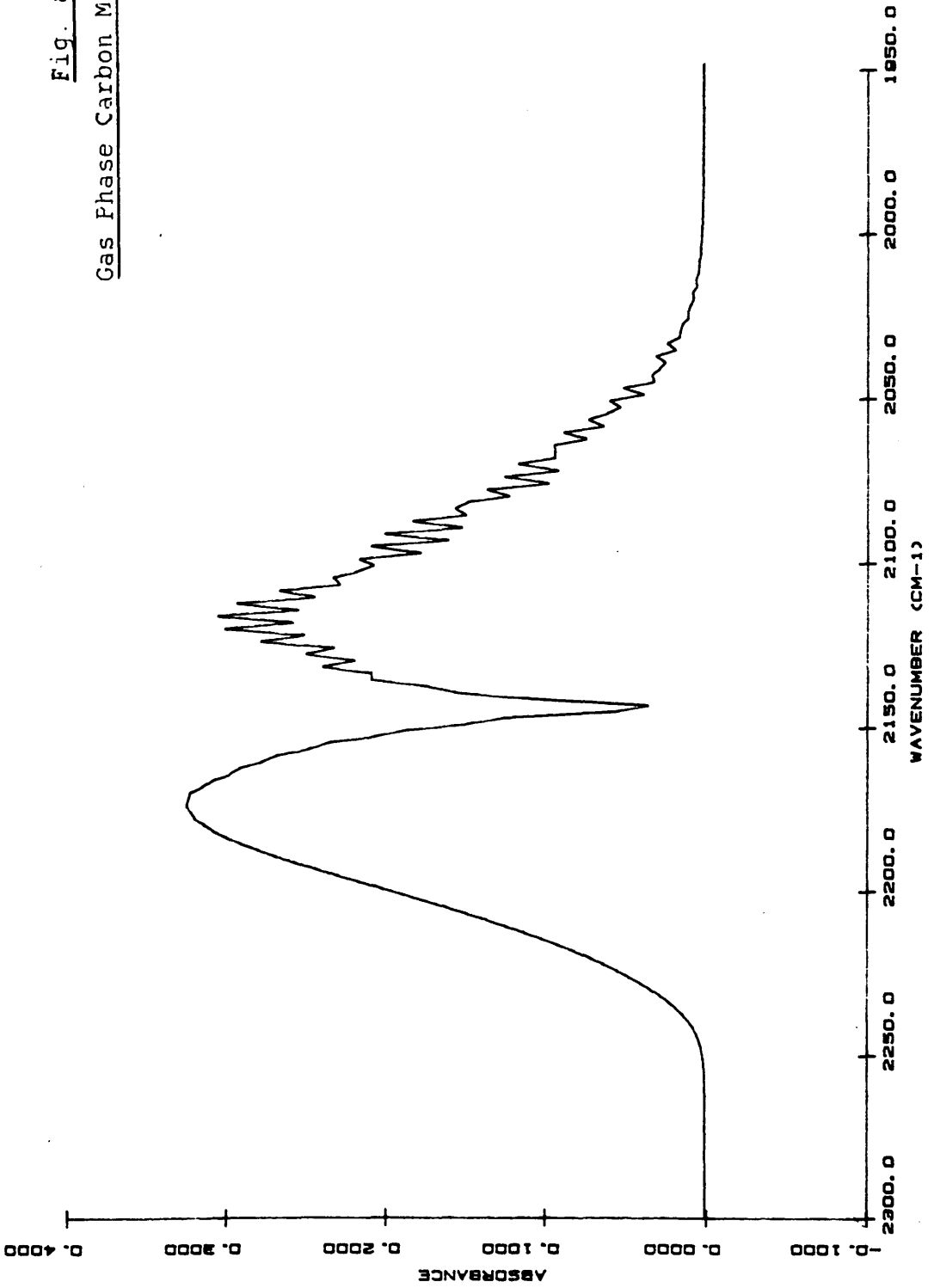


Fig. 8.2

Carbon Monoxide on Rh/Al₂O₃

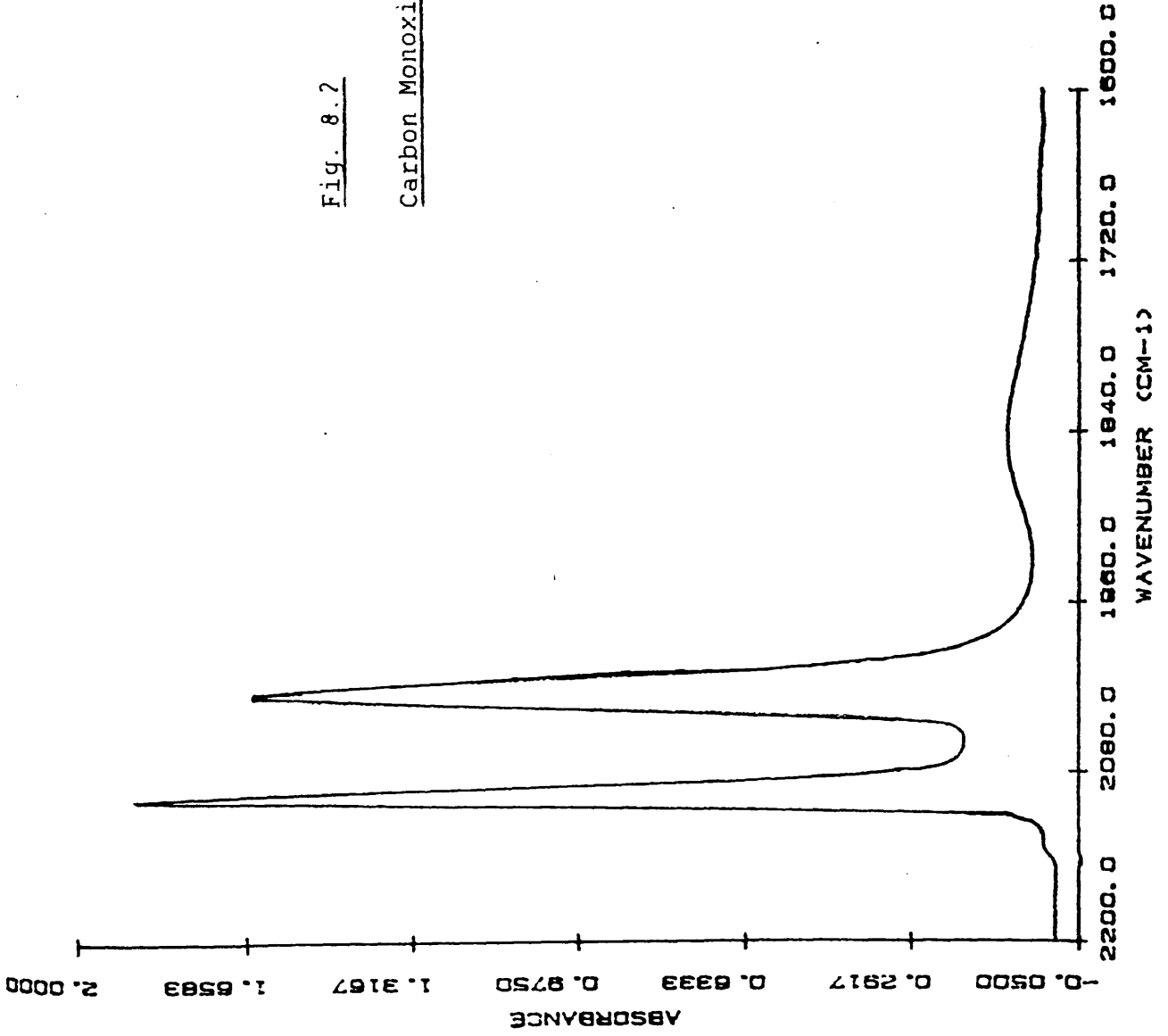
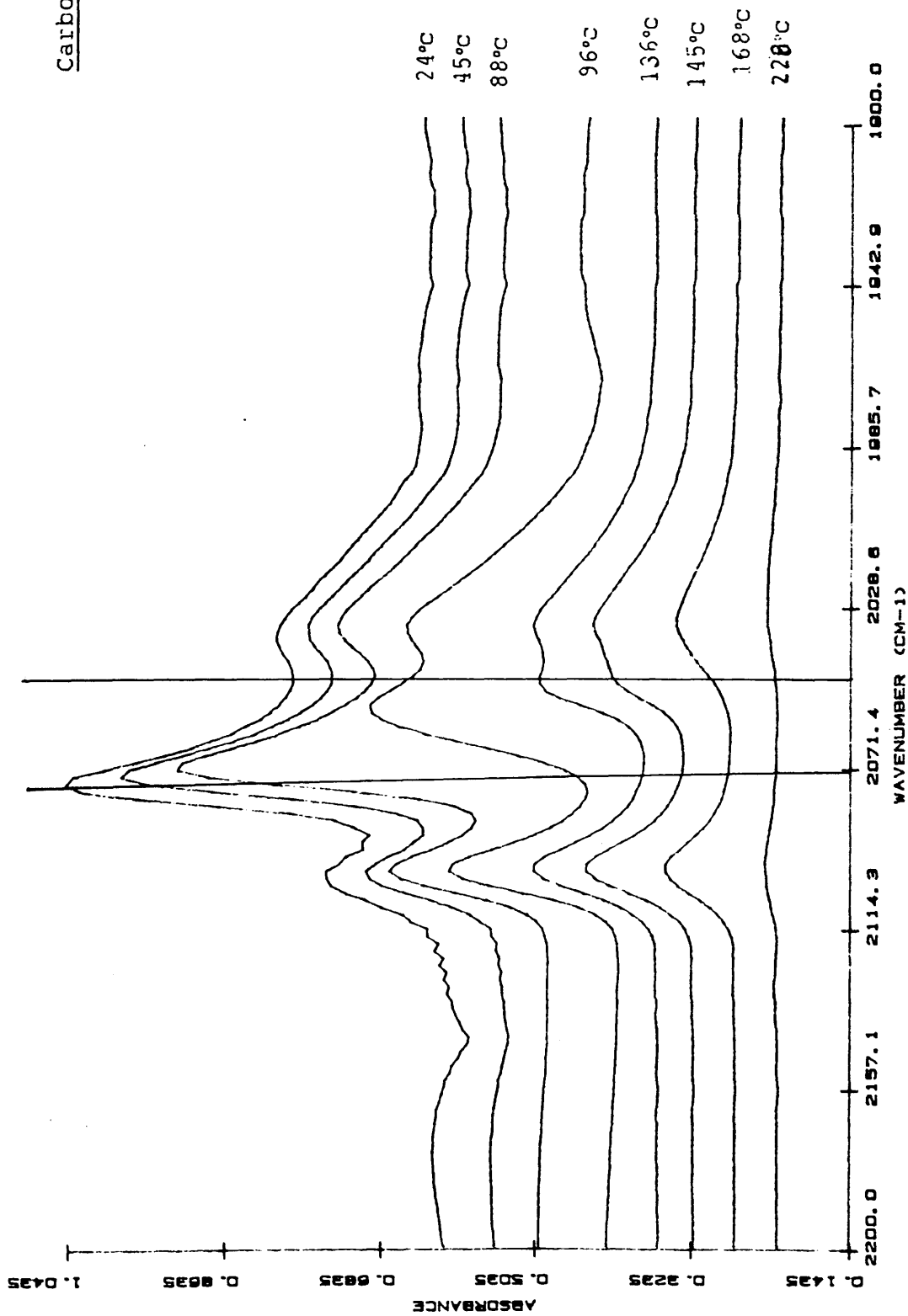


Fig. 8.3

Carbon Monoxide Desorption
From Rh/Al₂O₃



At ambient temperatures the spectra contained peaks at 2100 cm^{-1} and 2036 cm^{-1} as before, however, there was little evidence in this spectrum for a broad peak at about 1850 cm^{-1} and a very strong peak had appeared at 2075 cm^{-1} . There was also evidence at 2170 cm^{-1} and 2115 cm^{-1} for some remaining gas phase or physically adsorbed carbon monoxide which had not been removed from the surface by the helium carrier stream, this quickly disappeared as the temperature increased.

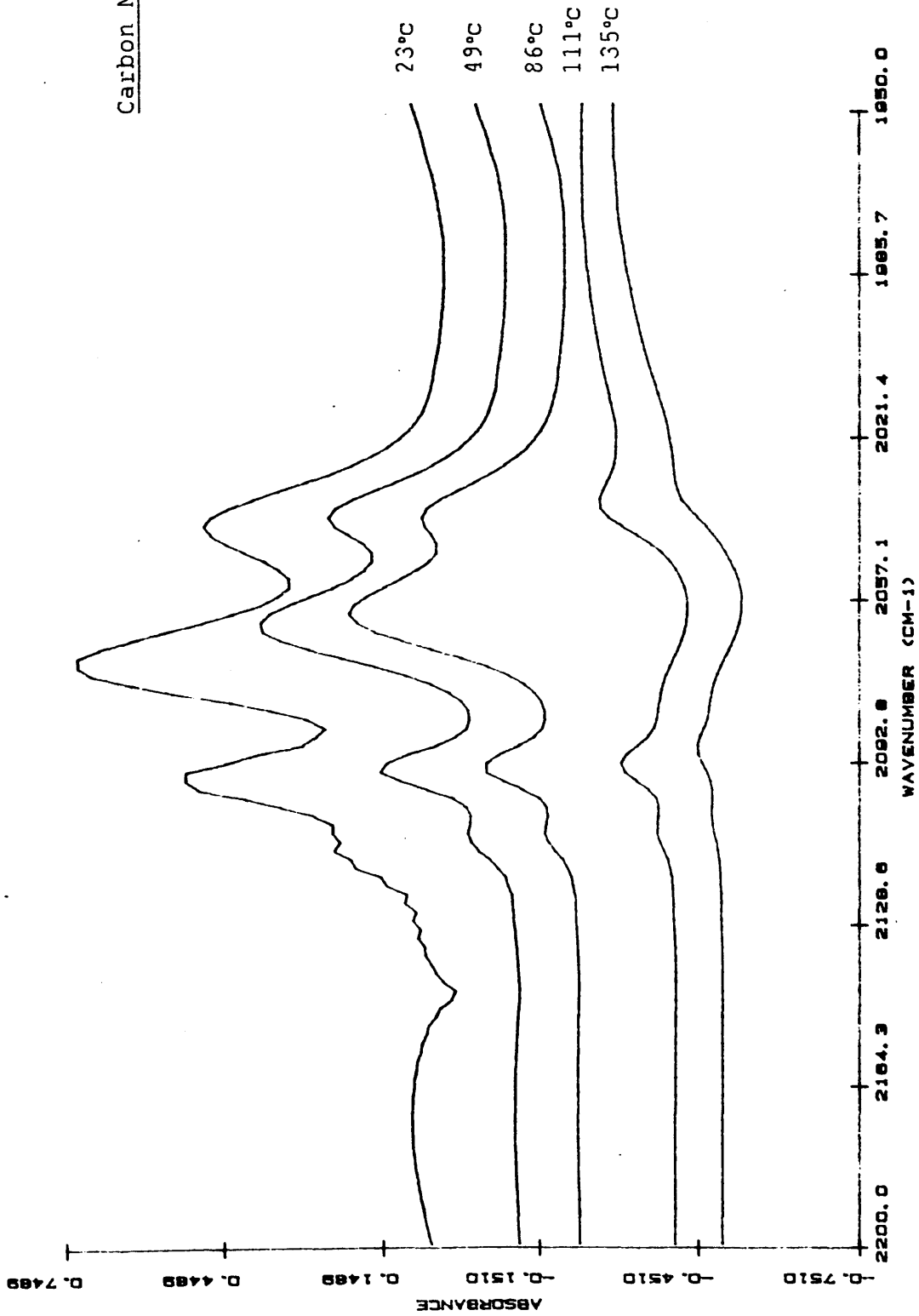
As the temperature increased and carbon monoxide desorbed from the surface, the peaks at 2100 cm^{-1} and 2036 cm^{-1} retained a constant position, while the 2075 cm^{-1} peak shifted from 2075 cm^{-1} at 24°C , to 2048 cm^{-1} at 130°C . The 2075 cm^{-1} peak also decreased most rapidly in intensity as the temperature was increased, the other peaks only starting to lose intensity above 100°C . By 245°C there was no evidence for any carbon monoxide remaining on the surface.

8.1.2 Carbon Monoxide Adsorption on Rh/SiO₂

When 2% Rh/SiO₂ was exposed to carbon monoxide, the spectrum shown in fig 8.4 was obtained. This spectrum consisted of three main peaks at 2095 , 2070 and 2042 cm^{-1} , together with some gas phase carbon monoxide and a small peak at 2108 cm^{-1} .

Fig. 8.4

Carbon Monoxide Desorption From Rh/SiO



As the temperature was increased, the 2070 cm^{-1} peak shifted to 2058 cm^{-1} and then disappeared completely between 86°C and 111°C . The positions of the other peaks remained constant, but by 135°C the species responsible for these peaks too, had all but desorbed .

The spectrum of carbon monoxide on the 5% Rh/SiO₂ catalyst is shown for comparison in fig 8.5. It consisted of three peaks at 2096 , 2064 and 2039 cm^{-1} , together with two broad peaks at 1886 cm^{-1} and 1630 cm^{-1} . A second sample of 5% Rh/SiO₂, however, had only two peaks in its spectrum (fig. 8.6) at 2102 cm^{-1} and 2023 cm^{-1} . These decreased steadily in intensity as the temperature was increased until, at approximately 165°C , there was very little carbon monoxide left on the surface .

8.1.3 Carbon Monoxide Desorption

The relative areas of the various peaks shown in figs 8.3 and 8.4 were measured by cutting out each peak and accurately determining its weight. It had been hoped to use the integrating capacity of the spectrometer to measure the peak areas, but, unfortunately, the peaks proved to be too close together for the computer to measure them accurately, and so this had to be done manually. The error on these measurements, however, was found to be less than ten percent. Figure 8.7 shows a plot of the area of the various peaks in fig 8.3 versus the temperature at which each of the

Fig. 8.5

Carbon Monoxide
on 5% Rh/SiO₂

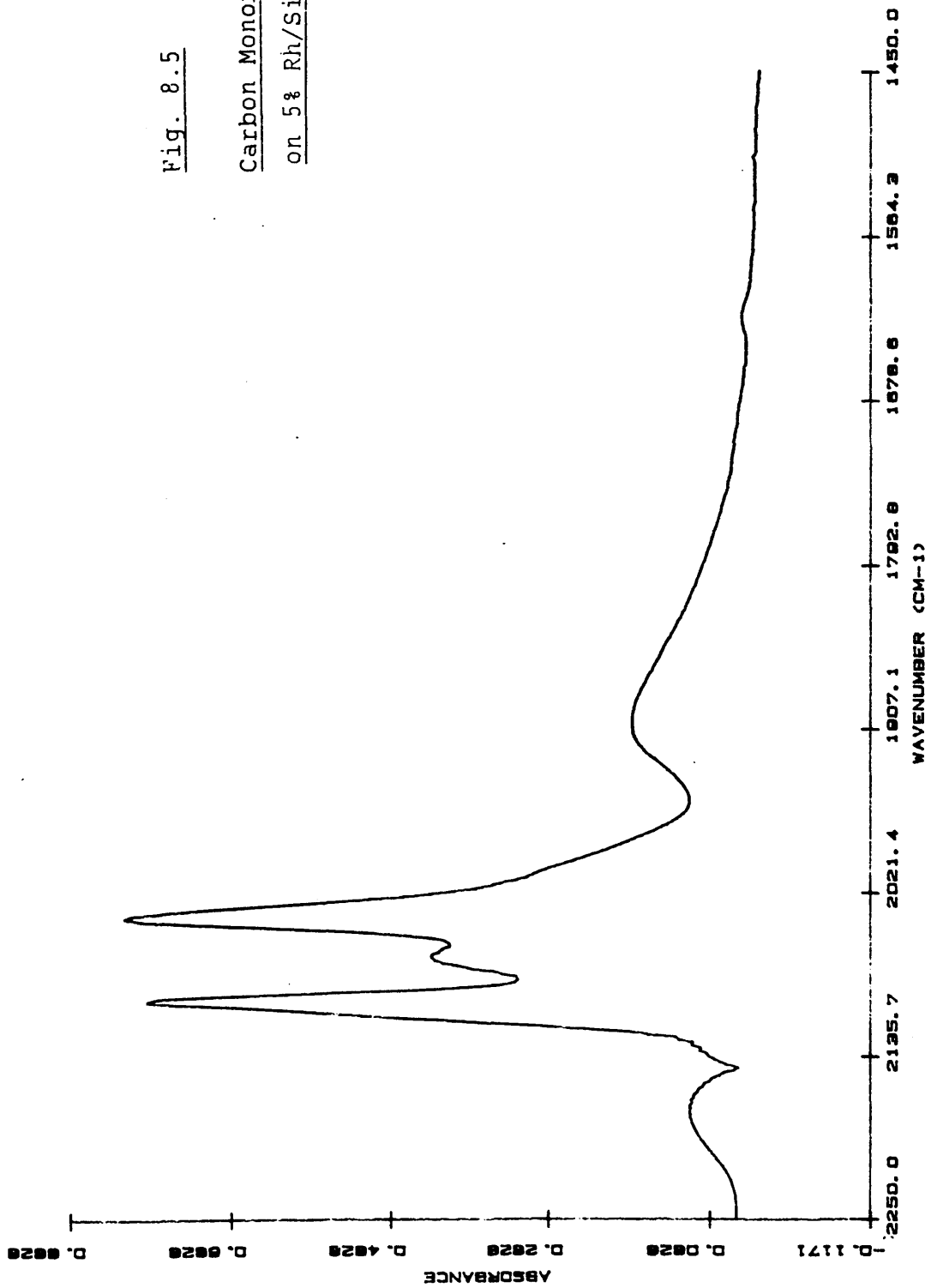


Fig. 8.6

Carbon Monoxide Desorption From Rh/SiO₂

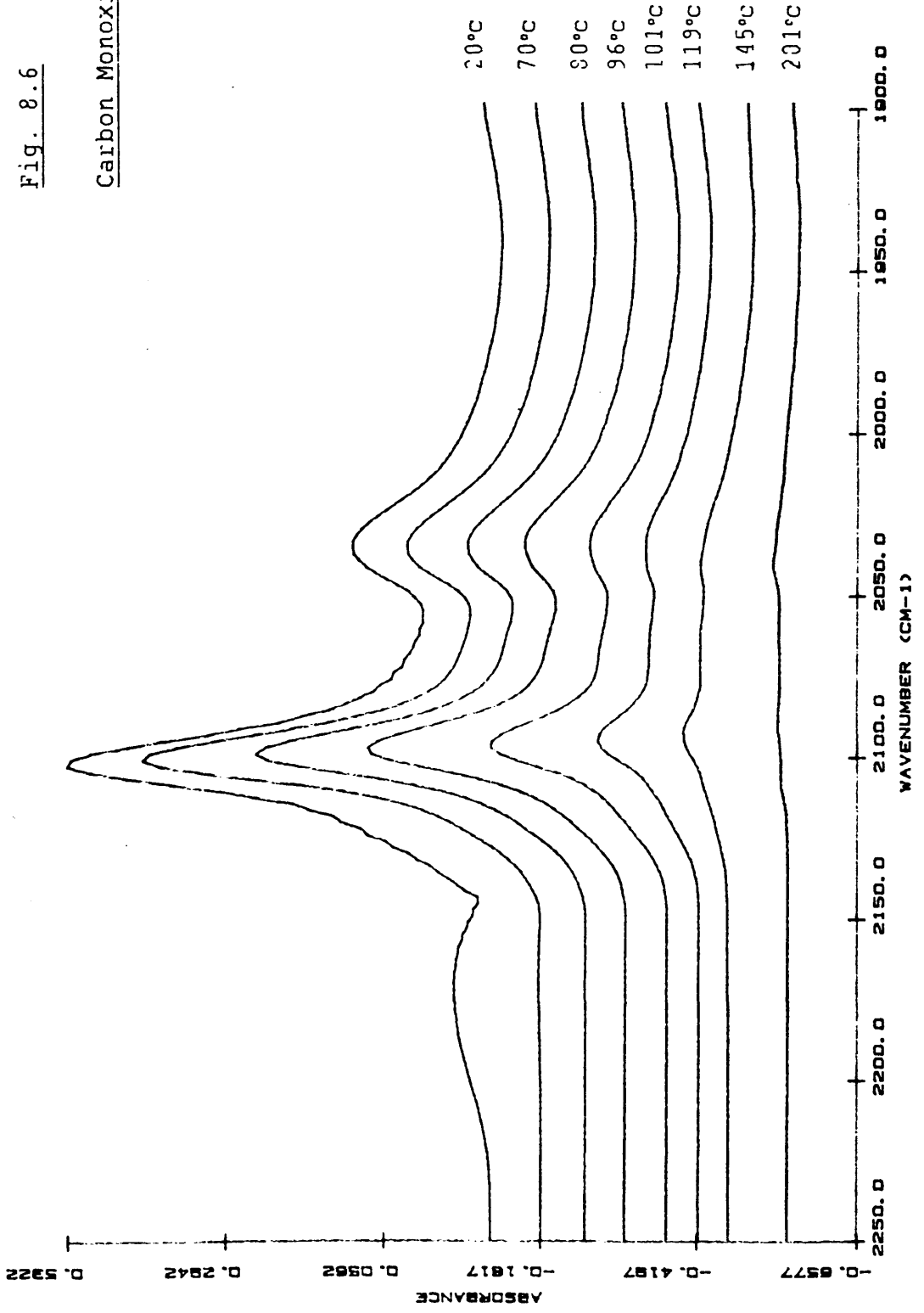
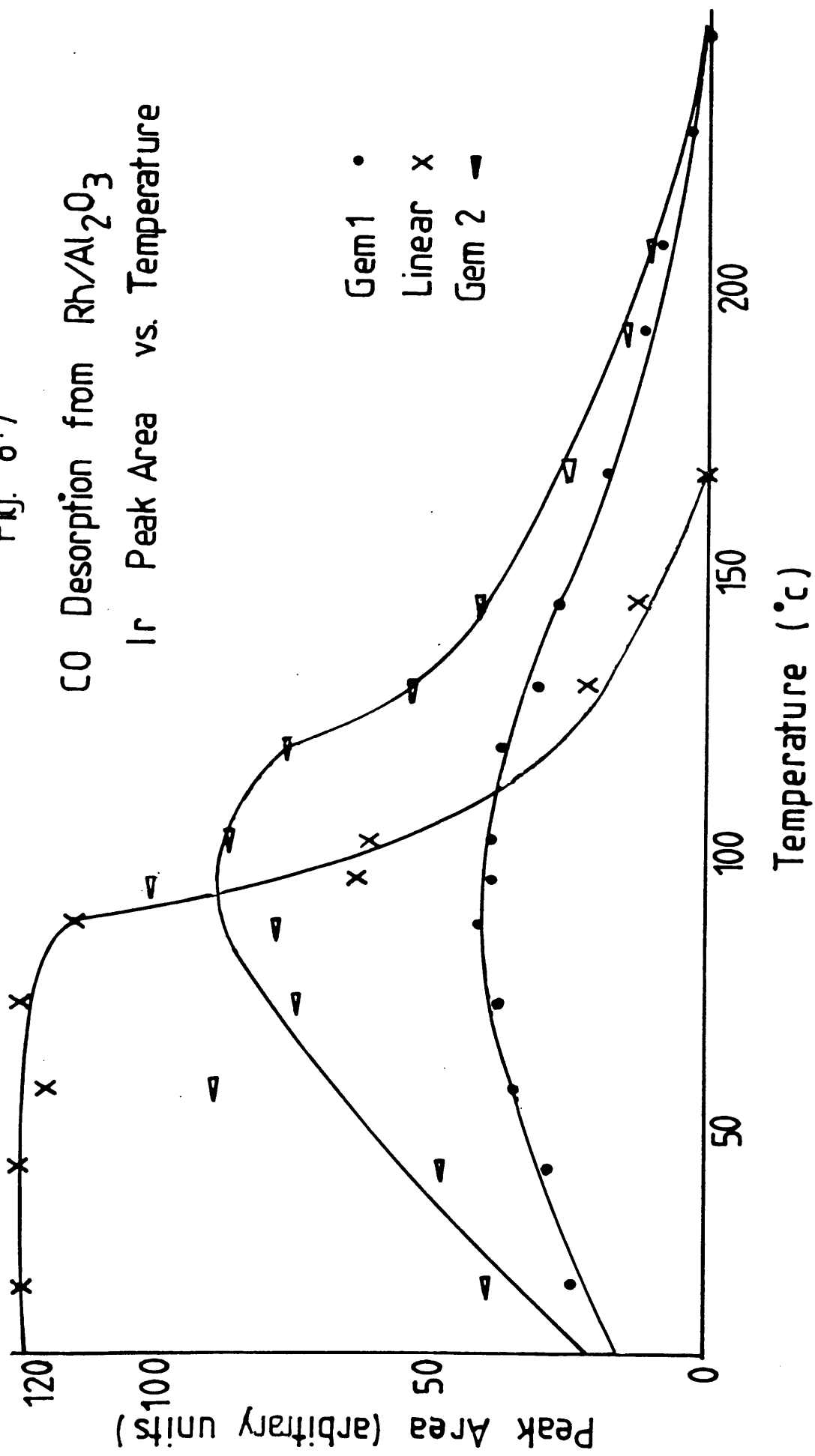


Fig. 8.7



spectra were taken. Whilst the area of the 2075 cm^{-1} peak behaved as expected, remaining fairly constant at the lower temperatures, before decreasing sharply at about 90°C , the other two peaks, at 2100 cm^{-1} and 2036 cm^{-1} , increased in intensity up to ca. 95°C , before decreasing as the temperature approached 240°C . The 2075 cm^{-1} peak disappeared at 170°C , whilst the other peaks were present until the temperature reached 240°C .

The area of the peaks in fig 8.4 were also plotted against the temperature of the spectrum, with the resulting graphs being shown in fig 8.8. From these graphs it can be seen that although the peaks at 2095 cm^{-1} and 2042 cm^{-1} do not increase in area as the temperature is raised, there appears to be a change in gradient of each of the lines at approximately 100°C .

8.1.4 The Influence of the Reduction Procedure on the Infra-red Spectrum of Adsorbed Carbon Monoxide

Each of the catalysts was reduced for thirty minutes under a flow of hydrogen, before being exposed to carbon monoxide for five minutes. Three of these reduction/adsorption cycles were carried out, with the infra-red spectrum of the surface being recorded after each one. The results are shown in figs 8.9-8.10.

Fig. 8.8

CO Desorption from
2% Rh/SiO₂

Ir Peak Area vs. Temperature

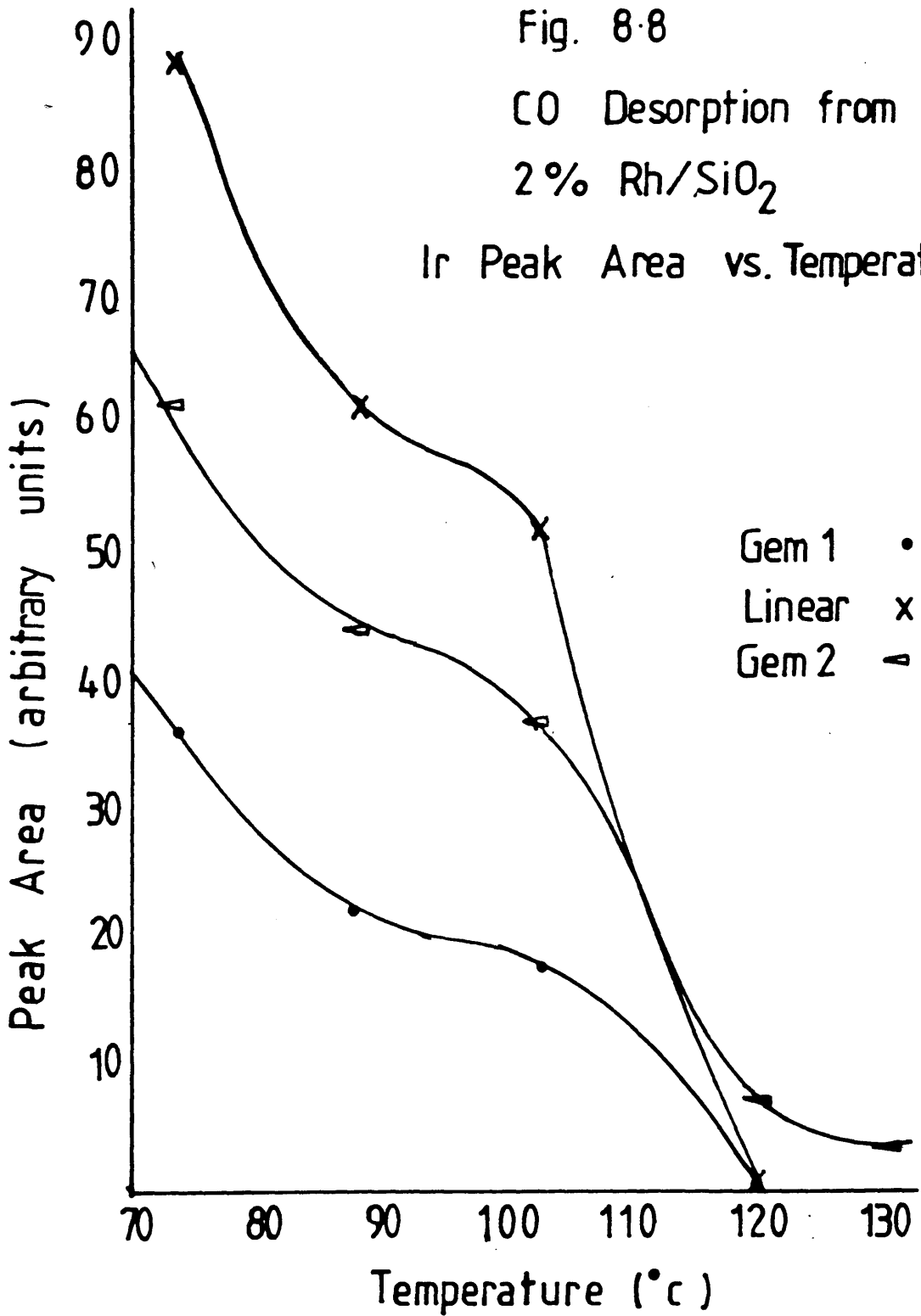


Fig. 8.9

Carbon Monoxide Spectra

The Effect of the Reduction procedure

Rh/Al₂O₃

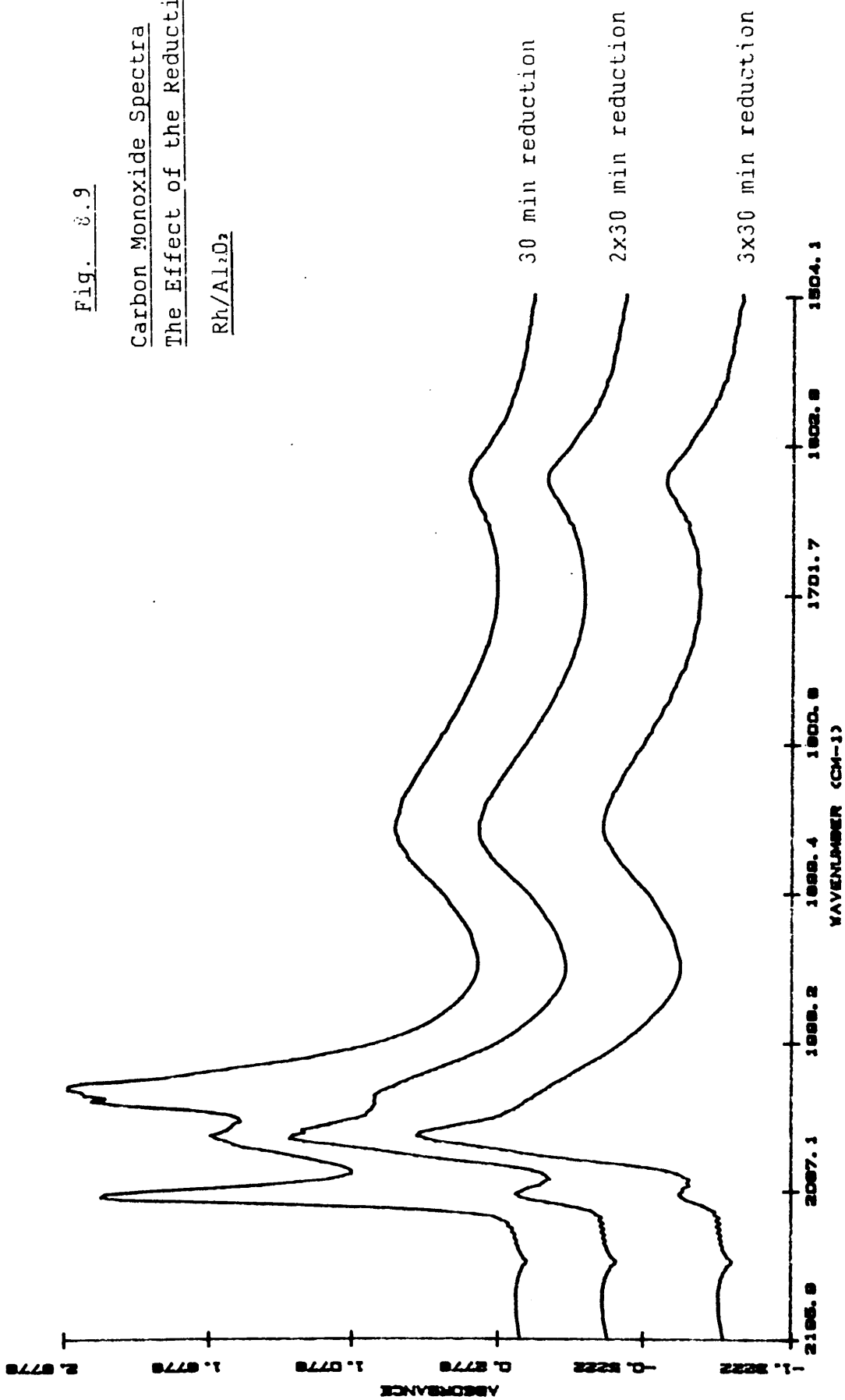
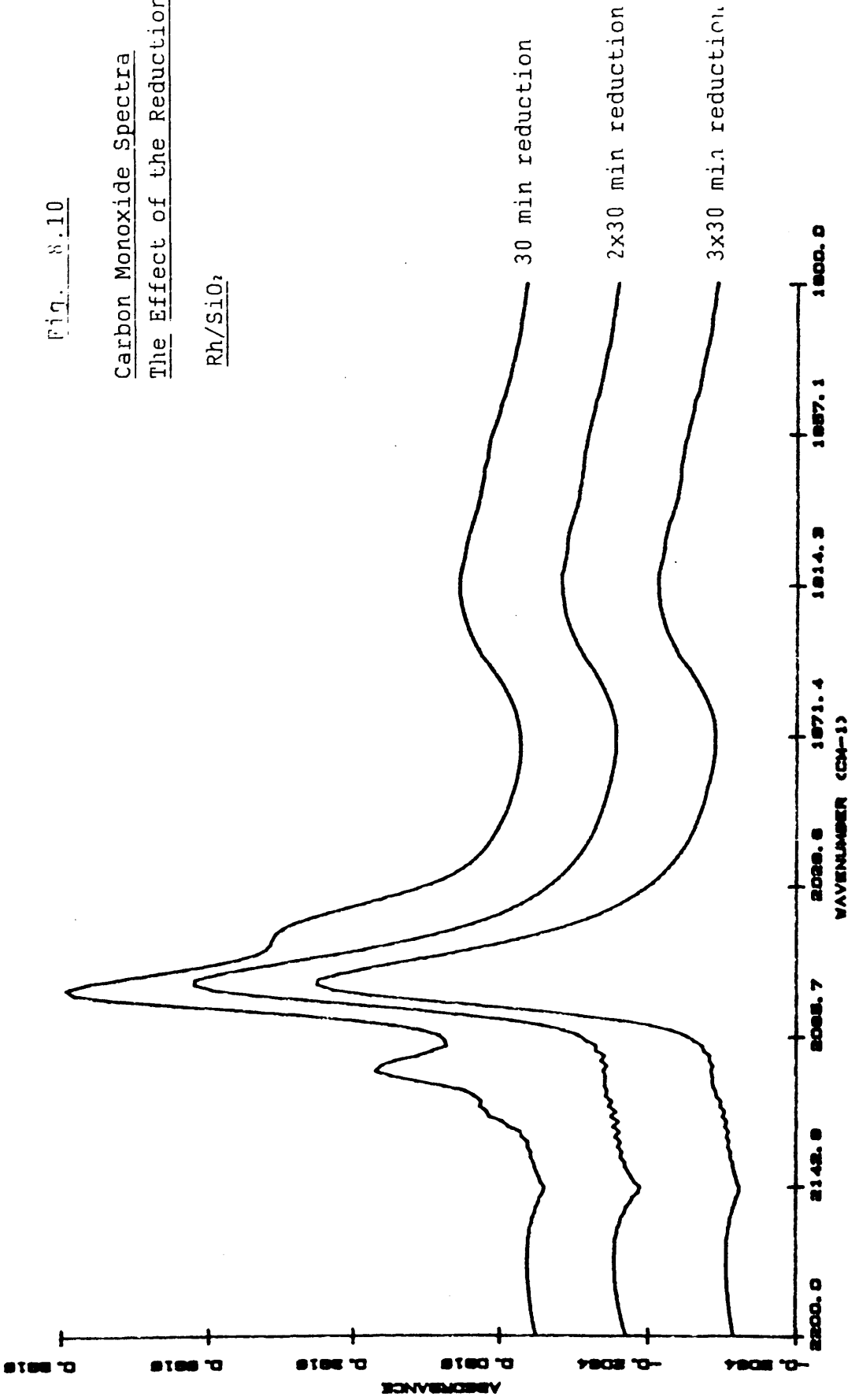


Fig. 8.10

Carbon Monoxide Spectra
The Effect of the Reduction Procedure

Rh/SiO₂



The initial Rh/Al₂O₃ spectrum consisted of five peaks at 2100, 2060, 2028, 1859 and 1632 cm⁻¹. The 2100 cm⁻¹ and 2028 cm⁻¹ peaks were much more intense than the peak at 2060 cm⁻¹. However, after two reduction cycles, the peak at 2060 cm⁻¹ was relatively more intense than the other two peaks, which were little more than shoulders at 2098 cm⁻¹ and 2035 cm⁻¹. The rest of the peaks appeared to be unaffected by the reduction treatment .

The same pattern was observed with the 2% Rh/SiO₂ catalyst. The bands at 2100 cm⁻¹ and 2034 cm⁻¹ were initially less intense than the central peak at 2066 cm⁻¹, and after two reduction cycles, only the 2066 cm⁻¹ peak, and one at 1940 cm⁻¹, remained .

8.1.5 Carbon Monoxide and Hydrogen Co-Adsorption

The co-adsorption of carbon monoxide and hydrogen on the Rh/Al₂O₃ and Rh/SiO₂ catalysts was investigated in order to identify some of the species present on the surface under reaction conditions.

The gas phase spectrum of the 1:2 CO/H₂ mixture, used in these experiments, was identical to that of pure carbon monoxide (fig 8.1).

8.1.5.1 THE CO-ADSORPTION OF CARBON MONOXIDE AND

HYDROGEN ON Rh/Al₂O₃

A freshly reduced sample of Rh/Al₂O₃ was saturated with the adsorption mixture at ambient temperature, before being flushed with helium for 5 minutes to remove any weakly held material. The results are shown in fig 8.11.

The main features are two peaks at 2096 cm⁻¹ and 2026 cm⁻¹, together with a smaller peak at 2129 cm⁻¹. There is also a significant amount of carbon dioxide on the surface as evidenced by the two peaks at 2361 cm⁻¹ and 2342 cm⁻¹ (see section 8.1.2). As the temperature was increased the intensity of the carbon monoxide peaks steadily decreased, until at 280°C, only carbon dioxide remained on the surface.

The catalyst was then cooled to 230°C and again exposed to the reaction mixture (fig 8.12). Apart from peaks due to gas phase carbon monoxide, a number of peaks appeared, the most intense of which occurred at 2046 cm⁻¹. A rather broad peak centred around 1840 cm⁻¹ also developed, together with three very small peaks at 1580, 1462 and 1340 cm⁻¹.

The catalyst was then maintained at 230°C overnight in a continuous flow of carbon monoxide and hydrogen, before a second spectrum was taken. This spectrum was very similar to the previous one, except that the peaks at 1580 cm⁻¹ and

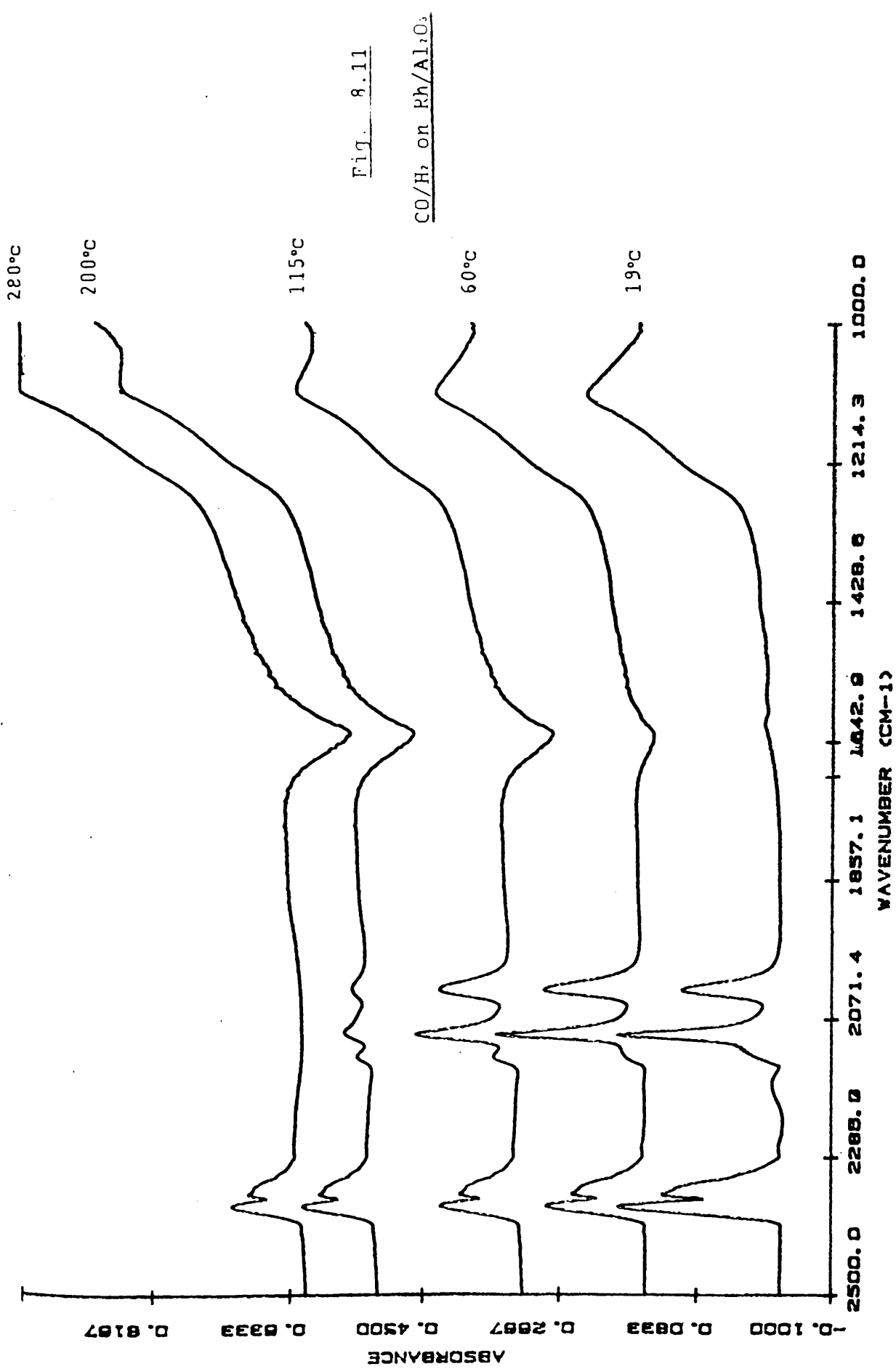
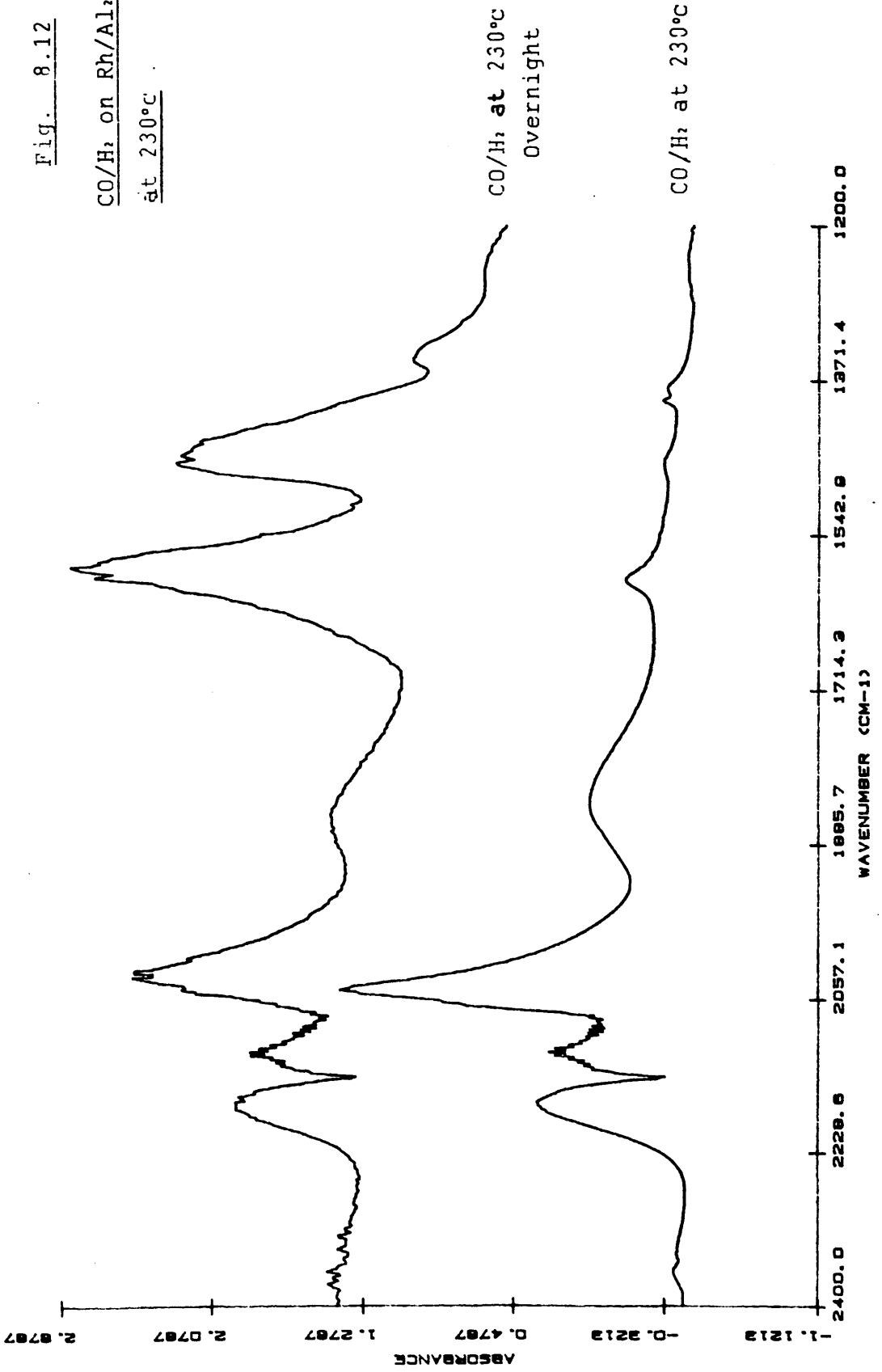


Fig. 8.11
CO/H₂ on Rh/Al₂O₃

Fig. 8.12

CO/H₂ on Rh/Al₂O₃
at 230°C



1462 cm^{-1} had grown quite considerably. All of the infrared peaks appeared to be stable to a five minute helium flush at 230°C,

A rhodium mirror was found to have formed on the inside of the catalyst holder during this prolonged period, at elevated temperatures, in the presence of carbon monoxide and hydrogen. The transmission of the catalyst sample was also severely reduced during this period.

8.1.5.2 THE CO-ADSORPTION OF CARBON MONOXIDE AND HYDROGEN ON Rh/SiO₂

When a 1:2 mixture of carbon monoxide and hydrogen was adsorbed, at room temperature, on to a sample of 5% Rh/SiO₂, the spectrum shown in fig 8.13 was obtained. This spectrum consisted of three bands at 2095, 2063 and 2037 cm^{-1} , together with a broader peak at ca. 1900 cm^{-1} . This spectrum did not show any evidence for carbon dioxide formation.

On the other hand, when a sample of 2% Rh/SiO₂ was exposed to the reaction mixture (fig 8.14), only two peaks were observed, at 2067 cm^{-1} and 1915 cm^{-1} . With this sample a sizeable amount of carbon dioxide was formed.

On heating the catalyst to 300°C, the peak at 2067 cm^{-1} shifted to 2051 cm^{-1} , and two small peaks appeared at 1828 cm^{-1} and 1587 cm^{-1} . The peaks due to carbon dioxide at 2360 cm^{-1} and 2342 cm^{-1} were significantly larger at 300°C

Fig. 3.13

CO/H₂ on RH/SiO₂

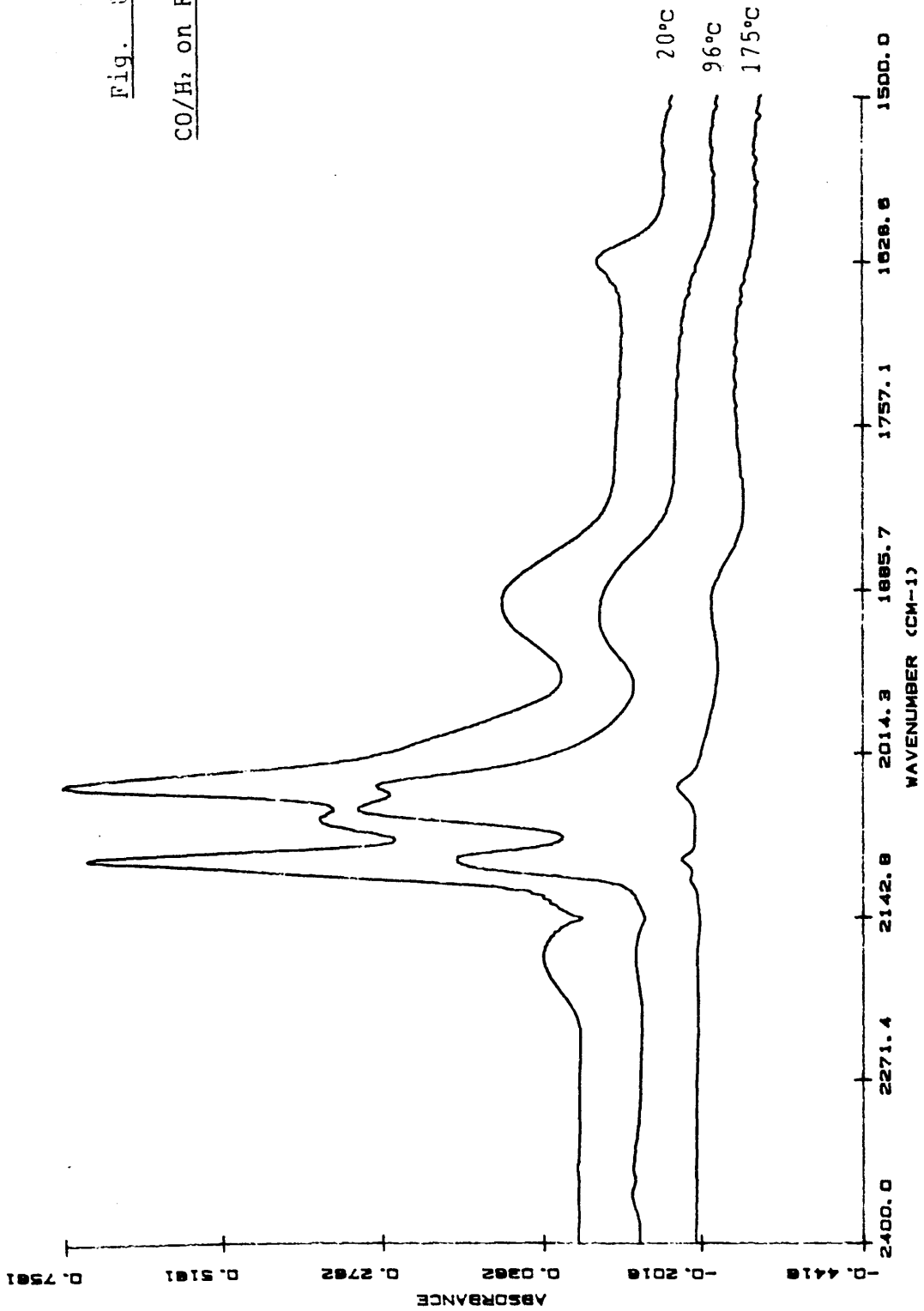


Fig. 8.14

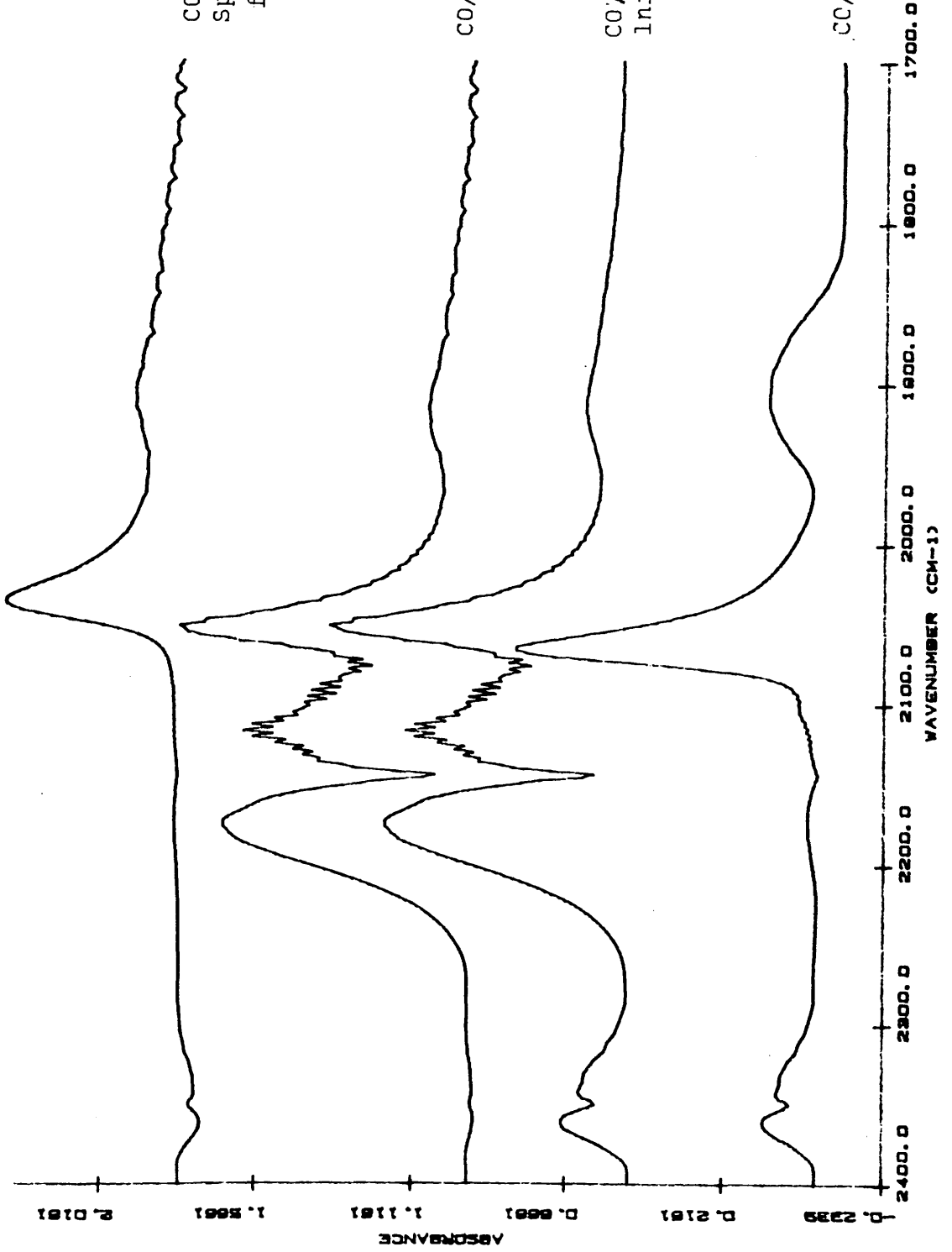
CO/H₂ On Rh/SiO₂ At 300°C

CO/H₂ at 300°C for 14 hr
Spectrum after a 10 mins
flush with He.

CO/H₂ at 300°C for 14 hr

CO/H₂ at 300°C
Initial Spectrum

CO/H₂ at 21°C



than at ambient temperature. After one hour at 300°C, however, the carbon dioxide doublet had, again, decreased in intensity.

After 14 hrs at 300°C, the spectrum was identical to that after one hour, under the reaction mixture, although the transmission of the catalyst sample had decreased substantially and a rhodium mirror had again been formed on the inside of the environmental cell.

After a ten minute flush with helium, the peaks at 2174 cm^{-1} and 2116 cm^{-1} (due to gas phase carbon monoxide) had completely disappeared and the peak at 2051 cm^{-1} had shifted to 2034 cm^{-1} , the rest of the spectrum remaining unchanged.

A summary of the results described in this section is presented in Table 8.1 overleaf.

8.2 CARBON DIOXIDE

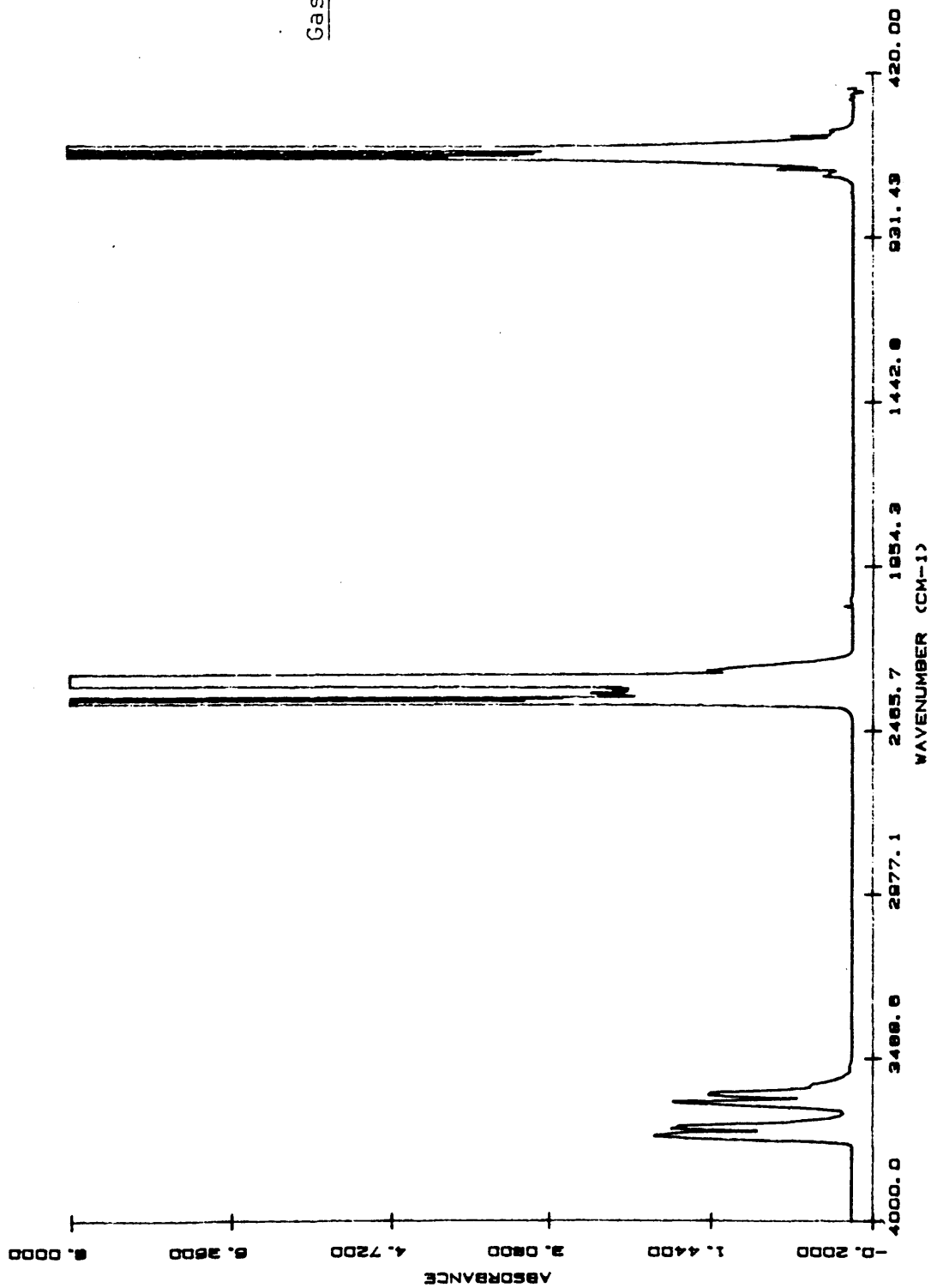
The gas phase spectrum of carbon dioxide is shown in fig 8.15. It consists of a doublet of doublets at 3727/3700 cm^{-1} and 3622/3600 cm^{-1} , together with two other doublets at 2377/2303 cm^{-1} and 678/657 cm^{-1} . With any of the catalysts under consideration any low wavenumber peaks will be completely obscured by support absorption and so, for practical purposes, can be ignored

Table 8.1 Carbon Monoxide Summary

	<u>Peak Position (cm-1)</u>	<u>Comments</u>
Gas Phase CO	2174 2115	
CO on Rh/Al ₂ O ₃ at 18°C	2100 2070 2036 1800-1900	2070 peak shifted to 2048 as the temperature increased (least stable species). All CO had desorbed by 245°C
CO/H ₂ on Rh/Al ₂ O ₃ at 18°C	2096 2026	Adsorbed CO ₂ was also observed.
CO/H ₂ on Rh/Al ₂ O ₃ at 300°C for 14 hr	2046 1580 1462 1344	Bands stable to 5 min flush. Rh mirror formed. Low transmission.
CO on Rh/SiO ₂ at 18°C	2100 2070 2035 1800-1900	2070 peak shifted to 2058 as the temperature is increased (least stable species). All CO had desorbed by 150°C
CO/H ₂ on Rh/SiO ₂ at 18°C	2095 2063 2037	Adsorbed CO ₂ was also observed.
CO/H ₂ on Rh/SiO ₂ at 300°C for 14 hrs	2051 1828 1587	2051 peak shifted to 2034 after helium flush. All other peaks were unaffected. CO ₂ concentration was initially higher at 300°C than 18°C but quickly fell again. Rh mirror formed. Low transmission.

Fig. 8.15

Gas Phase Carbon Dioxide



During these experiments the optical bench of the Nicolet spectrometer was not flushed with nitrogen, therefore, many of the spectra described in this chapter contain small bands at 2377 cm^{-1} and 2303 cm^{-1} due to atmospheric carbon dioxide. As the concentration of carbon dioxide was not constant with time, these bands can appear as either positive or negative peaks - depending on the relative concentrations of carbon dioxide present during the reference and the adsorption spectra.

8.2.1 CARBON DIOXIDE ON Rh/Al₂O₃

When carbon dioxide was adsorbed on Rh/Al₂O₃ at ambient temperature, the spectrum shown in fig 8.16 was obtained. It consists of a doublet of peaks at 2363 cm^{-1} and 2342 cm^{-1} , together with a small peak at 2273 cm^{-1} . Two very weak peaks were also detected at 2098 cm^{-1} and 2031 cm^{-1} , in the carbon monoxide region of the spectrum. The rest of the spectrum contained three well defined peaks at 1650, 1448 and 1227 cm^{-1} . Each of the peaks decreased in intensity as the temperature was increased, so that by 233°C , only two small peaks at 2362 cm^{-1} and 2342 cm^{-1} remained.

8.2.2 CARBON DIOXIDE ON Rh/SiO₂

When carbon dioxide was adsorbed on 5% Rh/SiO₂ (fig 8.17) the spectrum was very similar to that of

Fig. 8.16

Carbon Dioxide on Rh/Al₂O₃

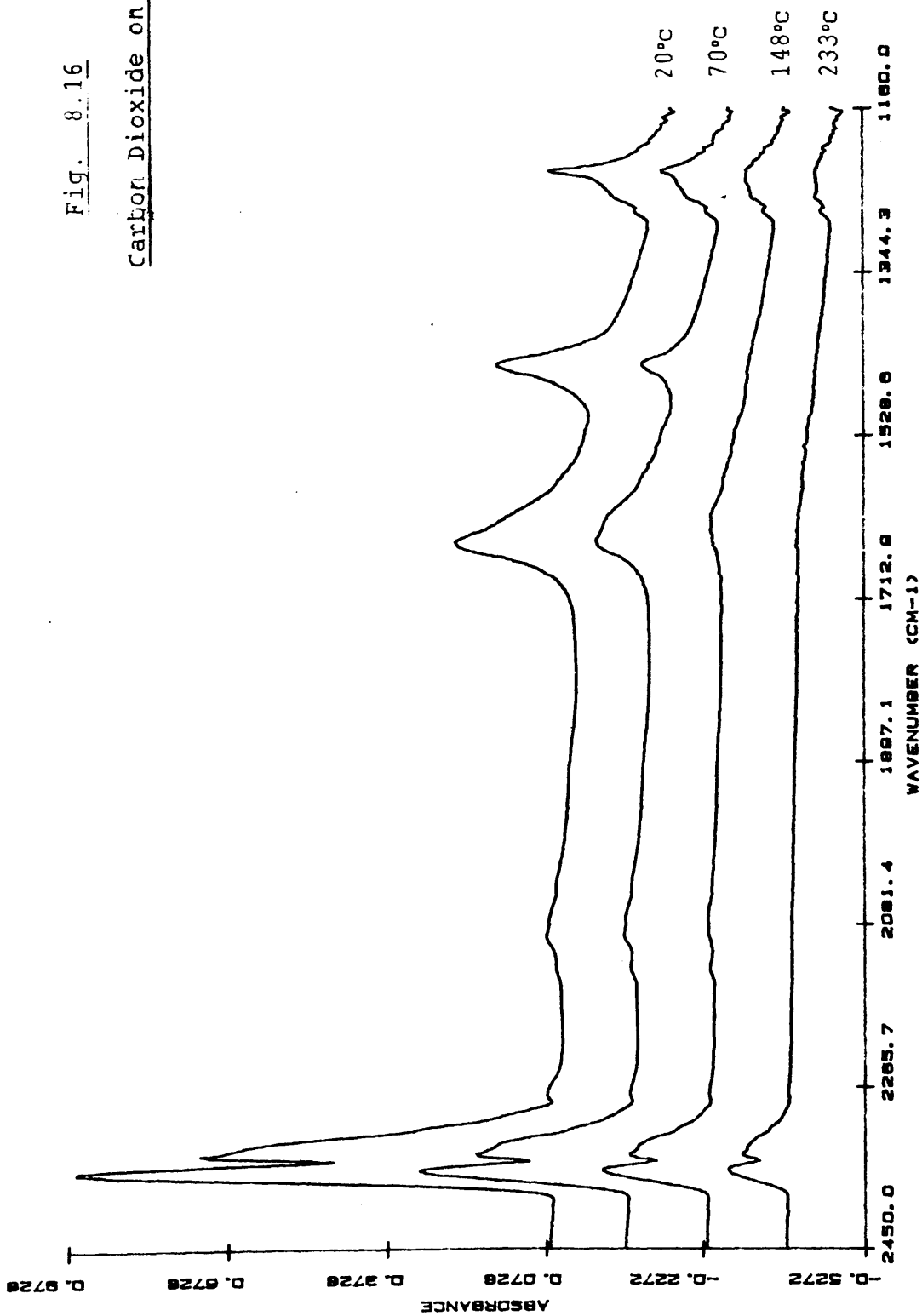
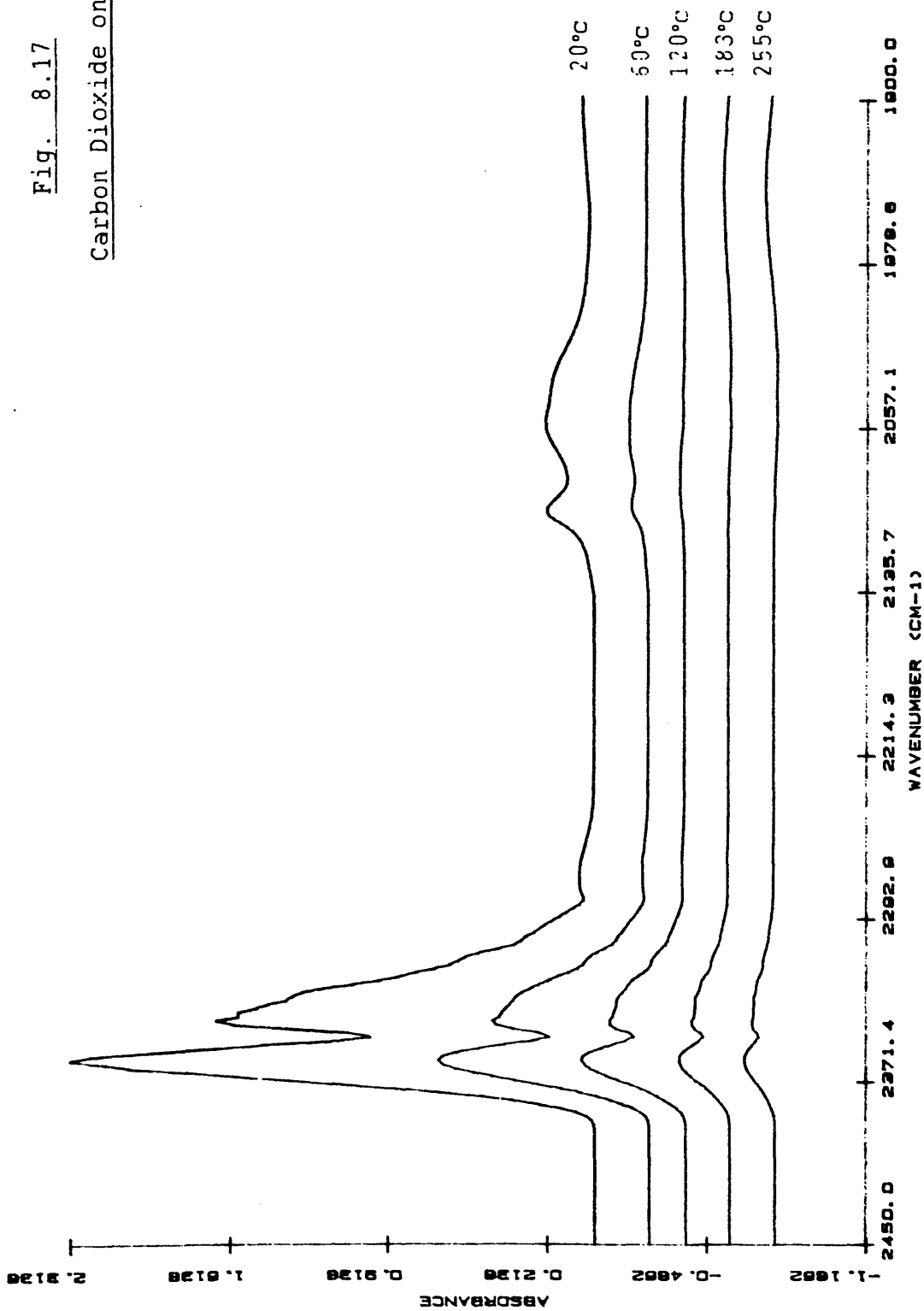


Fig. 8.17

Carbon Dioxide on Rh/SiO₂



Rh/Al₂O₃. The two main bands appeared at 2360 cm⁻¹ and 2341 cm⁻¹, with a small peak at 2274 cm⁻¹. Three weaker bands were detected at 2096, 2052 and 2031 cm⁻¹. These peaks had disappeared completely by 120°C, whilst the peaks at 2360 cm⁻¹ and 2341 cm⁻¹ were present up to 255°C. A very weak band was also detected at 1628 cm⁻¹. A summary of the results for carbon dioxide adsorption is shown in Table 8.2.

Table 8.1 Carbon Dioxide Summary

	Peak Positions (cm ⁻¹)
Gas phase CO ₂	3727/3700, 3622/3600, 2377/2303 678/657
CO ₂ on Rh/Al ₂ O ₃	2363, 2342, 2098, 2031, 1650, 1448, 1227
CO ₂ on Rh/SiO ₂	2360, 2341, 2096, 2052, 2031, 1628

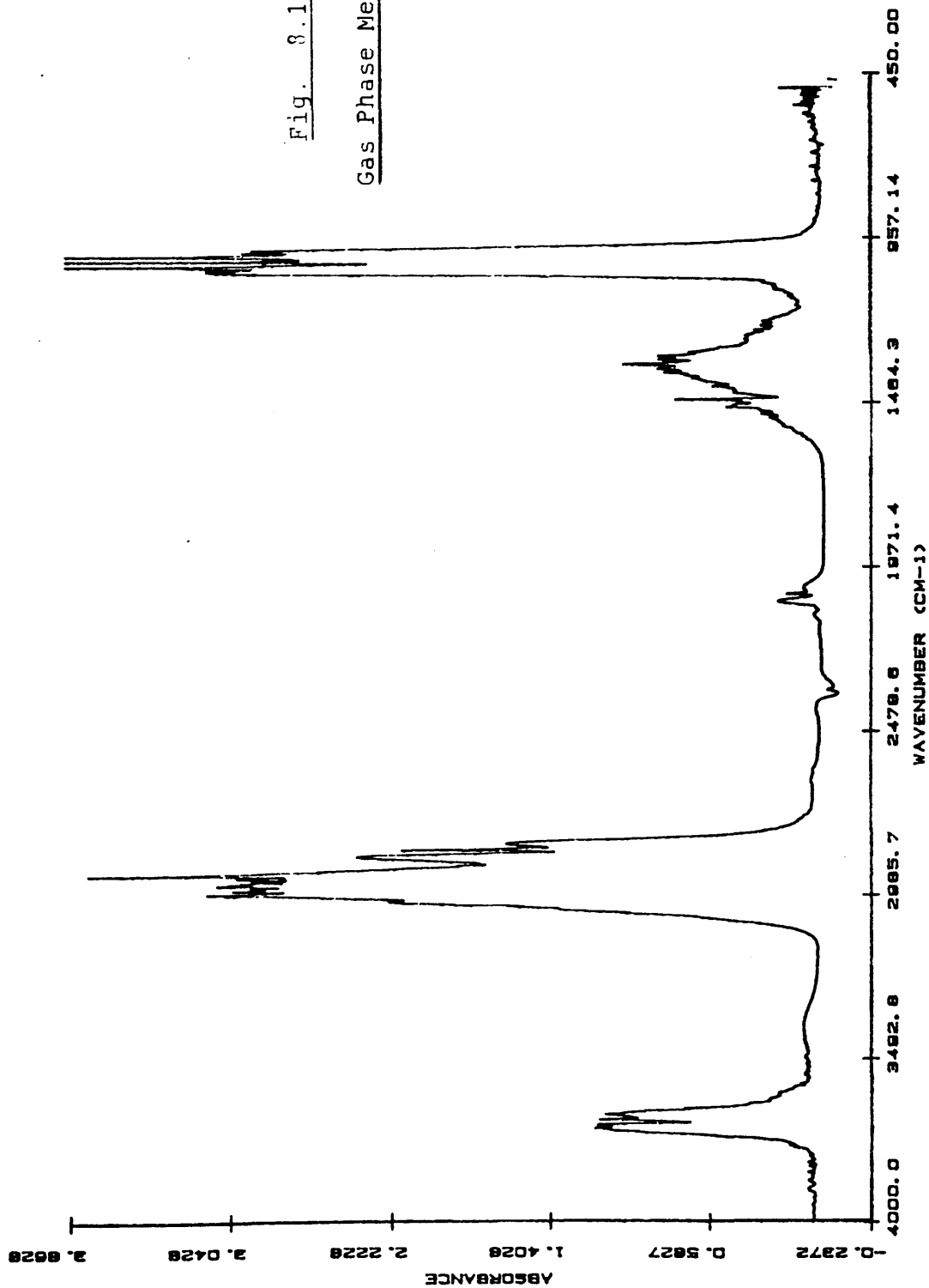
8.3 METHANOL ADSORPTION

The gas phase spectrum of methanol (fig 8.18) was obtained by slowly dripping AnalaR methanol into the helium carrier gas, passing through the empty environmental cell.

The spectrum consisted of a doublet of doublets at 3706 cm⁻¹ and 3681 cm⁻¹, a large peak between 2980 and 2870 cm⁻¹, two smaller bands at 1456 cm⁻¹ and 1343 cm⁻¹ and a very

Fig. 3.18

Gas Phase Methanol



intense band around 1040 cm^{-1} . Three very small peaks were also observed at 2070 , 2050 and 2031 cm^{-1} .

8.3.1 METHANOL ADSORPTION ON Rh/Al₂O₃

The spectrum obtained when methanol was passed over the Rh/Al₂O₃ catalyst is shown in fig 8.19. This ambient temperature spectrum was taken thirty minutes after the initial injection of methanol, in order to limit the amount of physically adsorbed methanol on the surface.

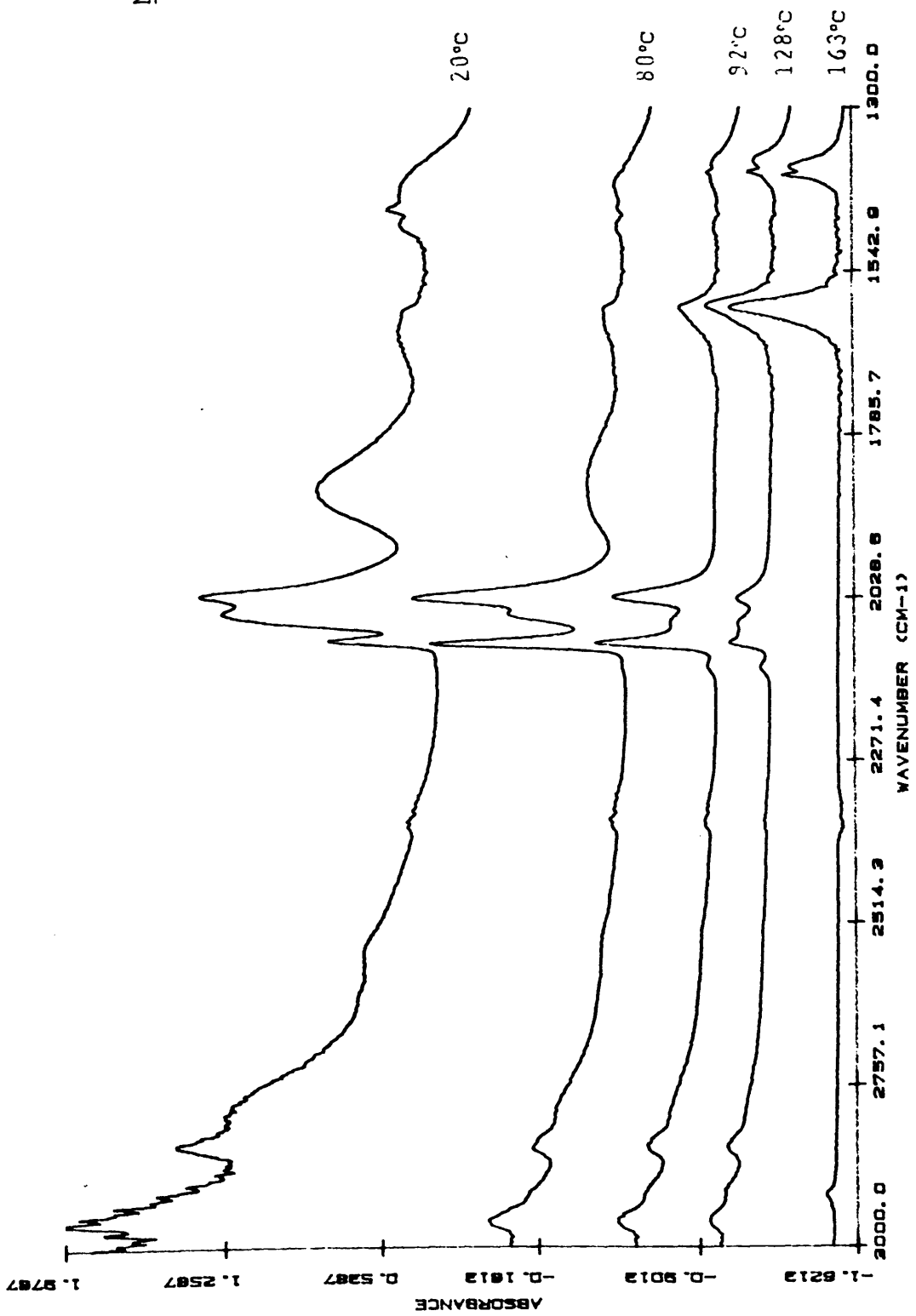
The spectrum consisted of two broad bands at 2953 cm^{-1} and 2847 cm^{-1} , which were probably due to some remaining physically adsorbed methanol. Two very weak peaks were observed at 2542 cm^{-1} and 2360 cm^{-1} . The major features of the spectrum, however, were the group of three peaks at 2096 , 2047 and 2024 cm^{-1} , with a broader band at ca. 1867 cm^{-1} , due to carbon monoxide on the surface. Smaller bands were also observed at 1635 , 1469 and 1449 cm^{-1} .

When the temperature of the catalyst was raised to 80°C , without any further addition of methanol, the peaks at 2096 , 2047 and 2024 cm^{-1} became sharper and better defined. The intensity of the 2096 cm^{-1} and 2031 cm^{-1} peaks growing at the expense of the central peak.

As the temperature was increased further the carbon monoxide peaks decreased in intensity, until at 163°C the

Fig. 8.19

Methanol on Rh/Al₂O₃



only features on the spectrum were the band at 1635 cm^{-1} and a doublet at 1391 cm^{-1} and 1381 cm^{-1} .

When methanol was adsorbed on $\text{Rh}/\text{Al}_2\text{O}_3$ at 285°C (fig 8.20), the spectrum consisted of bands due to gas phase carbon monoxide and physically adsorbed methanol, as well as bands at 2081 , 2053 , 2037 , 1847 and 1591 cm^{-1} . After a five minute flush with helium, the spectrum had simplified to a single peak at 2027 cm^{-1} , a broad one at 1847 and a sharp band at 1591 cm^{-1} . There was still some evidence at about 2900 cm^{-1} and 1400 cm^{-1} for the presence of a small amount of methanol on the surface.

8.3.2 METHANOL ADSORPTION ON Rh/SiO_2

The spectrum obtained 15 minutes after injecting methanol on to a pre-reduced sample of 2% Rh/SiO_2 is shown in fig 8.21. Apart from peaks at about 2950 cm^{-1} and 1450 cm^{-1} due to physically adsorbed methanol, the spectrum consisted of three peaks at 2857 , 2051 and 1450 cm^{-1} , with a very weak peak at 1688 cm^{-1} .

When the catalyst temperature was increased to 97°C the spectrum consisted of only two small bands at 2957 cm^{-1} and 2857 cm^{-1} .

When methanol was adsorbed on the catalyst at 288°C , the spectrum, taken 8 minutes after the initial injection of

Fig. 8.20

Methanol on Rh/Al₂O₃

at 285°C

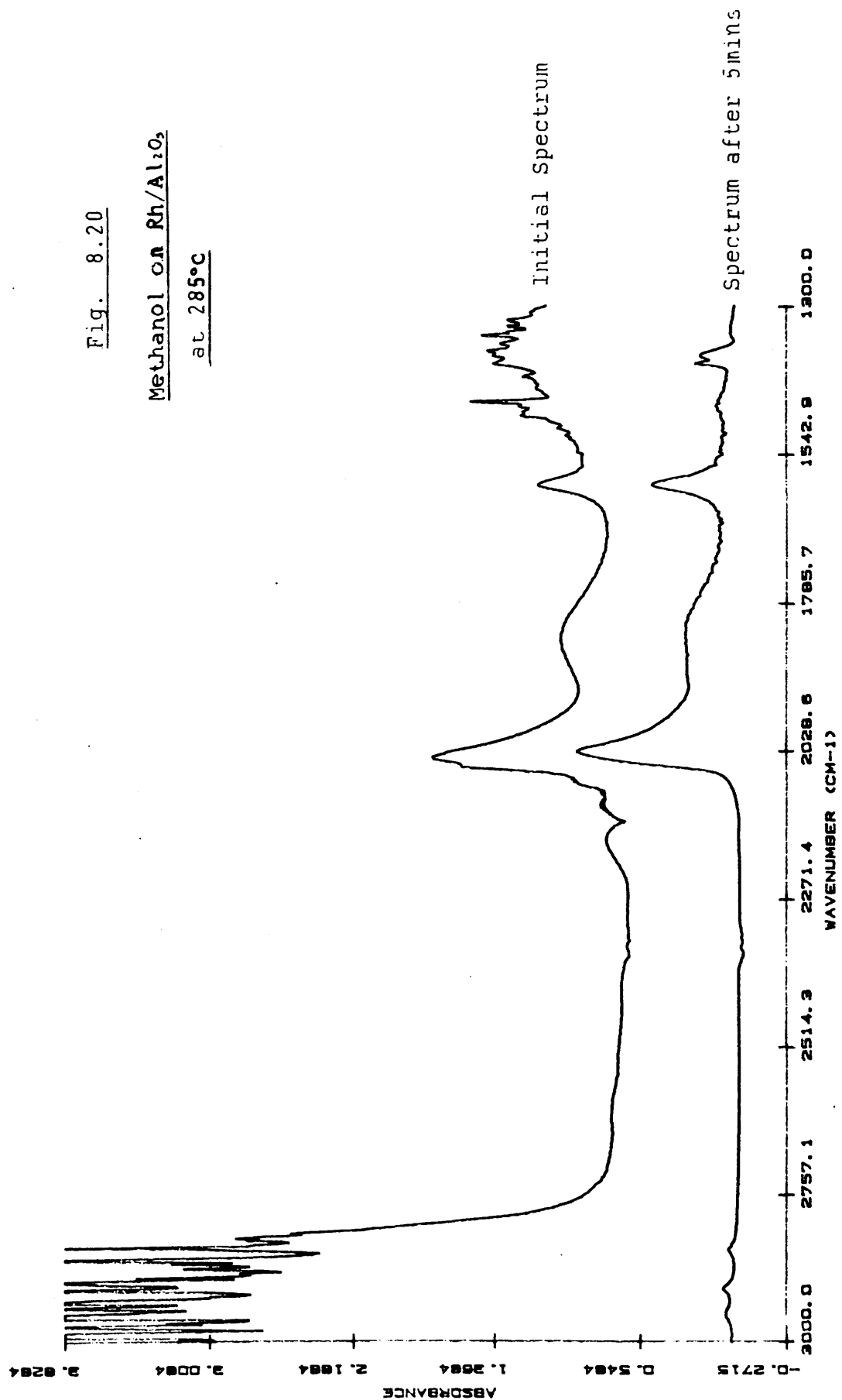
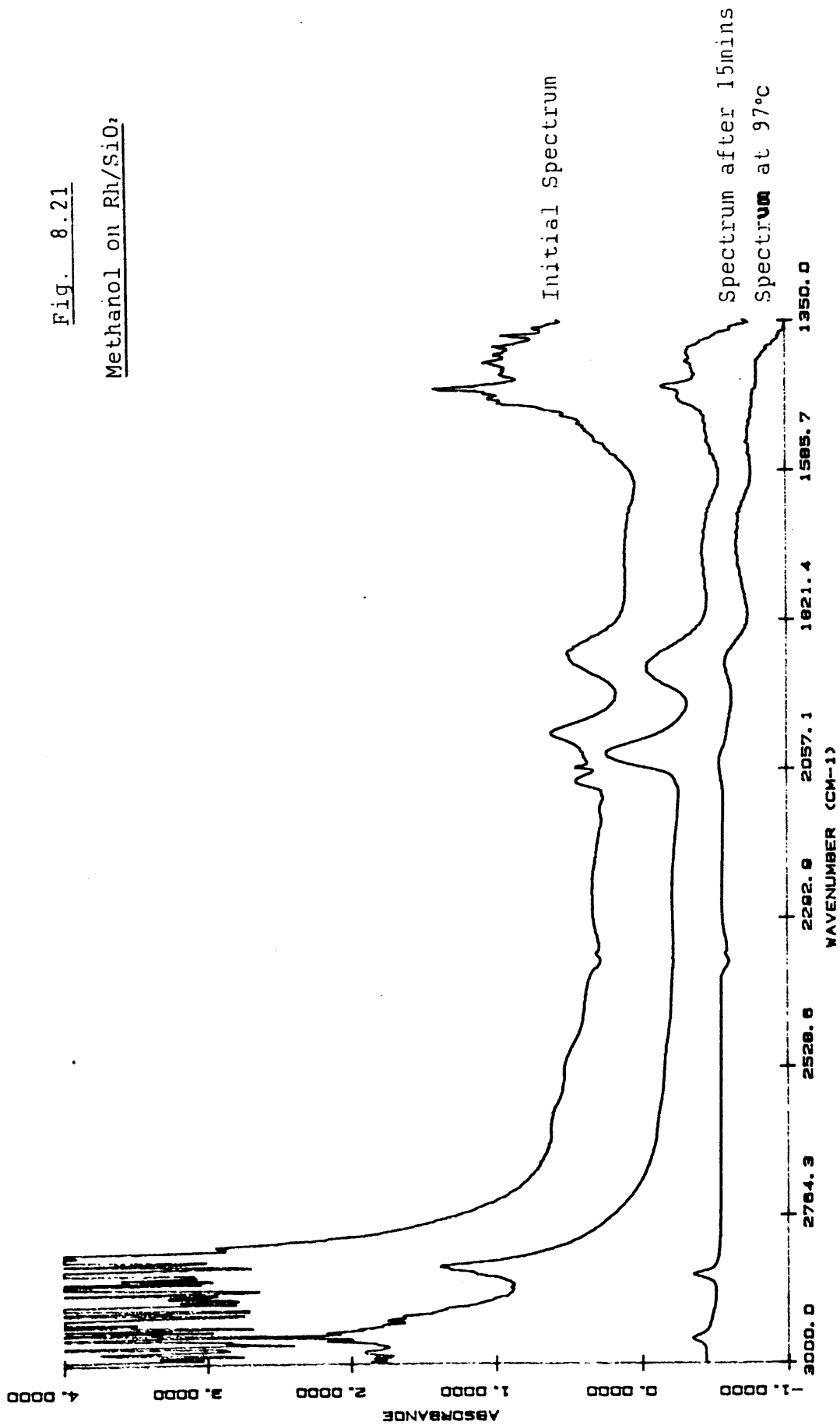


Fig. 8.21

Methanol on Rh/SiO₂



methanol (fig 8.22), consisted of two small peaks at 2957 cm^{-1} and 2855 cm^{-1} , together with a large peak at 2039 cm^{-1} and a smaller one at 1911 cm^{-1} .

The results of these experiments are summarised in Table 8.3.

Table 8.3 Methanol Summary

	Comments
MeOH on Rh/Al ₂ O ₃ at 18°C	Adsorbed CO detected (bands at 2096, 2047 and 2024 cm^{-1}), desorbing at 163°C. Peaks at 1635, 1391 and 1381 cm^{-1} grew as the temperature rose, and were the only remaining bands at 260°C.
MeOH on Rh/Al ₂ O ₃ at 285°C	Gas phase CO initially present. The only stable peaks were at 2027, 1847, 1591 and 1393/1380 cm^{-1} .
MeOH on Rh/SiO ₂ at 18°C	Adsorbed CO (2051 and 1876 cm^{-1}) had desorbed by 97°C, only stable bands were at 2957 and 2557 cm^{-1} .
MeOH on Rh/SiO ₂ at 288°C	Main peak at 2045 cm^{-1} shifted to 2039 cm^{-1} after 8 mins.

8.4 Ethanol Adsorption

The infra-red spectrum of gas phase ethanol is shown in fig 8.23. It consists of five bands of medium intensity situated at 3668, 1450, 1393, 1250 and 887 cm^{-1} , each of these bands being composed of several different peaks.

Fig. 8.22

Methanol on RH/SiO₂ at 288°C

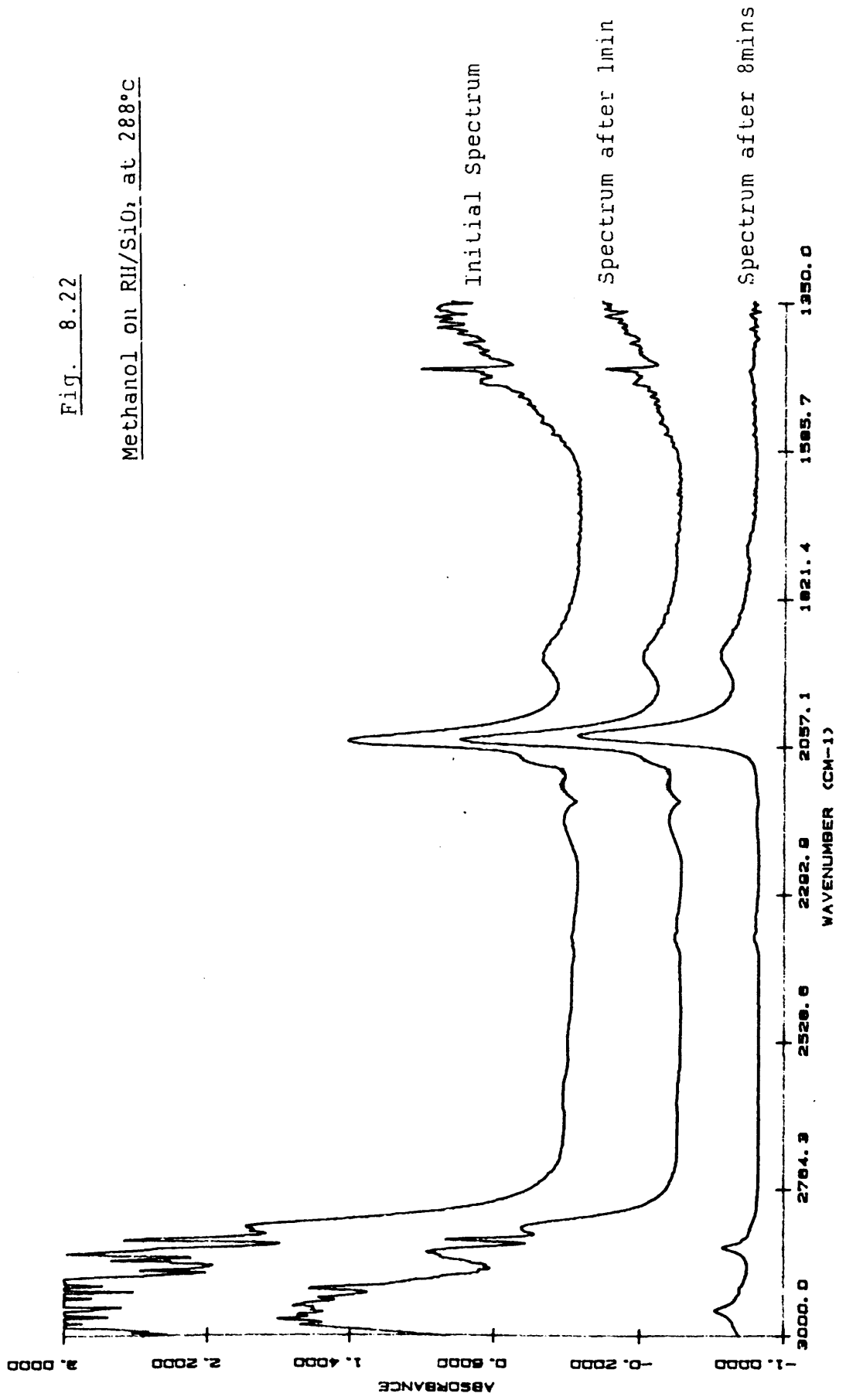
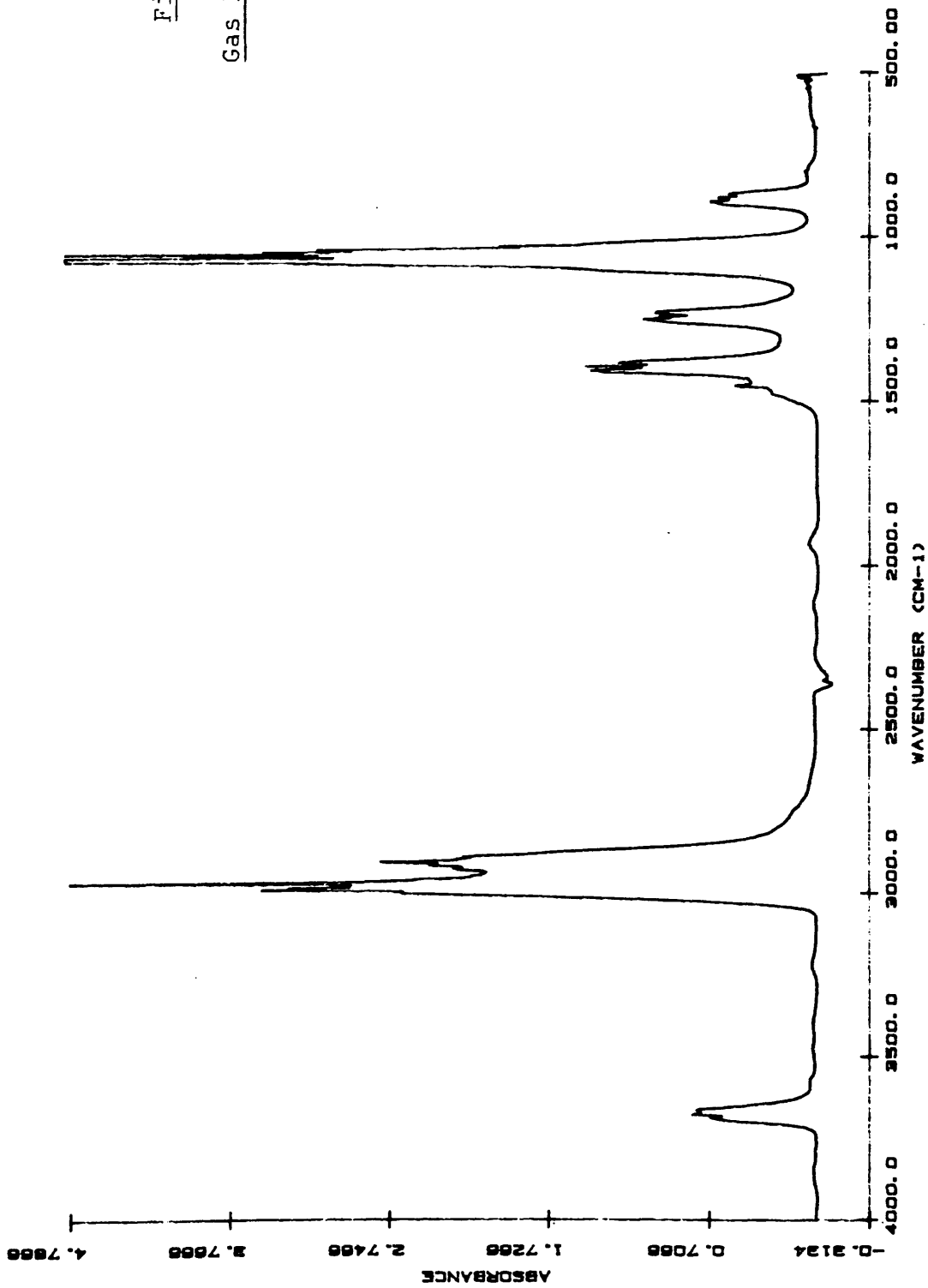


Fig. 2.23

Gas Phase Ethanol



Three rather intense bands appeared at 2987, 2968 and 2900 cm^{-1} , with a very sharp band at 1069 cm^{-1} .

8.4.1 ETHANOL ADSORPTION ON Rh/Al₂O₃

A freshly reduced sample of Rh/Al₂O₃ was exposed to ethanol in a stream of helium and the spectra, presented in fig 8.24, were recorded. Then, in a separate experiment, ethanol was injected in to a stream of hydrogen, and this was passed over the catalysts surface. The spectrum obtained is shown in fig 8.25.

The main features of the spectrum shown in fig 8.24 are the doublet of peaks at 1252 cm^{-1} and 1228 cm^{-1} , and the group of five peaks at 1476, 1449, 1406, 1395 and 1383 cm^{-1} . The rest of the room temperature spectrum is made up of two strong bands at 3000 cm^{-1} and 1000 cm^{-1} .

As the temperature was increased all of the above mentioned peaks decreased quite dramatically in intensity. This loss in intensity was accompanied by the growth of a group of four peaks at 2134, 2089, 2054 and 2033 cm^{-1} . These peaks reached a maximum at 160°C, but had disappeared completely by 221°C. Two peaks at 1574 cm^{-1} and 1460 cm^{-1} also increased in intensity as the temperature was raised, to become the only spectral feature at 221°C.

The spectra obtained when Rh/Al₂O₃ was exposed to ethanol in the presence of hydrogen, however, was slightly

Fig. 8.24

Ethanol on Rh/Al₂O₃
(in a flow of He)

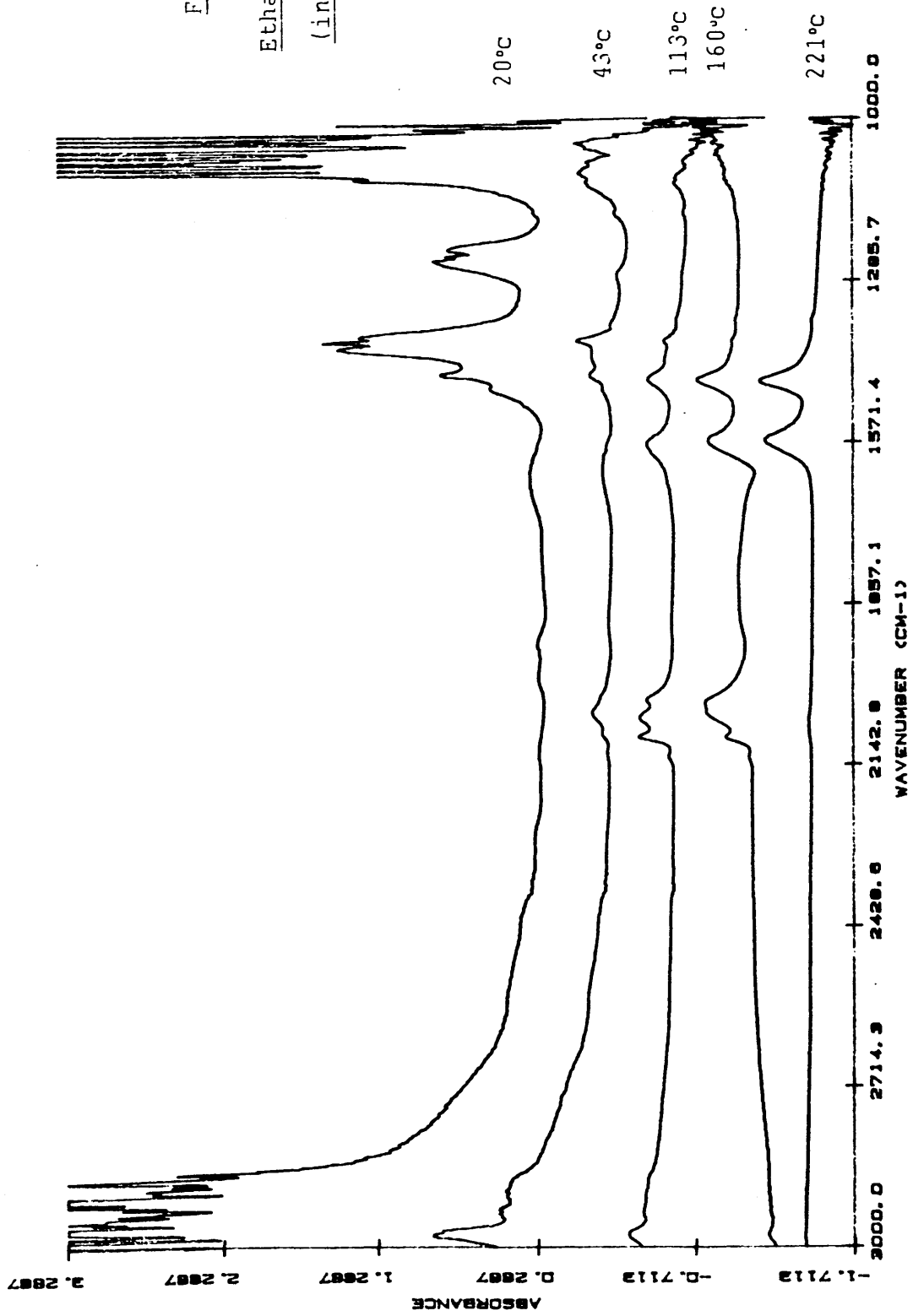
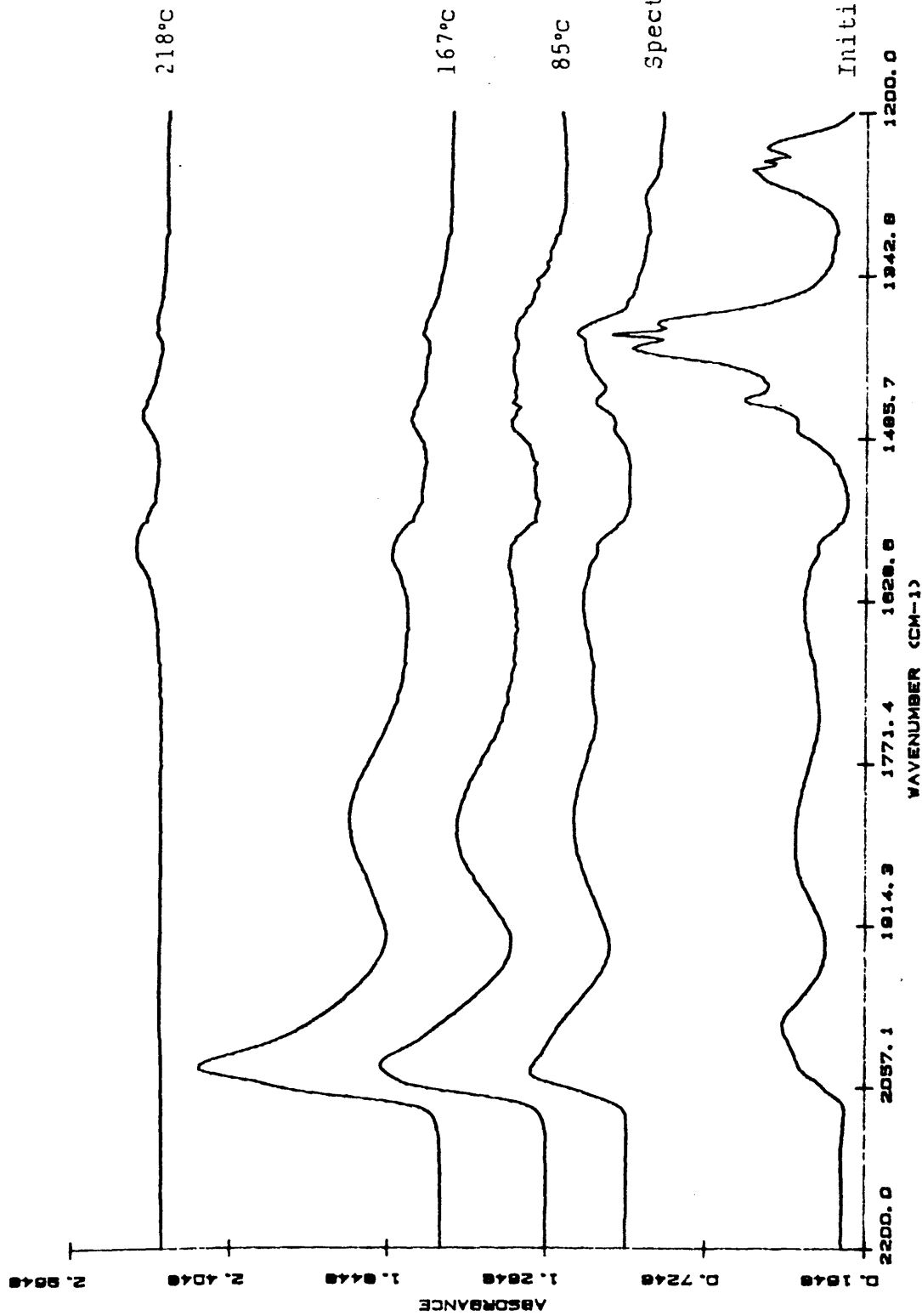


Fig. 0.25

Ethanol on Rh/Al₂O₃
(in a flow of H₂)



different. Two of its main features, at room temperature, were bands at 2048 cm^{-1} and 1826 cm^{-1} . Both of these bands increased in intensity as the temperature was increased, reaching a maximum at 167°C , before falling in intensity towards 218°C . The peak at 2048 cm^{-1} was found to shift to slightly lower wavenumbers as the temperature increased. The other peaks in the spectrum gradually lost intensity as the temperature increased until at 218°C , only three bands, at 1593 , 1471 and 1395 cm^{-1} remained.

When ethanol was adsorbed on a sample of $\text{Rh}/\text{Al}_2\text{O}_3$ at 277°C , the spectrum shown in fig 8.26 was obtained. The initial spectrum consisted of bands due to physically adsorbed or gas phase ethanol at 3000 - 2900 , 1450 - 1380 , 1246 - 1226 and 1000 cm^{-1} . Two bands due to gas phase carbon monoxide (2173 cm^{-1} and 2117 cm^{-1}) were detected as well as bands at 2007 , 1828 , 1570 and 1305 cm^{-1} .

When ethanol was adsorbed on this catalyst at high temperatures in the presence of hydrogen (fig 8.27), the spectrum was very similar to that described above. However, this spectrum, taken at 275°C , suggests that much more gas phase carbon monoxide was formed in the presence of hydrogen. The peak at 2007 cm^{-1} (fig 8.26) is not present in this spectrum, but a much sharper peak appears at 2037 cm^{-1} . The position and relative size of all of the other peaks remains constant. After a 3 minute flush with helium, the remaining peaks were at 1574 , 1451 and 2037 cm^{-1} .

Fig. 8.26

Etanol on Rh/Al₂O₃ at 277°C

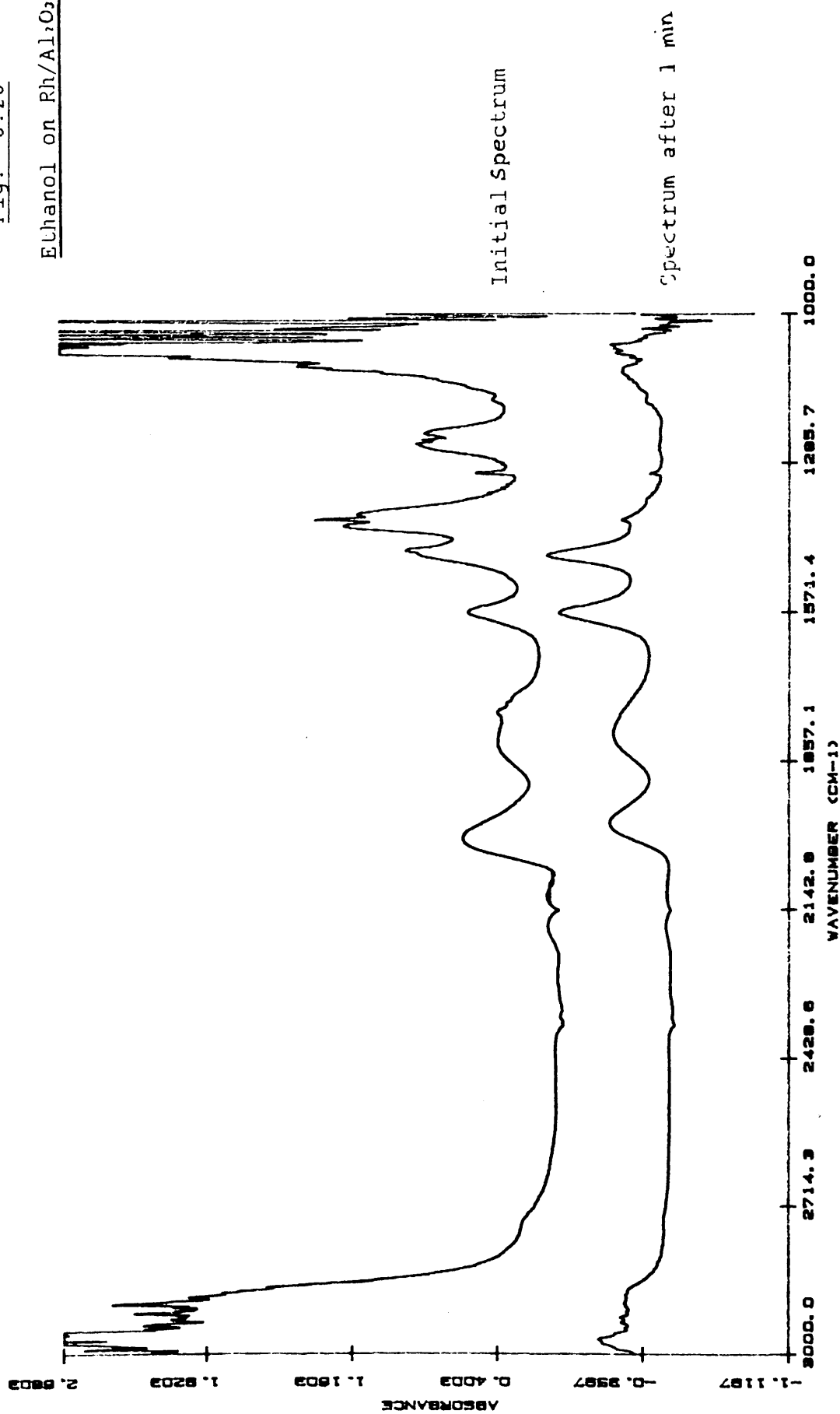
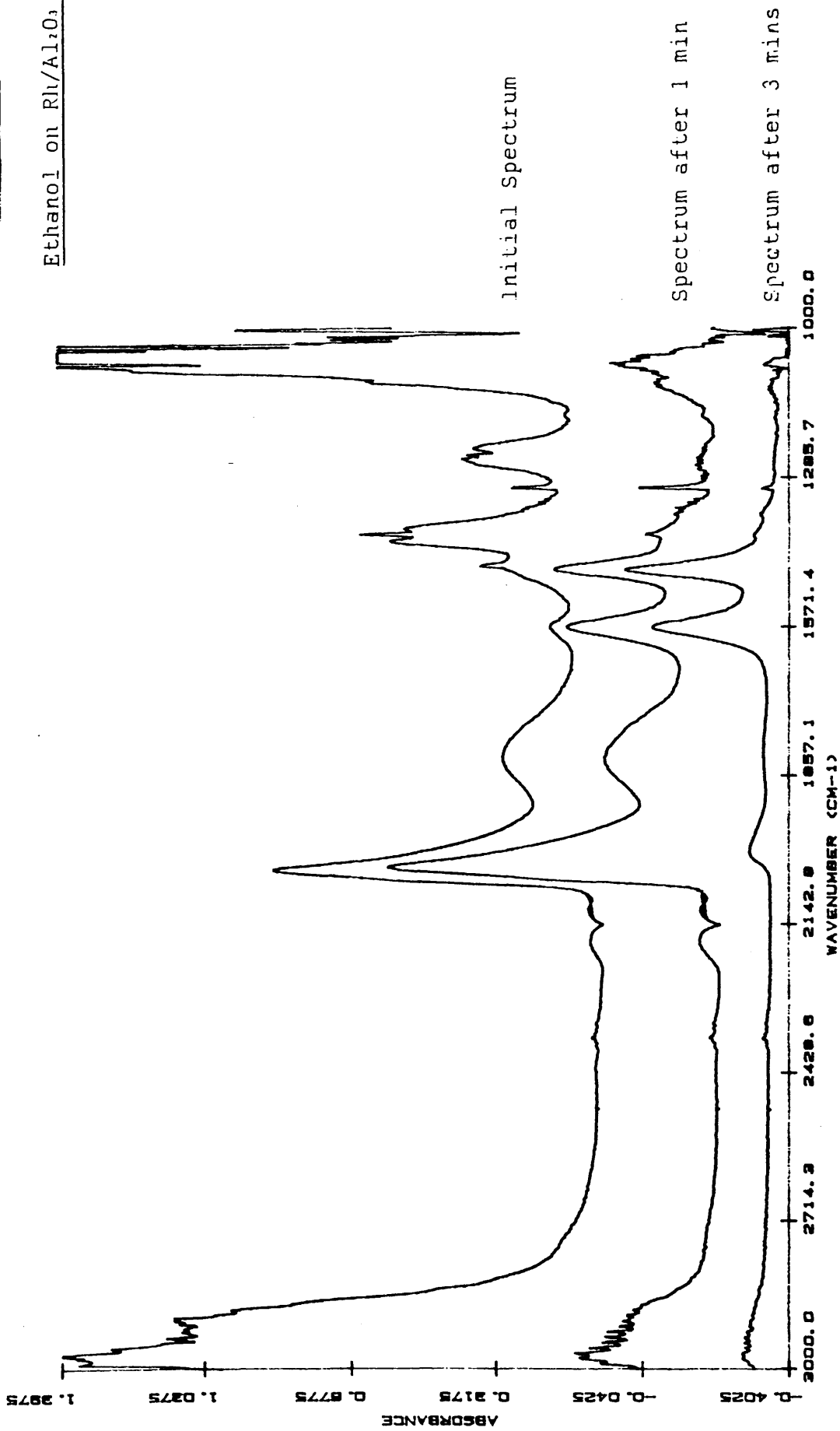


Fig. 8.27

Ethanol on Rh/Al₂O₃ at 275°C



8.4.2 ETHANOL ADSORPTION ON Rh/SiO₂

The infra-red spectrum of ethanol adsorbed on Rh/SiO₂ at ambient temperature is shown in fig 8.28. After 15 minutes in the helium stream, the spectrum was made up of a broad band centred around 2950 cm⁻¹ and another at about 1400 cm⁻¹ due to gas phase or physically adsorbed ethanol. Two rather weak bands 2016 cm⁻¹ and 1878 cm⁻¹ were also observed. As the temperature was increased all of these peaks gradually diminished in intensity until, by 195°C, they had all but disappeared.

When ethanol was adsorbed on to Rh/SiO₂ at elevated temperatures, the spectrum contained no bands, except those due to gas phase ethanol (fig 8.29).

Table 8.4 contains a summary of the results described in this section.

Fig. 8.28

Ethanol on Rh/SiO₂

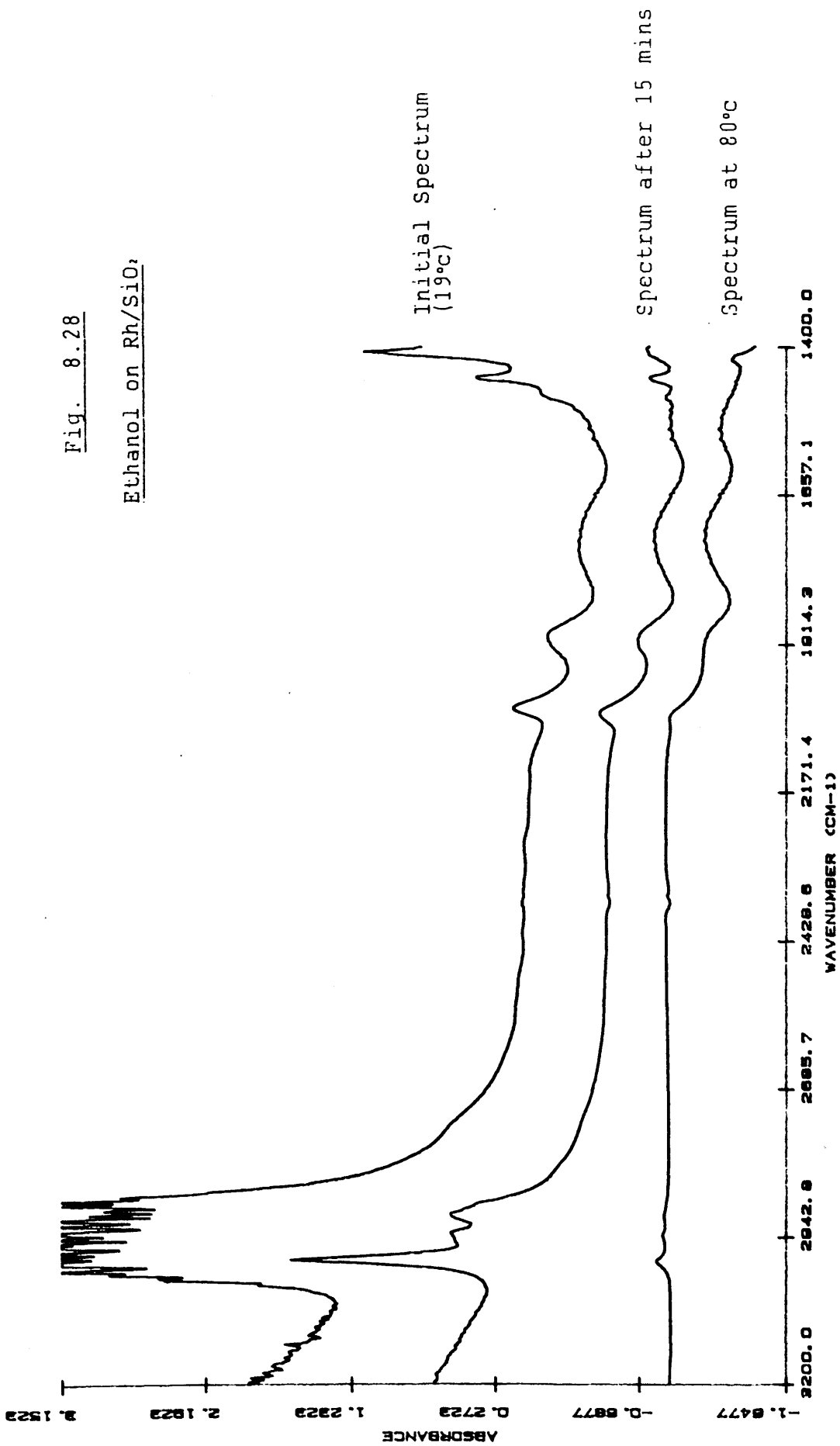


Fig. 6.29

Ethanol on Rh/SiO₂

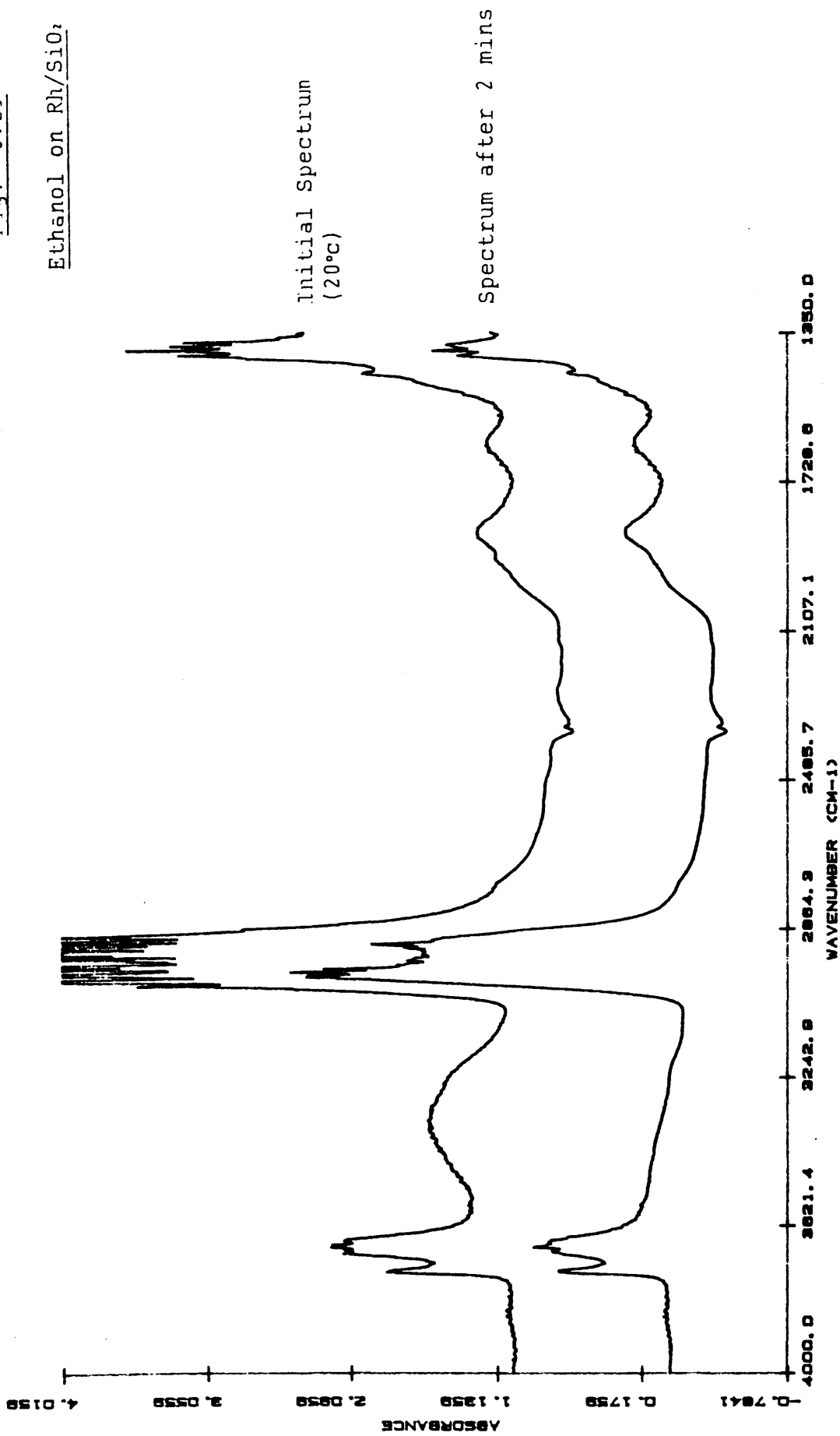


Table 8.4**Ethanol Summary****Comments**

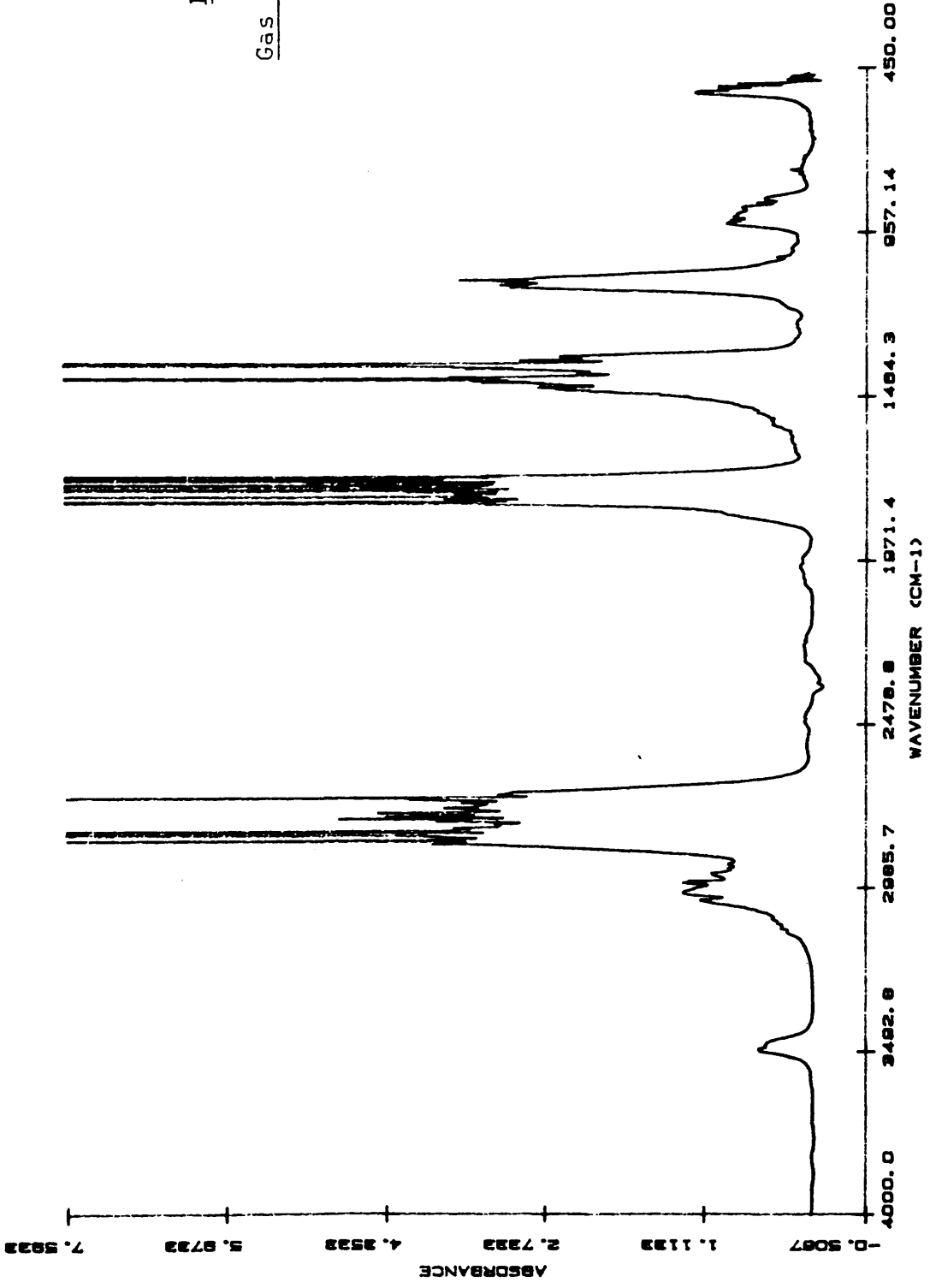
EtOH on Rh/Al ₂ O ₃ at 18°C in He	The concentration of adsorbed CO (2089, 2054 + 2033 cm ⁻¹) increased up to 160°C, but had desorbed by 221°C. Two peaks, stable at 221°C, increased with increasing temperature.
EtOH on Rh/Al ₂ O ₃ at 18°C in H ₂	More CO formed than in He, but only linear CO (2048 cm ⁻¹), up to a max at 167°C. All CO had desorbed by 218°C, where the only stable peaks were at 1593 and 1471 cm ⁻¹ .
EtOH on Rh/Al ₂ O ₃ at 277°C in He	Gas phase CO present as well as peaks at 2007, 1806, 1574 and 1460 cm ⁻¹ .
EtOH on Rh/Al ₂ O ₃ at 275°C in H ₂	More gas phase CO was present as well as peaks at 2037, 1826, 1574 and 1460 cm ⁻¹ .
EtOH on Rh/SiO ₂ at 18°C in He	Weak bands at 2019 and 1878 cm ⁻¹ as well as physically adsorbed EtOH
EtOH on Rh/SiO ₂	Only physically adsorbed EtOH detected

8.5 ACETALDEHYDE ADSORPTION

The gas phase spectrum of acetaldehyde (fig 8.30) consisted of a large number of peaks, the main bands appearing at approximately 3487, 3000, 2830 - 2700, 1750, 1390, 1106 and 930 cm⁻¹.

Fig. 8.30

Gas Phase Acetaldehyde



8.5.1 ACETALDEHYDE ADSORPTION ON Rh/Al₂O₃

The infra-red spectrum of acetaldehyde adsorbed on Rh/Al₂O₃ (fig 8.31) was taken one minute after the initial injection of acetaldehyde.

The spectrum consisted of a large number of small peaks, the most intense of which appeared at 1714 cm⁻¹. Three peaks at 2084, 2054 and 2020 cm⁻¹, which were probably due to adsorbed carbon monoxide, were also present. These became more intense as the temperature was increased to 70°C, but decreased in intensity above that temperature and had completely disappeared by 260°C.

At 70°C, the peak at 1714 cm⁻¹ had disappeared, while three small peaks, at 1697, 1667 and 1646 cm⁻¹, had grown in, by 150°C, these too had disappeared. The only remaining peaks at 190°C were those at 1573 cm⁻¹ and 1462 cm⁻¹, which increased in intensity as the temperature increased.

The spectrum of acetaldehyde adsorbed on the alumina support itself was also measured (fig 8.32). After 10 minutes in a 40 ml min⁻¹ flow of helium, this consisted of a large number of very sharp peaks, which showed a remarkable similarity to the spectrum of acetaldehyde adsorbed on the Rh/Al₂O₃ catalyst (fig 8.31). However, no adsorbed carbon monoxide was detected.

Fig. 8.31

Acetaldehyde on Rh/Al₂O₃

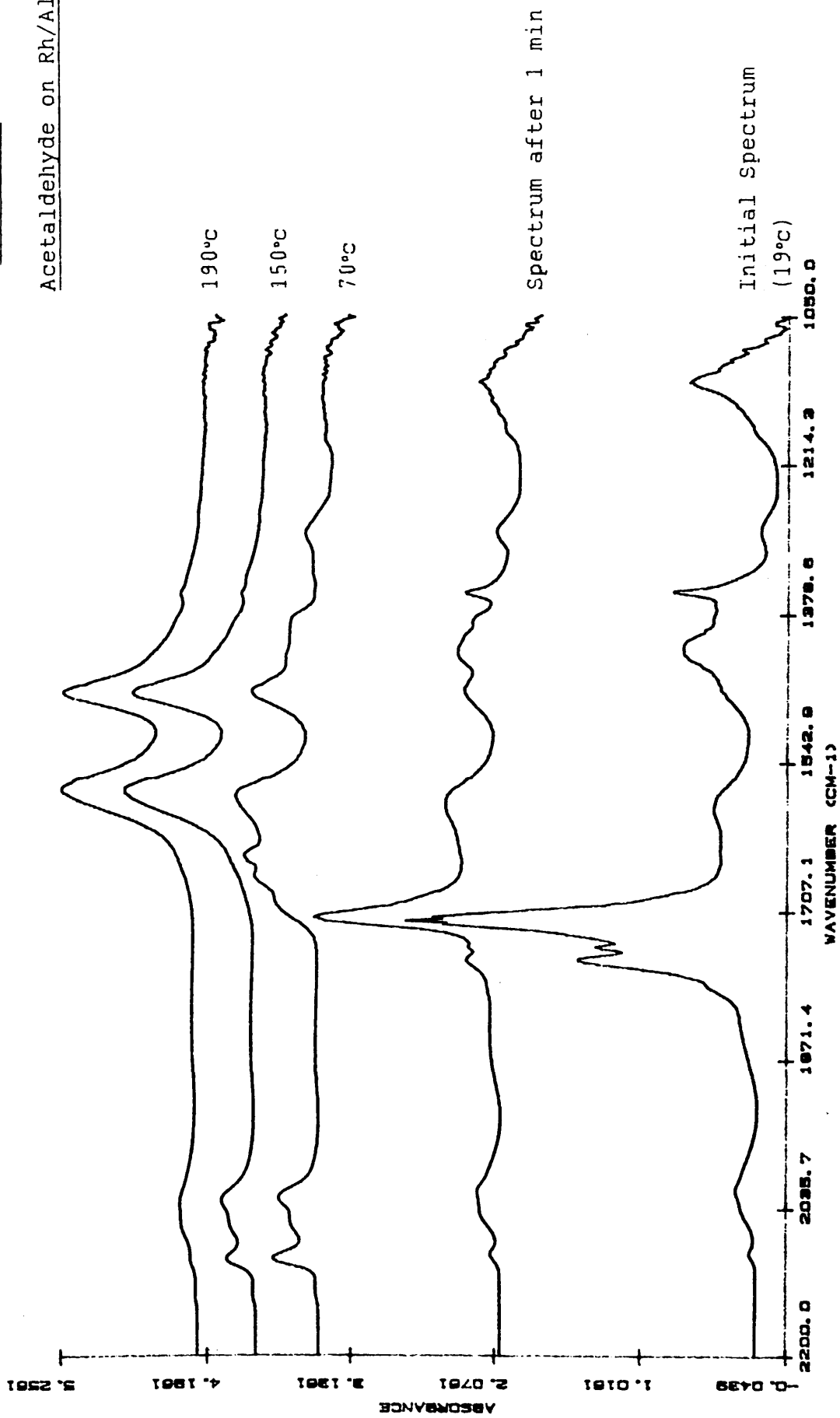
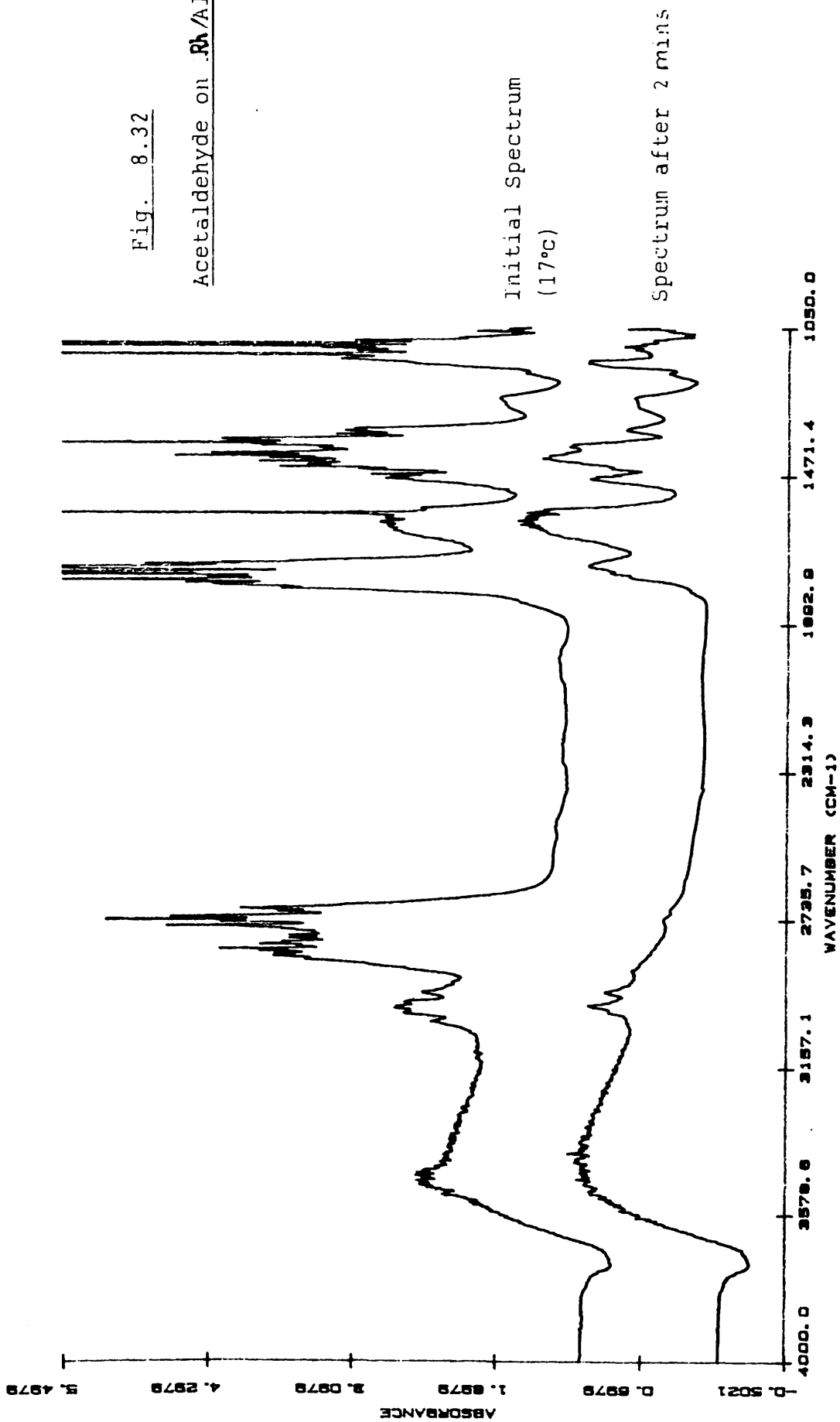


Fig. 8.32

Acetaldehyde on $\text{Rh}/\text{Al}_2\text{O}_3$



When acetaldehyde was adsorbed on Rh/Al₂O₃ at 280°C, the infra-red spectrum shown in fig 8.33 was obtained. One minute after the initial injection of acetaldehyde, the main features of the spectrum were two peaks at 1573 cm⁻¹ and 1462 cm⁻¹.

8.5.2 ACETALDEHYDE ADSORPTION ON Rh/SiO₂

Ten minutes after the initial injection of acetaldehyde, the infra-red spectrum of the 2% Rh/SiO₂ catalyst (fig 8.34) contained three main peaks at 2041, 1884 and 1720 cm⁻¹, together with some smaller peaks due to physically adsorbed or gas phase acetaldehyde. As the temperature was increased, all of the peaks decreased in intensity, except for the peak at 1640 cm⁻¹. This drop in intensity was most marked for the peak at 1720 cm⁻¹.

The infra-red spectrum of acetaldehyde adsorbed, at 270°C, on to Rh/SiO₂, is shown in fig 8.35. The spectrum consists of only two major bands, at around 2800 cm⁻¹ and 1770 cm⁻¹, due to physically adsorbed or gas phase acetaldehyde, neither of these bands was stable under the experimental conditions and their intensities were markedly reduced within one minute.

A summary of these results is shown in Table 8.5.

Fig. 8.33

Acetaldehyde on Rh/Al₂O₃
at 280°C

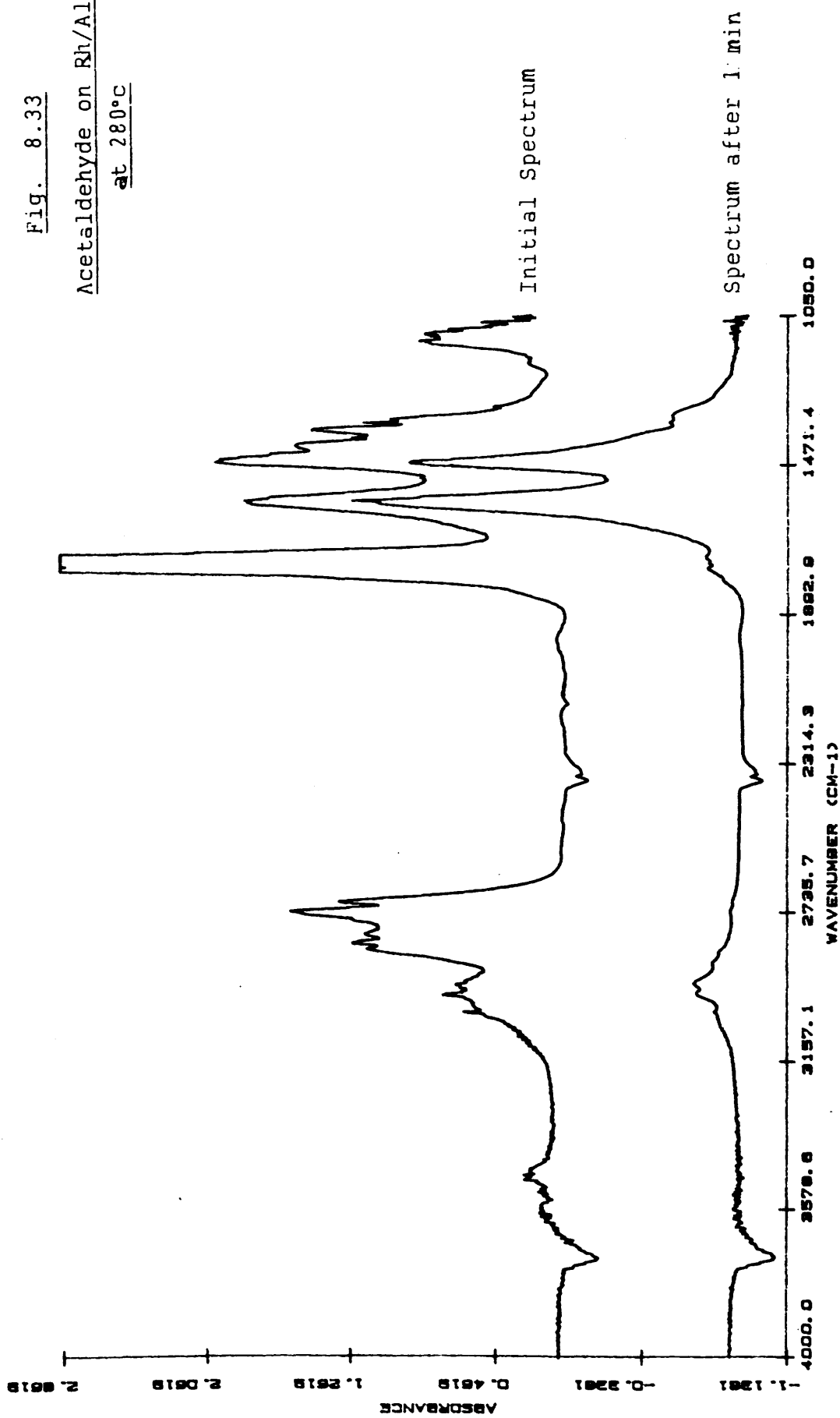


Fig. 8.34a

Acetaldehyde on Rh/SiO₂
(at 20°C)

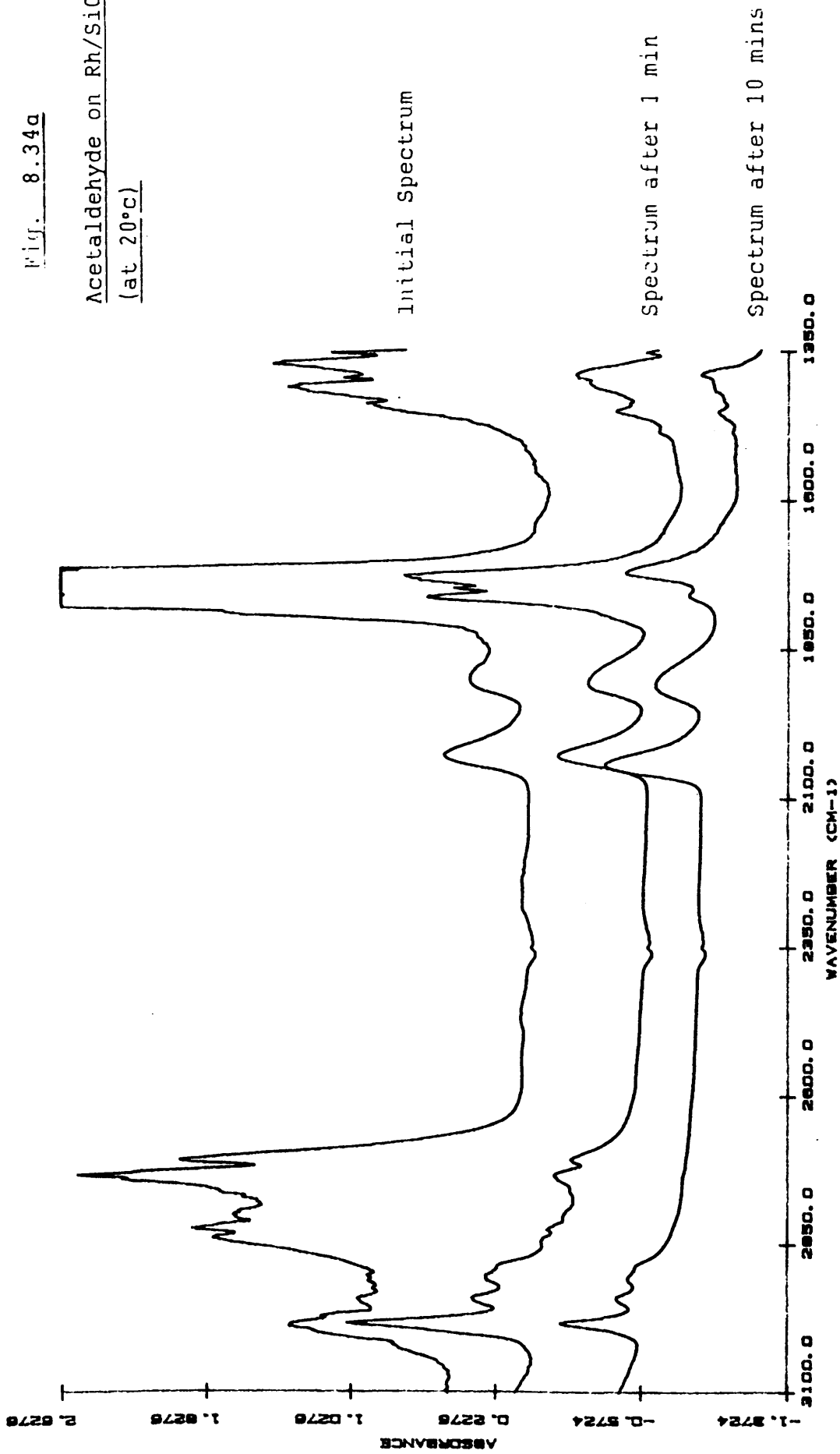


Fig. 8.34b

Acetaldehyde on Rh/SiO₂

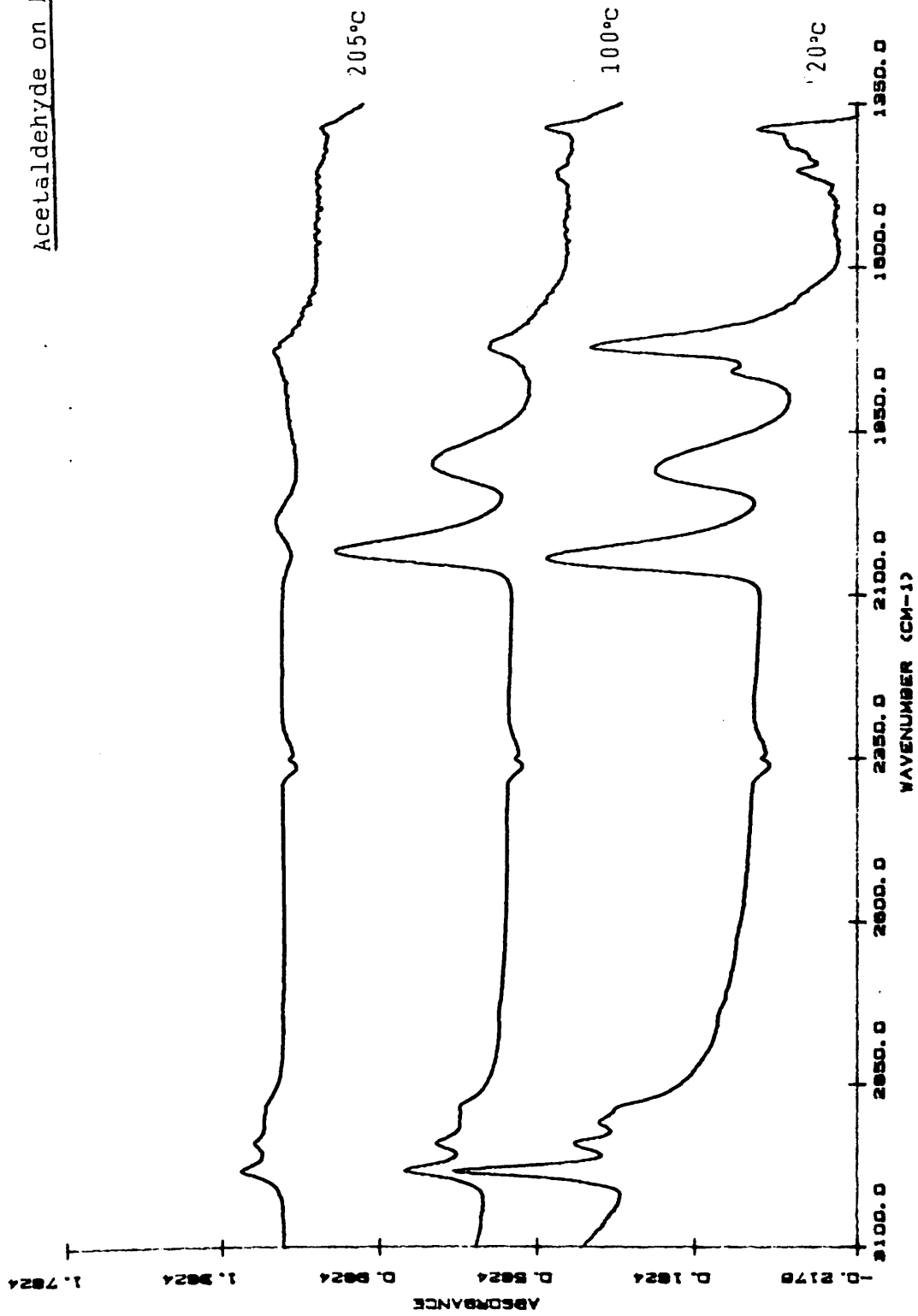


Fig. 8.35

Acetaldehyde on Rh/SiO₂
at 270°C

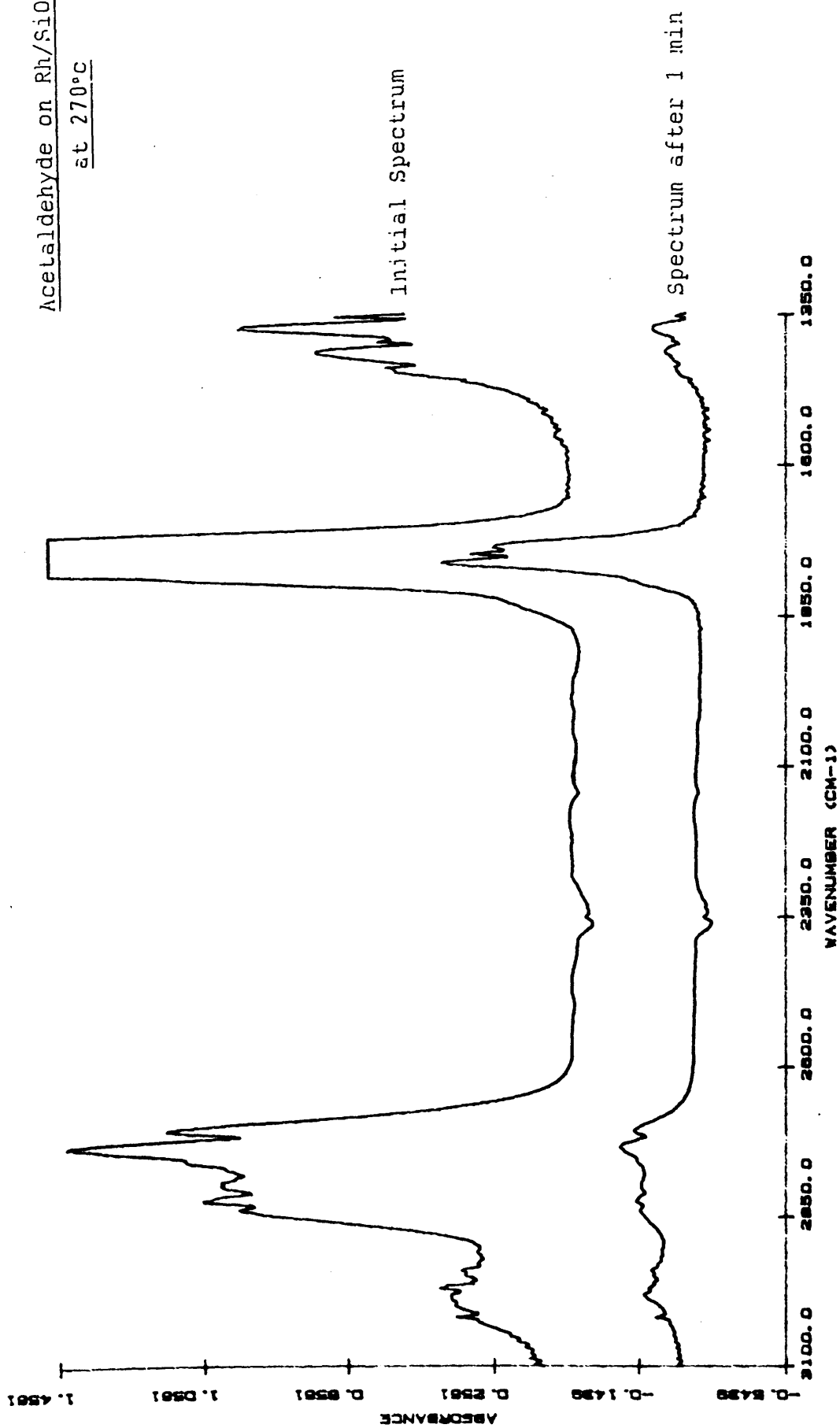


Table 8.5 Acetaldehyde Summary

	Comments
Acetaldehyde on Rh/Al ₂ O ₃ at 18°C	Adsorbed CO (2084, 2054 + 2020 cm ⁻¹) intensity rose initially, but complete desorption had occurred by 260°C. 1714 cm ⁻¹ --> 1693, 1667 + 1646 cm ⁻¹ All peaks, except those at 1513 + 1462 cm ⁻¹ , had disappeared by 150°C
Acetaldehyde on Rh/Al ₂ O ₃ at 280°C	Only stable peaks at 1573 + 1462 cm ⁻¹
Acetaldehyde on Al ₂ O ₃ at 18°C	No CO formed, otherwise very similar to acetaldehyde on Rh/Al ₂ O ₃
Acetaldehyde on Rh/SiO ₂ at 18°C	Main peaks at 2041, 1884 + 1720 cm ⁻¹ all decreased with increasing temperature while the 1720 cm ⁻¹ peak increased.
Acetaldehyde on Rh/SiO ₂ at 270°C	No stable bands.

CHAPTER 9

DISCUSSION

CHAPTER 9 DISCUSSION

9.1 THE CATALYST STRUCTURE

Upon reduction, each of the catalysts used in this study produced at least two distinct rhodium species. These have been identified, by TEM studies, as small easy to reduce rhodium particles, which may be in the form of 2-D rafts²⁹, and larger crystallites which are more difficult to reduce. This is clearly shown by the TPR profiles of the catalysts, each of which contain at least two, and in the case of Rh/MoO₃, as many as four peaks, all corresponding to different reduction processes. Similar results and conclusions have now been published by a number of groups³⁰, although the exact position and size of the TPR peaks appears to be very dependent on the experimental conditions. A selection of these results, together with those obtained in this study, are summarised in table 9.1.

Yao et al¹⁵⁶ reported similar TPR results, but suggested that the low temperature peak was due to the reduction of the larger crystallites, on the basis that the low temperature peak was enhanced by a prolonged and severe oxidation treatment before reduction. This would be expected to result in a higher proportion of the rhodium being present in the larger particles.

Table 9.1 TPR Summary

Catalyst	Peak Maxima (°C)	Reference
Rh/Al ₂ O ₃	120 ,240	This study
Rh/SiO ₂	105, 138	This study
Rh/MoO ₃	150, 190, 290, 500	This study
Rh/Al ₂ O ₃	100, 170	156
Rh/Al ₂ O ₃	110, 230	192
Rh/SiO ₂	70, 120, 400	71
Rh/SiO ₂	34, 74	72
Rh/MoO ₃	152 ,200 ,300-600	75
Rh/MoO ₃ /SiO ₂	170, 250, 430	71
RhCl ₃	110	
MoO ₃	410-500	This study
MoO ₃	300-800*	193

(* - depending on the H₂O content of the reducing mixture)

RhCl_3 itself has been shown to be reduced at 110°C ¹⁹² when no support is present, and yet each of these catalysts produced TPR peaks at significantly higher temperatures. Al_2O_3 , SiO_2 and MoO_3 therefore, stabilise at least some of the RhCl_3 against reduction, such that higher temperatures are needed for reduction. The ability of the catalyst supports to stabilise partially reduced rhodium species may be due to the formation of a mixed surface complex which is more difficult to reduce than the original metal precursor. This effect was found to be much more pronounced with those supports such as Al_2O_3 and MoO_3 which can interact strongly with the metal particles⁷¹, so that while $\text{Rh}/\text{Al}_2\text{O}_3$ was found to take up hydrogen at 240°C , the reduction of Rh/SiO_2 was complete by 140°C . Although a great deal of evidence now exists for the occurrence of Rh^+ species on the surface of supported rhodium catalysts, and many have speculated as to why this should be so, the mechanism is, as yet, far from clear.

A large number of hydroxyl groups are always present on these supported catalysts, as evidenced by the very intense peaks they produce in the ir spectra. These may have a substantial role to play in the stabilisation of the Rh^+ species, probably through the neutralisation or delocalisation of their positive charge. Each of the ir spectra of adsorbed carbon monoxide contained a small but very stable band at 2136 cm^{-1} . This band has now been assigned¹²⁴ to the adsorption of carbon monoxide on

unreduced Rh^{3+} ions, providing direct evidence for an unreduced phase of rhodium.

The amounts of hydrogen taken up by the samples of Rh/SiO_2 and $\text{Rh}/\text{Al}_2\text{O}_3$ during their TPR's suggest that less than 10% of the available Rh^{3+} ions have been reduced to Rh^0 . In view of the large amount of carbon monoxide which adsorbed on each of the catalysts, these results would appear to be rather low. However, this discrepancy may be due to a large room temperature uptake of hydrogen, which would have been masked by the peak caused by the initial switching of gases. The observed results may also be due to the large amount of water which was observed to desorb from these catalysts, during the reduction process.

On the other hand, the Rh/MoO_3 catalyst was found to adsorb more than twice the amount of hydrogen which would be required to reduce all of the Rh^{3+} ions, which were present, to Rh^0 . If, as seems likely, these experiments provide an underestimate of the amount of hydrogen that was taken up then this figure could, in reality, be even higher. This effect is caused by the spillover of dissociated hydrogen atoms from the metal particle on to the support. The small shoulder which appeared on the main peak at about 150°C , is probably due to the formation of catalytic sites which were capable of dissociating hydrogen and thus promoting spillover.

Although spillover and reverse spillover from the support to the metal particles, are believed to also occur on Rh/Al₂O₃ and Rh/SiO₂, experiments using isotopic labels have shown that spillover hydrogen can exchange with support hydroxyl groups, these catalysts do not display an increased uptake of hydrogen. This is because there is no mechanism whereby the spillover hydrogen can be "trapped" on the support.

On Rh/MoO₃, however, the spillover hydrogen forms a series of hydrogen bronzes, of the type H_{0.7}MoO₃²⁴, on the surface. These bronzes can then decompose to form the large amounts of water which are produced during the reduction of Rh/MoO₃ and partially reduced sub-oxides of the support.

Interactions can take place between the Al₂O₃ and SiO₂ supports, and hydrogen, to a limited extent, during the reduction process, through the formation and recombination of hydroxyl groups on the surface. This also leads to a desorption of water from the surface and the formation of a lower oxide, but since Al₂O₃ and SiO₂ are so difficult to reduce, this process is only likely to change the acidity of the surface rather than cause widespread reduction of the type found with Rh/MoO₃.

The TPR of the MoO₃ support itself consisted of a single peak in the range 400-500°C and hence the high temperature peak of Rh/MoO₃ can be assigned to the direct reduction of the support material by the reducing mixture.

The fact that MoO_3 took up less hydrogen than Rh/MoO_3 and that it did not adsorb any hydrogen below 400°C , points to the importance of the rhodium particles in the spillover of hydrogen and the reduction of the support.

Al_2O_3 and SiO_2 are only reduced at extremely high temperatures and so were, as expected, not found to take up any hydrogen in the TPR experiments, which only went up to a maximum temperature of 500°C .

Since the spillover of hydrogen is an extremely rapid process, the surface concentration of hydrogen at any one time on either the $\text{Rh/Al}_2\text{O}_3$ or the Rh/SiO_2 would be fairly low. This could have important implications for the activity of the catalyst in any reaction, such as the hydrogenation of carbon monoxide, where hydrogen was involved. As a catalyst's ability to promote spillover can drastically increase the concentration of hydrogen which is available on its surface for reaction.

The average particle sizes, as measured by TEM, show that the rhodium particles are somewhat larger on the Rh/MoO_3 catalyst than on the other two catalysts. Since MoO_3 has a much lower surface area than either of the other supports this is perhaps not surprising. However, the observed differences in dispersion are not enough to explain the much greater discrepancies which were observed in the amount of carbon monoxide which the catalysts adsorbed. Each of the techniques used in this study showed that much

less carbon monoxide was adsorbed on Rh/MoO₃ than on any of the other catalysts. The average rhodium particle on Rh/MoO₃ was found, from TEM measurements, to have a diameter of 4.29 nm and yet the diameter calculated from the amount of carbon monoxide which the sample adsorbed (section 5.2.1) was 55.2 nm. Since a higher proportion of the atoms are on the surface, and therefore available for adsorption on a small particle rather than a large one, these results imply that much of the surface area is unavailable for carbon monoxide adsorption on the Rh/MoO₃ catalyst.

The particle size of each of the other catalysts, calculated from the amount of carbon monoxide adsorbed, was also found to be slightly larger than that measured by TEM, however, the differences were very much smaller than those observed with Rh/MoO₃; 4.5 nm compared to 2.73 nm for Rh/SiO₂. These results therefore suggest that much more of the surface is available for adsorption, on these catalysts, than with the Rh/MoO₃ catalyst.

Many have speculated recently, on the migration of easily reduced support moieties on to the catalyst metal particles, thereby blocking, or changing the character of, the adsorption sites. Direct evidence for the occurrence of partially reduced support species on the metal particles of similar catalysts, such as Rh/TiO₂⁴⁹ and for systems where MoO₃ is used as a promoter, for example Rh/MoO₃/SiO₂⁷¹, have already been published. It therefore seems likely that

similar effects are being observed here. As well as the support material simply blocking the adsorption sites and so reducing the amounts of carbon monoxide adsorbed, it may also act by stabilising Rh^+ species on the surface which are known to adsorb carbon monoxide much less strongly than Rh^0 .

Since Al_2O_3 and SiO_2 are only reduced at elevated temperatures these catalysts would be unlikely to exhibit the similar effects.

9.2 THE ADSORPTION OF CARBON MONOXIDE

The adsorption of carbon monoxide on the catalysts used in this study is essentially a non-activated process, with very similar amounts of carbon monoxide being adsorbed under flow conditions at 0°C , 18°C or 250°C . The average heat of adsorption of carbon monoxide was calculated to be $93 \pm 6 \text{ kJmol}^{-1}$ for each of the catalysts. That the heats of adsorption should all be so similar is rather surprising when the very different behaviour, which each of the catalysts exhibited, is considered.

One explanation is that under the experimental conditions which were used, the catalyst did not attain equilibrium and so we are observing kinetic rather than thermodynamic differences between the catalysts. The adsorption of carbon monoxide on to Rh/MoO_3 was found to be a rather slow process, with equilibrium not being reached

even after 14 hours. Although the adsorption of carbon monoxide on $\text{Rh/Al}_2\text{O}_3$ was found to be very rapid in its initial stages, the process slowed considerably as saturation was approached. $\text{Rh/Al}_2\text{O}_3$ appeared to bind carbon monoxide much more strongly than Rh/MoO_3 could, since 93% of the adsorbed carbon monoxide was removed from the Rh/MoO_3 catalyst during a 30 minute evacuation whilst only 7% could be evacuated from the $\text{Rh/Al}_2\text{O}_3$ in the same period. After 6 hours, however, 15% of the surface carbon monoxide had been removed from the $\text{Rh/Al}_2\text{O}_3$, whilst little more had desorbed from the Rh/MoO_3 . This indicates that a very slow desorption process is occurring on the $\text{Rh/Al}_2\text{O}_3$ catalyst.

It should, however, be remembered that the figures which were quoted are average heats of adsorption and that the surface may contain a number of different sites, the average energies of which may happen to be very similar for each of the catalysts. Infra-red studies of the desorption of carbon monoxide from $\text{Rh/Al}_2\text{O}_3$ and Rh/SiO_2 have shown that linear carbon monoxide desorbs at significantly lower temperatures than the gem species, thus suggesting that linear carbon monoxide has a lower heat of adsorption than the gem.

A number of different species have been detected on these catalysts after the adsorption of carbon monoxide, whose different behaviour also reflects differences in their binding energies.

The carbon monoxide isotherms presented in section 5.2, clearly show that the adsorption of carbon monoxide proceeds in two distinct stages. In the primary region of the isotherm the surface concentration of carbon monoxide increases rapidly as carbon monoxide is introduced in to the system, while in the second region the increase is very much slower.

Although the overall behaviour of each of the catalysts was similar, the shapes of the individual isotherms were found to be very dependent on the catalyst support, especially in the secondary region of the isotherm. The Rh/Al₂O₃ catalyst reached saturation at fairly low pressures of carbon monoxide and adsorbed very little in the secondary region of the isotherm. While the Rh/MoO₃ sample adsorbed the majority of its surface carbon monoxide in the latter part of the curve and did not reach saturation even at pressures of 11 torr of carbon monoxide.

Carbon monoxide adsorbed in the primary region of the isotherm tended to be rather more strongly held than that in the secondary region of the curve. Since the primary region was not susceptible to room temperature evacuation, while carbon monoxide adsorbed in the second region was quickly removed from the surface. This suggests that two different types of site are present on the surface, each with its own heat of adsorption.

The first type of adsorption is relatively unaffected by the support and is associated with the metal particles themselves. The support, however, has a much greater degree of influence on the second type of site which may well be situated at the metal support interface.

It is proposed that it is the relative and absolute proportions of these two types of site which determines the overall shape of the isotherm. The fact that the Rh/MoO₃ catalyst had the highest proportion of secondary sites and therefore the highest degree of support interaction, lends evidence to the theory that partially reduced support species are present on the metal particles themselves.

A proportion of the adsorbed carbon monoxide could be evacuated from the surface of each of the catalysts, the magnitude of which was found to be support dependent and closely related to the amount of carbon monoxide adsorbed in the secondary region of the isotherm. Up to 38% of the remaining carbon monoxide could then be removed by a 40 mlmin⁻¹ flow of helium. This effect was also observed in each of the pulse-flow adsorption experiments, however, it was not possible in these experiments to measure the amount of material which was stripped, by the carrier stream, from the surface.

That the remaining carbon monoxide is composed of at least four different species is clearly demonstrated by the experiments described in chapter 6, where ¹³C¹⁶O and ¹²C¹⁸O

were adsorbed in a series of adsorption followed by desorption cycles on samples of Rh/SiO₂ and Rh/MoO₃.

After saturating the surface with a 1:1 mixture of heavy-atom labelled carbon monoxide, two desorption peaks were observed on raising the temperature to 320⁰C. As the low temperature peak consisted of unscrambled carbon monoxide, whilst that in the second peak was completely scrambled, this strongly suggests that two distinct species are desorbing. Smaller amounts of carbon monoxide and water were also observed to desorb.

These results are in reasonable agreement with those of the TPD experiments (the results of which are summarised in table 9.2) which were carried out in this, and other studies, using unlabelled carbon monoxide. Two desorption peaks were detected below 300⁰C for both Rh/SiO₂ and Rh/MoO₃.

Even after a thermal desorption, a substantial amount of material remained at the catalyst surface. Approximately half of this material, which was stable at 320⁰C, was found to exchange with unlabelled gas phase molecules of carbon monoxide, whilst the remainder appeared inert.

The surface residue, which is still present after the thermal desorption, then blocks some of the sites for carbon monoxide adsorption. The amount of carbon monoxide adsorbed by a sample of Rh/SiO₂ decreased progressively during a

Table 9.2 Carbon Monoxide Desorption

Catalyst	Desorption Temp (°C)	Reference
Rh/Al ₂ O ₃	200,330	This study
Rh/SiO ₂	110 (2 peaks),375	This study
Rh/MoO ₃	125,165	This study
Rh/Al ₂ O ₃	190-200	113
Rh/SiO ₂	175,394,574 (CO) 124,424 (CO ₂) 424, ~624 (H ₂)	72
Rh/TiO ₂	209	58
Rh(111)	204	115
Rh filament	209-245	96

series of adsorption / desorption cycles, until, after four cycles, a steady state was reached, when the equivalent of 1.65×10^{19} molecules of carbon monoxide had been retained by the surface. However, only 9.6×10^{16} molecules of carbon monoxide were retained by a much larger sample of Rh/MoO₃.

Several different surface species were also detected by infra-red spectroscopy on the Rh/Al₂O₃ and Rh/SiO₂ catalysts. Unfortunately, however, because of the very low transmission of MoO₃, it did not prove possible to obtain any spectra of the Rh/MoO₃ catalyst.

The first species produced two very intense peaks at 2100 cm⁻¹ and 2040 cm⁻¹, which have been assigned to the symmetric and antisymmetric stretching modes of gem , or twinned, carbon monoxide¹²⁹. The second species produced a broader band at approximately 2070 cm⁻¹, this was due to linear carbon monoxide. The broad feature, which was observed between 1800-1900 cm⁻¹, and which appeared to be made up of several ill-defined peaks, is ascribed to carbon monoxide coordinated between two or more rhodium atoms.

It is interesting to note that carbon monoxide can, to a limited extent, adsorb on MoO₃, even when no rhodium is present. However only 11% of the carbon monoxide which adsorbed on Rh/MoO₃, would adsorb on a similar sized sample of MoO₃ which had undergone an identical reduction

procedure. No carbon monoxide was found to adsorb on either of the other supports.

Since MoO_3 , unlike Al_2O_3 and SiO_2 , can undergo reduction under fairly mild conditions, these results suggest that carbon monoxide is causing a partial reduction of the support material. Some carbon monoxide may actually be present on the support of the Rh/MoO_3 catalyst under similar conditions.

When each of the catalysts was reduced by carbon monoxide, rather than hydrogen, they changed colour from the original pink to a very pale grey, rather than the dark grey/black colour which was produced when the catalysts were reduced under hydrogen. That none of the catalysts were found to adsorb any carbon monoxide after this treatment was probably due to the retention of carbon monoxide species on the surface and to the incomplete reduction of the RhCl_3 .

Carbon monoxide adsorbed on either the Rh/SiO_2 or the $\text{Rh}/\text{Al}_2\text{O}_3$ catalysts underwent complete and very rapid molecular exchange with any gas phase carbon monoxide which was present. However, no exchange took place with the Rh/MoO_3 catalyst, unless the gas phase had first been removed, whereupon complete exchange was found to occur.

These results prove that molecular exchange occurs between two surface species, so that sites have to be available for the adsorption of the incoming molecule if

exchange is to take place. If no such vacant sites are present then they can, as was the case with the Rh/MoO₃ catalyst, be created by evacuating off some of the adsorbed carbon monoxide.

For molecular exchange to take place, two molecules of carbon monoxide must be brought together in fairly close proximity, such that one molecule can displace the other from the surface. This process has been shown to occur readily with gem adsorbed carbon monoxide ^{121,132}, where two molecules are actually adsorbed on to the same rhodium atom, possibly through a transient Rh(CO)₃ species.

Although molecular exchange took place readily at room temperature, labelled carbon monoxide was not found to scramble on either Rh/SiO₂ or Rh/MoO₃ at ambient temperature. When a 1:1 mixture of ¹³C¹⁶O and ¹²C¹⁸O was adsorbed on to a freshly reduced sample of catalyst, none of the carbon monoxide which appeared in the effluent carrier gas had been scrambled. Yet previous experiments had shown that, under flow conditions, carbon monoxide was being continuously stripped from the surface. Hence, at least some of the effluent carbon monoxide must have been adsorbed on the catalyst surface.

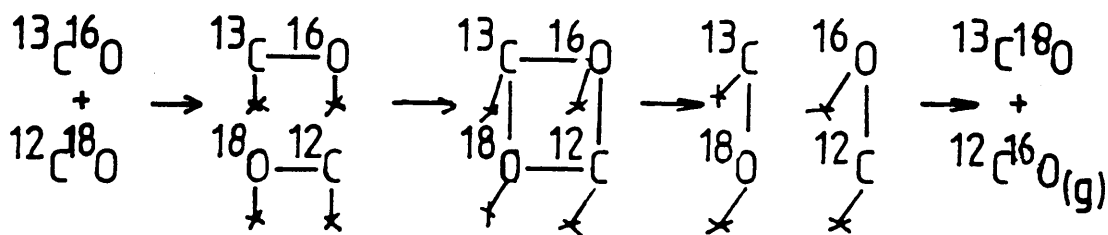
On slowly raising the catalyst temperature, the first and major desorption product was unscrambled carbon monoxide, implying that at low temperatures even the

strongly held carbon monoxide, which was not removed by the helium carrier stream, did not undergo scrambling.

At higher temperatures, however, the effluent carbon monoxide was completely scrambled, indicating the comprehensive breaking and reforming of the carbon - oxygen bond.

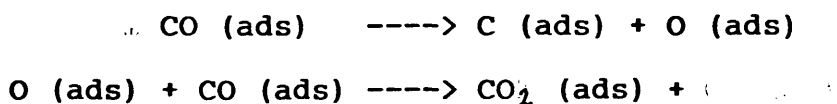
There are two main routes by which this could have been accomplished. The first route involves the complete dissociation of the adsorbed carbon monoxide in to surface carbon and oxygen atoms, with their subsequent recombination in to carbon monoxide. The second route to scrambled carbon monoxide is by a concerted process whereby two molecules of carbon monoxide are brought together, in the correct geometry, so that simultaneous bond making and breaking can take place, such that two new molecules of carbon monoxide are formed. The likely mechanism for this is shown below :-

Reaction Scheme 9.1



If the mechanism was a dissociative one then a great deal of carbon dioxide would be expected to be formed, due to the reactivity of adsorbed oxygen atoms and the large amount of carbon monoxide which was present.

Reaction Scheme 9.2



During the initial adsorption of carbon monoxide, on to the freshly reduced sample of Rh/SiO₂, a small amount of carbon dioxide was produced but, within three carbon monoxide pulses, its production quickly fell to zero. This was due to a small amount of highly reactive oxygen which was present on the catalyst surface due to either the incomplete reduction of the catalyst or to a very small amount of carbon monoxide dissociating on high energy sites in the initial stages of the adsorption.

Some carbon dioxide was formed both during the thermal desorption and during the high temperature adsorption of carbon monoxide, but much less was produced than would have been expected if the scrambled carbon monoxide had been formed through a completely dissociative mechanism.

No carbon dioxide formation was detected during the carbon monoxide adsorption isotherm or the infra-red experiments, even though elevated temperatures were used in the latter.

The labelling of the carbon dioxide which was produced was also inconsistent with a dissociative mechanism. Since

a 1:1 mixture of $^{13}\text{C}^{16}\text{O}$ and $^{12}\text{C}^{18}\text{O}$ was used in these experiments, the carbon dioxide formed from the dissociation of carbon monoxide should statistically have been a 1:1:1:1 mixture of $^{13}\text{C}^{16}\text{O}_2$: $^{12}\text{C}^{16}\text{O}^{18}\text{O}$: $^{13}\text{C}^{16}\text{O}^{18}\text{O}$: $^{12}\text{C}^{18}\text{O}_2$. The carbon dioxide which was formed, however, was found to be heavily enriched with ^{16}O , with no C^{18}O_2 being detected.

Although these observations may be the result of the rapid exchange of dissociated oxygen atoms with surface hydroxyl groups, this process would require the migration, without reaction, of highly active oxygen atoms from the metal particles on to the support, and this would appear unlikely in the presence of large amounts of carbon monoxide.

Less carbon dioxide was produced, even at elevated temperatures, than the amount of material which was left on the surface after each adsorption /desorption cycle. If the formation of carbon dioxide was via the simple disproportionation reaction shown in Reaction Scheme 9.2, then this would not be the case.

Even if the oxygen atoms were not able to readily react with carbon monoxide, they would be expected to exchange rapidly with the surface hydroxyl groups which were always present. This would result in the scrambled carbon monoxide being heavily enriched with ^{16}O , and this was not found to be the case.

That a large amount of scrambled carbon monoxide should be desorbed from the surface at high temperatures would be unlikely if a significant amount of carbon monoxide dissociation was taking place. Since, if, upon dissociation, the carbon and oxygen atoms were far enough apart for recombination not to take place, the oxygen atom would be more likely to react with the numerous molecules of carbon monoxide which would be present than the much scarcer carbon atoms.

After thermal desorption at 320°C, scrambled carbon monoxide was displaced from the catalyst surface by gas phase, unlabelled, carbon monoxide. If dissociation had occurred to any great extent, then most, if not all, of the surface oxygen atoms would have reacted with carbon monoxide to form carbon dioxide. Even if oxygen atoms were still present on the surface after the desorption process, they would be expected to react with the adsorbing carbon monoxide at ambient temperature, rather than the surface carbon atoms. The scrambled carbon monoxide was not found to be enriched with ^{16}O , although after prolonged exposure at elevated temperatures some exchange with the numerous hydroxyl groups would be expected. That this was not the case, is yet more evidence against a completely dissociative mechanism.

Although, there has been a great deal of interest in the recent literature ^{106,109,112} as to whether carbon

monoxide can readily dissociate on rhodium catalysts, the consensus of opinion at the present time appears to be that although carbon monoxide can dissociate to a slight extent at surface defects, this was only significant at much higher temperatures than were employed in the present study.

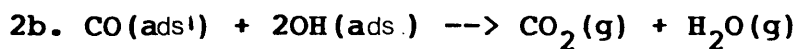
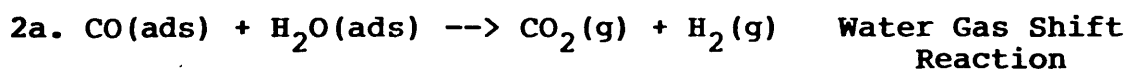
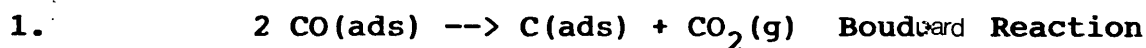
The evidence from these experiments, that a carbon containing species is stable on the catalyst surface at 320°C is somewhat at odds with the findings from the radiotracer experiments that nothing is stable on the surface above 300°C. The infra-red experiments on the other hand imply that the only species stable on the surface above about 250°C was a carbonate species. Even if the surface carbon monoxide was present as dissociated atoms of carbon and oxygen, or as molecules of carbon monoxide adsorbed parallel to the surface and, as such, was undetectable by infra-red spectroscopy, any ^{14}C on the surface, in whatever form, should still have been detectable by the direct monitoring technique. Only if the material had migrated in to the bulk would these results be expected, yet the rapid exchange of at least some of this material, clearly illustrates its accessibility. This discrepancy may, however, be a consequence of the slight differences in the conditions, which are unavoidable when using several different experimental systems.

It may be concluded that the available evidence is much more consistent with a concerted mechanism for the

scrambling of carbon monoxide, which produces scrambled carbon monoxide without the need for the molecules complete dissociation. Scrambling through the type of intermediate shown in Reaction Scheme 9.1 would be expected to produce the full range of isotopically labelled carbon monoxide, as was in fact found to be the case. This carbon monoxide would not be expected to be enriched with ^{16}O , because at no time would the carbon atom be in a position to react with a surface hydroxyl group. Nor would the oxygen atoms be in a position to exchange with the hydroxyl groups, as they too would be firmly co-ordinated.

During the thermal desorption of carbon monoxide however, substantial amounts of ^{16}O enriched carbon dioxide were produced. The possible mechanisms are :-

Reaction Scheme 9.3



Reaction 1) would necessitate the dissociation of one molecule of carbon monoxide for every molecule of carbon dioxide produced and would, therefore, lead to a build up of material on the surface. However, this mechanism cannot

account for the large amount of material which was stable on the surface, nor can it account for the observed isotopic distribution of the carbon dioxide produced.

The two very closely related reactions shown in mechanism 2) would, however, explain the higher than expected amounts of ^{16}O which were present in the carbon dioxide, as the vast majority of the surface water or hydroxyl groups would not be labelled. That large numbers of hydroxyl groups were always present on these catalysts is clearly demonstrated by the very intense infra-red bands observed at $3600\text{--}3800\text{ cm}^{-1}$. Water molecules are also likely to be available on the surface because of the vast amounts of water which are produced during the reduction procedure.

Although, no gas phase hydrogen was detected in this study, other groups have been able to detect its production during the desorption of carbon monoxide. Much of the hydrogen which is formed would, moreover, be expected to spillover on to the support. It is therefore not possible with the information available to choose between the two reactions involved in mechanism 2). It may well be that both reactions are important and that the relative proportions of each depend on the reaction conditions.

The surface scrambling of ^{13}C and ^{18}O labelled carbon monoxide would appear to have a fairly high activation energy. No scrambling was observed at room temperature and yet large amounts of scrambled carbon monoxide were observed

in the effluent gas stream when carbon monoxide was adsorbed at 250°C. This may be due to the difficulties involved in forcing two molecules of carbon monoxide into close enough proximity to form the square planar intermediate complex required. An alternative explanation, however, is that it is the lower surface concentration of carbon monoxide which is present at 250°C and not a high activation energy, which promotes the scrambling reaction at high temperatures.

If the transition complex is formed from two doubly bonded molecules of carbon monoxide which are adsorbed parallel to the surface, then its formation may be limited by the availability of sufficient vacant sites. It has been reported ¹⁹⁴, from infra-red studies, that the relative concentration of bridged carbon monoxide, which is also multiply co-ordinated, increases as the surface concentration of carbon monoxide falls.

Saturation was not reached during the high temperature adsorption of carbon monoxide because of the continuous desorption of carbon monoxide, in the helium stream.

Fairly substantial amounts of carbon dioxide were also produced during the high temperature adsorption of carbon monoxide, this was again heavily enriched with ¹⁶O, suggesting that this reaction may also have a relatively high activation energy.

The material which was thermally stable but exchange inert, may be present as unreactive graphitic or sub-surface carbon.

When unlabelled carbon monoxide stable on the surface at 320°C, was exposed to labelled carbon monoxide, large amounts of unlabelled carbon monoxide were detected in the effluent gas stream. Similar experiments and results have been reported elsewhere ¹¹⁷.

Infra-red studies of the three forms of adsorbed carbon monoxide which are infra-red active, strongly imply that the gem carbon monoxide is formed on small isolated sites, whilst the linear and bridged species are formed on the larger rhodium particles. The gem peaks retained a constant position with changing coverage and are therefore relatively unaffected by interactions with other neighbouring species. This implies that they are present on isolated sites, which were at first thought to be atomic in nature¹²⁹. However, the current evidence now suggests that they are formed on small 8-10 atom particles or on 2-D rafts¹⁴⁹. Others suggest ^{43,118} that because of their nature these sites carry a slight positive charge, but a great deal of further work is needed in this area before any definitive conclusions can be drawn.

The linear peak, on the other hand, is shifted from 2040 cm^{-1} to 2075 cm^{-1} as the surface concentration of carbon monoxide is increased. Due to the increased

interactions between the molecules at high coverage causing a weakening of the Rh-CO bond. This occurs through a decrease in the number of electrons which are available for back donation and the subsequent strengthening of the C-O bond. Linear carbon monoxide is therefore believed to form on the larger metal crystalites. Bridged carbon monoxide¹⁹⁴ has also been observed to shift slightly with coverage and this together with the obvious geometric constraint on a doubly bonded species imply that it too must be found on the larger particles.

The 5% Rh/SiO₂ catalyst with its higher metal loading and generally larger particles, tended to show a higher linear/gem ratio than the 2% catalyst, in agreement with the above conclusions. However, the linear/gem ratio was found to vary enormously from sample to sample, suggesting that the metal loading is only one of a number of factors which control the particle size and so the infra-red spectra of these catalysts.

When the infra-red spectrum of adsorbed carbon monoxide was taken after a series of reduction /adsorption cycles, the peaks due to gem carbon monoxide were found to decrease quite dramatically after each cycle, whilst the linear peak was relatively unaffected. This implies that the number of very small particles on which gem carbon monoxide can form, is falling during the reduction process due to sintering of

the metal particles. Alternatively, if the gem sites really are ionic in character then they may simply be being reduced to metallic sites during the prolonged reduction procedure.

Carbon monoxide adsorption isotherms taken after similar reduction/adsorption cycles also revealed a progressive fall in the amount of carbon monoxide adsorbed by the catalyst. This was principally due to a reduction in the amount of carbon monoxide adsorbed in the primary region of the isotherm, again implying a loss of adsorption sites due to sintering of the metal particles.

When a freshly reduced sample of Rh/Al₂O₃ was saturated with carbon monoxide, the area of the various infra-red peaks which were formed were studied as a function of increasing temperature. As can be seen in fig 8.7, the linear peak behaved as expected, remaining constant until about 90°C, before decreasing sharply in area at higher temperatures and disappearing at 170°C. The two gem peaks, on the other hand, increased in area as the temperature was increased, reaching a maximum at approximately 95°C, before decreasing and subsequently disappearing at 245°C. The increase in area was more pronounced with the asymmetric gem peak, because of its overlap with the linear peak. However, the symmetric peak, which was completely separate, also exhibited an increase in area as the temperature increased.

These results suggest that the amount of gem carbon monoxide on the surface is increasing at higher

temperatures, possibly at the expense of the linear carbon monoxide. Solymosi¹⁴³ has reported that on adsorbing carbon monoxide, the gem species was only produced very slowly on a sample of Rh/Al₂O₃ which had undergone a high temperature reduction. Although this process was reported to go much faster when gas phase carbon monoxide was present. The high temperature reduction would have resulted in a high proportion of the rhodium being present in fairly large particles, and yet in the presence of carbon monoxide "gem-sites", which are only believed to occur on very small particles, were slowly being formed.

These and other related results¹⁴⁹⁻¹⁵¹ imply that carbon monoxide can disrupt large rhodium particles, to form the small isolated sites on which gem carbon monoxide can form. This process has been reported as being accelerated by the moderately high temperatures used in these experiments¹⁵⁰. It is therefore believed that the observed spectra are due to a combination of two processes: the slow disruption of the metal particles by surface carbon monoxide and the desorption of that carbon monoxide as the temperature increases.

No such increase in the area of the gem peaks was observed when carbon monoxide was desorbed from Rh/SiO₂, although a change of gradient in both the linear and the gem graphs was detected at approximately 100°C (fig 8.8). It may, therefore, be that the disruption of rhodium

crystallites by carbon monoxide is a support dependent process, which reflects the supports ability to stabilise the isolated gem sites.

9.3 THE ADSORPTION OF CARBON DIOXIDE

Much less carbon dioxide was found to adsorb on each of the rhodium catalysts, relative to the amount of carbon monoxide adsorbed. Furthermore, the carbon dioxide which did adsorb was much more weakly held. All of the adsorbed carbon dioxide could be removed by evacuation from the Rh/SiO₂ and Rh/MoO₃ catalysts in a 30 minute period, whereas only 20% and 80% respectively of the adsorbed carbon monoxide was labile. These observations may be a consequence of the much greater steric constraints on the adsorption of carbon dioxide. Carbon dioxide is a far larger molecule than carbon monoxide, therefore, steric interactions during its adsorption would be such that significantly less carbon dioxide would be able to adsorb on a given surface area. The back-bonding which is an important feature of the adsorption of carbon monoxide is absent from the adsorption of carbon dioxide and so the adsorbate/adsorbent bond would be expected to be significantly weaker.

Carbon dioxide adsorption appears to have a fairly high activation energy, with more carbon dioxide being adsorbed at 100°C than at ambient temperature. This may again be a consequence of the greater steric interactions between adsorbed molecules.

The adsorption was found to be a rather slow process, with only partial equilibrium being reached in the duration of these experiments, which was up to 14 hrs. This meant that the adsorption isotherms, which were obtained for carbon dioxide proved to be fairly ill-defined. The adsorption isotherms for the Rh/SiO₂ and Rh/MoO₃ catalysts contained no evidence for a primary region and were, to a best approximation, linear. The Rh/Al₂O₃ isotherm did, on the other hand, contain an initial region where the surface count rate increased rapidly with pressure, before tailing off. The fact that 60% of the adsorbed carbon dioxide was stable on Rh/Al₂O₃, whilst all of the adsorbed carbon dioxide was removed by evacuation from the other catalysts, may be related to these differences in the shape of the adsorption isotherms. That is, while some carbon dioxide adsorbs on to the metal particles of the Rh/Al₂O₃ catalyst, possibly through the dissociative adsorption of carbon dioxide, the other catalysts could only adsorb carbon dioxide rather weakly on to their supports. The gradients of the isotherms were very support dependent, with the Rh/MoO₃ catalyst adsorbed ten times the amount of carbon dioxide that a similar sample of Rh/SiO₂ did. None of the catalysts

used in this study reached saturation even at pressures of 5.2 torr of carbon dioxide.

The adsorption of carbon dioxide on to the catalyst supports may be due to the re-oxidation of the partially reduced support material by the carbon dioxide. As discussed earlier MoO_3 has been shown to undergo a partial reduction during the reduction procedure, which may be reversed by the adsorption of carbon dioxide. Direct evidence has been published for the adsorption of carbon dioxide on the Al_2O_3 support itself¹⁹⁵.

No molecular exchange of labelled carbon dioxide was observed in the presence of unlabelled gas phase molecules, presumably because of the difficulties in getting two such large molecules in to sufficiently close proximity for exchange to take place. No equivalent of the gem carbon monoxide species has yet been reported for carbon dioxide.

Carbon dioxide was found to decompose to a slight extent on the catalysts, even at room temperature. The infra-red spectra of carbon dioxide adsorbed on samples of $\text{Rh}/\text{Al}_2\text{O}_3$ or Rh/SiO_2 were all dominated by two very intense bands at 2363 cm^{-1} and 2342 cm^{-1} , due to gas phase or weakly adsorbed carbon dioxide. Three small but very stable carbonate bands were also observed at 1650, 1448 and 1223 cm^{-1} . But even after room temperature adsorption, bands due to adsorbed carbon monoxide were always detected. This

carbon monoxide could only have come from the dissociation of carbon dioxide. The carbon dioxide peaks decreased very rapidly in intensity as the temperature was increased, suggesting again that the carbon dioxide is not very strongly held on the surface. That no gas phase carbon monoxide was detected during the static adsorption of carbon dioxide is probably a result of the adsorption of the carbon monoxide formed. As will be discussed later in this chapter, carbon monoxide was observed, in this study, to adsorb even on surfaces which were saturated with carbon dioxide.

Although the infra-red bands at 1650, 1448 and 1223 cm^{-1} have long been assigned to carbonate bands, it is only recently¹⁹⁶ that inorganic chemists have produced complexes containing carbon dioxide ligands of the type shown below.



One such complex is $\text{RhCl}(\text{CO}_2)(\text{Bu}^n_3\text{P})_2$ which has infra-red bands at 1660, 1550 and 1220 cm^{-1} . That these complexes have proved difficult to produce and are very unstable is generally reflected in the rather poor adsorption of carbon dioxide on these rhodium catalysts. Carbonyl compounds on the other hand are numerous, easy to produce and, on the whole, very stable.

9.4 THE ADSORPTION OF OXYGEN

All of the catalysts investigated adsorbed large amounts of oxygen, which probably resulted in more than a superficial oxidation of the surface. This is strongly suggested by the fact that the percentage dispersion calculated from the amount of oxygen the catalyst adsorbed was much higher than that calculated from either the amount of carbon monoxide the catalyst adsorbed or the TEM studies. This was especially true for the Rh/MoO₃ catalyst where a dispersion of 0.89% was calculated from the adsorption of carbon monoxide, whilst the dispersion from oxygen adsorption if it is assumed that one atom of oxygen adsorbed on each rhodium atom, was 57%.

Although the Rh/Al₂O₃ and Rh/SiO₂ catalysts reached saturation very quickly, the Rh/MoO₃ catalyst did not reach saturation during the period of these experiments.

Very little of the adsorbed oxygen was desorbed from any of the catalysts during the TPD procedure. Rh/Al₂O₃ produced a small desorption peak at approximately 480°C, whilst Rh/SiO₂ desorbed very small amounts of oxygen at 225°C and 435°C. However, the Rh/MoO₃ catalyst did not desorb any oxygen below 500°C, the highest temperature which could be reached in these experiments. Together these results show that the adsorbed oxygen on Rh/MoO₃ is rapidly reoxidising the support material which was partially reduced

during the reduction and hence the calculation of dispersion from the oxygen chemisorption figures is, in this case, almost certainly not valid. The oxygen may also react to reform some of the hydroxyl groups which were lost from each of the catalysts during the reduction.

9.5 THE COMPETITIVE ADSORPTION OF CARBON MONOXIDE, CARBON DIOXIDE, HYDROGEN AND OXYGEN

9.5.1 THE COMPETITIVE ADSORPTION OF CARBON MONOXIDE AND HYDROGEN

The presence of hydrogen was found to increase the amount of carbon monoxide adsorbed by each of the catalysts by 20-35%. Similar observations have also been reported for the co-adsorption of carbon monoxide and hydrogen on rhodium films ¹⁹⁷, although the exact behaviour was very dependent on the ratio of carbon monoxide and hydrogen used, as high concentrations of carbon monoxide were found to displace hydrogen from the surface. The authors explained their results in terms of a co-operative interaction, or complex formation, between carbon monoxide and hydrogen on the surface.

The effect of hydrogen admission on to a surface saturated with carbon monoxide was very rapid, with the

majority of the increased adsorption taking place within the first five minutes. The extra carbon monoxide, which was adsorbed in the presence of hydrogen, was firmly bound to the surface and could not be removed by evacuation, even from the Rh/MoO₃ catalyst.

One explanation for these observations is that the carbon monoxide and hydrogen are reacting together on the surface to form a formate species. These species have been detected on working catalysts by many groups¹³⁷, but since formates are known to decompose rapidly on rhodium³⁹, it may be that these species are either formed on or migrate to the catalyst support. Alternatively, the co-adsorption of carbon monoxide and hydrogen may result in a restructuring of the catalyst surface, such that more active sites for carbon monoxide adsorption are produced.

When carbon monoxide and hydrogen were co-adsorbed on a freshly reduced sample of Rh/Al₂O₃, the infra-red spectrum of the surface consisted of bands due to gem carbon monoxide and peaks at 2361 cm⁻¹ and 2342 cm⁻¹ due to a substantial amount of carbon dioxide. Carbon dioxide was also detected when a sample of 2% Rh/SiO₂ was subjected to an identical procedure. However, no carbon dioxide production was observed with the 5% Rh/SiO₂ catalyst. This suggests that the carbon dioxide is formed from the reaction of adsorbed carbon monoxide with a small amount of highly reactive oxygen, which is still present on the surface, even after

reduction. Similar results have already been discussed for the adsorption of carbon monoxide under flow conditions on a sample of Rh/Al₂O₃.

As the temperature of the catalyst was increased, the adsorbed carbon monoxide slowly desorbed from the surface. The carbon dioxide on the other hand, proved, quite unexpectedly, to be more stable, even at 280°C fairly substantial peaks still remained. However, as will be discussed in more detail later, there is evidence to suggest that carbon dioxide formed from the surface reaction of carbon monoxide and oxygen is more stable, on the catalyst surface, than carbon dioxide adsorbed from the gas phase.

In order to gain a better understanding of what occurs on a working catalyst under reaction conditions, freshly reduced samples of catalyst were exposed to a 2:1 mixture of hydrogen and carbon monoxide at 300°C for up to 14 hrs. The initial infra-red spectra consisted of peaks due to linear carbon monoxide (2046 cm⁻¹ for Rh/Al₂O₃ and 2051 cm⁻¹ for Rh/SiO₂), bridged carbon monoxide and carbonates, as well as gas phase carbon monoxide. No gem carbon monoxide was detected on any of the catalysts in agreement with a number of other studies^{32,142,144}, which have reported that only linear and bridged carbon monoxide is observed at high temperatures in the presence of hydrogen.

The lack of gem carbon monoxide under these conditions has caused a considerable amount of debate. Solymosi¹⁴⁰ has

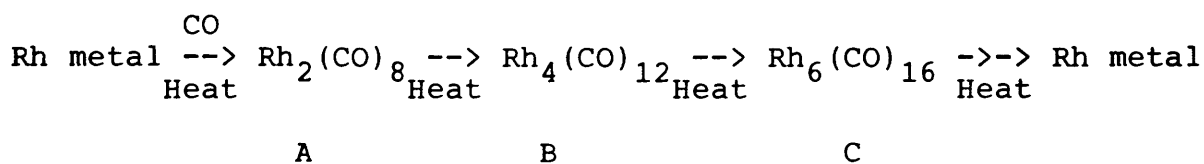
suggested that it indicates the formation of a $\text{Rh}(\text{CO})(\text{H})$ species which prevents the formation of gem carbon monoxide. However, since the adsorption of carbon monoxide is far stronger than that of hydrogen, other groups believe that even if this species is produced, adsorbing molecules of carbon monoxide would tend to displace the hydrogen atoms to form gem carbon monoxide. The present results can be interpreted in terms of hydrogen preventing the disruption of the metal particle by carbon monoxide and so inhibiting the formation of the gem sites. Evidence for the disruption of rhodium particles by carbon monoxide has been discussed earlier and it has also been reported that hydrogen inhibits the process¹⁵³, so that only linear and bridged carbon monoxide are detected.

After 14 hrs at 300°C , no new features had appeared on the $\text{Rh}/\text{Al}_2\text{O}_3$ spectrum, although the carbonate bands at 1590, 1462 and 1344 cm^{-1} were considerably more intense, due perhaps, to the formation of formate species on the surface or to a slow build up of carbon dioxide from the water gas shift reaction. A small amount of carbon dioxide was detected in the initial high temperature spectrum of Rh/SiO_2 , but this quickly desorbed from the surface. The peak due to linear carbon monoxide shifted slightly from 2067 cm^{-1} to 2057 cm^{-1} after 14 hrs at 300°C , indicating a drop in the surface concentration of carbon monoxide, upon evacuation the peak shifted still further to 2034 cm^{-1} .

This effect was a consequence of the build up of carbonaceous material on the surface during these experiments as was demonstrated quite clearly by the considerable fall in the transmission of the samples after, 14 hrs at 300°C.

That a rhodium mirror should have formed on the inside of the sample holder during these experiments may have been due to the formation and decomposition of a series of rhodium carbonyl clusters at the fairly high temperatures which were employed. Reaction scheme 9.4 depicts one possible reaction pathway from a small but unstable rhodium dimer to fairly large clusters, which would then lose their remaining carbonyls to form the metallic mirror.

Reaction Scheme 9.4



Species A-C have all been reported in the literature and are known to decompose easily into the next complex in the reaction scheme ¹⁹⁸. Rhodium clusters containing as many as twenty two rhodium atoms and thirty seven carbonyl groups have also been reported, these too were found to be unstable.

9.5.2 THE COMPETITIVE ADSORPTION OF
CARBON DIOXIDE AND HYDROGEN

It has been reported¹³⁹ that the presence of hydrogen increases the amount of carbon dioxide adsorbed by supported rhodium catalysts. In this study, however, it was found that the presence of hydrogen caused an initial decrease in the amount of carbon dioxide adsorbed by each of the catalysts, through the displacement of the rather weakly held carbon dioxide by hydrogen. The small subsequent increase in the amount of carbon dioxide on the surface is probably only a consequence of the long contact times used in these experiments. This slow adsorption of carbon dioxide, when the system was allowed to equilibrate overnight may even be, in part, the result of the reverse water gas shift reaction, as any carbon monoxide which is formed would be expected to be strongly adsorbed by the surface.

Reaction Scheme 9.5



Less carbon dioxide was found to adsorb on the Rh/MoO₃ catalyst when hydrogen was present.

9.5.3 THE COMPETITIVE ADSORPTION OF CARBON MONOXIDE AND CARBON DIOXIDE

Preadsorbed carbon monoxide was found to drastically reduce the amount of carbon dioxide, which a sample of Rh/Al₂O₃ could adsorb, from that which would be expected to adsorb in the absence of carbon monoxide. Since carbon monoxide is more strongly bound to rhodium surfaces than carbon dioxide, it is not surprising that carbon monoxide should block carbon dioxide adsorption. Adsorbed carbon monoxide has been reported³⁴ to produce a similar site blocking effect when it blocks the spillover of hydrogen atoms from the metal atoms on to the support, but has no effect on any hydrogen which may already be present on the support.

Much more interesting and more difficult to explain, were the observations that both the Rh/SiO₂ and the Rh/MoO₃ catalysts actually adsorbed more carbon dioxide when they were pre-covered with carbon monoxide. This effect may have been caused by the formation of more active sites for the adsorption of carbon dioxide, by the more thorough reduction of the catalyst surface produced by the carbon monoxide than was possible with hydrogen. This, however, seems unlikely in view of the fact that samples of catalyst reduced by carbon monoxide adsorbed no further carbon monoxide. It appears likely, therefore, that the pre-adsorbed carbon monoxide has increased the amount of carbon dioxide the

catalyst can adsorb by increasing the surface area of the catalyst through its disruption of the rhodium crystallites.

The adsorption isotherms of carbon monoxide adsorbed on samples of Rh/Al₂O₃ and Rh/SiO₂ which were pre-covered with carbon dioxide, were very similar in shape to those observed on a freshly reduced surface.

Both Rh/Al₂O₃ and Rh/SiO₂ were found to adsorb less carbon monoxide when the surface was covered with carbon dioxide. This may be a result of the carbon dioxide, or even the carbon monoxide formed from carbon dioxide dissociation, blocking some of the sites for carbon monoxide adsorption. On the other hand, the amount of carbon monoxide adsorbed by the Rh/MoO₃ catalyst was found to increase slightly on the pre-treated surface. Although the increase was within the experimental error of the experiment, it probably reflects the proportionally higher amounts of carbon dioxide which adsorb on the support of the Rh/MoO₃ catalyst compared to that adsorbed on the other supports. This means that less of the carbon dioxide would be present on the metal to block the adsorption of carbon monoxide.

9.5.4 THE COMPETITIVE ADSORPTION OF CARBON MONOXIDE AND OXYGEN

Less carbon monoxide was found, not surprisingly, to adsorb on pre-oxidised samples of Rh/Al₂O₃ and Rh/SiO₂ than

on freshly reduced ones. However, the pre-oxidised sample of Rh/MoO₃ adsorbed nearly four times as much carbon monoxide as any of the freshly reduced ones, with, moreover, a higher proportion of the adsorbed carbon monoxide being stable to evacuation.

These observations are probably due to the surface concentration of oxygen being higher, after evacuation, on Rh/MoO₃ than on any of the other catalysts. When large amounts of gas phase oxygen were admitted to catalysts saturated with carbon monoxide, all of the catalysts were found to adsorb more carbon monoxide. This increase in the adsorption of carbon monoxide is due to the reaction of carbon monoxide with adsorbed oxygen atoms on the surface. That the pre-oxidised sample of Rh/MoO₃ should contain more of these active oxygen atoms is probably due to the partially reduced nature of the support, after the standard reduction procedure. The oxygen may adsorb directly on to the support and then possibly spill back over on to the metal particles. The loss of adsorption capacity observed with the oxidised samples of Rh/Al₂O₃ and Rh/SiO₂ was probably a result of a loss of active sites due to the partial oxidation of the metal surface by the oxygen, without the compensating reductive reactions of carbon monoxide.

Since Rh/MoO₃ adsorbed more carbon dioxide than any of the other catalysts, it would be expected that this catalyst

would also exhibit the largest increase in carbon monoxide adsorption, under oxidising conditions. As much of the carbon dioxide adsorbed on Rh/MoO₃ appears to be associated with the support, then it is probable that the carbon dioxide formed from the oxidation of carbon monoxide would also be present on the support.

Further evidence for the formation of carbon dioxide on these catalysts comes from the adsorption isotherms obtained when carbon monoxide was adsorbed on to catalyst samples saturated with oxygen. Under these conditions the amount of ¹⁴C on the surface showed a linear increase with the amount of carbon monoxide present. This produced isotherms which were very similar in shape to those obtained when carbon dioxide itself was adsorbed on to the catalysts. That the catalysts did not appear to reach saturation also suggests that the carbon dioxide which is formed is present on the support.

It should however, be noted that none of the material adsorbed in these experiments could be subsequently removed from the surface by a 30 minute period of evacuation. On a freshly reduced sample of Rh/MoO₃ however, 93% of the surface carbon monoxide and all of the adsorbed carbon dioxide could be evacuated from the surface. The surface species are therefore different from those which are formed when either carbon monoxide or carbon dioxide are adsorbed from the gas phase on to a freshly reduced catalyst.

Although its exact structure is still unknown, the available evidence is consistent with a carbonate ion on the support.

Carbon monoxide and oxygen probably adsorb on different surface sites, on each of the catalysts which were studied, as neither totally blocked the adsorption of the other, nor did oxygen displace any carbon monoxide from the surface. This is in contrast to the report by Jackson⁸² that pre-adsorbed carbon monoxide inhibits the adsorption of oxygen, although this effect was found to be very dependent on the metal precursor.

9.5.5 THE COMPETITIVE ADSORPTION OF CARBON DIOXIDE AND OXYGEN

The presence of oxygen, whether by the pre-oxidation of the surface or by the co-adsorption of carbon dioxide and oxygen, results in a dramatic decrease in the amount of carbon dioxide which was adsorbed by each of the catalysts. The more oxygen that was present the more dramatic were its results. This was a consequence of the loss of adsorption sites caused by the oxidation of the metal particles. There is no mechanism whereby the catalyst could counteract this effect, as carbon dioxide is a much poorer reducing agent than carbon monoxide, therefore less carbon dioxide can adsorb on to the surface.

RHODIUM CATALYSTS9.6.1METHANOL

When methanol is adsorbed on either Rh/Al₂O₃ or Rh/SiO₂ at room temperature, the initial infra-red spectrum was made up principally of bands due to gas phase or physically adsorbed methanol. This weakly held material was gradually removed from the surface by the helium carrier stream. Of more significance, with the Rh/Al₂O₃, was the appearance in the infra-red spectrum of fairly intense bands due to carbon monoxide and carbonates on the surface.

While a small amount of carbon monoxide was observed in the reference spectrum of methanol, probably due to its decomposition in the infra-red beam, the Rh/Al₂O₃ catalyst promoted the decomposition of methanol to carbon monoxide.

The room temperature adsorption of methanol on Rh/SiO₂ produced features at 2000, 1876 and 1678 cm⁻¹ which were not due to physically adsorbed methanol. While the latter bands can be identified as being due to bridged carbon monoxide and carbonates respectively, the first peak is more difficult to assign. If it were due to linear carbon monoxide, then it would be expected to appear at much higher wavenumbers. These results are, however, entirely

consistent with the observations of Yang, who reported ¹²⁹ that when carbon monoxide is adsorbed in the presence of hydrogen or water, both of which are likely to be methanol decomposition products, the peak due to linear carbon monoxide was found to shift to lower wave numbers by as much as 50 cm^{-1} . He also reported that under these conditions the peak due to bridged carbon monoxide increased in intensity. This was also observed in this study when methanol decomposed at room temperature on $\text{Rh}/\text{Al}_2\text{O}_3$ or Rh/SiO_2 .

As the temperature was increased, surface carbon monoxide gradually desorbed from the surface of the $\text{Rh}/\text{Al}_2\text{O}_3$ sample, until at 163°C only the carbonate bands remained in the spectra. During this period the gem carbon monoxide peaks were observed to increase in intensity at the expense of the linear one. This effect can once again be ascribed to the slow disruption of the metal crystallites by the adsorbed carbon monoxide. The carbonate bands at 1635, 1391 and 1381 cm^{-1} were found to increase in intensity as the temperature rose and were still stable at 260°C .

On Rh/SiO_2 , all of the major spectral features had disappeared by 97°C , suggesting that the products of methanol decomposition were more strongly held on the $\text{Rh}/\text{Al}_2\text{O}_3$ than the Rh/SiO_2 catalyst. This is in accordance with the TPD studies of carbon monoxide which were carried out on these catalysts, as discussed earlier. While

material was desorbed from the Rh/SiO₂ at temperatures as low as 110°C, no desorption peak was detected for Rh/Al₂O₃ until nearly 200°C.

The infra-red spectra of both catalysts also exhibited two weak bands at approximately 2950 cm⁻¹ and 2850 cm⁻¹ due to C-H groups on the surface, but these bands were not stable above 160°C.

When methanol was adsorbed on a sample of Rh/Al₂O₃ at 285°C, as well as the bands due to adsorbed carbon monoxide and carbonates, peaks due to a quantity of gas phase carbon monoxide were also present. However, after five minutes all of this gas phase material had been removed by the carrier stream. This implies that, as expected, the decomposition of methanol is more rapid at 285°C than at 18°C, but that no new species were formed.

Similar results were also obtained with the Rh/SiO₂ catalyst, a weak band in the C-H stretching region again being observed.

It should be noted that no gem carbon monoxide was detected during the high temperature decomposition of methanol, probably because of the large amounts of hydrogen which would also be present on the surface. As already discussed, no gem carbon monoxide was detected during the high temperature co-adsorption of carbon monoxide and hydrogen, because hydrogen is believed to inhibit the

disruption of the metal particles by carbon monoxide, and so prevents the formation of the "gem" sites.

9.6.2 ETHANOL

The influence of hydrogen on the adsorption of ethanol on Rh/Al₂O₃ was investigated by adsorbing the ethanol in a stream of either helium or hydrogen. In helium, the room temperature adsorption of ethanol produced an infra-red spectrum which contained only bands due to physically adsorbed ethanol. As the temperature increased, however, bands due to gem, linear and bridged carbon monoxide all developed, reaching a maximum at 160°C, whereafter they decreased in intensity, until at 220°C the carbon monoxide had all desorbed.

These findings are rather at odds with the TPD results which suggest that carbon monoxide desorbs from Rh/Al₂O₃ in two stages, the first around 200°C and the second at 330°C. If all of the infra-red active carbon monoxide desorbs in the low temperature peak, then it is conceivable that the second peak is due to that carbon monoxide which is adsorbed parallel to the surface and is, as such, infra-red inactive. The same may also be true of the other catalysts which all exhibited two adsorption bands (110°C + 375°C for Rh/SiO₂ and 125°C + 165°C for Rh/MoO₃).

Carbonate bands were observed at approximately 100°C and slowly increased in intensity up to 220°C.

When a hydrogen carrier gas was used, however, linear and bridged carbon monoxide were observed even when ethanol was adsorbed at room temperature. Carbonate bands were also identified, although they were found to be less intense in the presence of hydrogen. As the temperature increased the amount of carbon monoxide on the surface also increased. Although a great deal more carbon monoxide was formed when hydrogen rather than helium was used as the carrier gas, its concentration reached a maximum and it desorbed, at the same temperature, as carbon monoxide which was formed in the absence of hydrogen.

The peak due to linear carbon monoxide was observed at a higher wavenumber and was also narrower in line-width than was detected when a flow of helium was used as the carrier. This may, as reported by Wells¹⁹⁷, be a direct consequence of the higher concentration of carbon monoxide which was present on the surface when hydrogen was present, as discussed earlier. The increased stretching frequency being a consequence of the higher degree of interaction between adsorbed molecules at high coverages and the subsequent strengthening of the C-O band which results. One explanation for the reduction in line width is that at low coverages carbon monoxide is randomly adsorbed on to a wide variety of sites with various energies. This produces

a rather broad line-width. At higher coverages, however, the increased interaction between neighbouring molecules results in a decrease in the overall heat of adsorption of carbon monoxide. This reduces the bonding differences between the molecules and, in effect, makes the adsorbed molecules more equivalent, thereby reducing the line-width. Several weak bands were observed in the C-H stretching region, but these appeared to be less stable than those formed during the adsorption of methanol .

When ethanol was adsorbed on Rh/Al₂O₃ at 275°C, its behaviour was very similar to that observed when methanol was adsorbed. Both linear and gas phase carbon monoxide were observed, although the linear peak appeared at only 1979 cm⁻¹ when helium was used as the carrier gas. The initially intense peaks due to physically adsorbed ethanol were quickly reduced by its desorption and/or decomposition at these high temperatures, while stable carbonate peaks grow in at 1574 cm⁻¹ and 1455 cm⁻¹.

When ethanol was adsorbed on Rh/SiO₂ at room temperature, the only bands observed, apart from those due to physically adsorbed ethanol, were small peaks at 2019cm⁻¹ and 1878 cm⁻¹, due to linear and bridged carbon monoxide, which were not stable above 80°C. When ethanol was adsorbed at 272°C, only bands due to physically adsorbed ethanol could be detected.

It therefore appears that while methanol will decompose readily on either catalyst, Rh/Al₂O₃ is a much better catalyst for the decomposition of ethanol than is Rh/SiO₂. The presence of hydrogen and, not suprisingly, elevated temperatures were also found to enhance the decomposition of ethanol on Rh/Al₂O₃.

If the principle of microscopic reversibility holds true then those catalysts which are active in the decomposition of ethanol, should also be active in its formation from carbon monoxide and hydrogen. I.C.I.'s very active, low temperature methanol formation catalysts have been shown to readily decompose methanol²⁰¹. Jackson et al.¹⁹⁹, have reported that not only was the selectivity of their Rh/Al₂O₃ catalysts higher for ethanol than that of their Rh/SiO₂, but its turnover frequency and the amount of ethanol it produced per second were also significantly higher than that of the Rh/SiO₂. This is in complete agreement with the above hypothesis .

9.6.3 ACETALDEHYDE

Acetaldehyde was found to decompose to carbon monoxide on both the Rh/Al₂O₃ and the Rh/SiO₂ catalysts at room temperature. On Rh/Al₂O₃ both gem and linear carbon monoxide were formed, but on Rh/SiO₂ only the linear species was formed. This is a reflection of the ease with which carbon monoxide can disrupt the metal particles on Rh/Al₂O₃

to form the smaller "gem sites". On Rh/SiO₂, however, as witnessed by the infra-red studies which were carried out on carbon monoxide desorption, this process does not appear to occur as readily.

The surface concentration of carbon monoxide increased as the temperature went up, reaching a maximum at approximately 70°C, before desorbing completely at about 200°C, with both catalysts. This implies that once again the decomposition of simple oxygenates occurs more readily on these catalysts at higher temperatures. Fairly intense carbonate bands formed in the spectrum of Rh/Al₂O₃ as the temperature was increased, and were the only stable species on the surface above 200°C. No such bands, however, were observed with the Rh/SiO₂ catalyst. Small bands in the C-H stretching region were also detected on both catalysts, these were stable at temperatures as high as 200°C.

A very similar spectrum to that observed when acetaldehyde was adsorbed on Rh/Al₂O₃ was also obtained when acetaldehyde was adsorbed on the Al₂O₃ support itself. It is, however, important to note that no carbon monoxide was observed and, therefore, the decomposition of acetaldehyde did not take place in the absence of any rhodium particles. It would appear, therefore, that while acetaldehyde, and possibly some of the other oxygenates, may be present on the support material, its decomposition can only take place on the metal.

In contrast to what was observed with the decomposition of ethanol and methanol, Rh/SiO₂ appeared to be a better catalyst for acetaldehyde decomposition, possibly because of the acetaldehyde having a higher stability on Al₂O₃ than on SiO₂. At elevated temperatures the adsorption of acetaldehyde on either of the catalysts produced only bands due to physically adsorbed acetaldehyde.

REFERENCES

1. P.Sabatier and J.B. Senderens a) C.R.Acad.Sci. Paris 134 514 (1902), b) German Patent No. 293787 (1913)
2. F.Fischer and H.Tropsch Brennst. Chem. 4 276 (1923)
3. G.C.Chinchen, K.C. Waugh and D.A.Whan Applied Catal. 25 101 (1986)
4. W.Klien, M.Berger, A.Eisenbeis, J.Kadelka and J.Schlupp J. Mol. Catal. 13 95 (1981)
5. E.Poels and V.Ponec in "Catalysis" ed. G.C.Bond and G.Webb (Specialist Periodic Reports). The Royal Society of Chemistry, London Vol.6 p.196 (1983)
6. V.Ponec in "Catalysis" ed. G.C.Bond and G.Webb, (Specialist Periodic Reports). The Royal Society of Chemistry, London Vol.5 p.48 (1982)
7. M.Ichikawa Bull. Chem. Soc. Jpn. 51 2273 (1978)
8. R.L.Pruett Ann. N. Y. Acad. Sci. 295 239 (1977)
9. C.K.Brown and G.Wilkinson J. Chem. Soc.(A) 1970 p.2753
10. H.Orita, S.Naito and K.Tamaru Chem. Lett. 1983 p.1161
11. M.Ichikawa J. Chem. Soc. Chem. Comm. 1978 p.566
12. G.C.Bond in "Heterogeneous Catalysis - Principles and Applications". Claredon, Oxford . 2nd ed p.97
13. S.C.Chuang, J.G.Goodwin and I.Wender J. Catal. 95 435 (1985)
14. S.Naito, H.Yoshioka, H.Orita and K.Tamaru Proc. 8th Inter. Cong. Catal.,Berlin Vol. 3 p.207 (1984)
15. D.G.Castner, R.L.Blackadder and G.A.Somorjai J. Catal. 66 257 (1980)
16. V.L.Kuznetzov, A.V.Romonenko, I.L.Mudrakovskii, V.M.Matikhin, V.A.Schmochkov and Y.I.Yermakov Proc. 8th Inter. Cong. Catal.,Berlin Vol. 5 p.3 (1984)
17. P.R.Watson and G.A.Somorjai J. Catal. 74 282 (1982)
18. M.A.Vannice J. Catal. 37 449 (1975)
19. M.M.Bhasin, W.J.Bartley, P.C.Ellgen and T.P.Wilson J. Catal. 54 120 (1978)
20. H.Fujitsu, N.Ikeyama and I.Mochida J. Catal. 100 279 (1986)

21. K.Fujimoto, M.Kameyoma and T.Kunugi J. Catal. 61 7 (1980)
22. M.A.Logan and G.A.Somorjai J. Catal. 95 317 (1985)
23. G.C.Bond and R.Burch in "Catalysis", ed. G.C.Bond and G.Webb (Specialist Periodic Reports), The Royal Society of Chemistry, London Vol.6 p.27 (1983)
24. S.D.Jackson, B.J.Brandreth and D.Winstanley Applied Catal. 27 325 (1986)
25. T.Iizuka, Y.Tanaka and K.Tanabe J. Catal. 76 1 (1982)
26. C.S.Keller and A.Bell J. Catal. 71 288 (1981)
27. F.Fajula, R.G.Anthony and J.H.Lunsford J. Catal. 73 237 (1982)
28. D.J.C.Yates, L.L.Murrell and E.B.Prestridge J. Catal. 57 41 (1979)
29. J.C.Vis, H.F.J.von t'Blik, T.Huizinga, J.van Grondelle and R.Pins J. Catal. 95 333 (1985)
30. C.Wong and R.W.McCabe J. Catal. 107 535 (1987)
31. H.Arakawa, K.Takeuchi and T.Matsuzaka Chem. Lett. 1984 p1607
32. Y.Tanaka, T.Iizuka and K.Tanabe J. Chem. Soc., Faraday Trans. 1 78 2215 (1982)
33. R.R.Cavanagh and J.T.Yates Jr J. Catal 68 22 (1981)
34. T.M.Apple, P.Gajardo and C.Dybowski J. Catal. 68 103 (1981)
35. J.C.Conesa, P.Malet, A.Munoz, G.Munuera, M.T.Sainz, T.Sanz and J.Saria Proc. 8th Inter. Cong. Catal., Berlin Vol.5 p217 (1984)
36. A.Bertuccio and C.O.Bennett Applied Catal. 35 329 (1987)
37. F.Solymosi, A.Erdohelyi and T.Bansagi J. Chem. Soc., Faraday Trans. 1 77 2645 (1981)
38. P.G.Gopal, R.L.Schneider and K.L.Watters J. Catal. 105 366 (1987)
39. F.Solymosi, T.Bangsagi and A.Erdohelyi J. Catal. 72 166 (1981)
40. B.J.Kip, F.Dirne, J.van Grondelle and R.Pins Applied Catal. 25 43 (1986)
41. S.L.T.Andersson and M.S.Scurrrell J. Catal. 59 340 (1979)

42. M.Primet J. Chem. Soc., Faraday Trans. 1 74 2570 (1978)
43. S.D.Worley, C.A.Rice, G.A.Mattson, C.W.Curtis, J.A.Cuin and A.R.Tarrer J. Phys. Chem. 86 2714 (1986)
44. G.van der Lee, B.Schuller, H.Post, T.L.F.Favre and V.Ponec J. Catal. 98 522 (1986)
45. J.R.Katzer, A.W.Sleight, P.Gajardo, J.B.Michel, E.F.Gleason and S.McMillan Faraday Discussions of the Chemical Society No72 p121 (1981)
46. H.A.Dirske, P.W.Lednor and P.C.Versloot J. Chem. Soc. Chem. Comm. 1982 p814
47. G.M.Schwab, J.Block and D.Schultze Agnew. Chem. 71 101 (1958)
48. D.E.Resasco and G.L.Haller J. Catal. 82 279 (1983)
49. G.L.Haller, V.E.Henrich, M.McMillan, D.E.Resasco. H.R.Sadeghi and S.Sakellson Proc. 8th Inter. Cong. Catal., Berlin Vol 5 p 135 (1984)
50. M.A.Vannice in "Catalysis - Science and Technology" ed. J.R.Anderson and M.Boudart, Springer - Verlag Vol 3 p 139 (1982)
51. F.Solymosi I.Tombacz and J.Kosztá J. Catal. 95 578 (1985)
52. S.H.Chien, B.N.Shelimov, D.E.Resasco, E.H.Lee and G.L.Haller J. Catal. 77 301 (1982)
53. H.R.Sadeghi and V.E.Henrich J. Catal. 87 279 (1984)
54. M.E.Levin, M.Salmeron, A.T.Bell and G.A.Somorjai J. Catal. 106 401 (1987)
55. A.G.T.M.Bastein, W.J.van der Boogert, G.van der Lee H.Luo, B.Schuller and V.Ponec Applied Catal. 29 243 (1987)
56. R.P.Underwood and A.T.Bell Applied Catal. 34 289 (1987)
57. H.R.Sadeghi and V.E.Henrich J. Catal. 109 1 (1988)
58. D.N.Belton, Y.M.Sun and J.M.White J. Catal. 102 338 (1986)
59. P.Meriaudeau, O.H.Ellestad, M.Dufax and C.Naccache J. Catal. 75 243 (1982)
60. G.van der Lee and V.Ponec Catal. Rev. - Sci. Eng. 29 183 (1987)
61. S.Kesraoui, R.Oukaci and D.G.Blackmond J. Catal. 105 432 (1987)

62. D.G.Blackmond, J.A.Williams, S.Kesraoui and D.S.Blazewick J. Catal. 101 496 (1986)
63. B.J.Kip, E.G.F.Hermans and R.Pins Applied Catal. 35 141 (1987)
64. G.Marcelin, J.Elester and S.F.Mitchell J. Catal. 102 240 (1986)
65. S.C.Chaung, J.G.Goodwin Jr and I.Wender J. Catal. 92 416 (1985)
66. B.J.Kip, P.A.T.Smeets, J.van Grondelle and R.Pins Applied Catal. 33 181 (1987)
67. G.C.Bond and D.G.Richards Applied Catal. 28 303 (1987)
68. R.Queau, L.Labroue and P.Poilblanc J. Catal. 69 249 (1981)
69. F.Solymsi, M.Pasztor and G.Rakhely J. Catal. 110 413 (1988)
70. J.S.Rieck and A.T.Bell J. Catal. 99 278 (1986)
71. F.G.A.van der Berg, J.H.E.Gleezer and W.M.H.Sachtler J. Catal. 93 340 (1985)
72. R.P.Underwood and A.T.Bell J. Catal. 109 61 (1988)
73. T.P.Wilson, P.H.Kasai and P.C.Ellgen J. Catal. 69 193 (1981)
74. B.J.Kip, E.G.F.Hermans, J.H.M.C.van Wolput, N.M.A.Hermans, J.van Grondelle and R.Pins Applied Catal. 35 109 (1987)
75. D.Yu-Hua, C.De-An and T.Khi-Rui Applied Catal. 35 77 (1987)
76. B.J.Kip, P.A.T.Smeets, J.H.M.C.van Wolput, H.W.Zandergen, J.van Grondelle and R.Pins Applied Catal. 33 157 (1987)
77. W.M.F.Sachtler, D.F.Shriver, W.B.Hollenberg and A.F.Lang J. Catal. 92 429 (1985)
78. M.Ichikawa and K.Shikakura "New Horizons in Catalysis", Proc. 7th Inter. Cong. Catal., Tokyo 1980 p 925
79. E.W.Thornton, H.Knozinger, B.Tesche, J.J.Rafalko and B.C.Gates J. Catal. 62 117 (1980)
80. S.L.T.Andersson, K.L.Watters and R.F.Howe J. Catal 69 212 (1981)

81. T.Beringhelli, A.Gervasini, F.Marazzoni, D.Stumoto,
S.Martinegro, L.Zanderighi and F.Pinna
Proc. 8th Inter. Cong. Catal., Berlin 1984 Vol 5 p 63
82. S.D.Jackson Unpublished Results
83. E.A.Hyde, R.Rudham and C.H.Rochester
J. Chem. Soc., Faraday Trans. 1 79 2405 (1983)
84. B.Brandreth, S.D.Jackson and D.Winstanley
J. Catal. 102 433 (1986)
85. S.D.Worley, C.A.Rice, G.A.Mattson, C.W.Curtis, J.A.Guin
and A.R.Tarrer J. Chem. Phys. 76 20 (1982)
86. P.Watson and G.A.Somorjai J. Catal. 72 347 (1981)
87. J.S.Brinnen, J.L.Schmitt, W.R.Doughman, P.J.Acharn,
L.A.Siegel and W.N.Delgass J. Catal. 40 295 (1975)
88. A.Amariglio, A.Elbiache and H.Amariglio J. Catal.
98 355 (1986)
89. D.C.Koningsberger, J.B.A.D.van Zon, H.F.J.van't Blik,
G.J.Yisser and R.Pins J. Phys. Chem. 89 4075 (1985)
90. D.Duprez, J.Barraut and C.Geron Applied Catal. 37
105 (1988)
91. Y.Iwasawa, T.Hayasaka and S.Ogasawara Chem Lett.
1983 p131
92. Y.Kobori, H.Yamasaki, S.Niato, T.Onishi and K.Tamara
Chem. Lett. 1983 p553
93. I.Toyoshima and G.A.Somorjai Catal. Rev.- Sci. Eng.
19 105 (1979)
94. J.T.Yates, P.A.Thiel and W.H. Weinberg Surf. Sci. 84
427 (1979)
95. V.V.Gorodetskii, B.E.Nieuwenhuys, W.M.H.Sachtler and
G.K.Boreskov Surf. Sci. 108 225 (1981)
96. V.V.Gordoetskii, V.A.Sobyorvin, A.R.Cholack and
M.Y.Smirnov Proc. 8th Inter. Cong. Catal., Berlin
Vol 3 p 323 (1984)
97. K.Christmann and G.Ertl Surf. Sci. 60 365 (1976)
98. B.J.Kip, F.B.M.Duivenvoorden, D.C.Koningsberger and
R.Pins J. Catal. 105 26 (1987)
99. S.E.Wanke and N.A.Dougharty J. Catal. 24 367
(1972)
100. H.F.J.van't Blik and R.Pins J. Catal. 99 239
(1986)

101. J.Sanz and J.M.Rojo J. Phys. Chem. 89 4974
(1985)
102. K.Kawasaki, M.Shibata, H.Miki and T.Kioka
Surf. Sci. 81 370 (1979)
103. P.A.Serman and G.C.Bond Catal. Rev. - Sci. Eng.
8 211 (1974)
104. G.Herinci-Olive and S.Olive in " The Chemistry of
the Catalyzed Hydrogenation of Carbon Monoxide "
Springer - Verlag 1984 p 23
105. G.Blyholder J. Phys. Chem. 68 2772 (1964)
106. L.H.Dubois and G.A.Somorjai Surf. Sci. 91 541 (1980)
107. K.Nakamoto in " Infrared Spectra of Inorganic and
Co-ordination Compounds " 2nd ed. p 260
108. J.T.Yates Jr., E.D.Williams and W.H.Wienberg
Surf. Sci. 91 562 (1980)
109. V.V.Gorodetskii and B.E.Nieuwenhuys Surf. Sci. 105
199 (1981)
110. C.T.Campbell and J.M.White J. Catal. 54 289
(1978)
111. D.G.Castner and G.A.Somorjai Surf. Sci. 83 60 (1979)
112. D.G.Castner, L.Dubois, B.Sexton and G.A.Somorjai
Surf. Sci. 103 L134 (1981)
113. A.Erdohelyi and F.Solymosi J. Catal. 84 446 (1983)
114. K.Guilhooley, S.D.Jackson and S.Rigby J. Chem. Soc.
Faraday Trans. 1 82 431 (1986)
115. P.A.Thiel, E.D.Williams, J.T.Yates Jr. and W.H.Weinberg
Surf. Sci. 84 54 (1979)
116. E.D.Williams, P.A.Thiel, W.H.Weinberg and J.T.Yates Jr.
J. Chem. Phys. 72 3496 (1980)
117. S.D.Jackson Unpublished Results
118. R.R.Cavanagh and J.T.Yates Jr. J.Chem. Phys. 74
4150 (1981)
119. H.C.Yao and W.G.Rothschild J.Chem. Phys. 68 4774
(1978)
120. S.Zhong J. Catal. 100 270 (1986)
121. H.C.Eckstrom, G.G.Possley, S.E.Hannum and W.H.Smith
J. Chem. Phys. 52 5435 (1970)
122. J.T.Yates Jr., T.M.Duncan, S.D.Worley and R.W.Vaughan
J. Chem. Phys. 70 1219 (1979)

123. J.T.Yates Jr., T.M.Duncan and R.W.Vaughan
J. Chem. Phys. 71 3908 (1979)
124. C.A.Rice, S.D.Worley, C.W.Curtis, J.A.Guin and
A.R.Tarrer J. Chem. Phys. 74 6487 (1981)
125. R.C.Jacklevic, L.Elle and H.C.Yao Surf. Sci. 171
279 (1986)
126. R.C.Jacklevic, L.Elle and H.C.Yao Proc. 8th Inter.
Cong. Catal., Berlin Vol. 3 p 37 (1984)
127. R.M.Kroeker, W.C.Kaska and P.K.Hansma J. Catal. 57
72 (1979)
128. T.M.Duncan, J.T.Yates Jr. and R.W.Vaughan
J. Chem. Phys. 73 975 (1980)
129. A.C.Yang and C.W.Garland J. Phys. Chem. 61 1504
(1957)
130. C.W.Garland and J.R.Wilt J. Chem. Phys. 36 1094
(1962)
131. L.F.Dahl, C.Martell and D.L.Wampler J. Am. Chem.
Soc. 83 1761 (1961)
132. H.P.Wong and J.T.Yates Jr. J. Catal. 89 79 (1984)
133. M.P.Keyes and K.L.Watters J. Catal. 100 477 (1986)
134. D.E.Morris and H.B.Tinker J. Organometallic Chem.
49 C53 (1973)
135. M.Laniecki and R.L.Burwell J. Colloid. Interface Sci.
75 95 (1980)
136. P.S.Braterman in " Metal Carbonyl Spectra " 1st ed.
Academic Press , New York , 1975
137. F.Solymosi, I. Tombacz and M.Kocsis J. Catal. 75 78
(1982)
138. F.Solymosi and M.Pasztor J. Catal. 104 312 (1987)
139. F.Solymosi, A.Erdohelyi and M.Kocsis J. Catal. 65
428 (1980)
140. M.A.Vannice Catal. Rev.- Sci. Eng. 14 153 (1976)
141. S.D.Jackson J. Chem. Soc., Faraday Trans. 1, 81
2225 (1985)
142. S.D.Worley, G.A.Mattson and R.Caudill
J. Phys. Chem. 87 1671 (1983)
143. F.Solymosi and M.Pasztor J. Phys. Chem. 89 4789
(1985)

144. P.Basu, D.Panayatov and J.T.Yates Jr. J. Am. Chem. Soc. 110 2074 (1988)
145. P.Gelin, Y.Ben Taarit and C.Naccache J. Catal. 59 357 (1979)
146. M.Primet, J.C.Vedrine and C.Naccache J. Mol. Catal. 4 411 (1978)
147. A.K.Smith, F.Hugues, A.Theolier, J.M.Basset, R.Ugo, G.M.Vanderighi, J.L.Bilhou, V.Bilhou-Bougnol and W.F.Graydon Inorganic Chem. 18 3104 (1979)
148. G.Blyholder and L.Orgi Adv. in Sci. and Tech. 4 1 (1987)
149. H.F.van't Blik, J.B.A.D.von Zon, T.Huizinga, J.C.Vis, D.C.Koningsberger and R.Pins J. Phys. Chem. 87 2264 (1983)
150. G.Bergeret, P.Gallezot, P.Gelin, Y.Ben Taarit, F.Lefebure, C.Naccache and R.D.Shannon J. Catal. 104 279 (1987)
151. D.C.Koningsberger, H.F.J.von't Blik, J.B.A.D. von Zon and R.Pins Proc. 8th Inter. Cong. Catal., Berlin Vol. 5 p 123 (1984)
152. F.Solymosi, T.Bansagi and E.Novak J. Catal. 112 183 (1988)
153. F.Solymosi and M.Pasztor J. Phys. Chem. 90 5312 (1986)
154. F.Solymosi and A.Erdohelyi J. Catal. 70 451 (1981)
155. T.Iizuka and Y.Tanaka J. Catal. 70 449 (1981)
156. H.C.Yao, S.Japor and M.Shef J. Catal. 50 407 (1977)
157. G.L.Kellogg Surf. Sci. 171 359 (1986)
158. Y.Kim, S.K.Shi and J.M.White 61 374 (1980)
159. G.L.Kellogg J. Catal. 92 167 (1985)
160. J.Kiss and F.Solymosi Surf. Sci. 177 191 (1986)
161. F.Solymosi, A.Berko and T.I.Tanoczi Surf. Sci. 141 533 (1984)
162. J.E.Demuth and H.Ibach Chem. Phys. Lett. 60 395 (1979)
163. D.Al-Mawlawi and J.M.Saleh J. Chem. Soc., Faraday Trans. 1, 77 2965 (1981)

164. D.Al-Mawlawi and J.M.Saleh J. Chem. Soc., Faraday
Trans. 1 , 77 2977 (1981)
165. J.B.Benzinger and R.J.Madix J. Catal. 65 36 (1980)
166. R.G.Greenler J. Chem. Phys. 37 2094 (1962)
167. T.Matsushima and J.M.White J. Catal. 44 183 (1976)
168. B.A.Marrow J. Chem. Soc., Faraday Trans. 1, 70
1527 (1974)
169. C.S.John and M.S.Scurr~~ell~~ in " Catalysis " ,
ed. C.Kemball and D.A.Dowden, (Specialist Periodic
Reports) The Royal Society of Chemistry, London .
Vol. 1 p 136 (1977)
170. F.Solymosi and A.Erdohelyi J. Catal. 91 327 (1985)
171. J.T.Yates Jr., S.D.Worley, T.M.Duncan and R.W.Vaughan
J. Chem. Phys. 70 1225 (1979)
172. J.T.Yates Jr. and R.R.Cavanagh J. Catal. 74 97
(1982)
173. M.A.Vannice J. Catal. 50 228 (1977)
174. A.Takeuchi and J.Katzer J. Phys. Chem. 85 937
(1981)
175. A.Takeuchi and J.Katzer J. Phys. Chem. 86 2438
(1982)
176. F.Solymosi, A.Erdohelyi and T.Bansagi J. Catal. 68
371 (1981)
177. B.A.Sexton and G.A.Somorjai J. Catal. 46 167 (1977)
178. A.Takeuchi and J.Katzer J. Catal. 82 351 (1983)
179. G.A.Somorjai Catal. Rev.- Sci. Rev. 23 189 (1981)
180. T.Fukushima, H.Arakawa and M.Ichikawa
J. Phys. Chem. 89 4440 (1985)
181. S.D.Jackson, B.J.Brandreth and D.Winstanley
J. Catal. 106 464 (1987)
182. H.Orita, S.Naito and K.Tamaru J. Chem. Soc. , Chem.
Comm. 1985 p 150
183. H.Orita, S.Naito and K.Tamaru J. Catal. 90 183 (1984)
184. T.Loek, F.Favre, G.van der Lee and V.Ponec
J. Chem. Soc., Chem. Comm. 1985 p230
185. G.van der Lee and V.Ponec J. Catal. 99 511 (1986)
186. T.Fukushima, H.Arakawa and M.Ichikawa J. Chem. Soc.
Chem. Comm. 1985 p 729

187. W.M.H.Sachtler, D.F.Shriver and M.Ichikawa
J. Catal. 99 513 (1986)
188. Y.Amenomiya J. Catal. 57 64 (1979)
189. A.Takeuchi, J.R.Katzer and R.W.Crecely J. Catal. 82
474 (1983)
190. W.Lui, C.L.Bao, D.M.Ren and T.T.Tsang Surf. Sci.
180 153 (1987)
191. a) S.J.Thomson and J.L.Wishlade Trans. Faraday Soc.
58 1170 (1962)
b) D.Cormack, S.J.Thomson and G.Webb J. Catal. 5
224 (1966)
192. G.D.M^CLellan Ph.D. Thesis ,University of Auckland
(1987)
193. C.Dall'Agnol, A.Gervasini, F.Morazzoni, F.Pinna,
G.Strukul and L.Zanderighi J. Catal. 96 106 (1985)
194. P.Arnoldy, J.C.M. de Jonge and J.A.Mouliyn
J. Phys. Chem. 89 4517 (1985)
195. H.Orita, S.Naito and K.Tamaru J.Catal. 112 176
(1988)
196. S.Evitt Ph.D. Thesis, The University of Glasgow
(1986)
197. F.A.Cotton and G.Wilkinson in " Advanced Inorganic
Chemistry ", John Wiley and Sons , New York , 4th ed.
1980 p 116
198. M.G.Wells, N.W.Cant and R.G.Greenler
Surf. Sci. 67 541 (1977)
199. " Dictionary of Organometallic Compounds "
Chapman and Hall , Vol 2 p 1650
200. K.Gildhooley, S.D.Jackson and S.Rigby Applied
Catal. 21 349 (1986)
201. L.Chan and G.L.Griffin Surf. Sci. 173 160 (1986)

But...